Fakultät für Medizin

Role of E2A SUMOylation during productive infection with Human Adenovirus Type 5

Miona Stubbe

Vollständiger Abdruck der von der Fakultät für Medizin der Technischen Universität München zur Erlangung des akademischen Grades einer

Doktorin der Naturwissenschaften (Dr. rer. nat.)

genehmigten Dissertation.

Vorsitz: Prof. Dr. Percy A. Knolle

Prüfer*innen der Dissertation:

1. Prof. Dr. Sabrina Schreiner
2. apl. Prof. Dr. Thomas Floss
3. Prof. Dr. Thomas Stamminger

Die Dissertation wurde am 10.05.2022. bei der Technischen Universität München eingereicht und durch die Fakultät für Medizin am 13.12.2022. angenommen.

Table of contents

Abstract

Human Adenoviruses (HAdV) are non-enveloped viruses containing a linear, double-stranded DNA genome surrounded by an icosahedral capsid with type-specific antigens. HAdVs are often non-pathogenic for healthy individuals. However, in the absence of protective immunity, HAdV infections can become lethal as a result of uncontrolled immunopathology and processes, which are still far from being understood in detail.

To ensure proper replication, DNA viruses express early viral genes to degrade or displace key regulators of cellular antiviral and immune response. In contrast, host-cells repress infection events through a network of transcriptional repressors and activators that typically regulate cellular homeostasis. The nuclear domains thought to be in charge for repressing viral DNA genomes are PML nuclear bodies (PML-NBs), interferon inducible, dot-like nuclear structures. Despite the fact that PML-NBs exhibit antiviral activity, many viruses including HAdVs position their genomes next to these structures via up to now unknown mechanism. PML-NBs represent the hotspots for host SUMO posttranslational modification. In HAdV infected cells these “SUMO factories” are located next to newly established replication centers indicated by the viral marker protein E2A.

This work demonstrates that E2A represents a novel target of the host SUMOylation machinery, orchestrating essential E2A functions. Mimicking removal of SUMOylated E2A from the infected cell by generation of HAdV variants with mutations in the SUMO conjugation motif repressed viral replication properties. Furthermore, we observed that E2A SUMO PTM might impact HAdV gene splicing and packaging of the viral genome. The data shown here clearly illustrate the influence of E2A SUMOylation on PML-NBs subcellular localization. Biochemical analyses revealed that SUMO modified E2A interacts with PML and Sp100A. These interactions represent the so far unknown molecular bridge between HAdV replication centers and PML tracks, enabling the virus to utilize their transcription activating capacities. On the other hand, to prevent condensation of the viral chromatin, Sp100HMG being an epigenetic modulator and repressive factor for efficient HAdV infection is counteracted by active entrapment into HAdV replication centers on an E2A SUMOylation-dependent manner.

HAdVs are classified as DNA tumor viruses due to their oncogenic capacity in non-permissive mammalian cells. They have developed intricate mechanisms to counteract host DNA damage response, including the activity of the cellular tumor suppressor p53. Several HAdV

proteins are known to inhibit p53-mediated transcriptional activation, however even though it has been reported that temperature-sensitive mutations within E2A gene affect HAdV-mediated transformation, the connection between E2A and p53 has so far not been reported.

Here, we identified E2A to be involved in the inhibition of p53-mediated transcription. E2A recruits p53 to HAdV replication centers during infection and to E2A containing domains in transfection settings. SUMOylated E2A promotes p53 degradation and E1B-55K interaction with PML-V that causes elevated p53 SUMOylation and subsequent inhibition of the transcription activating properties of the tumor suppressor. Additionally, functional E1B-55K prevents E2A binding to p53. In the absence of other viral factors E2A induces E1B-55K nuclear localization, reduces E1B-55K levels and SUMO PTM, thereby preventing E1B-55K-mediated p53 SUMOylation. Moreover, SUMOylated E2A interacts with Ubc9 and triggers the reduction of p53 SUMOylation, indicating the existence of an additional concept used by the virus to inhibit p53 activity using the HAdV DNA-binding protein E2A.

Taken together, these data reveal a novel E2A SUMOylation based mechanism employed by HAdV to exploit beneficial cellular components and to simultaneously counteract the host antiviral and DNA damage response.

Zusammenfassung

Humane Adenoviren (HAdV) sind unbehüllte Viren, die ein lineares, doppelsträngiges DNA-Genom enthalten, das von einem ikosaedrischen Kapsid mit typspezifischen Antigenen umgeben ist. HAdVs sind für gesunde Personen selten pathogen. In Abwesenheit einer schützenden Immunität können HAdV Infektionen tödlich verlaufen durch unkontrollierte Immunpathologie und Prozesse, die noch nicht im Detail verstanden sind.

Um eine ordnungsgemäße Replikation zu gewährleisten, exprimieren DNA Viren frühe virale Gene, die wichtige Regulatoren der zellulären antiviralen Maßnahmen und der Immunantwort abbauen oder antagonisieren. Als Gegenantwort unterdrücken die Wirtszellen die Infektion durch ein Netzwerk von transkriptionellen Repressoren und Aktivatoren, die normalerweise die zelluläre Homöostase regulieren. Die nukleären Domänen, von denen man annimmt, dass sie für die Repression des viralen DNA Genoms verantwortlich sind, sind PML-Kernkörper (PML-NBs), Interferon-induzierbare, punktförmige nukleäre Strukturen. Obwohl PML-NBs antivirale Aktivität aufweisen, positionieren viele Viren, einschließlich HAdVs, ihre Genome über einen bisher unbekannten Mechanismus an diesen Strukturen. PML-NBs stellen die Hotspots für posttranslationale SUMO Modifikationen dar. In HAdV-infizierten Zellen befinden sich diese "SUMO-Fabriken" in der Nähe von neu etablierten Replikationszentren, die durch das virale Markerprotein E2A angezeigt werden.

Diese vorliegende Arbeit zeigt, dass E2A ein neuartiges Zielprotein der Wirts-SUMOylierungsmaschinerie darstellt, welche essentielle E2A Funktionen orchestriert. Ein künstliches Blockieren der E2A-SUMOylierung durch Generierung von HAdV-Varianten mit Mutationen im SUMO-Konjugationsmotiv unterdrückt die viralen Replikationseigenschaften. Darüber hinaus scheint die E2A-SUMO-PTM das HAdV-Genspleißen und die Verpackung des viralen Genoms zu beeinflussen. Die hier gezeigten Daten verdeutlichen den Einfluss der E2A-SUMOylierung auf die subzelluläre Lokalisierung von PML-NBs. Biochemische Untersuchungen zeigten außerdem, dass SUMO-modifiziertes E2A mit PML und Sp100A interagiert. Diese Interaktionen stellen die molekulare Brücke zwischen HAdV-Replikationszentren und PML Strukturen dar und ermöglichen es dem Virus, deren transkriptionsaktivierende Kapazitäten zu nutzen. Um die Kondensation des viralen Chromatins zu verhindern, wird andererseits dem

repressiven Faktor Sp100HMG durch aktive Verdrängung in HAdV Replikationszentren auf eine E2A-SUMOylierungs-abhängige Weise entgegengewirkt.

HAdVs werden aufgrund ihrer onkogenen Kapazität in nicht-permissiven Säugetierzellen als DNA Tumorviren klassifiziert. Sie haben komplizierte Mechanismen entwickelt, um der zellulären DNA Schadensantwort entgegenzuwirken, einschließlich der Aktivität des zellulären Tumorsuppressors p53. Es ist bekannt, dass mehrere HAdV Proteine die p53-vermittelte Transkriptionsaktivierung hemmen. Obwohl berichtet wurde, dass temperatursensitive Mutationen innerhalb des *e2a* Gens die HAdV-vermittelte Transformation beeinflussen, wurde über einen Zusammenhang von E2A und p53 bisher nicht berichtet.

In dieser Arbeit wurde zum ersten Mal die Beteiligung von E2A an der Hemmung der p53-vermittelten Transkription nachgewiesen. E2A rekrutiert p53 zu HAdV Replikationszentren während der Infektion und zu E2A-haltigen Domänen in Transfektionsreihen. E2A-SUMOylierung unterliegt der HAdV-vermittelten Hemmung der p53-vermittelten Transaktivierung. SUMOyliertes E2A fördert den p53 Abbau und die E1B-55K Interaktion mit PML-V, was zu einer erhöhten p53-SUMOylierung und anschließender Hemmung der transkriptionsaktivierenden Eigenschaften des Tumorsuppressors führt. Auf der anderen Seite verhindert funktionelles E1B-55K die Bindung von E2A an p53. In Abwesenheit anderer viraler Faktoren induziert E2A die nukleäre Lokalisation von E1B-55K, reduziert die E1B-55K-Spiegel und das SUMO-PTM und verhindert dadurch die E1B-55K-vermittelte p53-SUMOylierung. Darüber hinaus interagiert SUMOyliertes E2A mit Ubc9 und vermindert die p53-SUMOylierung, was auf die Existenz eines zusätzlichen Konzepts hinweist, das vom Virus verwendet wird, um die p53-Aktivität mithilfe des HAdV-DNA-bindenden Proteins E2A zu hemmen.

Zusammengenommen zeigen die vorliegenden Daten einen neuartigen, auf E2A-SUMOylierung basierenden Mechanismus, den das HAdV einsetzt, um gleichzeitig nützliche zelluläre Komponenten zu nutzen und der antiviralen und DNA-Schadensantwort des Wirts entgegenzuwirken.

1 Introduction

1.1 Adenoviruses

1.1.1 Classification and pathogenesis

Adenoviruses (Ads) were discovered in 1953 and named according to the human adenoid tissue from which they were first isolated (Hilleman and Werner 1954; Rowe et al. 1953). They belong to the family Adenoviridae that comprises of more than 100 different serotypes that infect broad range of vertebrates. Depending on the host specificity adenoviruses are divided into six genera: *Mastadenoviruses* infecting mammals, *Aviadenoviruses* infecting birds, *Siadenviruses* infecting amphibians and birds, *Atadenoviruses* infecting ruminant, reptile, avian and marsupial hosts, *Ichtadenoviruses* infecting fish and *Testadenoviruses* infecting turtles (Benkő et al. 2022). Human Adenoviruses (HAdV) belong to genera *Mastadenoviruses* and are classified into seven species (A-G), according to their agglutination properties (Bailey and Mautner 1994).

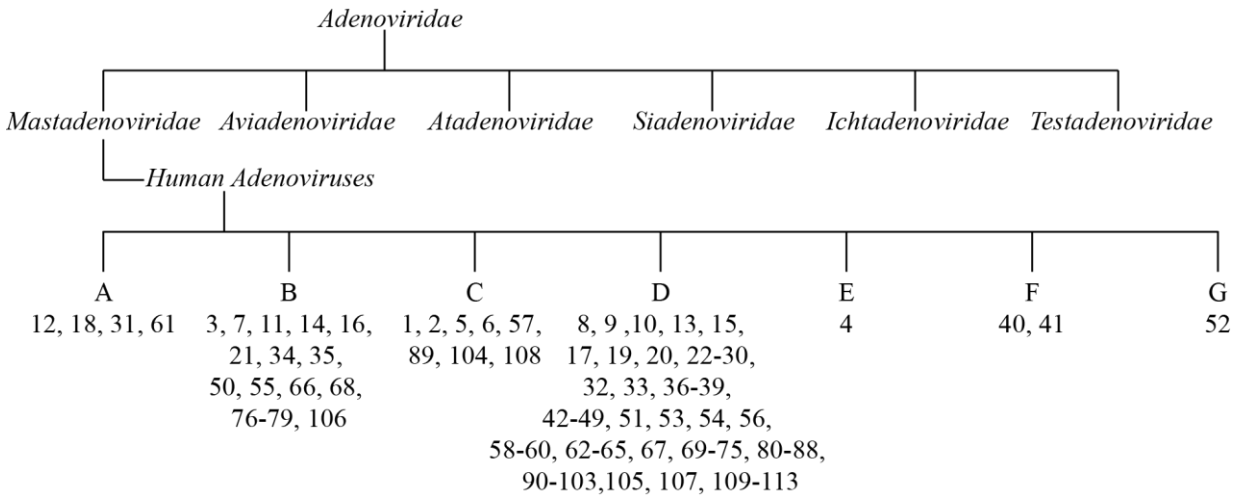

Figure 1: Classification of adenoviruses. Schematic representation of the Adenoviridae family. Human Adenovirus species are indicated by letters A-G according to the International Committee of the Taxonomy of Viruses (ICTV) (Harrach and Kajon 2012; Davison, Benko, and Harrach 2003; Benkő et al. 2022). Numbers 1-113 indicate human classified adenovirus genotypes according to (http://hadvwg.gmu.edu/).

There are 113 genotypes of HAdV known (http://hadvwg.gmu.edu/) and they are additionally divided using several characteristics like sequence homology and oncogenicity in rodents (Dhingra et al. 2019; Hage et al. 2015; Hashimoto et al. 2018; Yoshitomi et al. 2017; Benkő et al. 2022; Ismail et al. 2018). HAdV2 and HAdV5 are the most studied HAdV types also

used as for clinical vector development (Shenk 2001). First oncogenic adenovirus found was HAdV-12 that causes sarcomas in newborn hamsters (Trentin, Yabe, and Taylor 1962). This finding led to classification of HAdVs in the group DNA tumor viruses and numerous subsequent studies investigating transforming potential of adenoviruses. Intriguingly, DNA of HAdV B and D types was detected in pediatric brain tumors (Kosulin et al. 2007). Moreover, adenovirus DNA of C types was found in T-lymphocytes within various human sarcomas (Kosulin et al. 2013). Furthermore, HAdV-5 E1A/E1B oncogenes cause complete transformation of human mesenchymal stem/stroma cells (hMSCs) in tissue culture (Speiseder et al. 2017). Nevertheless, the solid causative association between HAdV infection and human tumors, has not been established up till now.

Most HAdV species are spread worldwide, with different abundancies dependent on geographic region and time period (Ampuero et al. 2012; Ishiko et al. 2008; Lin et al. 2004). It is estimated that they infect already 80% of the children by the age of five. AdV were first discovered as susceptive causative agents of common cold (Enders et al. 1956; Hilleman and Werner 1954; Rowe et al. 1953). Even though this original assumption was proven wrong, HAdV infection can lead to wide spectrum of human diseases due to their broad tissue tropism, where they mainly target differentiated epithelial cells (Boyer, Denny, and Ginsberg 1959). Particular groups of AdV can lead to different symptoms such as upper and lower respiratory tract infections (Ampuero et al. 2012; Esposito et al. 2013), keratoconjunctivitis (Jawetz 1959), gastroenteritis (Celik et al. 2015; Chhabra et al. 2013) or urinary tract infections (Hofland, Eron, and Washecka 2004; Numazaki et al. 1973). AdV most often associated with disease in humans are HAdV-C1, -C2, -C5, -B3, -B7, -B21, -E4 and -F41 (Lion 2014). HAdV infection is usually mild and self-limiting, however in rare cases it can lead to severe complications such as pneumonia, meningoencephalitis, hepatitis, or myocarditis (de Ory et al. 2013; Detrait et al. 2015; Echavarria 2008; Shauer et al. 2013). The most severe outcomes of HAdV infections have been reported in newborns and immunocompromised patients such as transplant recipients or patients suffering from AIDS (Berciaud et al. 2012; Krilov 2005; Lion 2014). Serious complications in immunocompromised patients are especially caused by HAdV-C types (Lion et al. 2010). Moreover, infection with the evolving strain HAdV 14p1 can be lethal even in healthy patients (Louie et al. 2008). Even though HAdV infections can be life-threatening, specific treatment is not available. Therefore, therapy of severe infections is often only symptomatic (Lion et al. 2003; Lion et al. 2010; Treacy et al. 2010).

Alternative is the treatment with common antiviral drugs, such as the nucleotide analog cidofovir or the nucleoside analog ribavirin (Ganapathi et al. 2016; Gavin and Katz 2002). However, promising progress in improving HAdV therapy has been made by recent discovery that arsenic trioxide exhibits strong antiviral activity in cell culture models (Hofmann et al. 2020). Additionally, T4 and A5/80 phage preparations showed inhibitory effects on HAdV replication, opening up novel possibilities for research of antiviral strategies (Przybylski et al. 2019).

1.1.2 Structure and genome organization

HAdVs are non-enveloped viruses with icosahedral capsid, ranging in size from 80 to 110 nm. HAdV capsid is composed out of nine structural proteins (Rux and Burnett 2004). The structural proteins belong to two main groups: the capsid and the core proteins. The capsid proteins termed as the major capsid proteins are hexon (II), penton base (III) and fiber (IV), while the minor capsid proteins are pVI, pIIIa, pVIII and pIX. Terminal protein (TP), μ, pVII, pV and IVa2 and the viral protease are termed as the core proteins (Nemerow et al. 2009; Russell 2009; Vellinga, Van der Heijdt, and Hoeben 2005).

The main subunit of the capsid is a structure called capsomere. The capsid consists of 252 capsomeres: 240 homotrimeric hexons (II) forming 20 triangular facets with 12 pentons composed out of penton bases (III) with fibers (IV) protruding from each vertex (Nemerow et al. 2009; Russell 2009). The fiber knob mediates the attachment of adenovirus to the host cell through interaction with the coxsackie/adenovirus receptor CAR (Bergelson et al. 1997; Wu et al. 2003). Even though the CAR receptor is commonly used by most adenovirus species, it is known that different cellular receptors are primarily used by certain adenoviruses, such as CD46 in case of species B (Gaggar, Shayakhmetov, and Lieber 2003).

Minor structural capsid proteins stabilize the capsid by association with the internal or external surfaces of the capsid. They serve as the ‘cement’ between individual hexons, as well as between hexons and pentons (Furcinitti, van Oostrum, and Burnett 1989; Liu et al. 2010; Perez-Berna et al. 2009; Stewart, Fuller, and Burnett 1993). Even though it was originally thought that the minor capsid proteins perform only the structural role in capsid stabilization, it was also shown that they have additional crucial functions within the host cell. For example, pVI is supporting viral endosomal escape and removes the transcriptional repressor death domain associated protein (Daxx) leading to the activation of the E1A promoter (Schreiner et al. 2012; Wiethoff et al. 2005).

The core proteins VII, V and µ are in a tight complex with the adenoviral DNA, condensing it into nucleosome-like state. The core protein V (pV) links the virion core to the capsid by connecting the pVI and the penton base. Protein VII (pVII) is presumed to have homologous functions to cellular histones as it condenses the viral DNA into repetitive nucleoprotein complexes, similar functions to pVII are also assumed for small peptide called µ (Everitt, Lutter, and Philipson 1975; Harpst, Ennever, and Russell 1977; Russell and Precious 1982). DNA replication is initiated by 55 kDa terminal proteins (TP), covalently attached to 5'ends (Pronk, Stuiver, and van der Vliet 1992; Rux and Burnett 2004; Tamanoi and Stillman 1982). Moreover, the IVa2 protein has a role in viral DNA packaging (Zhang et al. 2001; Ahi, Vemula, and Mittal 2013), and the viral protease cleaves the precursor proteins to enable the viral maturation (Webster et al. 1989).

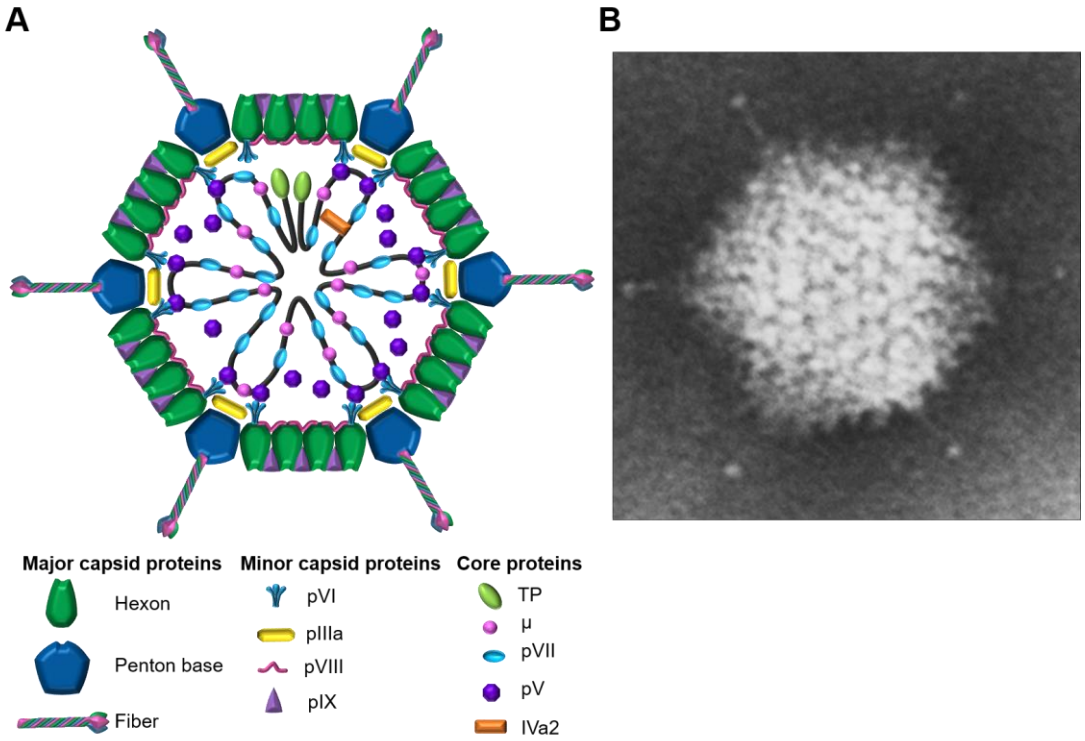

Figure 2: HAdV virion structure. (A) Schematic representation of the HAdV type 5 viral particle with indicated structural proteins. Viral DNA is represented by black line within the capsid. **(B)** *Mastadenovirus* picture acquired by electron microscopy (Mei, Harrach, and Wadell 2011).

Capsid harbors linear, double-stranded (ds) DNA genome, 26-45 kDa in size, flanked by 43-369 bp inverted terminal repeats (ITRs) at both ends. ITRs serve as replication origins during viral DNA replication (Davison, Benko, and Harrach 2003). The genome of HAdV consists of

nine different transcription units that encode 40 different regulatory proteins and two non-coding RNAs (virus associated RNAs). There are five early (E1A, E1B, E2, E3, E4), three delayed (IX, IVa2, E2 late) and one major late transcription unit (MLTU). MLTU is under control of *major late promoter* (MLP) and after processing generates five late mRNAs (L1, L2, L3, L4, L5) (Davison, Benko, and Harrach 2003; Berk 2007). All HAdV5 mRNAs except the virus associated RNAs (VA-RNAs), are synthesized by RNA polymerase II. VA-RNAs are transcribed by RNA polymerase III (Weinmann, Raskas, and Roeder 1974).

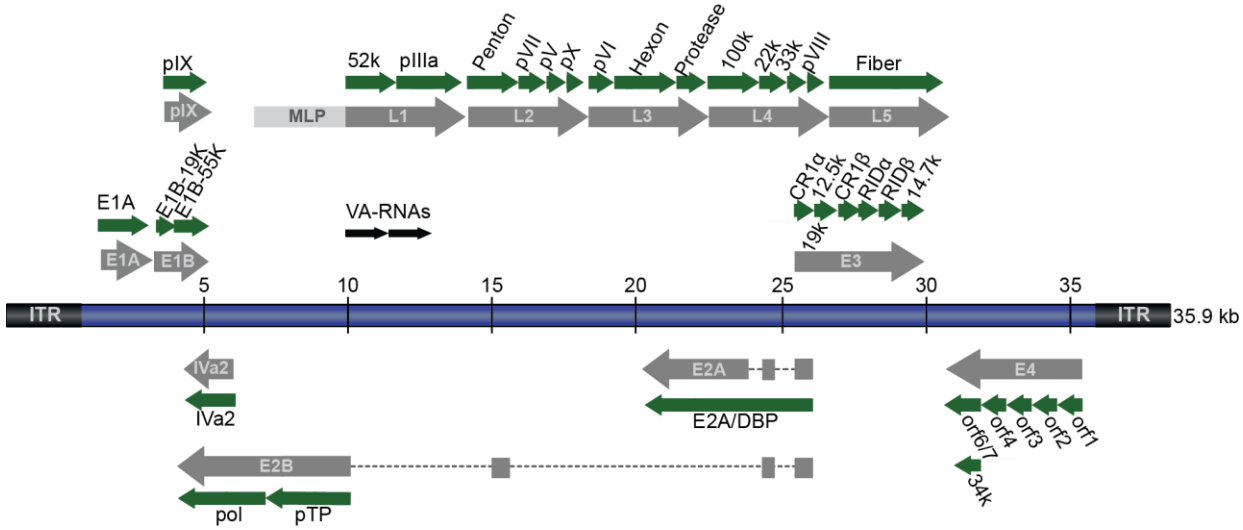

Figure 3: Organization of the HAdV genome. Schematic representation of the HAdV-C2 genome as a representative of HAdV-C types. The viral DNA is shown in blue. Organization of early (E1A, E1B, E2A, E2B, E3, E4), delayed (IX, IVa2) and late (L1-L5) transcription units is represented in gray; E: early; L: late; ITR: inverted terminal repeat. Expressed proteins are presented in green and virus-associated RNAs (VA-RNAs) in black. Arrows represent indicated orientation.

1.1.3 The adenoviral life cycle

HAdVs most often infect post-mitotic resting, differentiated epithelial cells of the respiratory and gastrointestinal tract (Boyer, Denny, and Ginsberg 1959; Wold 2007). In addition, there are several tumor and primary cell lines that can be infected by HAdVs in tissue culture. HAdVs infection in human cells is lytic resulting in death of these cells. Contrarily, in animal cells, especially rodent cell lines, HAdV infection is abortive (Garnett et al. 2009; Gustafsson et al. 2007; Kosulin et al. 2007; Liebermann et al. 1996). The adenoviral lytic cycle is divided into early and late phase. The early phase includes adsorption, particle disassembly and early gene expression. Viral DNA replication initiates the late phase during which late viral gene expression, virus progeny production and viral release occur (Berk 2007).

HAdV attaches to the cell via knob domain of the fiber protein by interaction with the CAR receptor, or CD46 receptor for species B (Roelvink et al. 1998). Efficient uptake of the virus is mediated by interaction of Arg-Gly-Asp (RGD) motif of penton base protein and surface integrins (Mathias et al. 1994; Stewart et al. 1997; Wickham et al. 1994). Viral particles enter the cell via clathrin-mediated endocytosis (Greber et al. 1993; Varga, Weibull, and Everitt 1991). The virus escapes from endosome into the cytosol in order to avoid the cellular immune response. This process takes place via drop in the pH and pVI that permeabilize the endosomal membrane (Greber et al. 1993; Wiethoff et al. 2005). Partially uncoated virions are transported along microtubules to microtubule organizing center (MTOC) from where they associate with the nuclear pore complex and the viral DNA bound to pVII is imported into the nucleus (Bremner et al. 2009; Dales and Chardonnet 1973; Greber et al. 1997; Greber and Way 2006).

Early phase of adenoviral life cycle starts with the import of viral DNA into the nucleus and it is initiated by first adenoviral protein expressed, E1A. E1A is the major adenoviral transcription factor that induces transcription of other early genes E1B to E4 (Avvakumov, Sahbegovic, et al. 2002; Avvakumov, Wheeler, et al. 2002; Moran et al. 1986). However, before the E1A expression, pVI promotes the activation of the E1A promoter and E1A-dependent promoters, initiating the onset of HAdV DNA transcription in the absence of other viral proteins (Schreiner, Burck, et al. 2013; Schreiner et al. 2012; Schreiner et al. 2010). Early viral proteins perform broad range of functions and establish the optimal environment for virus replication. E1A and E4 are known to induce the cell cycle progression by leading the cells to the S-phase and E1B, E4 and E3 proteins counteract antiviral host cell response by inhibiting apoptosis, growth arrest or immune response (Berk 1986b, a; Debbas and White 1993; Harlow et al. 1986; Nevins 1981; Windheim, Hilgendorf, and Burgert 2004). The E2 transcriptional unit E2A encodes for viral DNA binding protein (E2A), while the E2B unit encodes for the viral DNA polymerase (Pol) and the precursor of the terminal protein (pTP). The main function of these proteins is in HAdV DNA replication, which starts with their accumulation (de Jong, van der Vliet, and Brenkman 2003; Shenk 2001). Additional functions essential for virus replication are performed by proteins expressed from E4 region E4orf1, E4orf2, E4orf3, E4orf4, E4orf6 and E4orf6/7 (Tauber and Dobner 2001).

The late phase of HAdV life cycle starts with the onset of viral DNA replication and transcription of the major late transcription unit (MLTU) into one 29 kbp precursor mRNA that is

alternatively spliced into around 20 different mRNAs belonging to five families of late mRNAs (L1-L5) (Nevins and Darnell 1978). L4-22K and L4-33K mediate transcriptional and posttranscriptional changes of MLTU to facilitate the expression of late mRNAs. Moreover, IVa2 is activates MLTU and cooperates with L4-22K and L4-33K (Ali et al. 2007; Farley, Brown, and Leppard 2004; Lutz and Kedinger 1996; Morris and Leppard 2009; Morris, Scott, and Leppard 2010; Tormanen et al. 2006). Viral late mRNAs are efficiently synthesized, transported to the cytoplasm and translated, but the host mRNA transport and translation are shut-off during the late phase of infection (Beltz and Flint 1979). The multimerization of hexon and penton monomers takes place in the cytoplasm, while the virion assembly occurs in the host nucleus. This final step of HAdV life cycle is regulated by late (L4-100K, -33K, -22K), intermediate (IVa2) and early regulatory (E1B-55K, E4orf6, E2A) proteins (Ahi, Vemula, and Mittal 2013; Fessler and Young 1999; Hong et al. 2005; Horwitz, Scharff, and Maizel 1969; Velicer and Ginsberg 1970). The completion of the viral life cycle takes place 24-36 h after infection and results in the host cell lysis and the release of $1x10^4$ viral particles (Tollefson et al. 1996).

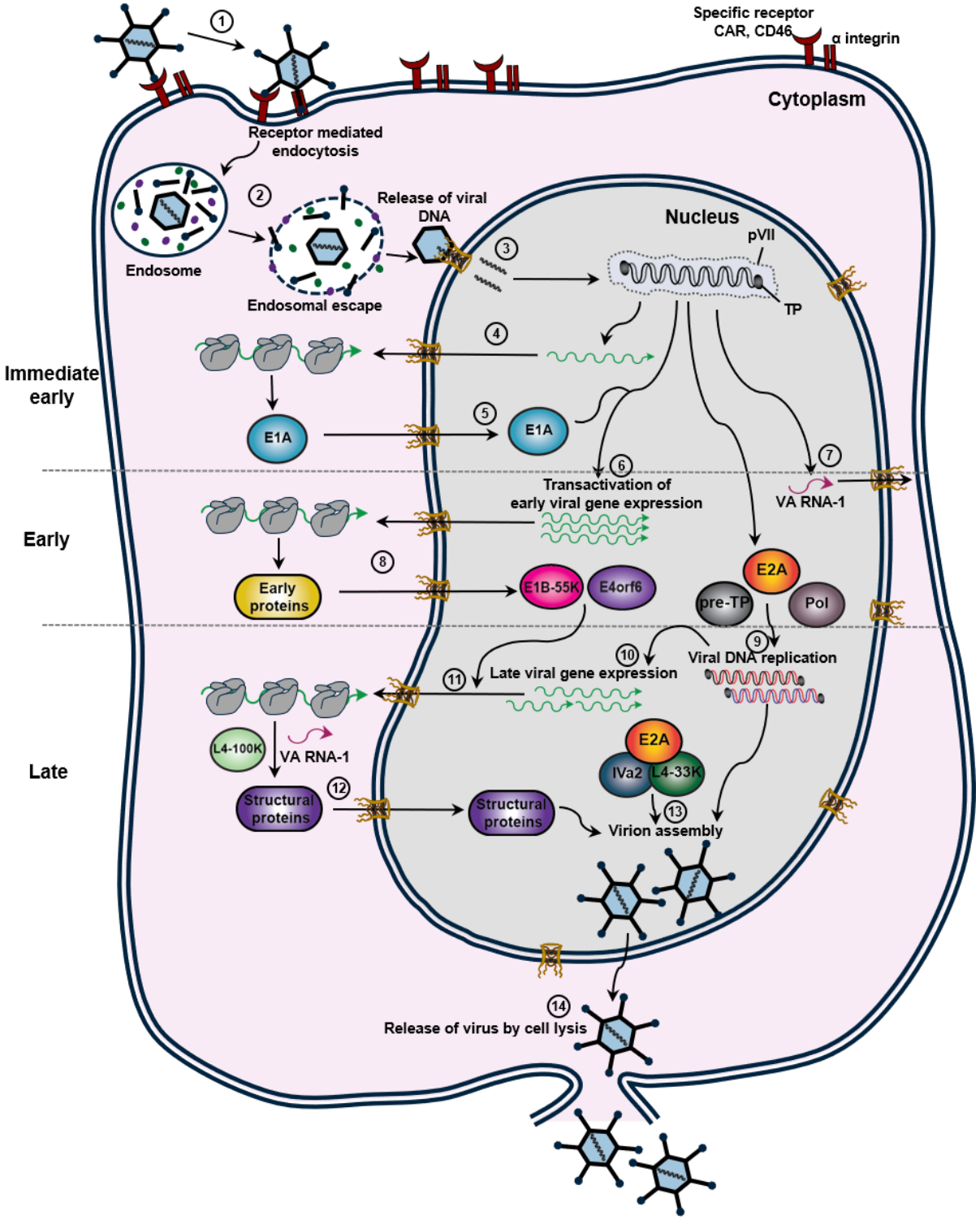

Figure 4: HAdV life cycle. In the immediate early phase, the virus attaches to a host cell via interaction between the fiber and the specific receptor (CAR or CD46) on the host cell surface (1). The virus enters the cell via endocytosis dependent on the interaction of the structural protein penton base with a cellular integrin. Prior to the entry into the cytoplasm viral particles are partially disassembled (2). After uncoating, the viral genome in association with core protein VII is imported into the nucleus (3). Immediate-early E1A gene is transcribed by the host cell RNA polymerase II and E1A mRNAs is exported to the cytoplasm (4). E1A proteins are synthesized

by the cellular translation machinery and imported into the nucleus (5). During the early phase, E1A controls transcription of both cellular and viral genes. E1A promotes transcription of the early adenoviral genes by cellular RNA polymerase II (6). Additionally, in the early phase of infection, RNA polymerase III transcribes VA-RNAs (7). The early pre-mRNAs (E1B to E4) are exported to the cytoplasm, translated and imported into the nucleus (8). Late phase starts with the onset of viral DNA replication controlled by viral replication proteins E2A, TP and Pol. Replicated viral DNAs are used as templates for further rounds of replication or for transcription of late genes (9). Late promoters are activated by viral DNA replication, but IVa2 and L4 proteins maximize transcription from MLP unit (10). Late mRNAs species are exported into the cytoplasm by the E1B-55K and E4orf6 proteins (11). VA-RNAs and L4-100K protein are required for efficient translation of late mRNAs. L4-100K is a chaperone for assembly of trimeric hexons which are imported into the nucleus with the other structural proteins. L4-100K also mediates the host shut-off (12). Within the nucleus, capsids are assembled, DNA is packaged via packaging signal located near the end of the genome, as well as the E2A, IVa2 and L4-33K proteins that assemble a packaging complex (13). Precursor proteins in immature virions are cleaved by the viral L3 protease into their mature forms to generate mature infectious virions. Progeny virions are released via the host cell lysis (14) (MacLachlan and Dubovi 2011).

1.1.4 Structure and function of HAdV DNA binding protein (E2A)

Early E2A region of the HAdV genome encodes the viral DNA-binding protein (E2A), detectable as early as 2 hours after infection and expressed at substantial levels throughout infection cycle (Voelkerding and Klessig 1986). In order to be able to provide sufficient amounts of E2A protein during infection, E2A region contains both early (E2E) and late (E2L) promoter (de Jong, van der Vliet, and Brenkman 2003). E2A is 529 amino acid phosphoprotein with an apparent size of 72 kDa on sodium dodecyl sulfate (SDS)-polyacrylamide gels. The unusual structure of the N-terminal part of the molecule and the extensive phosphorylation at several serine and threonine residues contribute to the aberrant gel mobility (Cleghon et al. 1989; Axelrod 1978; Linne, Jornvall, and Philipson 1977; Linne and Philipson 1980). E2A predominantly accumulates in the nucleus, but in the late phase of infection a cytoplasmic subclass can be detected (Sugawara et al. 1977; Voelkerding and Klessig 1986; Deppert, Walser, and Klockmann 1988).

HAdV E2A was first detected as a single-stranded DNA-binding protein (van der Vliet and Levine 1973), but it also binds to double-stranded DNA (Fowlkes et al. 1979) and RNA (Cleghon and Klessig 1986). E2A binds to DNA on a sequence unspecific manner, whereas association to ssDNA is cooperative (van Amerongen, van Grondelle, and van der Vliet 1987) and to dsDNA non-cooperative (Stuiver and van der Vliet 1990). E2A is anisometric and therefore it can be cleaved by mild treatment with several proteases in to a 26 kDa N-terminal domain, (for HAdV5, aa 1-173) and a 44 kDa C-terminal domain, (for HAdV5, aa 174-529) (Klein, Maltzman, and Levine 1979; Linne and Philipson 1980). The C-terminal E2A domain is highly conserved between serotypes (Ariga et al. 1980; Kitchingman 1985; Tsernoglou et al. 1985). Tree conserved regions

on the C-terminal part, CR1, CR2 and CR3 at aa 178-186, aa 322-330 and aa 464-476 are involved in nucleic acid binding (Neale and Kitchingman 1989). C-terminal part of E2A (aa 510 to 529) also forms a protruding C-terminal arm with a hook. Crystallography studies showed strong differences in the orientation of the E2A C-terminal arm, a consequence of flexibility around so-called hinge region (aa 512 to 515). This flexibility supports the E2A DNA unwinding activity during replication initiation processes. Furthermore, the C-terminal arm enables the formation of E2A protein chains, by hooking into another E2A molecule to form a multiprotein complex (Dekker et al. 1997; Kanellopoulos et al. 1996; Tucker et al. 1994). Additionally, binding of Zn to the region required for metal ion binding, located between aa 273 and 286, facilitates E2A interaction with ssDNA (Tucker et al. 1994).

In contrast, the N-terminal domain is not conserved among adenovirus serotypes (Cleghon and Klessig 1986). Nearly all the protein phosphorylation sites are in the N-terminal part of E2A (Cleghon et al. 1989; Klein, Maltzman, and Levine 1979). Remarkably high E2A phosphorylation increases the molecule solubility and prevents unspecific interactions with other molecules. Moreover, N-terminal domain contains an unusually large proportion of proline and acidic/basic residues (Cleghon et al. 1993; Cleghon et al. 1989). At least two distinct nuclear localization sites are localized at the N-terminal part of E2A, at aa 42 to 46 and aa 84 to 89 (Morin, Delsert, and Klessig 1989; Cleghon et al. 1989).

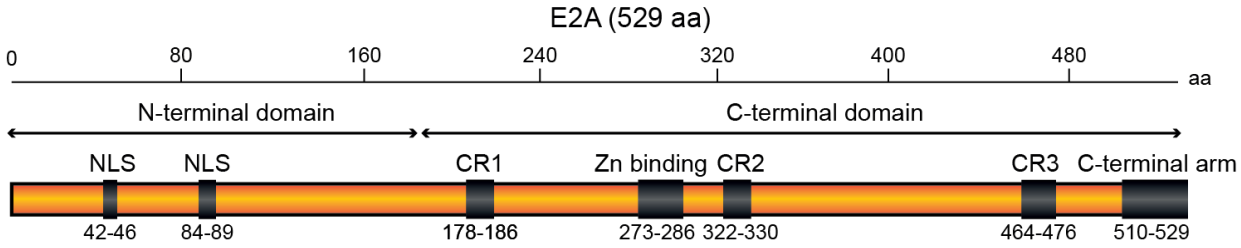

Figure 5: Structure of HAdV DNA binding protein, E2A. Black boxes represent known functional domains in E2A. N-terminal domain contains nuclear localization signals (NLS). C-terminal region harbors conserved regions, labeled CR1-3, Zn binding region and C-terminal arm.

E2A is involved in regulation of the viral gene expression (Carter and Blanton 1978), mRNA stability (Babich and Nevins 1981), host range determination (Morin, Delsert, and Klessig 1989), splicing of late viral mRNAs (Anderson 1981; Anderson and Klessig 1984; Kruijer, van Schaik, and Sussenbach 1981), virion assembly (Ahi, Vemula, and Mittal 2013) and maturation (Nicolas et al. 1983) and cell transformation (Rice, Klessig, and Williams 1987). However, the

main function attributed to this protein is in viral DNA replication (Hay et al. 1995; Schilling, Weingartner, and Winnacker 1975; van Breukelen et al. 2003; van Breukelen et al. 2000). E2A promotes efficient binding of polymerase by modulating the origin conformation during the initiation of DNA replication (van Breukelen et al. 2003). E2A is also important for the elongation phase of DNA replication where it is engaged in unwinding of dsDNA template. Moreover, E2A protects the displaced single strand maintaining it in a form of a rigid nucleoprotein fiber (Monaghan, Webster, and Hay 1994; Zijderveld, Stuiver, and van der Vliet 1993). Due to its essential role in replication E2A is widely regarded as marker protein for viral replication centers (RC) (Puvion-Dutilleul, Pedron, and Cajean-Feroldi 1984).

1.1.5 Structure and function of HAdV replication centers

Replication centers of DNA viruses that replicate in the nucleus are non-membranous structures usually formed adjacent to defined nuclear domains, such as PML-NBs, nuclear speckles or nucleolus (Doucas et al. 1996; Everett 2001; Ishov and Maul 1996; Jul-Larsen et al. 2004; Maul 1998; Maul, Ishov, and Everett 1996; Sourvinos and Everett 2002; Spector and Lamond 2011; Wang et al. 2010). The assembly of replication centers in the nucleus is accompanied by the vast reorganization of the major components of nuclear domains, such as PML-NBs, interchromatin granules (IG), paraspeckles, cajal bodies (CB), and nucleoli (Schmid et al. 2014). Replication centers of nucleus replicating viruses both promote efficient viral replication and simultaneously support suppression of the host antiviral response (Schmid et al. 2014).

Upon infection, HAdV DNA localizes to PML-NBs that are reorganized in PML tracks by HAdV protein E4orf3 (Ishov and Maul 1996). Besides E2A, additional adenoviral proteins such as L4-33K, IVa2, L4-22K, viral DNA polymerase, pTP, Penton, Fiber, pIX, E4orf4, E4orf6 and E1B-55K localize to HAdV RCs (Hidalgo and Gonzalez 2019). Interestingly, HAdV E2A has been proposed to target PML-NBs independently on other viral components (Komatsu, Nagata, and Wodrich 2016). RC formation is accompanied by recruitment of components from PML-NBs, nucleoli, CB, IG and nuclear domains that regulate RNA biogenesis to these viral compartments (Besse and Puvion-Dutilleul 1995; Bridge et al. 1995; Hiscox 2002; James et al. 2010; Rodrigues et al. 1996). HAdV replication centers size varies between 0.5 and 5 μm in diameter. Even though they are not limited by membranous structures, HAdV RCs contain morphologically and functionally distinguishable subsections (Hidalgo et al. 2016). Not actively replicated or

transcribed dsDNA localizes in the centers of RCs. HAdV E2A is associated with ssDNA in the peripheral replicative zone (PRZ) where active replication and transcription take place. As a consequence of the active transcription the clusters of IG accumulate around RCs and enable late transcription and splicing (Hidalgo et al. 2016; Murti, Davis, and Kitchingman 1990; Pombo et al. 1994; Puvion-Dutilleul et al. 1994; Puvion-Dutilleul and Puvion 1990). Interestingly, during infection SUMO-1 localizes outside of RC, whereas SUMO-2 and SUMO-3 are mainly detected inside RC, showing similar pattern to E2A (Hidalgo et al. 2016).

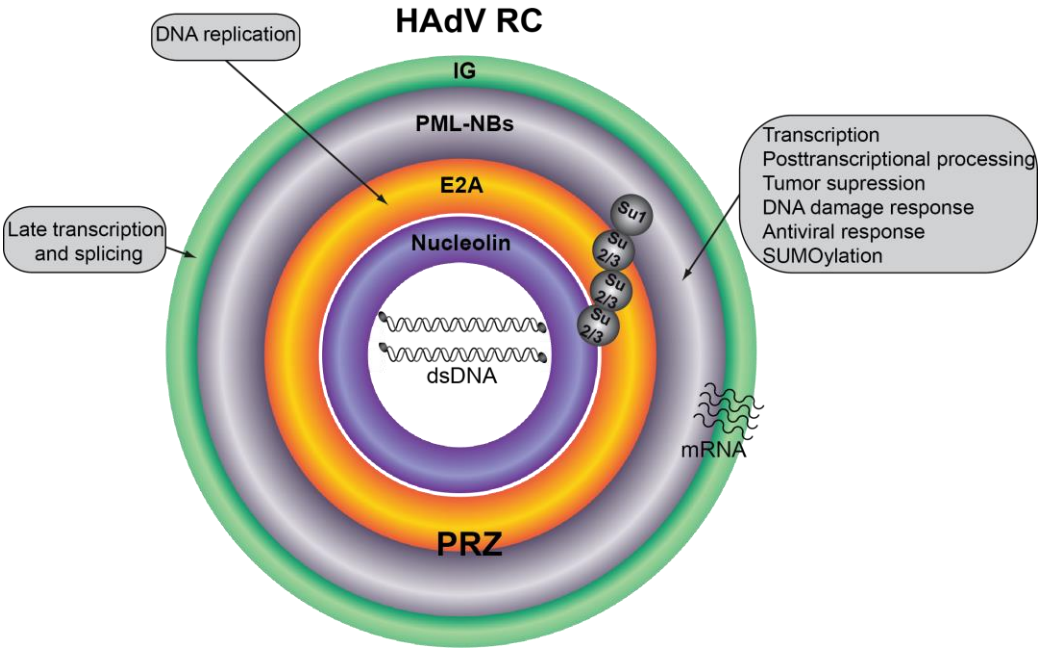

Figure 6: Schematic representation of HAdV replication centers. Interchromatin granules region (IG) is represented in green, PML nuclear bodies (PML-NBs) in grey, E2A in orange, and Nucleolin in purple. After the entry in the nucleus, HAdV DNA localizes next to PML-NBs. HAdV protein E4orf3 relocalizes PML-NBs into track like structures. Different viral proteins and nuclear components are recruited to PML tracks leading to the formation of viral RCs. RCs contain different compartments. E2A localizes at the peripheral replicative zones (PRZ), where viral DNA replication and early transcription occur. Nucleolin colocalizes with E2A in later stages of infection. Splicing and late transcription take place at the IG region that localize next to RCs. SUMO-1 (Su1) localizes outside of RCs, while SUMO-2 and -3 (Su2/3) localize inside the RCs together with E2A.

Except for the recruitment of components from various cellular domains to the HAdV replication centers, components of DNA repair machinery, tumor suppressor proteins, signal transduction factors and innate immune response proteins also localize to HAdV RCs (Cardoso et al. 2008; Carson et al. 2009; Maul et al. 1998; Sohn and Hearing 2011; Hidalgo et al. 2016). Additionally, the host factors involved in cellular DNA replication such as Nuclear factor I (NFI)

are also recruited to HAdV RCs (Bosher, Dawson, and Hay 1992). Besides the positive factors for HAdV infection, inhibitory host factors are also sequestered to HAdV RCs and thereby inactivated. This enables the virus to counteract the host antiviral response and establish optimal conditions for viral replication (Ornelles and Shenk 1991; Schmid et al. 2014). Some negative factors are recruited to the HAdV RCs in the early infection but degraded in the later stages via E1B-55K/E4orf6 E3 ubiquitin ligase complex (Baker et al. 2007a; Blanchette et al. 2004; Gupta et al. 2013; Orazio et al. 2011; Schreiner, Burck, et al. 2013; Schreiner, Kinkley, et al. 2013; Stracker, Carson, and Weitzman 2002; Yondola and Hearing 2007; Dallaire et al. 2009). For example, restriction factor for HAdV infection, involved in regulation of DDR and chromatin structure SPOC1, is recruited to the viral RCs prior to E1B-55K/E4orf6 induced proteasomal degradation (Schreiner, Kinkley, et al. 2013). Similarly, the Bloom Helicase, a PML-NB component implicated in resection of DNA breaks, is localized at the HAdV RCs early during infection and is later degraded (Orazio et al. 2011). Additional repressive factors and proteins involved in DNA damage response such as ATR, ATRIP, RPA32, Rad9, Rad17, TOPBP1 and hnRNPUL1 are also sequestered to viral replication centers, pointing at the common trend during HAdV infection (Turnell and Grand 2012). Moreover, HAdV recruits cellular inhibitory factors such as Sp100 isoforms B, C and HMG, to RCs and thereby inactivates their repressive activity. However, Sp100A isoform is kept in PML tracks localized next to HAdV RCs to promote HAdV gene expression (Berscheminski et al. 2014). Another noteworthy example of the HAdV ability to simultaneously exploit and inhibit various host proteins is the manipulation of the Mre11, Rad50 and NBS1 (MRN) complex, in charged for sensing and repair of DNA damage. In early infection, RC components are relocalized to PML tracks by E4orf3. However, in the later stages of infection, Mre11 levels are decreased, Rad50 stays in the tracks and NBS1 gets sequestered to the viral RCs (Evans and Hearing 2005). These facts emphasize the dual role of HAdV RCs in both supplying the components necessary for efficient viral replication/transcription and inhibiting the host antiviral properties.

1.2 The role SUMO posttranslational modification during HAdV infection

1.2.1 The cellular SUMOylation machinery

The small ubiquitin-like modifier (SUMO) was first discovered in mammals as a covalent modification of GTPase activating protein RanGAP1 (Lee et al. 1998; Mahajan et al. 1997; Mahajan, Gerace, and Melchior 1998; Matunis, Coutavas, and Blobel 1996; Matunis, Wu, and Blobel 1998). This highly conserved protein family is found in all eukaryotes (Epps and Tanda 1998; Fraser et al. 2000; Johnson 2004; Jones et al. 2002). In multicellular organisms, SUMO conjugation happens in all tissues at all developmental stages (Chen, Mannen, and Li 1998; Joanisse, Inaguma, and Tanguay 1998; Kamitani et al. 1998; Kurepa et al. 2003; Lois, Lima, and Chua 2003; Shen et al. 1996). SUMO is grouped into the family of ubiquitin-like proteins (UBL) as it shows 18 % of sequence similarity with ubiquitin and these two proteins share similar structures and molecular mechanisms of attachment. The SUMO family comprises five SUMO isoforms, SUMO-1 to SUMO-5. However, SUMO-1 to 3 are considered as the main SUMO family members (Hay 2005; Saitoh and Hinchey 2000; Wang and Dasso 2009). It is still not certain if SUMO-4 can be conjugated to target proteins *in vivo* and its expression has been detected only in kidneys, lymph nodes and spleen (Bohren et al. 2004; Owerbach et al. 2005). SUMO-5 has so far not been confirmed on protein level (Liang et al. 2016). SUMO-2 and SUMO-3 are often termed as SUMO-2/3 as they show 95% sequence similarity but only about 45% of sequence identity with SUMO-1 (Hay 2005; Saitoh and Hinchey 2000; Wang and Dasso 2009). The sequence of SUMO-2/3 contains a conserved acceptor lysine residue which enables them to form polymeric chains, while SUMO-1 can only be found in mixed SUMO chains indicating its role as a chain terminator (Matic et al. 2008; Tatham et al. 2001).

SUMO attachment most often takes place at the consensus site ψKXE (ψ for a hydrophobic amino acid and X for any amino acid) (Rodriguez, Dargemont, and Hay 2001). However, especially in the stress conditions, target SUMOylation becomes less stringent leading to SUMO attachment to non-consensus motifs (Hendriks and Vertegaal 2016; Pichler et al. 2017). SUMO binds to its substrates through an isopeptide bond between C-terminal carboxyl group of SUMO and the ε-amino group of a lysine residue in the substrate protein, increasing its molecular weight by 20 to 40 kDa. SUMOylation is a three-step enzymatic reversible pathway, analogous to

ubiquitin conjugation (Hay 2007; Johnson 2004). Prior to activation, all SUMO isoforms are proteolytically processed by sentrin specific proteases (SENPs), from its precursor to produce a conserved C-terminal di-glycine motif (Hay 2007; Mukhopadhyay and Dasso 2007). In the second step of SUMO conjugating pathway the catalytic domain of the activating enzyme E1 specifically recognize the C-terminal di-glycine motif on mature SUMO as a substrate and forms a thioester bond with consumption of ATP (Desterro et al. 1999; Hay 2005; Lois and Lima 2005). E1 is a heterodimeric protein composed of Sae1 and Sae2 subunits. Sae1 has a structural role while the Sae2 contains catalytically active cysteine and performs most of the tasks required for E1 function. E1 enables the formation of an additional thioester bond leading to transfer of SUMO proteins to the conjugating enzyme E2, also called Ubc9 (Desterro, Thomson, and Hay 1997; Okuma et al. 1999). Ubc9 contains an active site with a cysteine residue that enables the direct SUMO binding to the SCMs within the target proteins. Through the mediation of Ubc9, appropriate E3 SUMO ligase leads to the formation of an isopropyl bond between the C-terminal di-glycine residues of SUMO and an ε-amino group of a lysine residue within target SCM (Rodriguez, Dargemont, and Hay 2001). E3 enzymes perform mostly structural function, maintaining SUMO and Ubc9 in a favorable relative orientation. E3 ligase kinetically facilitates the SUMO conjugation, but it is not absolutely required for the process (Bernier-Villamor et al. 2002; Seeler and Dejean 2003).

The pattern of SUMO attachment is dynamic and varies during the cell cycle and in response to different stimuli. SUMOylation is a reversible modification and deSUMOylation involves SENPs that release the target protein, in a process analogous to SUMO maturation (Mukhopadhyay and Dasso 2007).

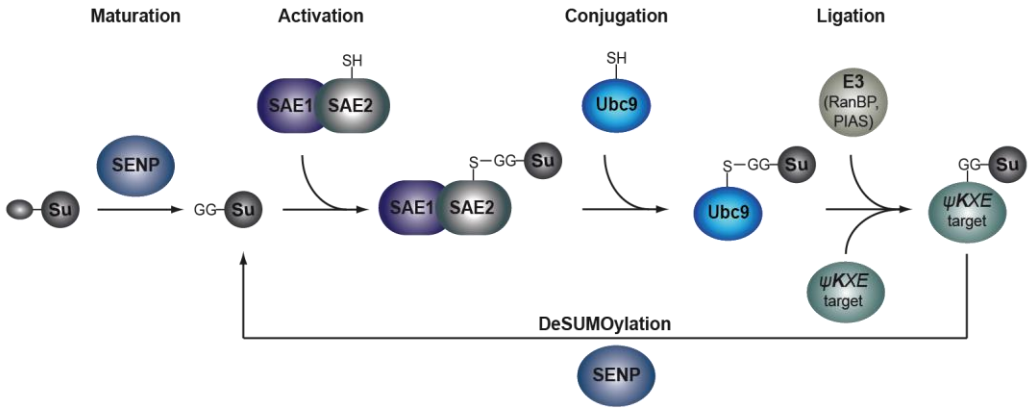

Figure 7: SUMO conjugation pathway. SUMO specific protease (SENP) processes the SUMO precursor to expose the di-glycine motif (GG). SUMO in activated state is conjugated to target proteins harboring the SUMO

conjugation motif (ψKXE). Enzymatic cascade involved in this process consists of SUMO activating enzyme E1 (SAE1/2), a SUMO conjugating enzyme E2 (Ubc9) and a SUMO ligase E3 (e.g., RanBP, PIAS). Specific SENPs are able to deconjugate SUMO from target proteins (Seeler and Dejean 2003).

SUMOylation affects wide range of cellular processes such as transcription, nucleocytoplasmic transport, protein degradation, mRNA splicing, ribosome biogenesis, apoptosis, DNA repair, recombination, chromatin organization and PML-NBs formation (Bossis and Melchior 2006; Hay 2005; Hendriks and Vertegaal 2016; Seeler and Dejean 2003; Ishov et al. 1999; Shen et al. 2006; Keiten-Schmitz, Schunck, and Muller 2019; Mitra et al. 2020). High diversity of SUMOylation functions derives from its ability to reversibly alter protein role by regulating their stability, activity, subcellular localization, and their interactions with other proteins (Hendriks and Vertegaal 2016). As SUMOylation regulates such vast number of cellular functions, it is not surprising that many viruses have acquired mechanisms to modulate this process for their benefit (Everett, Boutell, and Hale 2013).

1.2.2 HAdV-mediated manipulation of the host SUMOylation pathway

Several HAdV proteins have been connected to the modulation of the host SUMO conjugation pathway. Early HAdV protein E1A is not the SUMO substrate itself, but it directly interacts with the SUMO conjugating enzyme Ubc9 leading to the suppression of polySUMOylation (Hateboer et al. 1996; Knipscheer et al. 2007; Yousef et al. 2010). The lack of polySUMOylation could alter the targeting of SUMOylated proteins by SUMO-dependent ubiquitin ligases (STUBLs) for proteasomal degradation (Prudden et al. 2007; Sun, Leverson, and Hunter 2007; Weisshaar et al. 2008; Xie et al. 2007). Moreover, the E1A interaction with Ubc9 affects PML localization as well as the localization of E1A itself (Yousef et al. 2010). Interestingly, E1A reduces SUMOylation of the retinoblastoma tumor suppressor protein (pRB), leading to its inhibition and consequent E2F-dependent transcriptional activation and S-phase induction (Ledl, Schmidt, and Muller 2005).

E4orf3 is another HAdV protein that interacts with Ubc9 even though it is not the target of the host SUMOylation machinery (Sohn and Hearing 2019). E4orf3 acts as an E3 SUMO ligase promoting the SUMOylation of for various cellular proteins involved in the DNA damage response (Sohn and Hearing 2016a, b). Mre11 and Nbs1 are transiently SUMOylated by E4orf3 before their levels decrease due to E1B-55K/E4orf6-dependent proteasomal degradation (Sohn and Hearing

2012). Additionally, E4orf3 increases TFII-I and TIF-1γ SUMO PTM prior to their proteasomal degradation via E4orf3-dependent pathway (Bridges et al. 2016; Forrester et al. 2012; Sohn and Hearing 2016a). Moreover, E4orf3 also acts as an E4 SUMO elongase leading to polySUMOylation indicating the possibility that E4orf3 recruits so far unknown cellular STUbL to selectively target some of its SUMO substrates for proteasomal degradation (Sohn and Hearing 2016a, b).

HAdV protein E1B-55K harbors SUMO conjugation motif and can be SUMOylated on the lysine residue 104 with SUMO isoforms 1, 2 and 3 (Wimmer et al. 2013; Endter et al. 2001). E1B-55K also binds to the SUMO conjugating enzyme Ubc9, but that interaction occurs independently on the E1B-55K SUMO PTM (Wimmer et al. 2013). It has been recently shown that host restriction factor for HAdV infection, transcriptional intermediary factor 1β (KAP1) promotes E1B-55K SUMOylation. KAP1 itself is deSUMOylated during HAdV infection alleviating epigenetic gene silencing (Burck et al. 2016). E1B-55K SUMOylation is crucial for E1B-55K nuclear localization (Kindsmuller et al. 2007). Moreover, E1B-55K SUMO PTM controls diverse functions of the viral protein, leading to the establishment of optimal conditions for efficient HAdV infection. E1B-55K acts as an E3 SUMO ligase and promotes HAdV-mediated inhibition of different host restriction factors (Sohn and Hearing 2016b). E1B-55K SUMOylates p53 and thereby inhibits the p53 activity on an E1B-55K SUMOylation-dependent manner (Muller and Dobner 2008; Pennella et al. 2010). Moreover, E1B-55K SUMOylates Sp100 isoform A promoting the complex formation between Sp100A and p53 within PML-NBs leading to the inhibition of Sp100A promoted p53 activation (Berscheminski et al. 2016). E1B-55K associates with PML isoforms IV and V on the SUMOylation-dependent manner (Wimmer et al. 2010). This interaction is crucial for the repression of p53 activity leading to the oncogenic transformation in conjunction with E1A (Wimmer et al. 2016). SUMO modified E1B-55K variant promotes SUMOylation and proteasomal degradation of the death-associated protein (Daxx), counteracting its antiviral activity (Schreiner et al. 2011). This process is further assisted by the cellular STUBL RNF4. E1B-55K promotes complex formation between RNF4, E1B-55K and Daxx in the insoluble matrix fraction. This leads to the SUMOylation and subsequent proteasomal degradation of Daxx (Muncheberg et al. 2018).

Contrary to the beneficial role of SUMOylation for E1B-55K viral replication promoting functions, host SUMO PTM machinery targets the HAdV core protein pV and inhibits its function.

Inactivation of three conserved SUMO conjugating motifs (SCMs) contained in pV enhances HAdV-mediated proteasomal degradation of inhibitory host factors, promoting the viral DNA synthesis, gene expression and progeny production (Freudenberger et al. 2018).

Taken together, these facts demonstrate the importance of SUMOylation pathway for efficient HAdV infection.

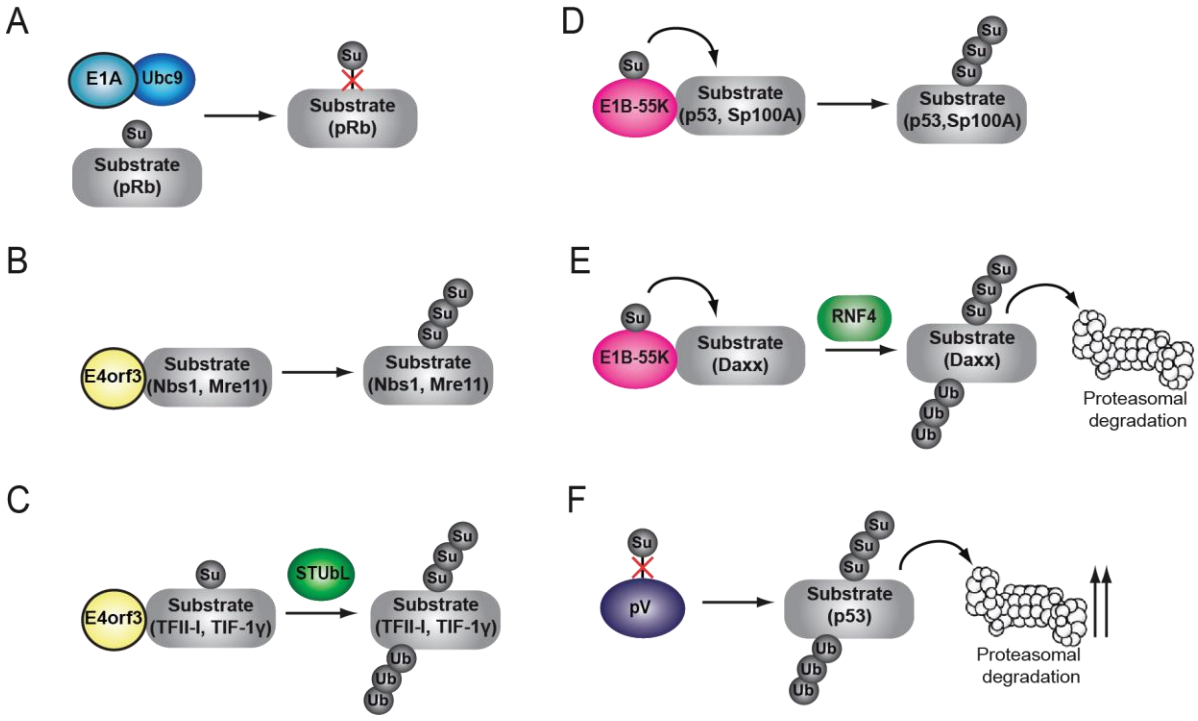

Figure 8: Schematic representation of the HAdV-mediated manipulation of the SUMOylation pathway. **(A)** E1A interacts with Ubc9 inhibiting the pRb SUMOylation. **(B, C)** E4orf3 is not SUMOylated but functions as a SUMO ligase for various substrates. **(D)** E1B-55K is SUMOylated and functions as a SUMO ligase for p53 and Sp100A. **(E)** E1B-55K leads to SUMOylation and subsequent proteasomal degradation of Daxx in cooperation with the STUbL RNF4. **(F)** Reduction of pV SUMOylation promotes proteasomal degradation of antiviral factors such as p53.

1.3 Structure and function of PML nuclear bodies (PML-NBs)

1.3.1 Organization of PML-NBs

PML nuclear bodies (PML-NBs), also referred to as PML oncogenic domains (POD) or nuclear domain-10 (ND10), are nuclear matrix associated multiprotein complexes, located in the inter-chromosomal space that can be detected in almost all human cell lines (Bernardi and Pandolfi 2014; Hodges et al. 1998; Plehn-Dujowich et al. 2000; Stuurman et al. 1992). PML-NBs have an average size of 0.2-1.0 µm and their number varies from 1-30 PML-NBs per nucleus. Their

amount, structure, composition, and function highly depend on cell cycle phase, differentiation stage and stress response (Ascoli and Maul 1991; Bernardi and Pandolfi 2007; Dellaire, Ching, et al. 2006; Dellaire, Eskiw, et al. 2006; Dyck et al. 1994; Koken et al. 1994; Lallemand-Breitenbach and de The 2010; Salomoni and Pandolfi 2002). PML-NBs appear as punctate nuclear structures in immunofluorescence images, however electron microscopy studies revealed that they are ring like structures with the shell composed out of PML and Sp100 proteins. In Addition, SUMO-1 mainly localizes in the PML-NBs shell, while the SUMO-2/3 chains also protrude into their interior (Shen et al. 2006). Nucleic acids are not detectable in the center of the ring that contains micro granular material, such as ribonucleoproteins (Lallemand-Breitenbach and de The 2010). DNA and RNA are located on the periphery of the ring, where PML-NBs connect with chromatin fibers (Boisvert, Hendzel, and Bazett-Jones 2000; Dellaire and Bazett-Jones 2004).

PML-NBs are dynamic structures that can harbor more than 166 proteins ether constitutively or transiently, depending on different conditions, such as stress, interferon expression, transformation, or viral infections (Van Damme et al. 2010). Main constitutive components of PML-NBs are the tumor suppressor PML (Promyelocytic leukemia protein), the transcriptional modulator Sp100 (Speckled protein 100 kDa), the chromatin remodeling factor Daxx (Death domain-associated protein 6), the Bloom Helicase (BLM) and the small ubiquitin-like modifier (SUMO) (Bernardi and Pandolfi 2007; Gorisch et al. 2004; Ishov et al. 1999). Proteins performing different cellular functions transiently localize within PML-NBs. Some of those proteins are the double-strand break repair protein Mre11, the tumor suppressors p53 and Rb, the heterochromatin protein HP1, the acetyltransferase CBP, the ubiquitin specific protease Usp7, and the transcriptional regulator ATRX. Additionally, 120 proteins have been identified to physically interact with PML (Guan and Kao 2015). Consequently, PML-NBs regulate exceptionally large number of cellular functions, such as transcription, senescence, apoptosis, inflammatory responses, metabolism, ageing, protein degradation, DNA damage response, oncogenesis, antibacterial and antiviral defense (Bernardi and Pandolfi 2014; Dellaire and Bazett-Jones 2004; Guan and Kao 2015; Sahin, Lallemand-Breitenbach, and de The 2014).

1.3.2 PML

Promyelocytic leukemia protein (PML) is the main scaffolding component of PML-NBs (Ishov et al. 1999). It was first identified in acute promyelocytic leukemia (APL), where the *pml*

gene was found fused to the retinoic acid receptor alpha gene as a consequence of a t(15;17) chromosomal translocation (Borrow et al. 1992; Chen and Chen 1992; Koken et al. 1994; Pandolfi et al. 1992; Weis et al. 1994). After its discovery, further research connected deregulation of PML with various cancer types, leading to its classification as a tumor suppressor (Salomoni and Pandolfi 2002).

In humans, the *pml* gene is alternatively spliced to express at least seven different PML isoforms (PML I-VII) (Bernardi and Pandolfi 2007; Jensen, Shiels, and Freemont 2001). Interferons and p53 regulate the transcription of the *pml* gene (de Stanchina et al. 2004; Stadler et al. 1995). N-terminal homo-multimerization domain, also termed as RBCC motif or the tripartite motif (TRIM) is present in all seven PML isoforms. RBCC motif consists of RING finger domain (R), two cysteine/histidine-rich B-Box domains (B) and an α-helical coiled-coil domain (CC) (Bernardi and Pandolfi 2007; Jensen, Shiels, and Freemont 2001). This motif is essential for dimerization and localization to the PML-NBs and it can be found in many SUMO or ubiquitin E3 ligases (Kentsis, Gordon, and Borden 2002; Meroni and Diez-Roux 2005). The C-terminal domain of human PML shows strong variability and it is responsible for different functions of PML isoforms (Nisole et al. 2013).

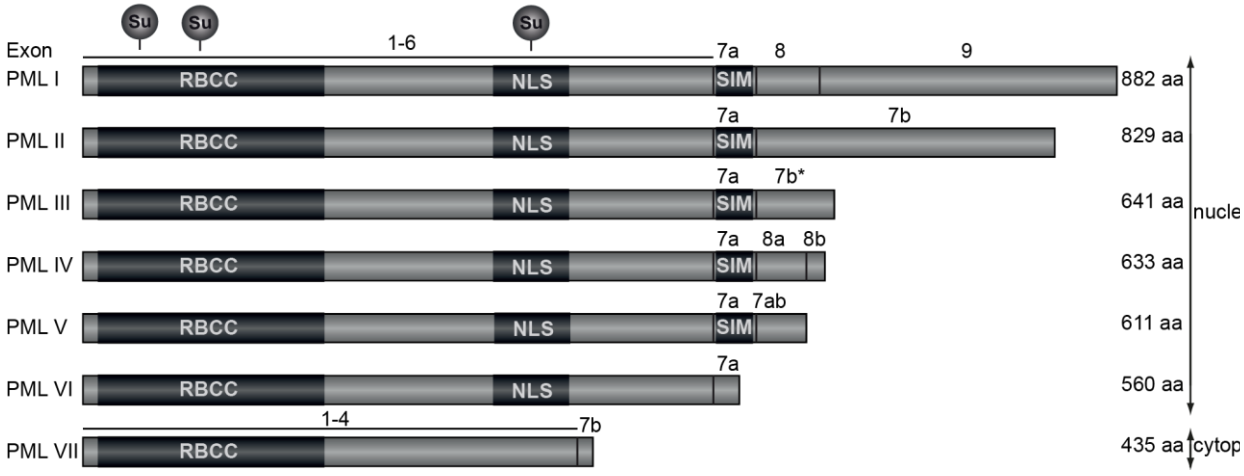

Figure 9: Main human PML isoforms. Domain organization of single PML isoforms is shown together with the exon structure indicated by numbers 1-9. RBCC (RING finger, B-box, coiled-coil domain), NLS (nuclear localization signal), SIM (SUMO interacting motif), Su (SUMO conjugation motif). (Jensen, Shiels, and Freemont 2001).

Posttranslational modifications, such as phosphorylation, acetylation, SUMOylation or ubiquitinylation, regulate PML functions (Ma et al. 2019). Proteasomal degradation of PML can be also triggered by phosphorylation by the Casein Kinase 2 (CK2) (Scaglioni et al. 2006).

Additionally, RING domain-containing ubiquitin E3 ligase RNF4 ubiquitinates poly-SUMOylated PML targeting it for proteasomal degradation (Lallemand-Breitenbach et al. 2008; Percherancier et al. 2009; Tatham et al. 2008). SUMOylation is essential for regulation of PML localization and nuclear bodies formation. SUMO interacting motif (SIM) is present in PML. That enables non-covalent interaction between PML and SUMO-modified proteins as well as formation of a 3D-PML network (Duprez et al. 1999; Lallemand-Breitenbach et al. 2001; Shen et al. 2006; Zhong et al. 2000). The covalent conjugation of SUMO and the non-covalent interaction of SUMO with the SIM of PML and associated proteins are necessary for formation and function of PML-NBs (Ishov et al. 1999; Shen et al. 2006; Zhong et al. 2000). All PML isoforms, except the nuclear PML-VI and the cytoplasmic PML-VII possess the SIM motif. However, PML-VI, as well as PML-III mutants, without their SUMO conjugation motifs (SCM) still form polymeric structures (Lallemand-Breitenbach et al. 2001; Shen et al. 2006). This can be explained by the model proposing formation of spherical PML network via establishment of disulfide bonds between cysteine residues of PML proteins assisted by the oxidation of PML by reactive oxygen species (ROS) (Sahin et al. 2014). Together with SUMO-SIM interactions, which are essential for recruitment of other SUMOylated proteins, acetylation and phosphorylation of PML further expand diversity of protein-protein interactions at the PML-NBs (Cheng and Kao 2012; Schmitz and Grishina 2012). Interestingly, inhibition of ubiquitinylation leads to increased SUMOylation of numerus cellular proteins and their subsequent association with PML-NBs (Sha et al. 2019).

1.3.3 Sp100

Sp100 (Speckled protein 100 kDa) was originally discovered as an autoantigen in primary biliary cirhosis patients (Szostecki et al. 1990; Szostecki et al. 1987; Szostecki et al. 1992). Further research defined Sp100 as transcriptional modulator, with both transcription-activating and -repressive capabilities, that can be induced by interferon (Grotzinger et al. 1996; Guldner et al. 1999; Lehming et al. 1998).

Alternative splicing of the *sp100* gene results in the expression of at least four different Sp100 isoforms termed Sp100A, Sp100B, Sp100C and Sp100HMG (Grotzinger et al. 1996; Guldner et al. 1999; Szostecki et al. 1990; Szostecki et al. 1992). All Sp100 isoforms have an N-terminal homogenously stained region (HSR) domain in charged for dimerization and localization to the PML-NBs (Sternsdorf et al. 1999). Sp100 B, C and HMG contain an additional SAND

(Sp100, AIRE-1, NucP41/45, and DEAF-1) domain, with high affinity towards DNA with unmethylated CpGs. Domains associated with chromatin such as Bromo-, PHD (plant homeo-domain) and HMG (High Mobility Group) domain are present only in Sp100 isoforms -C and -HMG (Baker, Allis, and Wang 2008; Bottomley et al. 2001; Burnett, Christensen, and Tattersall 2001; Isaac, Wilcox, and Taylor 2006; Lehming et al. 1998). All Sp100 isoforms contain a motif for interaction with the members of HP1 family which indicate possible involvement of Sp100 in regulation of chromatin architecture (Seeler et al. 1998). Furthermore, all Sp100 isoforms localize to the nucleus as they possess nucleus localization signal (NLS) (Sternsdorf et al. 1999). Additional common features or all Sp100 isoforms are the SIM domain and SCM at Lysine 297 (Sternsdorf et al. 1999; Sternsdorf, Jensen, and Will 1997).

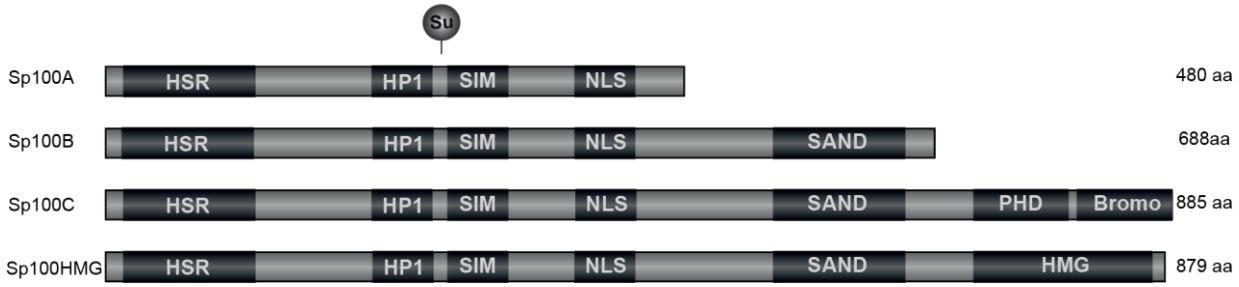

Figure 10: Main human Sp100 isoforms. Schematic representation of major human alternatively spliced Sp100 isoforms and their domain organization. HSR (Homogenous staining region), HP1 (Heterochromatin protein 1 interaction region), Su (SUMO conjugation motif), SIM (SUMO interacting motif), NLS (Nuclear localization signal), SAND (Sp100, AIRE-1, NucP41/45, DEAF1-domain), Bromo (Bromo domain), PHD (Plant Homeodomain), HMG (High Mobility Group domain) (Baker, Allis, and Wang 2008; Bottomley et al. 2001; Burnett, Christensen, and Tattersall 2001; Isaac, Wilcox, and Taylor 2006; Lehming et al. 1998; Seeler et al. 1998; Sternsdorf et al. 1999; Sternsdorf, Jensen, and Will 1997).

Even though the Sp100 represents the constitutive factor of PML-NBs, Sp100 SUMOylation is not required for nuclear body localization (Sternsdorf et al. 1999). SUMOylation of Sp100 most presumably regulates Sp100 interaction with HP1 and other non-histone chromosomal proteins (Seeler et al. 2001; Seeler et al. 1998). Sp100 isoforms perform different roles in transcriptional regulation, as Sp100A promotes chromatin decondensation while Sp100B -C and -HMG condense chromatin via their SAND domain (Newhart et al. 2013). The roles of these isoforms during HAdV infection also differ. Sp100A is kept in PML tracks and promotes HAdV gene expression, while Sp100B, -C and -HMG get translocated into viral replication centers as infection inhibiting factors (Berscheminski et al. 2014). Intriguingly, it has been shown that HAdV protein E2A can target and relocalize Sp100 independently on other viral factors (Komatsu, Nagata, and Wodrich 2016).

1.3.4 HAdV-mediated modulation of PML-NBs

One of the main functions of PML-NBs is the regulation of intracellular antiviral response (Everett and Chelbi-Alix 2007; Tavalai and Stamminger 2008). Genes for PML and PML-NBs associated factors are interferon-stimulated and can impair efficient virus replication (Chelbi-Alix et al. 1998; Regad and Chelbi-Alix 2001). Consequently, various DNA and RNA human viruses have developed mechanisms to counteract intrinsic defense of PML-NBs (Everett 2001; Everett and Chelbi-Alix 2007; Tavalai and Stamminger 2008). Nevertheless, many DNA viruses position their genomes next to PML-NBs where their replication and transcription take place (Doucas et al. 1996; Everett 2001; Ishov and Maul 1996; Jul-Larsen et al. 2004; Maul 1998; Maul, Ishov, and Everett 1996; Sourvinos and Everett 2002). This emphasizes an existence of more complex mechanism used by viruses to simultaneously counteract antiviral function of PML-NBs and exploit components of PML-NBs that promote efficient infection.

In case of HAdV, PML-NBs are reorganized in into track-like structures, through direct interaction of HAdV protein E4orf3 with PML-II (Carvalho et al. 1995; Doucas et al. 1996; Vink et al. 2015). In addition, E4orf3 also promotes HAdV-mediated modulation of cellular factors transiently present in PML-NBs such as tumor suppressor p53, the Mre11-Rad50-NBS1 (MRN) complex involved in DNA repair and the transcription factors TIF-1α, TIF-1γ and TFII-I (Liu et al. 2005; Araujo et al. 2005; Konig, Roth, and Dobbelstein 1999; Yondola and Hearing 2007; Vink et al. 2012; Sohn, Bridges, and Hearing 2015). The cellular transcriptional repressor Daxx is displaced from PML-NBs by adenoviral core protein pVI to promote activation of the E1A promoter (Schreiner et al. 2010). Moreover, E1A-13S trans activating capacity towards adenoviral genes is enhanced by the of E1A-13S interaction with PML-II (Berscheminski et al. 2013). Additionally, Sp100 isoform A exhibits transcription promoting capabilities and it is therefore, kept in PML tracks. Sp100A recruits histone acetyltransferases (HATs), creating the optimal microenvironment for activation of viral promoters (Berscheminski et al. 2014). On the other hand, numerous PML-NB components, and components of with inhibitory effect on viral replication such as p53, Mre11, ATRX, BLM are degraded by HAdV E3 ubiquitin ligase complex assembled by HAdV proteins E1B-55K and E4orf6 (Cardoso et al. 2008; Orazio et al. 2011; Schreiner, Burck, et al. 2013; Schreiner, Wimmer, and Dobner 2012). Additionally, HAdV E3 ubiquitin ligase complex also targets DNA-ligase IV and integrin α3 for proteasomal degradation (Baker et al. 2007b; Dallaire et al. 2009). Another example is previously mentioned cellular transcriptional

repressor Daxx, present in PML-NBs, that is proteasomally degraded by the early adenoviral protein E1B-55K that associates with PML-NBs during infection (Doucas et al. 1996; Leppard and Everett 1999). E1B-55K interacts with Daxx and recruits it into an E1B-55K/RNF4 complex, thereby leading to proteasomal degradation of the host factor (Muncheberg et al. 2018). The components of MRN complex are degraded in cytoplasmic aggresomes after relocalization from PML tracks (Araujo et al. 2005; Evans and Hearing 2005; Liu et al. 2005; Stracker, Carson, and Weitzman 2002), while E4orf3 mediates proteasomal degradation of TIF-1γ (Forrester et al. 2012). HAdV also counteracts antiviral factors such as Sp100 isoforms B, -C and -HMG by translocation into HAdV replication centers (Berscheminski et al. 2014). To counteract PML-NBs antiviral activity and prevent their reformation in late stages of the infection, HAdV protein pIX sequesters PML and PML associated proteins into clear amorphous inclusions (Rosa-Calatrava et al. 2003). These examples clearly illustrate dual role of PML-NBs in HAdV infection.

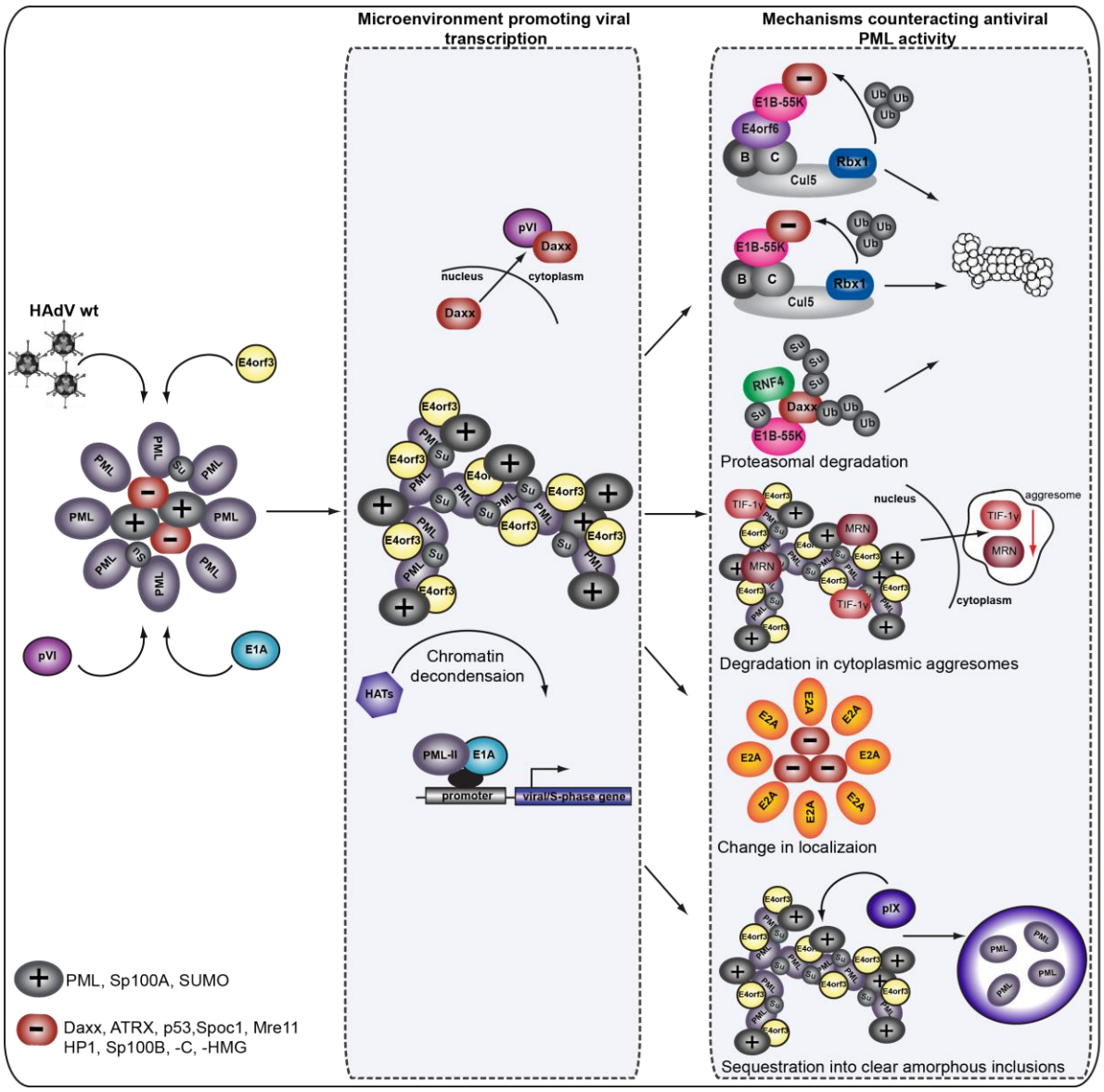

Figure 11: Schematic representation of the HAdV-mediated modulation of PML-NBs. Early adenoviral protein E4orf3 disrupts PML-NBs into tracks. Factors positive for HAdV infection remain in PML tracks. Sp100A, localized at the PML tracks, recruits HATs, creating a favorable microenvironment for activation of HAdV promoters. Adenoviral core protein pVI displaces Daxx from PML-NBs to promote activation of the E1A promoter. E1A interaction with PML-II promotes its transactivating activity towards HAdV genes. Negative factors are degraded by E3 ubiquitin ligase complex assembled by E1B-55K and E4orf6. E1B-55K can degrade and inhibit negative factors independently on E4orf6. E1B-55K promotes complex formation between RNF4, E1B-55K and Daxx leading to the SUMOylation and subsequent proteasomal degradation of Daxx. E4orf3 immobilizes components of the MRN complex and transcription factor TIF-1γ in PML tracks. They are degraded in cytoplasmic aggresomes after the release from the PML tracks. Some negative factors, such as Sp100 isoforms B, -C and -HMG, are counteracted by relocalization to HAdV RCs. pIX sequesters PML-NBs components into clear amorphous inclusions.

1.4 The role of tumor suppressor protein p53 during HAdV infection

1.4.1 Structure and function of the tumor suppressor protein p53

p53 was first identified in studies researching tumor induction by tumor viruses as cellular protein which co-immunoprecipitated with simian vacuolating virus 40 (SV40) large T-antigen protein (Kress et al. 1979; Lane and Crawford 1979; Linzer and Levine 1979; Smith, Smith, and Paucha 1979). WTp53 is a tumor suppressor protein, termed as the guardian of the genome, as it guards against tumor and virus replication. On the other hand, the mutated p53 version represents a potent oncogene (Brosh and Rotter 2009; Lane 1992).

The tumor suppressor protein p53 is a 393 aa protein with the molecular weight of 53 kDa (Kress et al. 1979; Lane and Crawford 1979; Linzer and Levine 1979; Smith, Smith, and Paucha 1979). It is composed out of five main regions, the transactivation domain (TAD), the proline-rich domain (P-rich), the DNA binding domain (DBD), the tetramerization domain (TD) and the regulatory C-terminal domain (REG) (Gu and Zhu 2012; Natan et al. 2011). TAD domain is in charged for binding to negative regulators, transcriptional coactivators and components of the transcription machinery (Di Lello et al. 2006; Lill et al. 1997; Teufel, Bycroft, and Fersht 2009; Thut et al. 1995). The proline rich region serves as a rigid linker that separated TAD from the DBD (Wells et al. 2008). DBD domain is thermodynamically and kinetically unstable and most of the cancer related mutations are located in this region (Butler and Loh 2006; Friedler et al. 2003; Petitjean et al. 2007). The p53 TD domain allows the oligomerization of this protein, and it is involved in DNA binding, protein–protein interactions, post-translational modifications, and p53 degradation (Chene 2001). TD domain also harbors nuclear export signal NES (Stommel et al. 1999). Two nuclear localization domains (NLS) are in the highly post translationally modified REG domain. This domain controls p53 subcellular localization (Gu et al. 2001; Nie, Sasaki, and Maki 2007), stability (Li et al. 2002; Nakamura, Roth, and Mukhopadhyay 2000), cofactor recruitment (An, Kim, and Roeder 2004; Chuikov et al. 2004) and DNA binding with emphasis on site specific DNA binding by induction of structural changes in DBD domain (Anderson et al. 1997; Laptenko et al. 2015; McKinney et al. 2004).

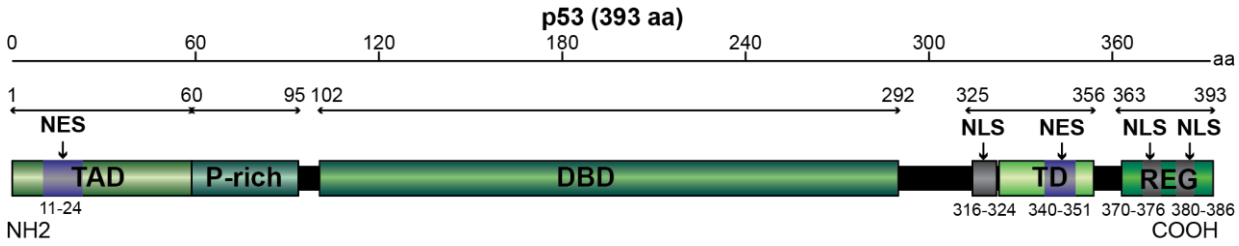

Figure 12: Schematic representation of p53 structure. Main functional p53 domains are represented in green; TAD (transactivation domain), P-rich (proline-rich domain), DBD (DNA binding domain), TD (tetramerization domain) and REG (regulatory C-terminal domain). Nuclear export signals (NES) are represented in blue and nucleus localization signals (NLS) in grey (Wesierska-Gadek 2018).

p53 activation is mainly triggered as a response to various stress signals such as DNA damage, oncogene activation, telomere erosion, nutrient deprivation, ribosomal stress and hypoxia. p53 activation ultimately leads to growth inhibition by induction of cell cycle arrest or apoptosis (Fischer 2017; Horn and Vousden 2007; Vousden and Prives 2009). Besides its major role in tumor suppression, p53 is involved in different physiological processes such as development, ageing and cell differentiation (Brady and Attardi 2010). Moreover, p53 plays an important role in antiviral innate immunity by both inducing apoptosis and enforcing the type I interferon response (Rivas, Aaronson, and Munoz-Fontela 2010). p53 primarily functions as a transcriptional factor that in tetrameric state binds to numerous target genes (Kitayner et al. 2006; McLure and Lee 1998; Riley et al. 2008). Interestingly, p53 can also bind to target genes under basal conditions, leading to their activation or inhibition (Allen et al. 2014; Sullivan et al. 2018). Target genes of p53 are involved in diverse cellular processes such as cell cycle arrest, apoptosis, senescence, autophagy, DNA repair, cellular metabolism and exosome secretion (Vousden and Prives 2009; Yu, Harris, and Levine 2006).

1.4.2 Regulation of p53 activity

The regulation of p53 activity is based on its localization, oligomerization and concentration (Rajagopalan, Huang, and Fersht 2011; Liang and Clarke 2001). In normal cells, nucleocytoplasmic translocation of p53 is tightly regulated during the cell cycle (Shaulsky, Ben-Ze'ev, and Rotter 1990). In transformed cells or fast growing normal cells, p53 is mainly located in the nucleus (Dippold et al. 1981; Rotter, Abutbul, and Ben-Ze'ev 1983), however abnormal cytoplasmic sequestration of p53 is associated with a subset of human cancers (Bosari et al. 1995; Moll et al. 1995; Moll, Riou, and Levine 1992). These reports suggest that the disruption of p53

function leading to tumorigenesis might be associated with defective p53 localization. The fact that NLS can be found on the p53 surface when the protein is in a monomeric shape and under surface when p53 is tetrameric, suggest possible regulation of p53 cellular localization by changes in its quaternary structure. Even though p53 enters the nucleus in oligomeric state, it has been suggested that the p53 monomeric state facilitates nuclear import (Liang and Clarke 2001). Oligomerization is important for p53 activation. Tetramerization of p53 promotes binding to p53 responsive elements leading to transactivation of p53-dependent genes (Stenger et al. 1994; Weinberg, Veprintsev, and Fersht 2004).

The main regulator of p53 function is the ubiquitin ligase mouse double minute 2 (Mdm2) protein, that physically associates with p53 (Cahilly-Snyder et al. 1987; Momand et al. 1992). The two molecules are linked to each other via autoregulatory negative feedback loop that maintains low cellular p53 levels in the absence of stress (Barak et al. 1993; Chen, Marechal, and Levine 1993; Picksley and Lane 1993; Wu and Levine 1997). p53 stimulates the expression of Mdm2, in turn Mdm2 inhibits p53 activity by stimulation of proteasomal p53 degradation in cytosol or nucleoplasm, promoting the p53 nuclear export or by inhibition of p53 transcriptional activity in a complex with MdmX (Haupt et al. 1997; Joseph, Zaika, and Moll 2003; Maki 1999; Shi and Gu 2012).

The role of PTMs is crucial for regulation of p53 levels and activity. p53 PTMs regulate the p53 function by influencing the strength of DNA binding, target gene selection and p53 stability. Besides ubiquitinylation that maintains low levels of p53 in non-stress conditions, the cellular tumor suppressor can also be acetylated, phosphorylated, methylated and SUMOylated (Kruse and Gu 2009). Repression of p53 activity by Mdm2-mediated ubiquitinylation is relieved in stress conditions. PTMs such as phosphorylation and acetylation prevent p53 ubiquitinylation by inhibiting p53 binding to Mdm2 or by blocking the site of ubiquitinylation (Hafner et al. 2019).

Phosphorylation of p53 is mediated by wide range of kinases, such as ATM/ATR/DNA-PK, and Chk1/Chk2 (Appella and Anderson 2001; Shieh et al. 2000). Phosphorylation of p53 occurs in response to various stress stimuli and modulates p53 interactions with other proteins and DNA. This p53 PTM affects sequence-specific DNA binding at promoters, acetylation of p53, ubiquitinylation of p53 and transcription stimulation, finally leading to p53 activation (Hafner et al. 2019; Kruse and Gu 2009).

Acetylation of p53 is elevated in stress conditions and it promotes efficient recruitment of cofactors, facilitates chromatin remodeling and activation of p53 target genes *in vivo* (Dornan et al. 2003). Most of p53 acetylation sites are located at the C-terminal REG domain (Gu and Roeder 1997). Acetylation of p53 is mediated by various acetyltransferases. One example is histone acetyltransferase CBP/p300, found mutated in various cancers (Goodman and Smolik 2000). Acetyltransferase PCAF, that interacts with CBP/p300, acetylates p53 on the different residue from that acetylated by p300 and leads to the increase of p53 DNA binding ability (Liu et al. 1999). Another p53 acetyltransferase, Tip60 activates p53 and it is implicated in both DNA repair and apoptosis (Tang et al. 2006). Additionally, p53 acetylation upon oncogene expression is also regulated by PML (Pearson et al. 2000). p53 acetylation is a reversible process. Deacetylation is mediated by histone deacetylase (HDAC) complexes containing HDAC1 or Sir2α/Sirt1 (Luo et al. 2001; Luo et al. 2000). This step is vital for restoring steady-state levels of p53 targets after completion of DNA damage repair and return of cells in normal homeostasis (Kruse and Gu 2009).

Methylation occurs at various lysine residues within p53 and has an ability to activate or repress p53 activity depending on the residue and the extent of methylation (Chuikov et al. 2004; Huang et al. 2010; Huang et al. 2006; Huang et al. 2007; Shi et al. 2007).

p53 is also a substrate for cellular SUMOylation machinery. It has been reported that SUMO-2/3 conjugation to proteins may have different consequences than SUMO-1 conjugation (Saitoh and Hinchey 2000; Wilkinson and Henley 2010). p53 can be SUMOylated both with SUMO-2/3 and SUMO-1, at the same lysine residue, K386 (Gostissa et al. 1999; Stindt et al. 2011). SUMO conjugating enzyme, Ubc9 directly interacts with p53. This interaction is promoted by p53 phosphorylation mediated by cell cycle checkpoint kinase 2 (Chk2), in response to DNA damage (Lin, Ohshima, and Shimotohno 2004). SUMO transfer from Ubc9 to p53 is facilitated by various cellular E3 ligases, such as Topors, the PIAS proteins and TRIM proteins (Bischof et al. 2006; Chu and Yang 2011; Weger, Hammer, and Heilbronn 2005). Various publications have shown that SUMO-1 modification of p53 results in increased, decreased or unchanged transcriptional activity (Gostissa et al. 1999; Kwek et al. 2001; Rodriguez et al. 1999; Schmidt and Muller 2002). Both activating and inhibiting properties of p53 SUMOylation, are also shown in case of p53 modification with SUMO-2/3 (Chang et al. 2010; Li et al. 2006; Stindt et al. 2011). This contradictory data illustrates the complexity of p53 regulation that so far has not been fully understood.

Cofactors recruitment further extends the complexity of p53 regulation, by contributing to activation of p53-dependent target genes. The cofactors act by modulating the strength of p53 binding to target promoters (Hafner et al. 2019). For example, the acetyltransferase p300 is needed for p53-dependent activation of p21 (Barlev et al. 2001). Moreover, p300 and p53 together recruit methyltransferase SETD1A, leading to histone modifications facilitating p53 functions (Tang et al. 2013). Additionally, E2F target proteins such as Apoptosis-stimulating of p53 protein 1 and 2 (ASPP1 and ASPP2) interact with p53 and promote p53-mediated activation of pro-apoptotic genes (Bergamaschi et al. 2004; Fogal et al. 2005; Samuels-Lev et al. 2001).

1.4.3 HAdV-mediated modulation of p53 activity

p53 plays an essential role in cell cycle arrest and DNA damage response as well as in antiviral innate immunity (Brosh and Rotter 2009; Lane 1992; Rivas, Aaronson, and Munoz-Fontela 2010). Different viruses, including HAdV, have developed various mechanisms to counteract cellular antiviral and DNA damage response and p53 activity (Speir et al. 1994; Casavant et al. 2006; Hermannstädter et al. 2009; Izumi et al. 2010; Liu and Marmorstein 2006; Maruzuru et al. 2013; Zhu et al. 1991; Ip and Dobner 2020).

The early HAdV protein E1A creates optimal conditions for productive virus infection by leading cells from G1 to S-phase. E1A, specifically E1A-12S, interacts with pRb (retinoblastoma protein) related proteins that suppress the activity of E2F family transcription factors through binding to their activation domains. E1A binding to pRb associated proteins enables their dissociation from E2F leading to the activation of E2F responsive genes, such as cyclin-dependent kinase 2 (CDK2), cyclin A/E or c-myc, required for the S-phase entry (Bagchi, Raychaudhuri, and Nevins 1990; Bandara and La Thangue 1991; Blais and Dynlacht 2004; Ghosh and Harter 2003; Ip and Dobner 2020). The removal of E2F from Rb causes the Mdm2 inhibition leading to p53 accumulation (Nakajima et al. 1998). It has also been reported that E1A triggers cell cycle arrest and apoptosis through p53 stabilization after E1A-mediated binding to acetyltransferase p300/CBP, causing the E2F stimulation (Ait-Si-Ali et al. 1998; Ip and Dobner 2020). E1A expression alone is also sufficient to induce p53 independent apoptosis through the interaction of the viral protein with p300 and Rb (Putzer et al. 2000). Additionally, E1A interacts with proteasome subunit 19S leading to inhibition of proteasome-dependent p53 degradation (Lowe

and Ruley 1993; Zhang et al. 2004). E1A-mediated p53 stabilization would lead the cells to apoptosis without the activity of adenoviral proteins that inhibit p53 through different mechanisms.

E1B-55K uses several mechanisms to inhibit p53 function. It inhibits p53-dependent transcription by direct interaction with the tumor suppressor, and subsequent tethering of the E1B-55K C-terminal repression domain to p53 target genes (Teodoro and Branton 1997; Yew and Berk 1992). Moreover, E1B-55K interacts with p53 and PCAF, modifies the interaction between the two cellular proteins and prevents PCAF-mediated p53 acetylation necessary for high DNA binding activity (Liu et al. 2000). To counteract host antiviral response, E1B-55K interacts with PML-IV and PML-V, causing p53 SUMOylation and inhibition of p53 transcriptional activity (Pennella et al. 2010; Wimmer et al. 2016). The E1B-55K nuclear export signal and the SUMO conjugation motif are required for E1B-55K-mediated nuclear-cytoplasmic relocalization of p53 and the complete inhibition of p53 activity (Endter et al. 2005; Endter et al. 2001). Furthermore, E1B-55K specifically interacts with the Sp100A isoform on a SUMOylation-dependent manner. This binding is essential for regulation of adenovirus-mediated transformation. Sp100A induced stimulation of p53 transcriptional activity is effectively eliminated when E1B-55K/Sp100A complex recruits p53. Sp100A exhibits tumor suppressive activity by stabilizing p53 transactivation and inhibiting E1A/E1B-55K-mediated transformation. To counteract this suppressive activity, E1B-55K SUMOylates Sp100A and sequesters it into the insoluble matrix of the nucleus or into cytoplasmic inclusions (Berscheminski et al. 2016).

E1B-55K associates with the HAdV protein E4orf6 to assemble the E3 ubiquitin ligase complex that amongst other antiviral factors also degrades p53 (Blanchette et al. 2004; Querido et al. 2001; Schreiner, Wimmer, and Dobner 2012). Moreover, HAdV E3 ubiquitin ligase complex also degrades acetyltransferase Tip60 to prevent transcriptional repression of the viral early protein E1A (Gupta et al. 2013). As Tip60 acetylates and thereby activates p53, the HAdV-mediated degradation of Tip60 might contribute to the inactivation of p53 (Tang et al. 2006). Furthermore, E4orf6 can counteract the p53 activity independently on other viral factors. E4orf6 directly interacts with p53 and prevents p53 binding to TBP-associated factor 3 (TAFII3), leading to the inhibition of p53-dependent transcriptional activation (Dobner et al. 1996). E4orf6 also inactivates p73, the protein from p53 family that can partially substitute the p53 functions (Higashino, Pipas, and Shenk 1998; Steegenga et al. 1999).

HAdV protein E4orf3 also modulates p53-mediated transcriptional activity. E4orf3 recruits the histone methyltransferase SUV38H1 and SUVH2 to p53 responsive elements causing H3K9me3 heterochromatin formation that prevents p53/DNA binding (Soria et al. 2010).

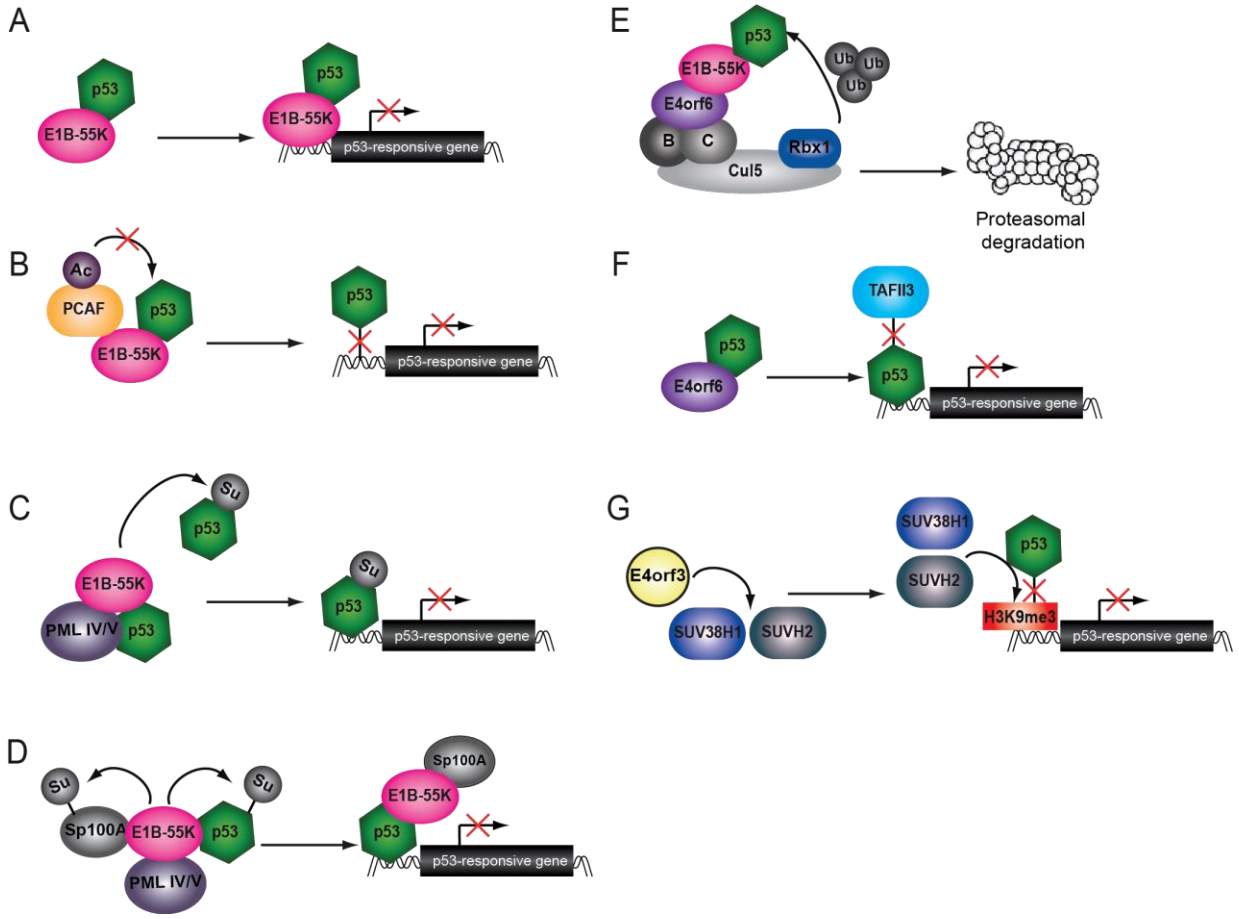

Figure 13: Schematic representation of HAdV-mediated p53 inhibition. (A) E1B-55K directly interacts with p53 and tethers its C-terminal domain to p53 target genes. **(B)** E1B-55K prevents PCAF-mediated p53 acetylation and reduces p53 DNA binding affinity. **(C)** E1B-55K SUMOylates and inhibits p53 through PMLIV/V interaction. **(D)** E1B-55K interacts with Sp100A and p53, SUMOylates them and promotes generation of p53/Sp100A complex leading to the inhibition of p53 transcriptional activity. **(E)** E1B-55K and E4orf6 generate E3- ubiquitin ligase complex that ubiquitinylates p53 leading to its proteasomal degradation. **(F)** E4orf6 interacts with p53 and disrupts it interaction with TAFII3 leading to inhibition of p53 transcriptional activity**. (G)** E4orf3 prevents p53/DNA binding by recruiting the histone methyltransferases SUV38H1 and SUVH2 to p53 responsive elements leading to H3K9me3 heterochromatin formation.

2 Material

2.1 Bacteria and cells

2.1.1 Bacterial strains

Table 1: Used bacterial strains.

Strain	Genotype	Reference
Escherichia coli DH5α	*sup*E44, Δ*lac*U169, (φ80d *lacZ*Δ *M15*), *hsd*R17, *rec*A1, *end*A1, *gyr*A96, *thi*-1, *rel*A1.	(Hanahan 1983)
XL2blue	recA1, endA1, gyrA96, thi-1, hsdR17, supE44, relA1, lac, [F'proAB, lacI q ΔZM15, Tn10 (Tetr), Amy, Camr]	Agilent Technologies

2.1.2 Mammalian cell lines

Table 2: Used mammalian cells.

Database no.	Cell line	Genotype	Reference
5	A549	Human lung carcinoma cell line expressing wild type p53	(Giard et al. 1973)
15	H1299	Human lung carcinoma cell line, derived from metastatic lymph node, p53 negative	(Mitsudomi et al. 1992)
16	HEK293	HAdV5-transformed, human embryonic kidney cell line; the E1 region is integrated into the genome and the adenoviral E1A and E1B gene products are stably expressed. Helper cell line.	(Graham et al. 1977)
9	2E2	293 cells stably expressing the Epstein-Barr virus nuclear antigen 1 (EBNA1), the tetracycline-dependent transcriptional silencer and the reverse Tet transactivator (rtTA2); all Ad5 early region 2 (E2) genes, and the early region 4 (E4) open reading frame 6 (ORF6) are stably expressed upon tetracycline induction.	(Catalucci et al. 2005)
1	HepaRG	Pseudo-primary human hepatoma cell line derived from HCV infected tissue	(Marion, Hantz, and Durantel 2010)

51	HepaRG shPML	HepaRG cell line with shRNA against six PML isoforms; shRNA 5'-AGATGCAGCTGTATCCAAG-3'	(Everett et al. 2006)
12	HepaRG-SUMO-2-His/HA	HepaRG cell line, stably expressing 6xHis/HA-SUMO-2	(Sloan et al. 2015)
20	HepaRG-His/HA	HepaRG cell line, stably expressing 6xHis/HA	(Sloan et al. 2015)
7	HeLa-Su2-His	Human cervix carcinoma cell line with HPV-18 genome integration, stably expressing 6xHis-SUMO-2	(Vertegaal et al. 2004)

2.1.3 Viruses

Table 3: Used viral strains.

Database no.	Adenovirus	Characteristics	Reference
1	HAdV wt	Wt HAdV-C5, H5*pg*4100, containing an 1863 bp deletion (nt 28602-30465) in the E3 region.	(Kindsmuller et al. 2007)
13	HAdV E2A SCM	HAdV E2A/DBP mutant containing lysine to arginine change at aa positions 94, 132 and 202.	This work (Stubbe et al. 2020)
2	HAdV E4orf6-	H5*pm*4154, E4orf6 null mutant, containing a stop codon in the E4orf6 region (AS 66)	(Blanchette et al. 2004)
3	HAdV E1B-55K-	H5*pm*4149, E1B-55K null mutant, containing four stop codons in the E1B-55K region (AS position 3, 8, 86 and 88)	(Kindsmuller et al. 2007)
30	HAdV E1B-55K NES	H5*pm*4101, Ad5 E1B-55K mutant containing three aa exchanges (L83/87/91A) within the NES of the E1B-55K sequence	(Kindsmuller et al. 2007)
31	HAdV E1B-55K SCM	H5*pm*4102, Ad5 E1B-55K mutant containing one aa exchange (K104R) within the SCM of the E1B-55K sequence	(Kindsmuller et al. 2007)
16	HAdV ΔE4orf3	H5*pm*4150, Ad5 E4orf3 mutant with an additional thymidine at position nt 34592, causing a frame shift mutation after codon 36	(Forrester et al. 2012)

2.2 Nucleic acids

2.2.1 Oligonucleotides

The following oligonucleotides were used for sequencing, PCR and site directed mutagenesis. All nucleotides were ordered from Metabion (Munich) and numbered according to the internal group *Filemaker Pro* database.

Table 4: Used oligonucleotides (from Metabion).

Database no.	Name	Sequence	Purpose
197	GAPDH-fwd	5'-CATCCTGGGCTACACTGA-3'	RT qPCR
198	GAPDH-rev	5'-TTGACAAAGTGGTCGTTG-3'	RT qPCR
181	E1A-fwd	5'-GTG CCCCATTAACCAGTTG-3'	RT qPCR
182	E1A-rev	5'-GGCGTTTACAGCTCAAGTCC-3'	RT qPCR
183	E2A-fwd	5'-GAAATTACGGTGATGAACCCG-3'	RT qPCR
184	E2A-rev	5'-CAGCCTCCATGCCCTTCTCC-3'	RT qPCR
189	Hexon-fwd	5'-CGCTGGACATGACTTTTGAG-3'	RT qPCR
190	Hexon-rev	5'-GAACGGTGTGCGCAGGTA-3'	RT qPCR
895	TUBB fwd	5'-TATCAGCAGTACCAGGATGC-3'	RT qPCR
896	TUBB rev	5'-TGAGAAGCCTGAGGTGATG-3'	RT qPCR
897	RPL30 fwd	5'-CAAGGCAAAGCGAAATTGGT-3'	RT qPCR
898	RPL30 rev	5'-GCCCGTTCAGTCTCTTCGATT-3'	RT qPCR
899	SAT2 fwd	5'-ATCGAATGGAAATGAAAGGAGTCA-3'	RT qPCR
900	SAT2 rev	5'-GACCATTGGATGATTGCAGTCA-3'	RT qPCR
901	HAdV P1 fwd	5'-CTTGCATGGCGTGTTAAATG-3'	RT qPCR

902	HAdV P1 rev	5'-GCCTCCATGAGGTCAGATGT-3'	RT qPCR
903	HAdV P3 fwd	5'-GGTGCACTTGGGAAATTTGT-3'	RT qPCR
904	HAdV P3 rev	5'-TATGGACGAATGCATGGAAA-3'	RT qPCR
905	HAdV P7 fwd	5'-TGACGAGGACGATGAGTACG-3'	RT qPCR
906	HAdV P7 rev	5'-GTTGCGTCTTGCATCATCTG-3'	RT qPCR
907	HAdV P11 fwd	5'-CTGTGGGTGATAACCGTGTG-3'	RT qPCR
908	HAdV P11 rev	5'-TAAAAGTAGGGCCCCTGTCC-3'	RT qPCR
909	HAdV P16 fwd	5'-AACGCCATAGTTGCTTGCTT-3'	RT qPCR
910	HAdV P16 rev	5'-ACGCCGTGATGGTAGAGAAG-3'	RT qPCR
686	pCMX-3b Flag out from E2A-fwd	5'-GCCAGTCGGGAAGAGGAGC-3'	Mutagenesis
688	pCMX-3b Flag out-fwd	5'-GGATCCGAATTCCTCGAGATC-3'	Mutagenesis
687	pCMX-3b Flag out-rev	5'-CATGGTACCTAGAAGCTTGG-3'	Mutagenesis
914	pCMX-fwd	5'-TAATACGACTCACTATAGGG-3'	Sequencing
915	pCMX-rev	5'-CCAATTATGTCACACCA-3'	Sequencing
911	Noah seq fwd 22332 bp	5'-CAGTGCGCAGATTAGGAGC-3'	Sequencing
912	Noah seq fwd 22903 bp	5'-GACCGTGCCCGGTCTGGG-3'	Sequencing
913	Noah seq fwd 23481 bp	5'-CGTGGTACTTGTCCATCAGC-3'	Sequencing
889	E2AK94R-fwd	5'-GAAGCGCCCTTCTCCCAGGCCCGAGCGCCCG-3'	Mutagenesis
890	E2AK94R-rev	5'-CGGGCGCTCGGGCCTGGGAGAAGGGCGCTTC-3'	Mutagenesis
891	E2AK132R-fwd	5'-GCTAATCAAGCATGGCAGAGGAGGTAAGCGCACAG-3'	Mutagenesis
892	E2AK132R-rev	5'-CTGTGCGCTTACCTCCTCTGCCATGCTTGATTAGC-3'	Mutagenesis

893	E2AK202R-fwd	5'-CCACCGGTGCTAATCAGGCATGGCAAAGGAGGTAAGCGCACAG-3'	Mutagenesis
894	E2AK202R-rev	5'-CTGTGCGCTTACCTCCTTTGCCATGCCTGATTAGCACCGGTGG-3'	Mutagenesis

2.2.2 Vectors

Table 5: Vector plasmids used for sub-cloning or as transfection controls.

Database no.	Name	Characteristics	Reference
12	pcDNA3	Expression vector for mammalian cells, CMV promoter	Invitrogen
18	pcDNA3-HA	Empty pcDNA3 vector with CMV promoter and N-terminal HA tag	Group database
21	pEYFP-C1	Empty pEYFP vector	Invitrogen
32	pCMX3b-Flag	Expression vector for mammalian cells, CMV promoter, N-terminal flag-tag	Group database
27	pCMX3b	Expression vector for mammalian cells, CMV promoter	This work
13	pEGFP-C1	Green Fluorescent Protein mut1 expressing vector for mammalian cells, CMV promoter, C-terminal protein fusion possible (GeneBank Accession #U55763)	Clontech
1	pTUM-1	Subcloning	Group database
4	pTUM-4	Subcloning	Group database

2.2.3 Recombinant plasmids

Table 6: Used DNA plasmids.

Database no.	Name	Vector	Insert	Reference
289	pFlag-E2A-wt	pCMX3b-flag	Ad5 E2A	Group data base
290	pFlag-E2AK94R	pCMX3b-flag	Ad5 E2A	This work
291	pFlag-E2AK132R	pCMX3b-flag	Ad5 E2A	This work
292	pFlag-E2AK202R	pCMX3b-flag	Ad5 E2A	This work
293	pFlag-E2AK94/132R	pCMX3b-flag	Ad5 E2A	This work
294	pFlag-E2AK94/132/202R	pCMX3b-flag	Ad5 E2A	This work
332	pGFP-E2A-SCM	pEGFP-C1	Ad5 E2A	Group data base
360	pGFP-E2A	pEGFP-C1	Ad5 E2A	Group data base
584	pE2A-wt	pCMX3b	Ad5 E2A	This work
585	pE2A-K94/132/202R (pE2A-SCM)	pCMX3b	Ad5 E2A	This work
779	pYFP-Sp100A	pEYFP-C1	Sp100A	Group data base
724	pYFP-Sp100HMG	pEYFP-C1	Sp100HMG	Group data base
61	pcDNA3-E1B-55K	pcDNA3	Ad5 E1B-55K	Group data base
187	pcDNA3-E1B-55K-HA	pcDNA3-HA	Ad5 E1B-55K	Group data base
52	pcDNA3-p53	pcDNA3	p53	Group data base
50	pcDNA3 6xHis Ubiquitin	pcDNA3	6xHis Ubiquitin with CMV promoter and N- terminal HA tag	Group data base
298	L4-Box	pTUM-4	Ad5 nt 21463-27103	(Groitl and Dobner 2007)
299	L4-Box E2A K94R	pTUM-4	Ad5 L4 region	This work
300	L4-Box E2A K132R	pTUM-4	Ad5 L4 region	This work

301	L4-Box E2A K202R	pTUM-4	Ad5 L4 region	This work
302	L4-Box E2A K94/132R	pTUM-4	Ad5 L4 region	This work
303	L4-Box E2A K94/132/202R	pTUM-4	Ad5 L4 region	This work
21	Ad5bac wt -E3 (Noah)	pTUM-1	Ad5 genome	(Groitl and Dobner 2007)
282	Ad5pTUM-1 E2A K94/132/202R	pTUM-1	Ad5 genome	this work

2.3 Antibodies

2.3.1 Primary antibodies

Table 7: primary antibodies used for western blot and immunofluorescence analysis.

Database no.	Antibody	Properties	Source
1	p53-DO1	Monoclonal mouse antibody raised against p53	Santa Cruz Biotechnology
18	p53 (FL-393)	Polyclonal rabbit antibody raised against p53	Santa Cruz Biotechnology
51	Ubc9 (C-12)	Monoclonal mouse Ab against Ubc9	Santa Cruz Biotechnology
61	β-actin (AC-15)	Monoclonal mouse antibody raised against β-actin.	Sigma Aldrich
16	PML (NB100-59787)	Polyclonal rabbit antibody raised against PML	Novus Biologicals
17	PML (sc-966)	Monoclonal mouse Ab raised against PML	Santa Cruz Biotechnology
133	SUMO (8A2)	Recombinant anti-SUMO-2 + SUMO-3 monoclonal mouse antibody	Abcam
39	GFP (ab290)	Polyclonal rabbit antibody raised against GFP	Abcam
19	Flag (M2)	Monoclonal mouse antibody raised against the flag-epitope	Sigma Aldrich

41	6-His	Monoclonal mouse antibody raised against 6xHis epitope.	Clontech
21	HA (3F10)	Monoclonal rat Ab; against the HA-tag	Kindly provided by Elisabeth Kremmer
45	E1A (M73)	Polyclonal rabbit antibody raised against HAdV5 E1A.	(Harlow, Franza, and Schley 1985)
49	E2A (B6-8)	Monoclonal mouse antibody raised against HAdV5 E2A protein.	(Reich et al. 1983)
52	E2A	Monoclonal rabbit antibody raised against HAdV5 E2A protein	Kindly provided by R.T. Hay
62	E1B-55K (2A6)	Monoclonal mouse antibody raised against HAdV5 E1B-55K protein.	(Sarnow, Sullivan, and Levine 1982)
94	E1B-55K (4E8)	Monoclonal rat antibody raised against the central region of HAdV5 E1B-55K.	(Kindsmuller et al. 2009)
34	E4orf6 (RSA3)	Monoclonal rat antibody raised against HAdV5 E4orf6.	Kindly provided by E.Kremmer (HMGU monoclonal antibody unit)
176	L4-100K (6B10)	Monoclonal rat antibody raised against HAdV5 L4-100K.	(Kzhyshkowska et al. 2004)
29	α-Ad5-L4-33K	Polyclonal rabbit antibody raised against HAdV5 L4-33K	(Wu, Guimet, and Hearing 2013)
22	α-Ad5-Pol	Polyclonal rabbit antibody raised against HAdV5 Polymerase	(Temperley and Hay 1991)
23	α-Ad5-pTP	Polyclonal rabbit antibody raised against HAdV5 TP	Kindly provided by R.T. Hay (Webster et al. 1997)
30	α-Ad5-IVa2	Polyclonal rabbit antibody raised against HAdV5 IVa2	(Ostapchuk et al. 2005)
43	Capsid (L133)	Polyclonal rabbit serum raised against HAdV5 capsid.	(Kindsmuller et al. 2007)

2.3.2 Secondary antibodies

Table 8: Secondary antibodies used for Western blot analysis.

Product	Dilution	Properties	Company
HRP-Anti-Mouse IgG	1:10000	HRP (horseradish peroxidase)-coupled; raised in sheep	Jackson/Dianova
HRP-Anti-Rabbit IgG	1:10000	HRP (horseradish peroxidase)-coupled; raised in sheep	Jackson/Dianova
HRP-Anti-Rat IgG	1:10000	HRP (horseradish peroxidase)-coupled; raised in sheep	Jackson/Dianova

Table 9: Secondary antibodies used for immunofluorescence analysis.

Product	Dilution	Properties	Company
647-anti-mouse	1:200	Alexa-647 conjugated goat anti-mouse-antibody	Thermo Scientific
647-anti-rabbit	1:200	Alexa-647 conjugated goat anti-rabbit-antibody	Thermo Scientific
647-anti-rat	1:200	Alexa-647 conjugated goat anti-rat-antibody	Thermo Scientific
488-anti-mouse	1:200	Alexa-488 conjugated goat anti-mouse-antibody	Thermo Scientific
488-anti-rabbit	1:200	Alexa-488 conjugated goat anti-rabbit-antibody	Thermo Scientific
568-anti-rabbit	1:200	Alexa-568 conjugated goat anti-rabbit-antibody	Thermo Scientific

2.4 Standards and markers

Table 10: Used standards and markers.

Product	Company
Quick-Load® 1 kb DNA Ladder	New England Biolabs
PageRuler Plus Prestained Protein Ladder	Pierce

2.5 Commercial systems

Table 11: Used commercial systems.

Product	Company
Plasmid Purification Mini, Midi und Maxi Kit	Qiagen
Protein Assay	BioRad
QuikChange Site-Directed Mutagenesis Kit	Stratagene
Lipofectamin® 2000	Invitrogen
Reverse transcription System	Promega

2.6 Chemicals, enzymes, reagents, equipment

Chemicals, enzymes, and reagents used in this study were obtained from Agilent, AppliChem, Biochrom, BioRad, Biozym, Carl Roth, Calbiochem, New England Biolabs, QIAGEN, Roche, Sigma Aldrich, Tetenal and Thermo Fisher Scientific. Cell culture materials, general plastic material as well as equipment were supplied by AGFA, Beckman Coulter, BioRad, Biometra, Brand, Consumer Electronics Association (CEA), Eppendorf GmbH, Falcon, GFL, Greiner, Integra, Hamilton Company, Harenstein, Heraeus, Heathrow Scientific, Hettich Zentrifugen, Kimberly-Clark Worldwide, LO Laboroptik, Meditrade GmbH, GE Healthcare, Bemis Company, Sarstedt, Scientific Industries, Thermo Fisher Scientific, VWR, Whatman and Zeiss.

2.7 Software and databases

Table 12: Used software tools.

Software	Purpose	Source
Acrobat X Pro	PDF data processing	Adobe
Adobe Photoshop CS6	Image processing	Adobe
Adobe Illustrator CS6	Image processing	Adobe
BioEdit 7.0.5.2	Sequence data processing	Open software (provided by Ibis Therapeutics Carlsbad)

CLC Sequence Viewer 6	Genome and sequencing analyses	CLC bio
Endnote X20	Reference management	Thomson Reuters
Excel 2010	Data processing	Microsoft
Filemaker Pro 14	Database management	Filemaker, Inc.
GPS-SUMO	Prediction of potential SCM and SIM motifs	The CUCKOO Workgroup
ImageJ	Signal intensity calculations	NIH
PowerPoint 2010	Presentation processing	Microsoft
R programing language	Biostatistical analysis	The Comprehensive R Archive Network (CRAN)
Serial Cloner	Genome and sequencing analyses	Serial Basics
Volocity	Microscopic image processing	PerkinElmer Inc.
Word 2010	Text processing	Microsoft

3 Methods

3.1 Bacteria

3.1.1 Culture and storage

Solid plate culture

Bacteria were plated on solid LB media containing 15 g/l agar with antibiotics (100 µg/ml ampicillin or 25 µg/ml kanamycin) and incubated at 30°C or 37°C overnight. Solid *E. coli* cultures were stored for several days at 4°C.

Liquid culture

For liquid culture of *E. coli*, single colonies were picked from agar plates and inoculated into sterile LB media containing appropriate antibiotic (100 µg/ml ampicillin or 25 µg/ml kanamycin). Cultures were incubated at 30°C or 37°C at 150 rpm overnight in an *Multitron* incubation shaker. Liquid *E. coli* cultures were stored for several days at 4°C.

Storage

Liquid cultures of single colony bacteria were centrifuged at 4,000 rpm for 10 min (*Rotina 420R*), at RT. The bacteria pellets were resuspended in 1 ml of solution containing 50% of sterile LB medium and 50% sterile 87% glycerol and kept in *CryoPure Tubes* in a *HeraeusTM Herafreeze* at -80°C for long-term storage.

Table 13: Components of LB medium.

LB Medium	Trypton Yeast extract NaCl (Autoclaved)	10 g/ 5 g/l 5 g/l

Table 14: Antibiotics used for selection.

Antibiotic solution (Sterile filtered; storage at -20 °C)	Ampicillin	50 mg/ml
	Kanamycin	25 mg/ml

3.1.2 Transformation of E. coli

Chemically treated competent DH5α bacteria were transformed in pre-cooled *Falcon® 2059 polypropylene round-bottom tubes*. In 100 µl of bacteria was added in 10 µl of diluted plasmid DNA (~200ng) and incubated on ice for 30 min, before applying the heat shock. The mixture was kept at 42°C for 30 s and subsequently cooled down on ice for 2 min. After the heat shock 1ml of LB media without antibiotics was added to the bacteria and incubated for 60 min at 37 °C at 220 rpm in an *Multitron* incubation shaker. The bacteria were plated on solid LB agar containing appropriate antibiotics and incubated overnight at 30°C/37°C.

3.2 Mammalian cell lines

3.2.1 Cultivation

Mammalian cells were cultured as a monolayer of adhesive cells in polystyrene cell culture dishes (12-well/ 6-well/ 100 mm/ 150 mm tissue culture dishes; Sarstedt) in Dulbecco's Modified Eagle Medium (DMEM; Sigma). Cell growth medium was supplemented with 0.11g/l sodium pyruvate, 10% fetal bovine serum, (FBS; Thermo Fisher Scientific) and 1% of penicillin/streptomycin solution (1000U/ml penicillin & 10mg/ml streptomycin in 0.9% NaCl; Sigma-Aldrich). For cultivation of hepatoma cell lines (HepaRG), 5 µg/ml bovine insulin (Sigma) and 0.5 µM hydrocortisone (Sigma) was added in the medium.

The cells in the culture were incubated at 37°C with 5% CO2 atmosphere (*Heraeus® BB16 Function Line*). The cell culture work was performed in sterile *Heraeus™ Laminair HLB 2448 GS* safety cabinet. For splitting, the confluent cells were washed with sterile PBS solution after removal of the media and incubated with trypsin solution 3-5 min on 37°C. After the cells were detached from the plate, trypsin activity was inhibited by addition of standard culture media. The mixture of cells, trypsin and media was transferred in 50 ml tubes and centrifuged for 3 min at 2000 rpm (*Heraeus™ Megafuge™ 40*). The supernatant was discarded after centrifugation and the cells were resuspended in appropriate culture medium. The cells were counted and seeded in a definite amount for experiments as described in (3.2.3) or split at ratio of 1:2 to 1:12 for further propagation.

Table 15: Composition of PBS.

PBS	NaCl	140 mM
	KCl	3 mM
	Na_2HPO_4	4 mM
	KH_2PO_4	1.5 mM
	(pH 7.3; autoclaved)	

3.2.2 Storage of mammalian cell lines

For long term storage of mammalian cells, the cultures were trypsinized and pelleted as described in section 3.2.1. The cell pellets were resuspended in pure FBS supplemented with 10% dimethyl sulfoxide DMSO (Sigma), transferred in *CryoTubes* (*CryoPure Tube*, Sarstedt) and slowly frozen to -80°C in *Mr. Frosty* freezing container (Nalgene Labware). The cells were stored at -80°C or in liquid nitrogen. For cultivation, frozen cells were thawed in 37°C water bath, pelleted to remove DMSO and subsequently resuspended in pre-warmed culture medium. Resuspended cells were seeded in an appropriate cell culture dish and incubated at standard conditions (3.2.1).

3.2.3 Cell number determination

Confluent cells were trypsinized, pelleted by centrifugation and resuspended in an appropriate volume of culture media, as described in section 3.2.1. Subsequently, 10 µl of resuspended cells was mixed with 10 µl of Trypan Blue solution and placed in *Neubauer* counting chamber (LO Laboroptik). Three manual counts (16 squares) were performed using the *Primovert* light microscope and the number of cells per ml was calculated using the following formula:

$$\text{cell number/ml} = \text{counted cells} \times 2^{(\text{dilution factor})} \times 10^4$$

Trypan blue was used to discriminate viable from dead cells.

Table 16: Composition of Trypan blue solution.

Trypan blue solution	Trypan Blue	0.15%
	NaCl	0.85%

After counting, 4-5 x 10^6 or 4-6 x 10^5 cells were seeded per 100 mm culture plate or 6-well respectively and incubated at 37°C and 5% CO_2, 24 h prior transfection (3.2.4) or infection (3.3.4).

3.2.4 Transfection by polyethylenimine

Mammalian cells were transfected using linear 25 kDa polyethylenimine (PEI; Polysciences). PEI was dissolved in Milli-Q water at a concentration of 1 mg/ml, set to pH of 7.2 with 0.1M HCl, filter sterilized (0.2 µm), aliquoted and stored at -80 °C.

For transfection, the cells were seeded as described in section 3.2.1. In order to ensure neutral pH, the standard cell culture media was replaced by DMEM media without supplements before transfection. DNA for transfection was dissolved in 1-3.6 ml of prewarmed DMEM media without supplements, PEI was added (5-10 µl per 1 µg DNA) and the mixture was vortexed. Transfection solution was incubated for 15-30 min at room temperature (RT) to generate DNA/PEI complex. The cells were incubated with the transfection solution for 3-5 h at standard conditions. Incubation time and the amount of transfection reagent was adjusted according to the cell type and the amount of DNA transfected as PEI exhibits toxicity to mammalian cells. After incubation, the transfection media was replaced by standard culture media. Cells were harvested 24-48 h post transfection.

3.2.5 Harvesting of mammalian cells

Mammalian cells were harvested 24-48 h after transfection or 8-96 h after infection. The cells were detached using cell scrapers, rinsed from the plates by PBS, transferred in 15 ml falcon tubes and centrifuged at 2000 rpm for 3 min at RT (*Rotina 420R*). After removal of supernatant, the cell pellets were washed once in PBS and centrifuged. The supernatant was discarded, and the cell pellets were stored at -20°C for subsequent experiments.

3.3 Adenovirus

3.3.1 Generating virus from DNA

To generate mutant viruses the viral genome was extracted from the recombinant bacmid by Pac I digestion. 2.4 x 10^6 of H1299 cells were seeded in 60 mm dish (Sarstedt) and after 24 h transfected with 8 µg of viral DNA using lipofectamine as transfection reagent. The mixture of viral DNA, lipofectamine and DMEM media without supplements was added to the cells, incubated for 6 h on 37 °C and changed to normal growth medium. After 5 days, cells were harvested, centrifuged at 2000 rpm for 5 min (*Rotina 420R*), and the cell pellet was resuspended

in 1 ml of DMEM. The viruses were released in medium by breaking the cells with three cycles of freezing in liquid nitrogen and thawing in 37°C water bath. Virus particles were separated from the cell debris by centrifugation at 4000 rpm for 10 min at RT (*Rotina 420R*). The virus-containing supernatant was used to infect 4 x 10^6 of H1299 cells in 100 mm dish (Sarstedt) and infectious viral particles were collected 3-5 d after infection by freezing/thawing as described above. This re-infection procedure was repeated until a cytopathic effect was observed in 90% of the cells. The preliminary virus solution was used to yield a high-titer virus stock.

3.3.2 Propagation and storage of high-titer adenovirus stocks

For establishment of high titer virus stocks, H1299 cells seeded in 150 mm dishes were infected with the virus obtained as described in previous section (3.3.1). Infected cells were incubated until the cytopathic effect was observed (3-5 d) at 37°C, harvested and centrifuged at 2000 rpm for 3 min (*Rotina 420R*). The infected cell pellet was resuspended in DMEM without supplements. The viral particles were released as described in section 3.3.1 and virus-containing supernatant was mixed with 87% glycerol (sterile, 10% final concentration) for preservation at -80 °C.

3.3.3 Titration of virus stocks

Virus stocks were titrated in HEK293 or 2E2 cells seeded in 6-well plates previously precoated with Poly-L-Lysine as described in (3.2.1). Virus titers were determined by calculation of number of fluorescence forming units (FFU) after immunofluorescence staining for the E2A (in HEK293 cells) or adenoviral capsid (in 2E2 cells). Virus stocks were diluted in DMEM without supplements by a factor 10^1-10^6 and 4 x 10^5 HEK293 or 2E2 cells per 6-well were infected with each virus dilution. After 24 h, the infected cells media was discarded and the cells were fixed with ice cold methanol at -20 °C for 15 min. Methanol was removed, the cells were air-dried at RT and stored at -20 °C or immediately used for immunofluorescence staining. Unspecific binding was blocked with TBS-BG on *Unitwist RT* shaker at RT for 1 h. The cells were incubated for 2-3 h at 4°C with an antibody solution containing the E2A specific antibody B6-8 (1:10 in PBS-T) or adenoviral capsid specific antibody (1:1000 in PBS-T). After three washes with TBS-BG the appropriate secondary Alexa Fluor 488-coupled secondary antibody (1:1000 in PBS-T) was added to the cells. After 2 h to overnight incubation at 4°C in dark, the stained cells were washed three

times with TBS-BG and infected cells were counted using a fluorescent *Axiovert 200 M* microscope (Zeiss). The total number of infectious particles per µl was calculated considering the virus dilutions as the mean value of several independent counts of vision field multiplied with the factor corresponding to the objective used for counting.

3.3.4 Adenovirus infection

The mammalian cells that reached the approximate confluence of 80-90 % were infected with adenovirus according to the experimental setup. Prior to the infection, the standard culture media was discarded and DMEM without supplements was added. Virus dilutions were prepared in an appropriate volume of DMEM without supplements and added to the cells. In order to calculate the amount of virus needed to achieve the MOI determined by experimental setup, the following formula was used:

$$V_{\text{virus stock solution}}\,(\mu l) = \frac{\text{total cell number}}{\text{virus titer (FFU/µl)}} \text{ x MOI (FFU)}$$

After 1-2 h of incubation at 37 °C, infection medium was replaced with the appropriate cell culture medium. The infected cells were harvested at time points, which were chosen according to the experimental setup.

3.3.5 Determination of virus yield

For determination of the progeny virion production the cells were seeded into the 6-well plates (3.2.1) and infected with adenovirus as described in 3.3.4. The infected cells were harvested 24, 48 and 72 h after infection, transferred into 15 ml reaction tube (Falcon) and centrifuged at 2000 rpm for 3 min (*Rotina 420R*). The supernatant was removed, the pellet washed in PBS and resuspended in 300, 400 or 500 µl of DMEM without supplements. The amount of DMEM used for resuspension was dependent on the harvesting time point. The virus particles were released from the cell suspension by 3 sequential freeze and thaw cycles as described in 3.3.2. After the centrifugation at 4000 rpm for 10 min (*Rotina 420R*) supernatant with the released virus particles was transferred into new a 1.5 ml reaction tube (Eppendorf) and stored at -20°C. Determination of

particle number in the virus solution was done by titration as described in 3.3.3, and the particle number produced per cell, termed as virus yield, was calculated using the following formula:

$$\text{FFU/cell} = \frac{\text{virus titer (FFU/µl)}}{\text{total cell number}} \text{ x } V_{\text{resuspension media volume}}$$

3.3.6 Determination of the viral DNA replication

To monitor viral DNA replication cells were infected according to the experimental setup and lysed with RIPA buffer as previously described in section 3.6.1. Total DNA was isolated by mixing 10 µg of the cell lysate with 10 µl proteinase K (2 mg/ml; Carl Roth). The reaction volume was adjusted to 90 µl with Milli-Q water containing 0.5 µl Tween-20. Samples were incubated for 1 h at 55 °C in *Eppendorf® Thermomixer Comfort 5355*. Proteinase K was inactivated by incubation at 95°C for 10 min and cooled down to 4°C. Samples were diluted 1:100 in nucleic acid-free water (Promega). For quantitative PCR analysis, described in section 3.5.3, 2 µl of sample was mixed with 12.5 µl of *Power SYBR Green PCR Master Mix* (Roche) and 10 µM concentration of appropriate primer pairs in total volume of 24 µl. Concentration of viral DNA was calculated based on standard curve obtained with quantitative PCR analysis for known concentrations of HAdV bacmid DNA.

3.4 DNA techniques

3.4.1 Preparation of plasmid-DNA from *E. coli*

Pre-culture was generated by inoculating a single bacteria colony picked from the agar plate in 5 ml of LB-medium supplemented with the appropriate antibiotics and incubated on 30 or 37°C at 150 rpm overnight in *Multitron* incubator. For large-scale plasmid-DNA preparations, 200-500 µl of pre-culture was inoculated in 500 ml of LB-medium supplemented with the appropriate antibiotics. After 16-24 h of incubation at 30°C or 37°C, 150 rpm (*Multitron*) the bacteria were pelleted by centrifugation at 4500 rpm for 20 min (*Rotixa 50 RS*). Plasmid DNA was extracted according to the manufacturer´s protocol using the *QIAGEN Plasmid DNA Purification Kit.*

Bacteria from 500 ml cultures were used for maxi DNA preparation. The bacteria pellet was resuspended in 10 ml of resuspension buffer P1 (QIAGEN). 10 ml of lysis buffer P2 (QIAGEN) and neutralization buffer P3 (QIAGEN) were added successively. The samples were

mixed, centrifuged for 30 min at 4500 rpm and the supernatants were loaded on Qiagen columns previously treated with 10 ml of equilibration buffer QBT (QIAGEN). After the samples ran through the column, they were washed twice with washing buffer QC (QIAGEN). DNA was eluted from the membrane using 15 ml of elution buffer QF (QIAGEN) and mixed with 12.5 ml of isopropanol. The DNA was precipitated by centrifugation at 4500 rpm for 60 min. DNA pellets were transferred in 1.5 ml Eppendorf tubes, washed once with 75 % (v/v) ethanol, centrifuged at 4500 rpm for 5 min and dried at 42°C. After resuspension in an appropriate amount of 10 mM Tris (pH 8.0), DNA concentration was measured using a *Nanodrop 2000c UV-Vis* spectrophotometer at a wavelength of 260 nm (3.4.2).

Midi DNA preparations were performed from bacteria pellets derived from 50 ml cultures. The pellets were resuspended in 1.2 ml of P1 buffer and split in two 2 ml Eppendorf tubes. 600 µl of P2 and P3 buffers were added to each tube successively. After mixing, the samples were centrifuged at 14800 rpm for 10 min. Supernatants were loaded on Qiagen columns equilibrated with 1 ml of QBT buffer. After the samples passed through the columns, they were washed twice with QC buffer. DNA was eluted using 840 µl of QF buffer, mixed with 700 µl of isopropanol and precipitated by centrifugation at 14800 rpm for 10 min. The DNA pellets were washed once with 75 % (v/v) ethanol, centrifuged at 14800 rpm for 5 min and dried at 42°C. DNA was resuspended in appropriate amount of 10 mM Tris (pH 8.0) and DNA concentration was measured (3.4.2).

Mini DNA preparations were done from 1 ml bacteria cultures, for analytical purposes. Bacteria pellets were resuspended in 300 µl of P1 buffer and 300 µl of P2 and P3 buffers were added successively. Salts and cellular debris were pelleted by centrifugation for 12 min at 14800 rpm. The supernatants were transferred in new 1.5 ml reaction tubes, 600 µl of isopropanol was added and precipitation was done by centrifugation at 14800 rpm for 12 min. DNA pellets were washed once with 75 % (v/v) ethanol, centrifuged at 14800 rpm for 5 min and dried at 42°C. The DNA pellets were rehydrated in appropriate volume of 10 mM Tris (pH 8.0) solution and DNA concentration was measured as described in the following section (3.4.2).

3.4.2 Quantitative determination of DNA concentrations

For the determination of DNA concentration, *Nanodrop 2000c UV-Vis spectrophotomet*er at a wavelength of 260 nm was used. Optical density of 1 corresponds to the absolute concentration of 50 µg/ml for double-stranded DNA or 33 µg/ml for single-stranded DNA. Ratio of

OD260/OD280 was used to assess DNA purity and it should be above 1.8 to assure high DNA purity and at 2.0 for high purity of RNA.

3.4.3 Agarose gel electrophoresis

Agarose was dissolved in TBE buffer to final concentration of 0.6-1.2 % (w/v), depending on the DNA fragment size, in order to make gels for analytical and preparative purposes. The agarose was melted in microwave oven, subsequently supplemented with 0.5 µg/ml ethidium bromide and the solution was poured in an appropriate gel tray with inserted combs. DNA discoloration was prevented by addition of ethidium bromide to a final concentration of 0.05 µg/ml in the positive side of the gel chamber. DNA samples were mixed with 6 x loading buffer, loaded in the gel pockets and subjected to agarose gel electrophoresis in 1 x TBE running buffer at 140 V for 1-2 h. DNA fragment size was determined using 100 bp or 1 kb DNA ladder. DNA was visualized under UV light at 365 nm using the *Gel Doc™ XR+* gel documentation system.

For preparative purposes, harmful UV radiation was minimized by supplementing agarose gels with 1 mM guanosine. DNA was extracted from gel slices cut under UV light at minimal wavelength of 365 nm by centrifugation at 20000 rpm for 1-2 h (*RC 5B Plus*; Sorvall), precipitated with isopropanol from the obtained supernatant, washed, dried and dissolved as described for plasmid DNA in (3.4.1).

Table 17: Composition of TBE buffer.

5 x TBE	Tris/HCl (pH 7.8)	450 mM
	Boric Acid	450 mM
	EDTA	10 mM

Table 18: Composition of DNA loading buffer.

6 x loading buffer	EDTA	10mM
	Glycerol	50% (v/v)
	Bromphenol blue	0.25% (w/v)
	Xylen Cyanol	0.25% (w/v)

Table 19: Composition of DNA ladder.

DNA ladder	100 bp or 1 kb ladder	100 µl
	6 x loading dye	100 µl
	Milli-Q water	400 µl

3.4.4 Polymerase chain reaction

Standard polymerase chain reaction (PCR) protocol was used for amplification of DNA template. Reaction was prepared in a 0.2 ml PCR reaction tube, by mixing 25 ηg of DNA template, 125 ηg of forward primer, 125 ηg of reverse primer, 1 µl of dNTP mixture, 5 µl of 10 x PCR reaction buffer, 1 µl of polymerase (PfuUltra II Fusion or Taq) and filling up until total volume of 50 µl with Milli-Q water. The thermocycler *PeqSTAR 96x universal gradient* was programmed as follows:

Table 20: PCR setup with indicated time periods, temperatures and number of cycling steps.

Pre-denaturation	2 min	95°C
Denaturation	1 min	95 °C
Annealing	30 sec-1 min	55 – 70 °C
Elongation	1 min/kb	72 °C
	(25-30 cycles)	
Final elongation	10 min	72 °C
Storage	∞	4 °C

The annealing and elongation steps were adjusted based on the DNA fragment length and theoretical primer melting temperature. To determine PCR efficiency 5 µl of PCR reaction was analyzed by gel electrophoresis (3.4.3).

3.4.5 Site-directed mutagenesis

To insert point mutations into target plasmids, suitable forward and reverse primers were designed and ordered from Metabion (Munich). Insertion of mutations was done by using *in vitro QuikChange™ Site-Directed Mutagenesis* kit (Agilent) according to the manufacturer's instructions. Mixture for PCR was made according to standard PCR protocol (3.4.4). Depending on the inserted mutation the PCR program was following:

Table 21: PCR setup with indicated time periods, temperatures and number of cycling steps.

Pre-denaturation	2 min	95 °C
Denaturation	1 min	95 °C
Annealing	45 sec	55 °C
Elongation	45 sec/kb (12-16 cycles)	68 °C
Final elongation	10 min	68 °C
Storage	∞	4 °C

After 12-16 cycles PCR efficiency was determined by examining 10 µl of PCR reaction product with gel electrophoresis (3.4.3). PCR mixture was incubated with DpnI for 1 h at 37°C to remove the template DNA. Afterwards, 10 µl of digestion product were used for transformation of chemical competent DH5α bacteria strain (3.1.2). Individual transformed colonies were picked and cultured in 5-50 ml of LB media supplemented with appropriate antibiotic (3.1.1). Plasmid DNA was prepared (3.4.1) and analyzed by restrictive digest, agarose gel electrophoresis and sequencing (3.4.7) before storage at 4°C and -20°C.

3.4.6 Cloning of DNA fragments

3.4.6.1 Enzymatic DNA restriction

For analytical purposes restriction digestions were done by incubating 0.5-1 µg of DNA with 3-10 U of suitable restriction enzyme at 37°C for 2 h. For preparative purposes, 50 U of enzyme was used digest 5-20 µg of DNA, at 37°C for at least 3 h. When necessary, the restriction fragments gained in various enzymatic restrictions were separated by agarose gel electrophoresis and isolated from preparative gels.

3.4.6.2 Ligation

To purify enzymatically restricted DNA fragments or PCR products synthesized for mutant generation, DNA was isolated from preparative gels using agarose gel electrophoresis (3.4.3) and isopropanol precipitation (3.4.1). Ligation was performed by mixing 20-100 ng vector DNA, insert DNA in a ratio of 1:3, 2 µl 10 x ligation buffer, 1 µl T4 DNA ligase (New England BioLabs) and Milli-Q water to a final volume of 20 µl. Ligation was performed overnight at 13°C (*Eppendorf® Thermomixer Compact*). Ligated plasmid DNAs were transformed into chemical competent E.coli (3.1.2), single clones were picked, cultured in 5-10 ml LB medium (3.1.1) and prepared plasmid

DNA was analyzed by restriction digestion (3.4.6.1), agarose gel electrophoresis (3.4.3) and sequencing (3.4.7).

3.4.7 DNA sequencing

For DNA sequencing 1 µg of DNA and 30 pmol of sequencing primer were mixed with Milli-Q water to achieve final volume of 17 µl. DNA sequencing was performed by Eurofins Genomics (Ebersberg) and the results were evaluated using BioEdit, BLAST and Serial Cloner.

3.4.8 Chromatin immunoprecipitation (ChIP) assay

The cells treated according to the experimental setup were crosslinked with 1% methanol-free formaldehyde (ThermoFisher Scientific) for 10 min at room temperature. Cross-linking reaction was stopped by addition of glycine to a final concentration of 125 mM, and the samples were incubated for 5 min at room temperature. Cells were washed two times with ice-cold PBS, harvested, and lysed in SDS buffer. Samples were incubated on ice for 10 min, sonicated for 15 min in *a Diagenode Bioruptor Pico* (30-s on-off intervals) and cleared by centrifugation two times for 10 min at 16,000 × g and 4 °C. For ChIP, sheared chromatin from 1.5×10^6 cells in 50 µl was combined with 9 volumes of ChIP dilution buffer and subjected to immunoprecipitation for 16 h at 4°C with mild rotation using the antibody against the examined protein, or the same amount of normal IgG. Samples were centrifuged for 10 min at 20,000 × g and 4°C to remove precipitated material, and the supernatants were combined with ChIP protein G magnetic beads (Millipore) binding to the examined protein and incubated for 2 h at 4°C with mild rotation. Immune complexes were washed successively with 1 ml each of low-salt buffer, high-salt buffer, and lithium chloride buffer, and twice with TE buffer. Elution of the chromatin-antibody complexes was performed by incubation with 150 µl freshly prepared elution buffer containing 1.5 µl proteinase K (Roche) at 62°C for 2 h, followed by a 10 min incubation step at 95°C. DNA was purified using the *MinElute PCR Purification Kit* from Qiagen according to manufacturer's instructions. DNA was eluted twice with 20 µl buffer EB, and 2 µl of the DNA solution was used as template DNA for qPCR with specific primers listed in Table 4.

Table 22: Composition of buffers used for ChIP analysis.

SDS buffer	Tris/HCl (pH 8.1)	50 mM
	EDTA	10 mM
	SDS	1%
ChIP dilution buffer	Tris/HCl (pH 8.1)	16.7 mM
	NaCl	167 mM
	EDTA	1.2 mM
	Triton X-100	1.1%,
	SDS	0.01%
Low salt buffer	Tris/HCl (pH 8.1)	20 mM
	NaCl	150 mM
	EDTA	2 mM
	Triton X-100	1 %
	SDS	0.1%
High salt buffer	Tris/HCl (pH 8.1)	20 mM
	NaCl	0.5 M
	EDTA	2 mM
	Triton X-100	1%
	SDS	0.1%
Lithium chloride buffer	Tris/HCl (pH 8.1)	10 mM
	LiCl	0.25 M
	EDTA	1 mM
	IGEPAL CA-630	1 %
	Deoxycholic acid	1%
TE buffer	Tris/HCl (pH 8.0)	10 mM
	EDTA	1 mM

Elution buffer	$NaHCO_3$	100 mM
	SDS	1 %

3.4.9 Formaldehyde-assisted isolation of regulatory elements (FAIRE)

The cells treated according to the experimental setup were harvested and chromatin was sheared as described in section 3.4.8. Sheared chromatin was diluted with one volume of TE buffer and a 100 µl portion (1.5×10^6 cells) was supplemented with 4 µl of 5 M sodium chloride solution and incubated for 4 h at 65°C to reverse cross-links and isolate total input DNA. After a brief cooling step on ice, the input sample was treated with 20-40 µg RNase A for 1 h at 37°C and with 2 µl proteinase K (Roche) for 1 h at 45°C before its final volume was adjusted to 333 µl with TE buffer. The input sample and a second, still cross-linked 333 µl portion of sheared chromatin (5×10^6 cells) were extracted twice with phenol/chloroform/isoamyl alcohol (25:24:1) and once with chloroform in 1.5 ml *MaXtract High Density tubes* (Qiagen). DNA from 200 µl of the aqueous phase was subsequently precipitated by the addition of 20 µl 3 M sodium acetate (pH 5.2), 20 µg glycogen (Roche), and 552.5 µl ethanol. This step was followed by an overnight incubation at −20°C. The precipitate was collected by centrifugation for 30 min at 16,000×g and 4°C, washed twice with 1 ml 70 % ethanol, air dried, and resuspended in 50 µl double-distilled water. Quantification of purified DNA (50 ng total DNA for cellular loci and 1.25 ng total DNA for viral loci) was done by qPCR using the *Brilliant III Ultra-Fast QPCR Master Mix* (Agilent Technologies) according to the manufacturer's instructions. Primer sequences are listed in Table 4.

3.5 RNA techniques

3.5.1 Preparation of total RNA from mammalian cells

After infected or transfected cells in 100 mm dishes or 6-well plates were harvested as described in section 3.2.5, the cell pellets were resuspended in 600 µl Trizol reagent (Thermo Scientific). Resuspended cells were ether frozen on -80°C or immediately further processed by addition of 200 µl Chloroform (Carl Roth). After vortexing each sample for at least 15 s (*Vortex-Genie 2*) and incubating for 3 min at RT, cell debris was pelleted at 12000 g for 15 min at 4 °C (*Heraeus™ FrescoTM 21 Microcentrifuge*) to perform phase separation. After this step, all further

processing of samples was performed on ice. The upper, transparent phase of supernatant that contains RNA was transferred into a new 1.5 ml Eppendorf tube with 600 µl isopropanol. The samples were thoroughly mixed and centrifuged at 12000 g for 15 min (*Heraeus™ FrescoTM 21 Microcentrifuge*) for RNA precipitation. The RNA pellet was washed with 1 ml of 75 % (v/v) EtOH (7500 g, 15 min, 4 °C; *Heraeus™ FrescoTM 21 Microcentrifuge*), air-dried and dissolved in 20 µl nuclease-free water. *Nanodrop 2000c UV-Vis spectrophotometer* was used to assess RNA purity and quantity. RNA was considered highly pure with a ratio of OD260/OD280 of ~2.0. RNA was stored at -80 °C or subjected to reverse transcription for quantitative RT-PCR.

3.5.2 Reverse transcription of RNA to cDNA

Reverse Transcription System (Promega) was used for reverse transcription of RNA to cDNA. The mixture for reverse transcription was prepared by combining 1 µg RNA in total volume of 10 µl in nuclease-free water with 3 µl nuclease-free water, 4 µl MgCl2 (25 mM), 2 µl 10 x reverse transcription buffer, 2 µl dNTP mixture (10 mM), 1 µl oligo$(dT)_{15}$ random primers, 0.5 µl recombinant RNasin® ribonuclease inhibitor and 0.7 µl AMV reverse transcriptase. The reverse transcription reaction was performed at 42°C for 45-60 min (*Eppendorf® Thermomixer Comfort 5355*) and it was inactivated by 5 min incubation at 95 °C. The cDNA was stored at -20 °C (*Liebherr*).

3.5.3 Quantitative PCR (qPCR)

RT-PCR was performed using a *LightCycler 480 Instrument II* in *FrameStar® 480/96* 96 well plates covered with adhesive seals. cDNA was diluted 1:50 to 1:100 for qPCR analysis in total volume of 4 µl and mixed with 0.5 µl of forward and reverse primer with concertation of 30 pmol and 5 µl of *LightCycler® 480* SYBR Green I Master (Roche). The PCR conditions for adenoviral mRNAs were as follows: 10 min at 95 °C, followed by 40 cycles of 30 s at 95 °C, 30 s at 62 °C and 30 s at 72 °C. The average threshold cycle (CT values) was determined from triplicate reactions and calculated relative to CT values for cellular GAPDH. The identities of the obtained products were confirmed by melting curve analysis.

3.5.4 RNA sequencing

RNA was isolated from whole-cell lysates as described in section 3.5.1. Strand specific, polyA-enriched RNA sequencing was performed as previously described (Haack et al. 2013). RNA integrity number (RIN) was determined with the *Agilent 2100 BioAnalyzer* (*RNA 6000 Nano Kit*, Agilent). For library preparation, 1 µg of RNA was poly(A) selected, fragmented, and reverse transcribed with the *Elute, Prime, Fragment Mix* (Illumina). A-tailing, adaptor ligation, and library enrichment were done according to the *TruSeq Stranded mRNA Sample Prep Guide* (Illumina). Quality and quantity of RNA libraries were assessed using the *Agilent 2100 BioAnalyzer* and the *Quant-iT PicoGreen dsDNA Assay Kit* (Life Technologies). RNA libraries were sequenced as 150 bp paired end runs on an *Illumina HiSeq4000* platform. Kallisto (version 0.46.1) was used to quantify transcript abundancies from paired-end RNA-seq reads (Bray et al. 2016). The index for Kallisto-pseudoalignment was built using the Genome Reference Consortium Human Build 38 patch release 13 (GRCh38.p13), (Yates et al. 2020). Differential gene expression was analyzed using the R package sleuth (version 0.30.0), (Pimentel et al. 2017). The R package goseq was used for gene ontology analysis (Young et al. 2010).

3.6 Protein techniques

3.6.1 Preparation of total cell lysates

All steps of sample preparation for protein analysis were performed on ice. To ensure proper solubilization of matrix-associated proteins RIPA lysis buffer was used. RIPA lysis buffer was freshly supplemented with 0.2 mM PMSF, 1 mg/ml Pepstatin A, 5 mg/ml aprotinin, 20 mg/ml leupeptin, 25 mM iodacetamide and 25 mM N-ethylmaleimide. Cell pellets, harvested as described in 3.2.5, were resuspended in appropriate volume of lysis buffer and incubated for 30 min on ice while vortexing every 10 min during that time (*Vortex-Genie 2*). After incubation, cell disruption and genomic DNA shearing was performed by sonification for 30 s at 5 °C with *Branson Ultrasonics SonifierTM* (0.8 output impulse/s). The cell debris and insoluble components were eliminated by centrifugation for 3 min, at 11000 rpm, at 4°C (*Heraeus™ FrescoTM 21 Microcentrifuge*) and the concentration of proteins was determined by spectrophotometry (*SmartSpecTM Plus*) using *Bradford* method (Bradford 1976) as described in the following section (3.6.2). Protein samples were transferred to new pre-cooled Eppendorf tubes, diluted in Milli-Q

water to the required concentration and boiled for 3 min at 95 °C (*Eppendorf® Thermomixer Comfort 5355*) with the appropriate amount of 5 x Laemmli buffer supplemented with β-mercaptoethanol. Protein lysates were stored at -20 °C for further analysis.

Table 23: Composition of RIPA buffer.

RIPA	Tris/HCl (pH 8.0)	50 mM
	NaCl	150 mM
	EDTA	5 mM
	Nonidet P-40	1 % (v/v)
	SDS	0.1 % (w/v)
	Sodium Desoxycholate	0.5 % (w/v)

Table 24: Composition of 5 x Laemmli buffer.

5 x Laemmli buffer	Tris/HCl (pH 6.8)	250 mM
	Glycerol	50 % (v/v)
	SDS	10% (w/v)
	Bromophenol blue	0.5 % (w/v)
	β-mercaptoethanol	5 % (w/v)

3.6.2 Quantitative determination of protein concentrations

For determination of protein concentration *Bradford-based BioRad Protein- Assay* (Bradford 1976) was used. 1 µl of protein solution was mixed with 799 µl of Milli-Q water and 200 µl of *Bradford Reagent* (BioRad) in semi-micro cuvettes sealed using *Parafilm® M All-Purpose Laboratory Film*. The samples were measured in *SmartSpec™ Plus* spectrophotometer at 595 nm against a blank of 800 µl of Milli-Q water and 200 µl of *Bradford Reagent*. The protein concentrations were calculated based on the standard curve made using BSA (Thermo Scientific) in concatenations 1-16 µg/µl.

3.6.3 Immunoprecipitation

Cell lysates were prepared as described in (3.6.1) using appropriate volumes of RIPA buffer supplemented with protease inhibitors and protein concentrations were measured as described in previous section (3.6.2). For pre-clearing, equal amounts (800-3000 µg) of total cell lysates were supplemented with 30 µl of Pansorbin cells (Calbiochem) and 1 mg of Sepharose A and incubated for 1-2 h at 4 °C in a rotator (*GFL 3025*). At the same time, appropriate amount of primary antibody was coupled to 3 mg of Sepharose A/sample by 1 h incubation in RIPA buffer at 4°C in a rotator (*GFL 3025*). Sepharose A used for pre-clearing and antibody coupling was previously swollen by 20 min incubation in RIPA buffer at 4°C in a rotator (*GFL 3025*). Sepharose A beads coupled with antibody were washed 2 times with 1 ml of RIPA buffer and resuspended in appropriate amount of RIPA buffer freshly supplemented with protease inhibitors. Protein lysates cleared by centrifugation (6000 rpm, 4 min, 4°C; *Heraeus™ FrescoTM 21 Microcentrifuge*) were mixed with equal amounts of Sepharose A beads coupled with antibody and incubated for 1-2 h at 4°C in a rotator (*GFL 3025*). Sepharose beads attached to precipitated protein complexes were pelleted (6000 rpm, 2 min, 4 °C; *Heraeus™ FrescoTM 21 Microcentrifuge*) and washed three times with 1 ml of RIPA buffer freshly supplemented with protease inhibitors. After washing, samples were boiled for 5 min at 95°C with 20 µl of *2 x Laemmli buffer* supplemented with β-mercaptoethanol. Eluted proteins were stored at -20 °C for further analysis.

Table 25: Composition of 2 x Laemmli buffer.

2 x Laemmli buffer	Tris/HCl (pH 6.8)	100 mM
	SDS	4 % (w/v)
	Bromophenol blue	0.2 % (w/v)
	Glycerol	20 %
	β-mercaptoethanol	2 % (w/v)

3.6.4 Denaturing purification and analysis of SUMO-conjugates

Two 100 mm dishes per sample of HeLa cells that stably express 6xHis-SUMO-2 or HepaRG cells stably expressing 6xHis/HA-SUMO-2 were transfected/infected with the appropriate expression factor/virus. Cells were harvested 24-48 h later, as described in (3.2.5). For

total protein analysis 10% of cells were separated and stored as pellets at -20°C or immediately lysed as described in section 3.6.1. The rest of cell pellet, used for Ni-NTA purification, was lysed in 5 ml of guanidinium-containing lysis buffer B1 supplemented with β-mercaptoethanol and stored at -80 °C or further processed by sonification three times for 10 s at 5°C, 0.8 output impulse/s (*Branson Ultrasonics Sonifier™*). 30 µl of Ni-NTA beads (Thermo Scientific) per sample previously washed in buffer B1 were added to the sonified cell lysates and incubated at 4°C for 24 h in rotator (*GFL 3025*). After the incubation, the samples were centrifuged at 4000 rpm for 10 min (*Rotina 420R*), washed once at 1000 g for 3 min at 4°C (*Heraeus™ FrescoTM 21 Microcentrifuge*) with 1 ml of buffer B1 and then once with 1 ml of each wash buffer B2 (pH8.0)/B3 (pH6.3). All three buffers were supplemented with β-mercaptoethanol (5 mM) as well as protease inhibitors aprotinin (10 U/ml), leupeptin (1 µg/ml) and pepstatin A (1 µg/ml). In order to elute proteins from Ni-NTA beads, the samples were supplemented with 20-40 µl of Elution buffer, mixed, incubated on RT for 10 min and boiled at 95°C for 5 min. The samples were kept on -20°C for further analysis.

Table 26: Composition of buffers used for Ni-NTA assays.

B1 (GuHCl lysis buffer)	GuHCl	6 M	
	Na_2HPO_4	94,7 %	0.1 M
	NaH_2PO_4	5,3 %	
	Tris/HCl (pH 8.0)	10 mM	
	Imidazole	20 mM	
	β-mercaptoethanol	5 mM	
B2 (wash buffer pH 8.0)	Urea	8 M	
	Na_2HPO_4	94,7 %	0.1 M
	NaH_2PO_4	5,3 %	
	Tris/HCl (pH 8.0)	10 mM	
	Imidazole	20 mM	
	β-Mercaptoethanol	5 mM	
B3 (wash buffer pH 6.3)	Urea	8 M	
	Na_2HPO_4	22.5 %	0.1 M
	NaH_2PO_4	77.5 %	
	Tris-HCl (pH 8.0)	10 mM	
	Imidazole	20 mM	
	β-Mercaptoethanol	5 mM	
Elution buffer	Imidazole	200 mM	

SDS	0.1% (w/v)
Tris/HCl (pH 6.8)	150 mM
Glycerol	30 % (v/v)
β-Mercaptoethanol	720 mM
Bromophenol blue	0.01 % (w/v)

3.6.5 SDS polyacrylamide gel electrophoresis (SDS-PAGE)

SDS-PAGE was used for separation of protein samples, prepared as described in sections 3.6.1, 3.6.3 and 3.6.4, according to their molecular weights. *Multigel* chambers (*Biometra*) were assembled as described in the manufacturer manufacturer's protocol. Polyacrylamide gels were made by diluting 30% acrylamide/bisacrylamide solution to the final concentration of 8-15 % with Milli-Q water and Tris. SDS, APS and TEMED were added, solution was mixed, 7 ml was loaded in each assembled gel chamber and the solution was covered with isopropanol. After the separating gel polymerized, lower percentage stacking gel was loaded on top and the 24 pocket combs were inserted. After fixing the hardened gels into the in *Multigel* SDS chambers, the samples were loaded in pockets and the gels were run in TGS-buffer at 15 mA/gel. Protein weights were determined using *PageRulerTM plus prestained* protein ladder. The separated proteins were transferred to the nitrocellulose membranes by Western blotting.

Table 27: Composition of gels used for SDS-PAGE analysis.

5 % stacking gel	Acrylamide solution (30 %)	17 % (v/v)
	Tris/HCl (pH 6.8)	120 mM
	SDS	0.1 % (w/v)
	APS	0.1 % (w/v)
	TEMED	0.01 % (v/v)
8 % separating gel	Acrylamide solution (30 %)	27 % (v/v)
	Tris/HCl (pH 8)	250 mM
	SDS	0.1 % (w/v)
	APS	0.1 % (w/v)
	TEMED	0.04 % (v/v)
10 % separating gel	Acrylamide solution (30 %)	34 % (v/v)
	Tris/HCl (pH 8)	250 mM
	SDS	0.1 % (w/v)
	APS	0.1 % (w/v)
	TEMED	0.04% (v/v)

12 % separating gel	Acrylamide solution (30 %)	40 % (v/v)
	Tris/HCl (pH 8)	250 mM
	SDS	0.1 % (w/v)
	APS	0.1 % (w/v)
	TEMED	0.04 % (v/v)

Table 28: Composition of TGS buffer.

TGS buffer	Tris	25mM
	Glycine	200 mM
	SDS	0.1 % (w/v)

3.6.6 Western blot

Protein transfer to nitrocellulose membranes

Proteins were separated by SDS-PAGE, described in previous section, and transferred to 0.45 μm nitrocellulose membranes (*Whatman*) using *Trans-Blot® Cell* chamber, according to manufacturer's protocol, in Towbin-buffer. Gels were placed on membranes between four (two from each side) *Whatman* blotting papers and two blotting pads in a plastic cassette. The gels, membranes, blotting papers and pads were soaked in Towbin-buffer before use. Completely wet transfer from gel to membrane was done in blotting transfer chamber filed with Towbin-buffer at 400 mA for 45-90 min. After the transfer, membranes were incubated 1 h on room temperature in PBS with 5% (w/v) non-fat dry milk to block unspecific binding of antibodies for nitrocellulose membrane.

Antibody staining

After removing of blocking solution membranes were washed with PBS-Tween three times. Membranes were incubated overnight in appropriate PBS-Tween solution of primary antibodies at 4°C on reciprocating shaker (*GFL 3016*). After the incubation primary antibody solution was removed, the membranes were washed three times with PBS-Tween and incubated for 2-3 h at 4°C in 1:5000 – 1:10000 dilution of secondary antibodies conjugated to horseradish peroxidase (HRP) in 3 % (w/v) non-fat dry milk in PBS-Tween.

Protein visualization by enhanced chemiluminescence

The membranes were washed three times with PBS-Tween after discarding the secondary antibody. Protein bands were visualized by enhanced chemiluminescence using a mixture of 10

ml substrate ECL-A, 100 µl of substrate ECL-B and 10 µl H_2O_2 and detected by X-ray films (CEA) using an *Agfa Curix 60* developing machine. Developed films were labeled, scanned and processed using *Photoshop CS6* (Adobe) and *Illustrator CS6* (Adobe). Protein signals were quantified using *ImageJ* (Wayne Rasband) program.

Table 29: Composition of Towbin buffer and PBS-T.

Towbin buffer	Tris/HCl pH (8.3) Glycine SDS Methanol	25 mM 200 mM 0.05 % (w/v) 20 % (v/v)
PBS-Tween	Tween-20 in 1x PBS	0.1 % (v/v)

Table 30: Composition of ECL-A and ECL-B solutions.

ECL-A	Tris/HCl (pH 6.8) Luminol sodium	100 mM 250 µg/ml
ECL-B	p-Coumaric acid in DMSO	1.25 µg/ml

3.6.7 Indirect immunofluorescence

Cells grown on glass coverslips were transfected or infected according to the experimental setup. Cell fixation was performed with 2% paraformaldehyde (PFA) at RT for 20 min or with ice cold methanol for 15 min at -20°C. The cells were permeabilized with PBS containing 0.5 % (v/v) Triton X-100 for 10 min at RT. Unspecific interactions were blocked with 1 x TBS-BG buffer for 1-2 h at RT. Subsequently, coverslips were incubated for 1 h at RT with 25 µl of primary antibody diluted in PBS according to company's datasheets. After discarding the primary antibody, coverslips were washed three times with 1 x TBS-BG buffer and incubated with 25 µl of the corresponding secondary antibodies diluted in PBS (1:200) for 1 h on RT in dark and wet environment. Following the secondary antibody incubation, coverslips were washed three times in 1 x TBS-BG buffer, dried and fixed on glass slides with 10 µl Mowiol glowing solution. Digital images were acquired with a *Nikon TiE microscope* equipped with *Perkin Elmer UltraView Vox System*, and further analyzed using *Volocity 6.2.1* software (PerkinElmer). Colocalization of

examined proteins was analyzed by determining the *Pearson's correlation* coefficient. Average minimal distances between structures determined by experimental setup were measured in 2D. Images were cropped using *Photoshop CS6* (Adobe) and assembled with *Illustrator CS6* (Adobe).

Table 31: Composition of TBS-BG.

TBS-BG	Tris/HCl, pH 7.6	20 mM
	NaCl	137 mM
	KCl	3 mM
	$MgCl_2$	1.5 mM
	Tween-20	0.05% (v/v)
	Sodium Azide	0.05% (w/v)
	Glycine	5% (w/v)
	BSA	5% (w/v)

Table 32: Composition of Mowiol.

Mowiol	Glycerin	6 g
	Mowiol	2.4 g
	0.2 M Tris/HCl, pH 8.5	12 ml, 0.2 M
	DABCO	0.1% (v/v)

3.6.8 Pretreatment of cells using cytoskeleton wash buffer

In order to remove soluble cytoplasmic proteins and loosely held nuclear proteins cells grown on cover slips were treated with the cytoskeleton wash buffer (CSK buffer) prior to immunofluorescence studies described in section 3.6.7. Before CSK treatment, the media was removed, and cells were washed once with PBS. After the removal of PBS, the ice-cold CSK buffer supplemented with the TritonX-100 to final concentration of 0.5% was added to the cells. After 4 min of incubation in CSK buffer on ice, the buffer was removed. The cells were washed with PBS and fixed according to the protocol described in chapter 3.6.7.

Table 33: Composition of CSK buffer.

CSK buffer	NaCl	100 mM
	Sucrose	300 mM
	$MgCl_2$ * 6H2O	3 mM
	PIPES	10 mM
	NaOH	pH 6.8

4 Results

4.1 SUMO modification of HAdV E2A

4.1.1 HAdV E2A is a novel viral target for cellular SUMO conjugation machinery

SUMOylation is the posttranslational modification where SUMO covalently attaches of the to a lysine residue of a substrate protein. Adenoviruses use this host SUMOylation machinery to enhance viral replication and evade cellular immune responses (Wimmer and Schreiner 2015). PML-NBs are hot spots for SUMOylation processes (Ishov et al. 1999; Shen et al. 2006; Zhong et al. 2000). During HAdV infection, PML-NBs are located next to viral RCs marked by HAdV protein E2A (Puvion-Dutilleul, Pedron, and Cajean-Feroldi 1984). Therefore, we hypothesized that E2A could represent a novel SUMOylation target.

To reveal if E2A is modified by SUMO-2, HepaRG cells stably expressing His/HA-SUMO-2 were transfected with constructs encoding for wt E2A (Fig. 14). Ni-NTA-purified His-SUMO-2 conjugates were subjected to immunoblotting analysis that showed an E2A signal at 72 kDa and higher migrating protein bands (Fig. 14, right panel, lane 2). As covalent SUMO attachment to a substrate protein results in a 20 to 40 kDa increase in the molecular weight (Zhao et al. 2004), it was concluded that these higher migrating bands indeed correspond to SUMOylated moieties of E2A.

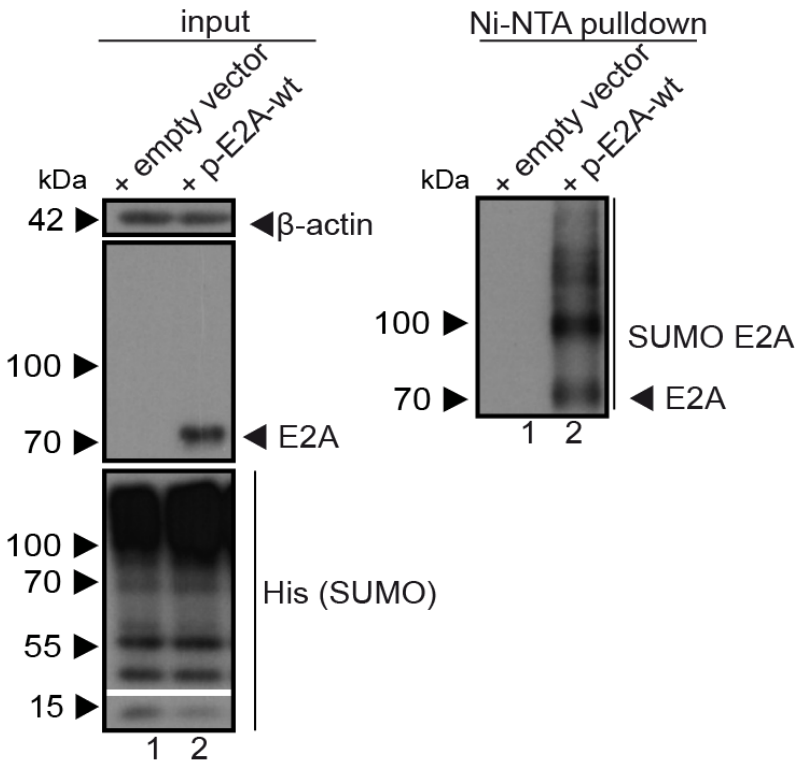

Figure 14: E2A is a novel substrate of the host cell SUMOylation machinery. HepaRG cells stably expressing His/HA-SUMO-2 were transfected with 5 µg of pE2A-wt. 30 h post transfection whole-cell lysates were prepared with guanidinium chloride buffer, subjected to Ni-NTA purification of His/HA-SUMO-2 conjugates and fractionated by SDS-PAGE before immunoblot analysis. Input levels of total cell lysates and Ni-NTA purified proteins were detected using mAb B6-8 (E2A), mAb 6-His (α-6xHis-tag) and mAb AC- 15 (α-β-actin). Molecular weights in kDa are indicated on the left, relevant proteins on the right.

4.1.2 Mutation of three SCMs in HAdV-C5 E2A reduces the attachment of SUMO

Data shown in section 4.1.1 demonstrate that E2A represents a novel target of the host SUMOylation machinery. Attachment of SUMO most frequently occurs at the consensus site ψKXE (ψ for a hydrophobic amino acid and X for any amino acid (Rodriguez, Dargemont, and Hay 2001). SUMO GPS software (Ren et al. 2009; Zhao et al. 2014) was used to detect lysine residues responsible for SUMO binding. All three SCMs identified in E2A do not correspond to classical consensus motifs, however it has been reported that SUMO can also attach to non-canonical motifs especially in the stress conditions (Hendriks and Vertegaal 2016; Pichler et al. 2017). Based on these findings, single SCM mutants pE2A-K94R, pE2A-K132R, pE2A-K202R were generated by exchanging the appropriate lysines for arginines by site-directed mutagenesis (Fig. 15). Additional double SCM mutant pE2A-K94/132R and triple SCM mutant pE2A-

K94/132/202R (pE2A-SCM) were created in order to achieve more complete reduction of E2A SUMOylation.

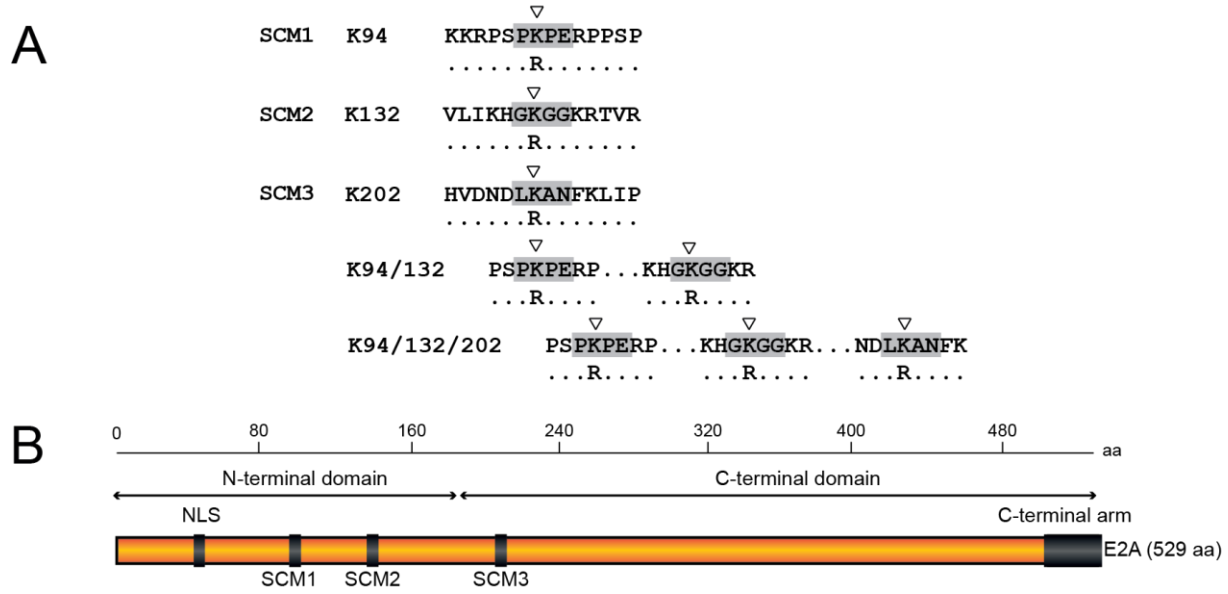

Figure 15: E2A harbors at least three SUMO conjugation motifs. (A) Amino acid sequences of possible SCMs in E2A. Arrow heads are pointing to the lysines which have been changed into arginines by site directed mutagenesis. (B) Schematic representation of E2A showing the locations of possible SCMs inside the E2A. Known protein domains are indicated by NLS (nuclear localization signal), N-terminal arm and C-terminal arm.

To investigate the effect of three SCM mutations on E2A SUMOylation, E2A wt and E2A SCM variants with Flag expressing epitopes were transfected into human cells stably expressing His-SUMO-2 (Fig. 16). Western blot analyses of Ni-NTA purified His-SUMO-2 conjugates revealed an E2A signal at 72 kDa and higher migrating protein bands, corresponding to SUMOylated moieties of the adenoviral protein (Fig. 16, right panel, lane 2). Moreover, less SUMO binding was detected to E2A K94R, K132R, K202R and pE2A-K94/132R, than to the wt protein (Fig. 16, right panel, lanes 3, 4, 5 and 6). Triple SCM mutant pE2A-K94/132/202R (pE2A-SCM) created to efficiently reduce SUMOylation of the viral factor, showed drastically diminished E2A SUMO conjugation (Fig. 16, right panel, lane 7), however a complete loss of SUMO PTM for the E2A protein was not observed.

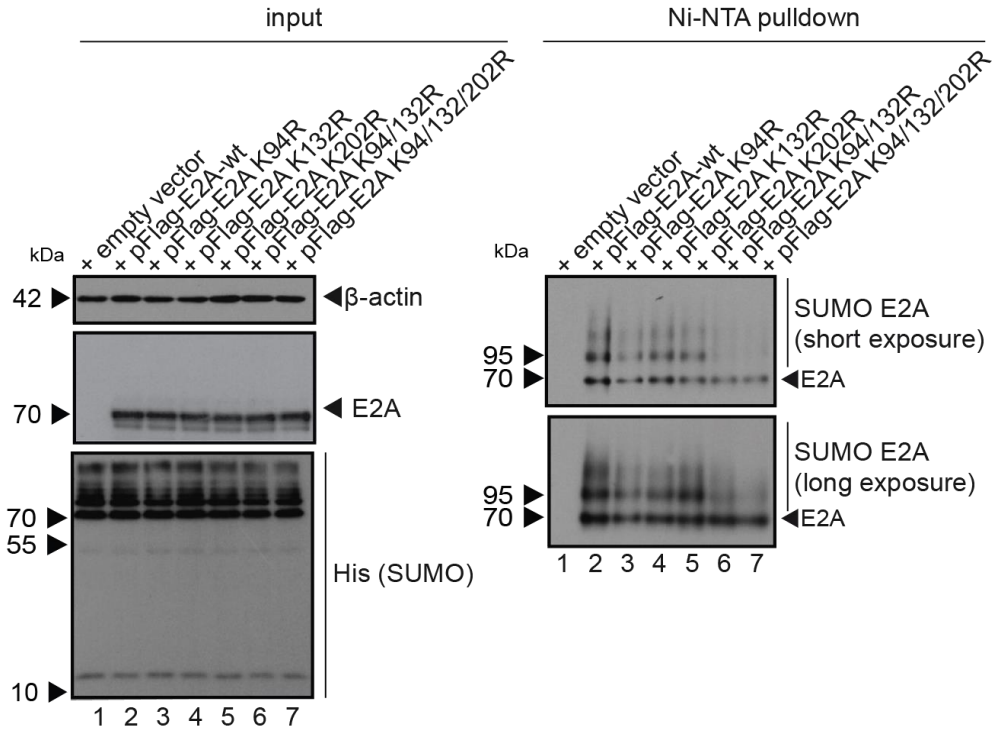

Figure 16: Validation of SCM mutations in the E2A open reading frame. HeLa cells stably expressing 6xHis-SUMO-2 were transfected with 5 µg of pCMX3b-Flag E2A (pFlag-E2A-wt) (lane 2) and pCMX3b-Flag E2A (pFlag-E2A) variants containing mutations in SCMs (lanes 3-7). The cells were harvested 48 h after transfection. Ni-NTA purification of 6xHis-SUMO conjugates was performed with whole-cell lysates prepared with guanidinium chloride buffer. After separation by SDS-PAGE, the samples were subjected to immunoblot analyses. Ni-NTA purified proteins and input levels of cell lysates were detected using mAb B6-8 (α-E2A), mAb 6-His (α-6xHis-tag) and mAb AC-15 (α-β-actin). Molecular weights in kDa are indicated on the left, relevant proteins on the right.

4.1.3 Ubc9 is essential to conjugate SUMO moieties to E2A

SUMOylation is a three-step enzymatic reversible pathway (Hay 2007; Johnson 2004). Ubc9 is the main SUMO conjugating enzyme of this process. Ubc9 enables the direct SUMO binding to the SCMs within the target proteins (Desterro, Thomson, and Hay 1997; Okuma et al. 1999). E3 SUMO ligases maintain SUMO and Ubc9 in a favorable relative orientation leading to the formation of an isopropyl bond between the C-terminal di-glycine residues of SUMO and an ε-amino group of a lysine residue within target SCM (Rodriguez, Dargemont, and Hay 2001). However, even though E3 enzymes facilitate the SUMO conjugation, they are contrary to Ubc9, not essential for the process (Bernier-Villamor et al. 2002; Seeler and Dejean 2003). HAdVs exploit the cellular SUMO conjugation pathway to promote viral infection using different mechanisms (Wimmer and Schreiner 2015). Three HAdV proteins were shown to directly interact with Ubc9. HAdV early protein E1A interferes with polySUMOylation via Ubc9 binding (Yousef

et al. 2010). Additionally, E4orf3 has been recently reported as novel Ubc9 interaction partner (Sohn and Hearing 2019). E1B-55K also binds to Ubc9. Interestingly, this interaction occurs on an E1B-55K SUMOylation independent manner (Wimmer et al. 2013).

HAdV E2A is a target of host SUMOylation machinery (4.1.1). To further investigate if Ubc9 interacts with E2A and thus serves as a SUMO conjugating enzyme for E2A, human cells were transfected with GFP tagged pE2A-wt and pE2A-SCM plasmids. Immunoprecipitation analysis of GFP tagged E2A followed by staining for endogenous Ubc9 revealed binding of E2A to Ubc9 (pGFP-E2A-wt; Fig. 17, right panel, lane 2). Moreover, this interaction was absent in samples prepared from cells transfected with the triple SCM mutant pE2A-K94/132/202R (pGFP-E2A-SCM; Fig. 17, right panel, lane 3). This data and the fact that the attachment of SUMO moieties to E2A showed the highest reduction in cells transfected with pE2A-SCM (Fig. 16, right panel, lane 7), prompted the usage of this variant in further investigations on the role of E2A SUMO PTM.

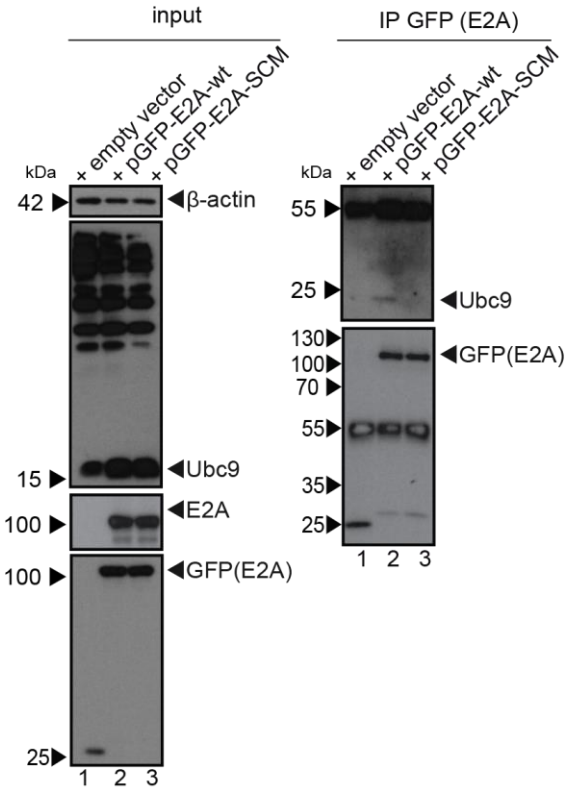

Figure 17: E2A interacts with Ubc9 on an E2A SUMOylation-dependent manner. 5 µg of pGFP-E2A-wt (lane 2) and pGFP-E2A-SCM (lane 3) was transfected into H1299 cells. Cells were harvested after 30 h and total-cell lysates were prepared. Immunoprecipitation was performed using pAb ab290 (α-GFP) and proteins were subjected to immunoblot analyses. Input levels of total-cell lysates and co-precipitated proteins were detected using mAb B6-8 (α-E2A), pAb ab290 (α-GFP), mAb C-12 (α-Ubc9) and mAb AC-15 (α-β-actin). Molecular weights in kDa are indicated on the left, relevant proteins on the right.

4.1.4 E2A SCM does not influence E2A ubiquitinylation

SUMO and ubiquitin PTM are posttranslational modifications that use similar three-step enzymatic cascade. Moreover, it is known that SUMO and ubiquitin can often compete for the same lysine residues within the conjugation motifs (Hay 2007; Johnson 2004). Those two processes are also connected by the process of SUMO-dependent ubiquitinylation, that involves specific ubiquitin ligases that recognize SUMO modified proteins, SUMO-targeted ubiquitin ligases (STUbLs) (Miteva et al. 2010).

To ensure that E2A SCM mutations do not affect Ubiquitin PTM, human cells were transfected with pE2A-wt and pE2A-SCM together with His-Ubiquitin (p6xHis-Ubi) (Fig. 18). Western blot analyses of Ni-NTA purified His-Ubi conjugates and total-cell lysates revealed a similar Ubiquitin PTM above 72 kDa, when E2A was detected with specific antibody after Ni-NTA purification (Fig. 18, right panel, lanes 5 and 6). This data led to the conclusion that E2A SCMs do not affect E2A ubiquitinylation.

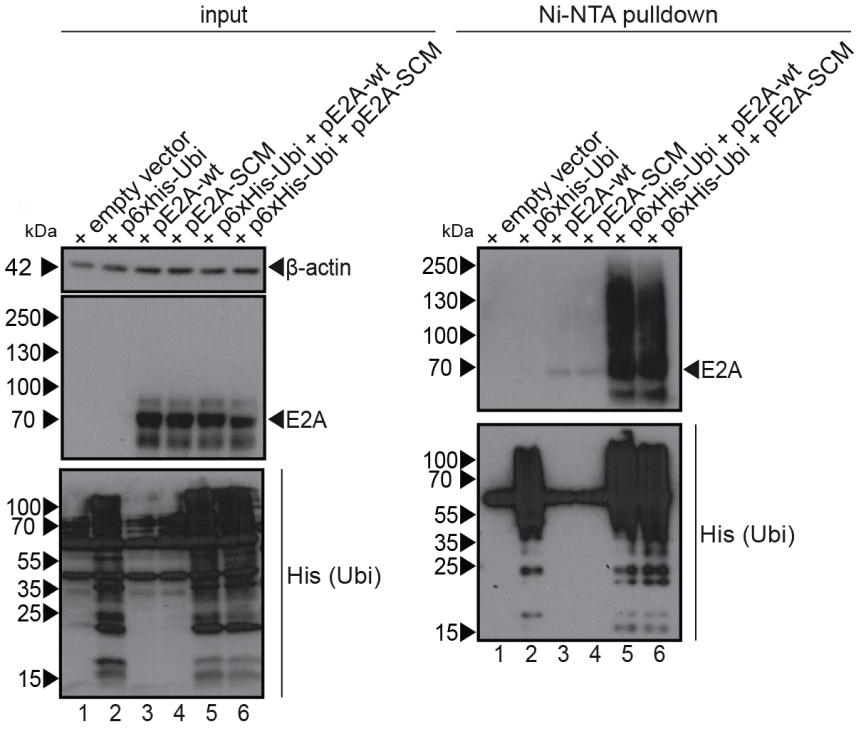

Figure 18: **E2A ubiquitinylation does not depend on E2A SUMO conjugation.** 10 µg of p6xHis-Ubi and 5 µg of pE2A-wt or pE2A-SCM was transfected in H1299 cells. Cells were harvested 30 h after transfection and whole-cell lysates were prepared with guanidinium chloride buffer. Ni-NTA purified 6xHis-SUMO conjugates were separated by SDS-PAGE and subjected to immunoblot analyses using mAb B6-8 (α-E2A), mAb 6-His (α-6xHis-tag) and mAb AC-15 (α-β-actin). Molecular weights in kDa are indicated on the left, relevant proteins on the right.

4.1.5 Generation of replication-competent E2A SCM HAdV-C5 virus mutant

The functions of single proteins in adenovirus infection can be reliably studied by generation of mutant adenoviruses. This approach involves two plasmid systems cloned in bacterial expression vectors by restriction site insertions. Small region-specific plasmid (L4-Box) was used for insertion of point mutations and ligated into a large viral bacmid to generate the 36 kb linear genome of adenoviruses containing desired mutations (Groitl and Dobner 2007). Required mutations can be easily inserted into small boxes using site-directed mutagenesis as described in the methods section (3.4.5). The mutated boxes are then cloned back into the viral genome.

To investigate the role of E2A SUMOylation during adenoviral infection, a mutant virus simulating the mutant pE2A-SCM construct was generated. Lysine residues K94/132/202 were exchanged by site-directed mutagenesis (3.4.5) into arginines to reduce SUMOylation of the viral protein (Fig. 19). The HAdV-C5 late region L4 from nt 21438-27081 (pL41513) was used for insertion of mutations into the E2A gene by site-directed mutagenesis, while plasmid Ad5bac wt-E3 (pHAdV wt) served as the DNA backbone to clone the mutations into the HAdV-C5 genome. L4 region from the pHAdV wt was enzymatically cleaved and exchanged by L4 region with inserted mutations cleaved away from the pTUM-4 part of the pL41513 plasmid. Subsequently, PacI digestion was used to release the viral DNA from the recombinant plasmid. To generate HAdV E2A SCM mutant virus, the viral DNA with appropriate mutations was transfected into H1299 cells. The viral progeny was amplified (3.3.1, 3.3.2), viral DNA was analyzed by restriction pattern analysis (3.4.6.1) and DNA sequencing (3.4.7).

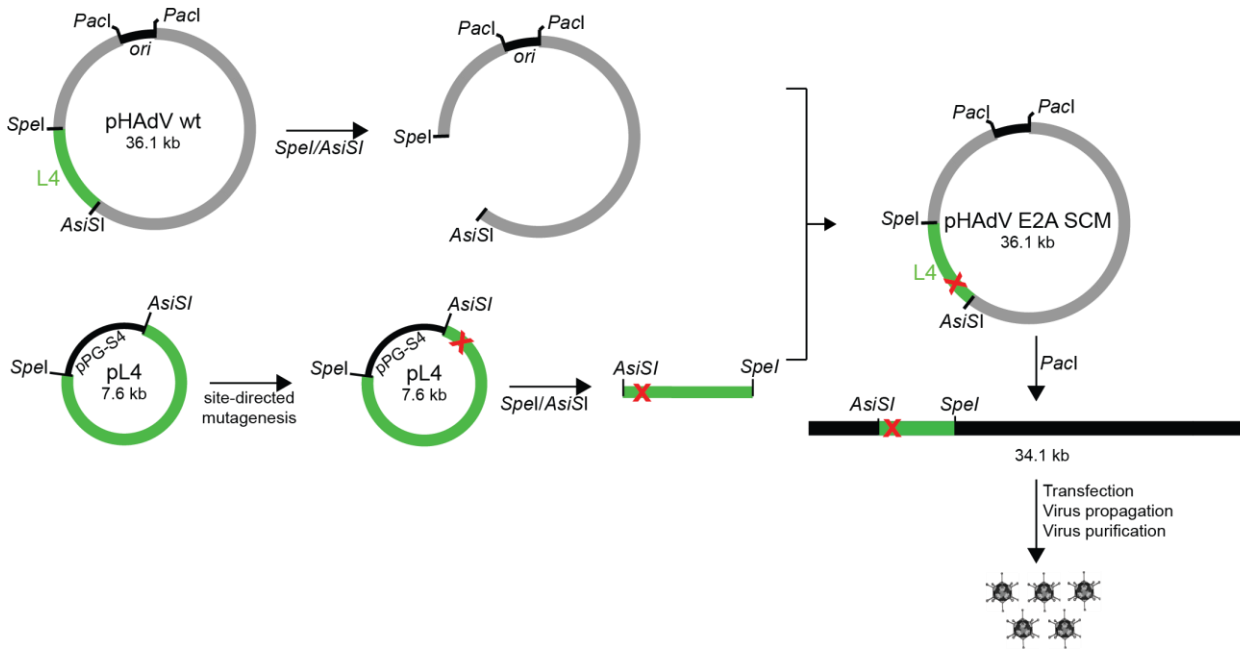

Figure 19: Generation of E2A SCM mutant virus. Point mutations were inserted into the e2a gene in the late HAdV region L4 from nt 21438-27081 (pL41513) using site-directed mutagenesis. The L4 plasmid and bacmid pHAdV wt were linearized by AsiSI and SpeI digestion. The 5.6 kb AsiSI/SpeI fragment from pHAdV wt was replaced with the corresponding fragment from the mutated pL4 construct. The viral genome was released by PacI digestion and used to transfect H1299 cells followed by virus propagation and isolation.

4.1.6 SCM mutant shows reduced E2A SUMO conjugation during infection

Experiments described in section 4.1.2 showed the strongest reduction of E2A SUMOylation when all three E2A SCMs were mutated. To increase the possibility of detectible E2A functional changes during HAdV infection, the triple E2A SCM mutant virus (HAdV E2A SCM) bearing lysine mutations in all three SCMs was generated. Therefore, detectable effects in further experiments can either be a joint result of the three mutations or a consequence of a single mutated SCM. The first step in characterization of the newly generated HAdV E2A SCM virus was to examine the pattern of E2A SUMO modification during E2A SCM mutant virus infection in comparison to wt adenovirus (HAdV wt) infection.

Analyses of Ni-NTA purified samples from infected HepaRG His/HA SUMO-2 cells revealed the reduction of E2A SUMO chains during infection with HAdV E2A SCM compared to HAdV wt infection (Fig. 20 A, right panel, lanes 5 and 6). E2A SUMOylation in E2A SCM mutant infected cells was 70 % less compared to HAdV wt infection (Fig. 20 B). These results concurred with the transfection experiments shown in section 4.1.2. This data confirmed E2A as a novel viral target of the cellular SUMO conjugation machinery and showed that triple SCM mutation of

K94/132/202 efficiently reduced but not completely abolished E2A SUMOylation during infection.

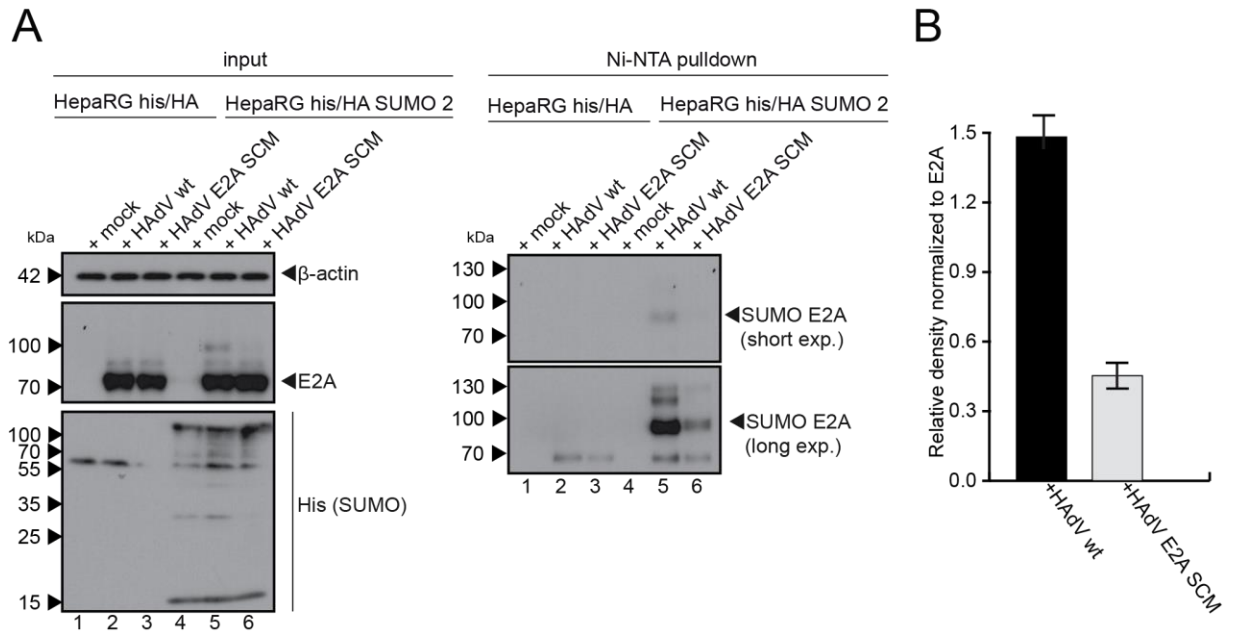

Figure 20: Validation of E2A SCM mutant virus. (A) HepaRG cells stably expressing His/HA or His/HA-SUMO-2 were infected with HAdV wt and HAdV E2A SCM mutant at a multiplicity of 20 FFU/cell. Harvesting was done 24 h p.i., whole-cell lysates were prepared with guanidinium chloride buffer, subjected to Ni-NTA purification of 6xHis-SUMO conjugates and separated by SDS-PAGE. Input levels of total-cell lysates and Ni-NTA purified conjugates were detected with mAb B6-8 (α-E2A), mAb 6xHis (α-6xHis-tag) and mAb AC-15 (α-β-actin). Molecular weights in kDa are indicated on the left, relevant proteins on the right. **(B)** Densitometric analysis of E2A SUMOylation levels in panel A (lanes 5 and 6), quantified with ImageJ (version 1.45s) software, normalized to the respective steady state E2A levels in HAdV wt and HAdV E2A SCM infected cells. Bar plot represents average values and standard deviations calculated based on three separate experiments.

4.2 The influence of E2A SUMOylation on efficiency of HAdV infection

4.2.1 E2A SUMOylation supports HAdV progeny production

Due to essential E2A functions in viral DNA replication (Hay et al. 1995; Schilling, Weingartner, and Winnacker 1975; van Breukelen et al. 2003; van Breukelen et al. 2000) as well as virion assembly (Ahi, Vemula, and Mittal 2013) and maturation (Nicolas et al. 1983), E2A SUMOylation effects on production of adenoviral progeny were investigated. Therefore, virus yield experiments (3.3.5) were performed in HepaRG cells infected with HAdV wt and HAdV E2A SCM viruses. The results obtained in these experiments revealed that progeny production depends on E2A SUMOylation at all three time points examined post infection. Compared to HAdV wt infection, a 62% reduction in viral progeny production was observed 24 h after infection

with HAdV E2A SCM virus. When compared to HAdV wt infection, production of viral progeny during HAdV E2A SCM infection was reduced by 41% after 48 h and reached 50% after 72 h (Fig. 21).

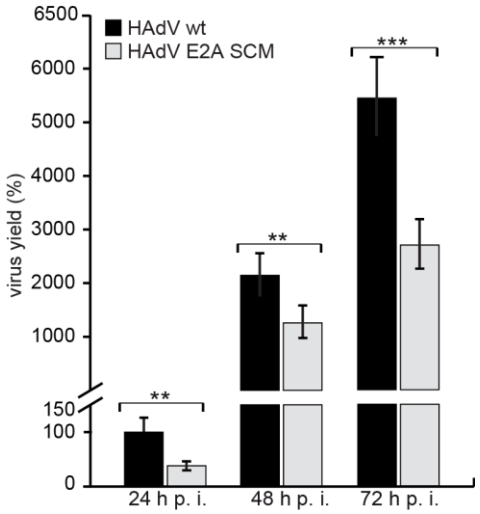

Figure 21: Viral progeny production is reduced during infection with E2A SCM mutant virus. Viral particles were harvested 24, 48 and 72 h p.i. and virus yield was determined by quantitative capsid immunofluorescence staining in 2E2 cells. Two-sided Mann-Whitney test was used to determine statistically significant differences.

4.2.2 E2A SUMOylation does not alter DNA binding capacity of the viral protein

E2A is HAdV DNA binding protein that interacts with single-stranded DNA (van der Vliet and Levine 1973), double-stranded DNA (Fowlkes et al. 1979) and RNA (Cleghon and Klessig 1986) on a sequence unspecific manner. SUMOylation has an ability to alter protein role through effects on various properties of its substrates (Hendriks and Vertegaal 2016). These facts and the above-mentioned finding showing importance of E2A SUMOylation for efficient progeny production (4.2.1), prompted the examination of E2A SUMO conjugation effects on E2A binding to the viral genome (Fig. 22).

ChIP assays were performed from cells transfected with pFlag-E2A-wt and pFlag-E2A-SCM constructs and subsequently infected with HAdV wt and HAdV E2A SCM, respectively. Mouse anti-Flag M2 antibody (Sigma-Aldrich, F3165), or normal mouse IgG (Sigma-Aldrich, I5381) was used for immunoprecipitation of the sheared chromatin 24 h post infection. A set of loci within the viral genome (P1, P3, P7, P11, P16) was selected to investigate E2A binding across the HAdV genome. The percentage of output versus input DNA was calculated and the obtained

results, demonstrated remarkably uniform distribution of E2A across all viral regions investigated, independent of E2A SUMO conjugation (Fig. 22).

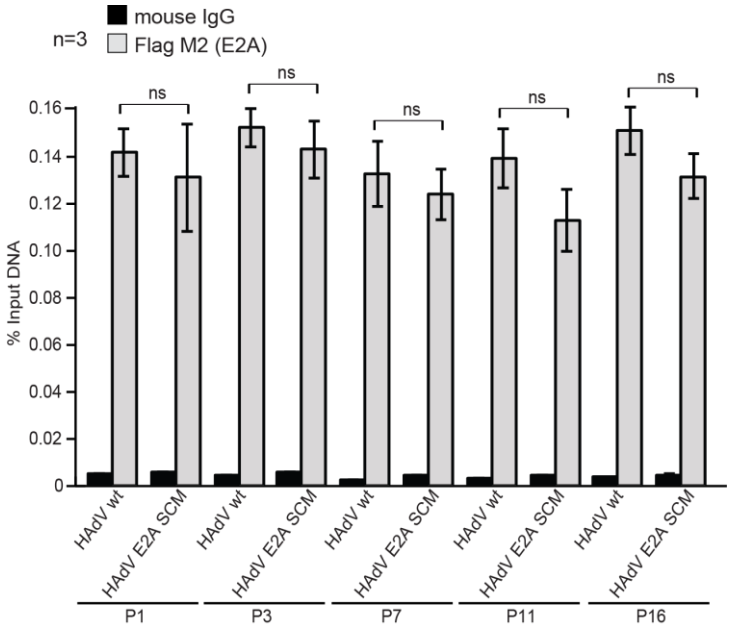

Figure 22: E2A SUMOylation does not affect the DNA binding of the viral protein. HepaRG cells were transfected with pFlag-E2A-wt or pFlag-E2A-SCM and infected after 4 h with the corresponding HAdV wt or HAdV E2A SCM at a multiplicity of 20 FFU/cell. 24 h after infection cells were subjected to ChIP with an antibody to the Flag epitope tag or normal mouse IgG and primers specific for five indicator loci in the HAdV genome (P1, P3, P7, P11, P16). The percentage of output versus input DNA was calculated and values are given as the mean ± standard deviation of three biological replicates. Student t tests were used to determine statistical significance.

4.2.3 E2A SUMOylation does not affect HAdV DNA replication

E2A performs various functions during HAdV life cycle, but the main function contributed to this protein is in viral DNA replication (Hay et al. 1995; Schilling, Weingartner, and Winnacker 1975; van Breukelen et al. 2003; van Breukelen et al. 2000). E2A is involved both in initiation (van Breukelen et al. 2003) and elongation phase of DNA replication (Monaghan, Webster, and Hay 1994; Zijderveld, Stuiver, and van der Vliet 1993). Due to this essential function E2A is termed as marker protein for viral replication centers (Puvion-Dutilleul, Pedron, and Cajean-Feroldi 1984). The data described in previous section (4.2.2) showed that E2A binding to DNA does not depend on SUMO modification of the viral protein. However, the fining from the virus yield experiment (4.2.1) demonstrating importance of E2A SUMOylation for HAdV progeny production suggest that the replication of HAdV DNA might be affected by this E2A PTM. To

test this hypothesis, viral DNA synthesis was monitored in E2A wt versus E2A SCM virus infected cells (Fig. 23). Interestingly, this data was consistent with the results observed when E2A binding to was DNA monitored (4.2.2) and there was no difference between the samples for each independent time point post infection.

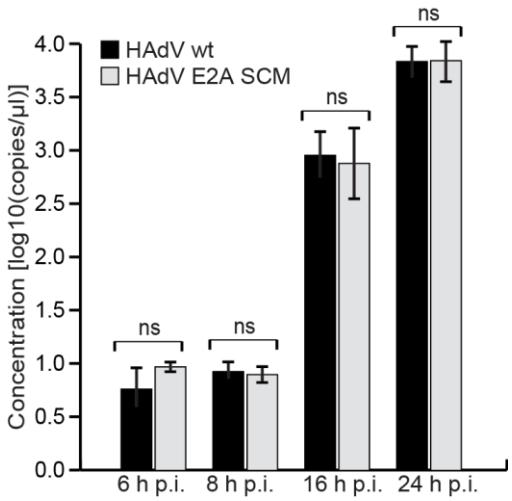

Figure 23: HAdV DNA replication does not depend on E2A SUMOylation. HepaRG cells were infected with HAdV wt or HAdV E2A SCM mutant at a multiplicity of 20 FFU/cell and harvested at indicated time points post infection. Genomic DNA was isolated from the cells and amplified by RT-PCR with primer pairs specific for an HAdV-C5 hexon. Standard curve with known concentrations of HAdV bacmid DNA was used to determine concentration of viral DNA. Statistics were calculated using a student´s t test.

4.2.4 E2A SUMOylation promotes HAdV protein synthesis

Even though E2A SCM mutations did not impair its function in HAdV DNA replication (4.2.3), the data described in section 4.2.1 demonstrated the requirement for this E2A PTM for efficient production of the viral progeny.

In order to analyze the behavior of adenoviral proteins during HAdV E2A SCM mutant virus infection compared to HAdV wt infection, time course experiment was performed in HepaRG cells. The cells were harvested 16 to 96 h after infection, lysed and subjected to immunoblot analysis (Fig. 24). The E1A protein levels, including all the splice forms of the viral protein, were strongly reduced during HAdV E2A SCM infection when compared to HAdV wt infection in all timepoints examined (Fig. 24, lanes 5 and 6, 8 and 9, 11 and 12, 14 and 15, 17 and 18). As E1A has the ability to enhance the transcription of different HAdV proteins it could be expected that also certain viral proteins be expressed to a lower extent than during HAdV wt infection. Interestingly, E2A SCM mutations did not affect E2A protein expression during HAdV E2A SCM infection (Fig. 24, lanes 5 and 6, 8 and 9, 11 and 12, 14 and 15, 17 and 18). Moreover,

the protein levels of the two main HAdV constituents of the viral ubiquitin ligase complex, E1B-55K and E4orf6 (Blanchette et al. 2004; Querido et al. 2001; Schreiner, Wimmer, and Dobner 2012), were not strongly affected by E2A SCM mutations (Fig. 24, lanes 5 and 6, 8 and 9, 11 and 12, 14 and 15, 17 and 18). Intriguingly, splicing of the two proteins was defective, namely E1B-156R, E1B-93R, E1B-84R and E4orf6/7 (Fig. 24, lanes 5 and 6, 8 and 9, 11 and 12, 14 and 15, 17 and 18) levels were strongly reduced during infection with E2A SUMOylation deficient virus. Furthermore, the levels of early HAdV protein E4orf3, involved in disruption of PML-NBs, were less in HAdV E2A SCM infection compared to HAdV wt infection in all examined time points (Fig. 24, lanes 5 and 6, 8 and 9, 11 and 12, 14 and 15, 17 and 18). Contrary to the data showing that E2A SUMOylation does not affect HAdV DNA replication (4.2.3), protein levels of two proteins involved in this process, HAdV polymerase (Fig. 24, lanes 14, 15 and 17, 18) and terminal protein (TP) (Fig. 24, lanes 14, 15 and 17, 18) were reduced during HAdV E2A SCM infection, compared to HAdV wt. Additionally, the reduction in levels of possible splice form of HAdV polymerase was also noted (Fig. 24, lanes 14, 15 and 17, 18). In case of TP, reduction of pre-terminal protein levels (pTP) in late time point of infection was detected (Fig. 24, lanes 17 and 18). The levels of proteins that are known to form HAdV DNA packaging complex together with E2A, IVa2 and L4-33K (Ahi, Vemula, and Mittal 2013) were also examined. IVa2 protein levels were not different in cells infected with HAdV E2A SCM virus when compared to HAdV wt infected cells (Fig. 24, lanes 5 and 6, 8 and 9, 11 and 12, 14 and 15, 17 and 18). Intriguingly, the protein levels of L4-33K were reduced only to a moderate extent, but the higher migrating band indicating possible PTM of the viral protein, was less pronounced during infection with HAdV E2A SCM mutant compared to HAdV wt infection (Fig. 24, 11 and 12, 14 and 15, 17 and 18). The levels of another protein expressed from MLTU, L4-100K, showed modest reduction in cells infected with HAdV E2A SCM, compared to HAdV wt infected cells (Fig. 24, lanes 5 and 6, 8 and 9, 11 and 12, 14 and 15, 17 and 18). Finally, reduced amount of HAdV Capsid protein expression during E2A SCM mutant virus infection compared to HAdV wt was observed (Fig. 24, lanes 5 and 6, 8 and 9, 11 and 12, 14 and 15, 17 and 18).

Observed reduction of certain HAdV protein levels during infection with E2A SUMOylation deficient virus as well as possible implications of E2A SUMOylation on HAdV gene splicing is in accordance with the virus yield data.

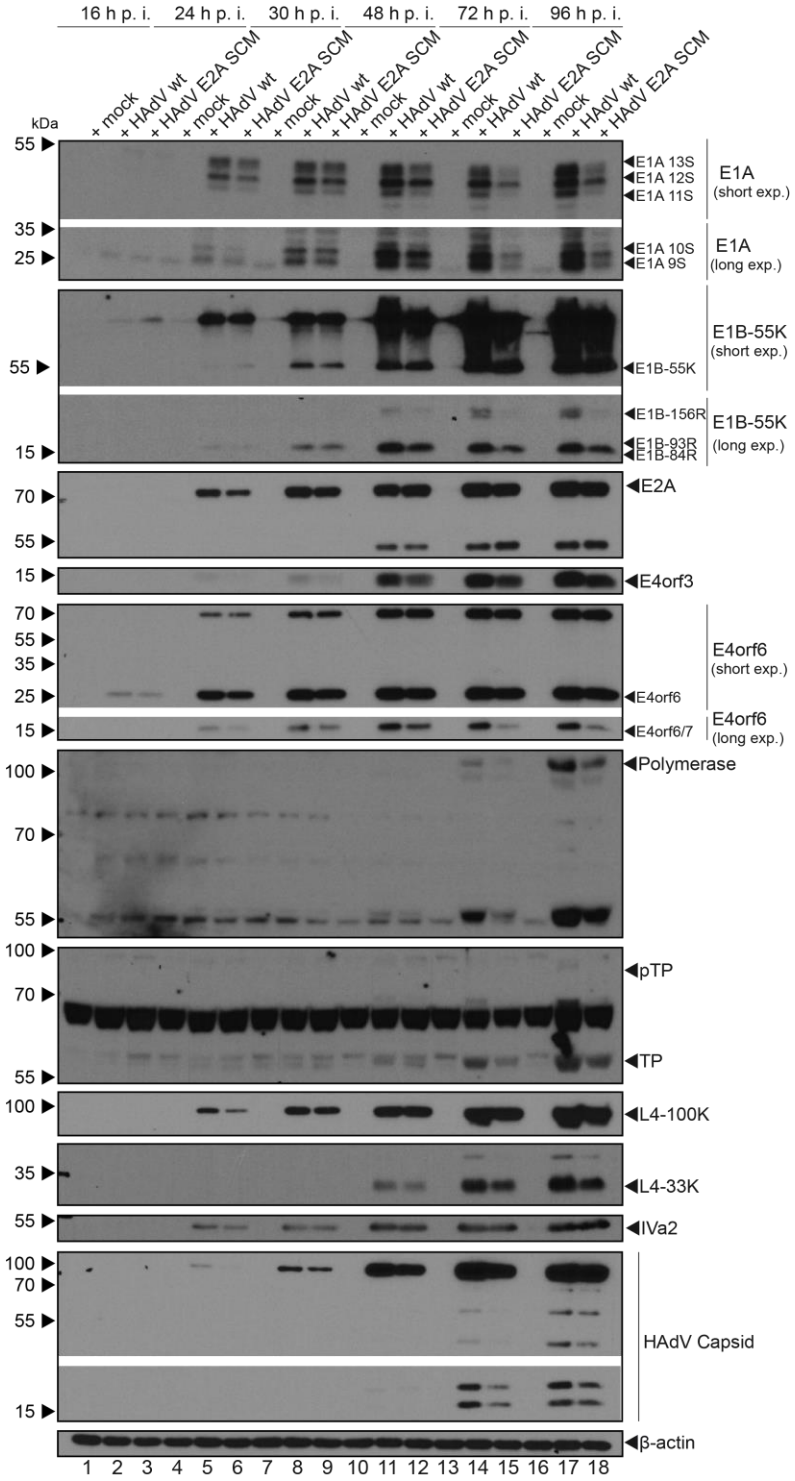

Figure 24: E2A SUMOylation is needed for efficient HAdV protein synthesis. HepaRG cells were harvested at 16, 24, 30, 48, 72 and 96 h after infection with HAdV wt and HAdV E2A SCM at a multiplicity of 20 FFU/cell. Total cell lysates were separated by SDS-PAGE and subjected to immunoblotting using following antibodies: mAb M73 (α-E1A), mAb 2A6 (α-E1B-55K), mAb B6-8 (α-E2A), mAb 6A11 (α-E4orf3), mAb RSA3 (α-E4orf6), mAb 6B10 (α-L4-100K), α-Ad5-Pol (α-Pol), α-Ad5-pTP (α-pTP/TP), α-Ad5-L4-33K (α- L4-33K), α-Ad5-IVa2 (α-IVa2), pAb L133 (α-capsid) and mAb AC-15 (α-β-actin). Molecular weights in kDa are indicated on the left, relevant proteins on the right.

4.2.5 E2A SUMOylation promotes late but not early HAdV mRNA synthesis

E2A is involved in regulation of viral gene expression (Carter and Blanton 1978), mRNA stability (Babich and Nevins 1981) and splicing of late viral mRNAs (Anderson 1981; Anderson and Klessig 1984; Kruijer, van Schaik, and Sussenbach 1981). These facts and the data described in previous section, showing promoting effect of E2A SUMOylation on protein synthesis of various HAdV proteins and their splice forms prompted the investigation of the influence of E2A SUMOylation on early and late HAdV mRNA production (Fig. 25).

HepaRG cells were infected either with HAdV wt or HAdV E2A SCM mutant virus and harvested 30 h after infection. Total RNA was isolated and reversely transcribed as described in (3.5.1 and 3.5.2). The resulting cDNA was amplified by RT-PCR (3.5.3) with primer pairs matching E1A and Hexon regions of the adenoviral genome. Contrary to the data demonstrating stimulating effect of E2A SUMO PTM on E1A protein synthesis, we did not detect significant difference in E1A mRNA expression during infection with HAdV E2A SCM mutant virus, compared to HAdV wt infection (Fig. 25 A). However, consistent with the virus yield (4.2.1) and late HAdV protein synthesis data (4.2.4), the Hexon mRNA levels in cells infected with HAdV E2A SCM mutant virus were 3.4 times less when compared to HAdV wt infected cells (Fig. 25 B).

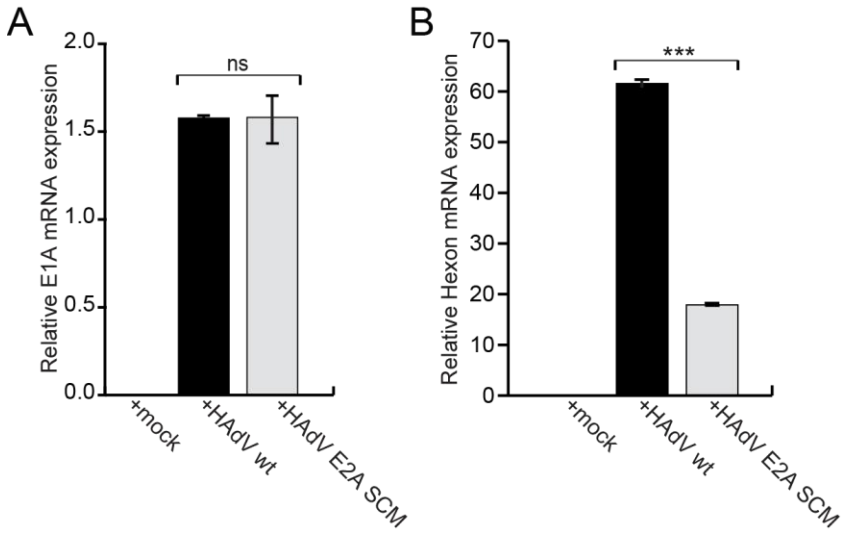

Figure 25: E2A SUMOylation supports late but not early HAdV mRNA production. HepaRG cells were infected ether with HAdV wt or HAdV E2A SCM virus at a multiplicity of 20 FFU/cell and harvested 30 h p.i. Total RNA was extracted, reverse transcribed and quantified by RT-PCR using primers specific for HAdV E1A **(A)** and Hexon **(B)**. The data was normalized to respective GAPDH mRNA levels. Statistics were calculated using a student´s t test.

4.3 Interaction of HAdV E2A with PML-NBs

HAdV RCs, marked by viral protein E2A (Puvion-Dutilleul, Pedron, and Cajean-Feroldi 1984) are located juxtaposed to PML-NBs which are reorganized into tracks by the virus (Doucas et al. 1996; Everett 2001; Ishov and Maul 1996; Jul-Larsen et al. 2004; Maul 1998; Maul, Ishov, and Everett 1996). Antiviral activity of PML-NBs is suppressed by disruption into tracks. Moreover, components of PML-NBs that negatively influence HAdV gene expression are either degraded by the HAdV E3 ubiquitin ligase complex (Berscheminski et al. 2013; Schreiner, Burck, et al. 2013; Schreiner, Kinkley, et al. 2013; Schreiner, Wimmer, and Dobner 2012; Schreiner et al. 2011; Schreiner et al. 2010) or inactivated by displacement into the interior of HAdV RCs (Berscheminski et al. 2014). HAdVs exploit certain components of PML-NBs to their benefit, but only when these factors are retained in PML tracks in close vicinity to RCs where active viral transcription takes place (Berscheminski et al. 2014; Berscheminski et al. 2013). PML-NBs are designated hotspots for SUMOylation processes (Van Damme et al. 2010). SUMOylation affects protein/protein interactions and subcellular localization of its substrates (Hendriks and Vertegaal 2016) and it is known that PML-NBs interact with SUMOylated proteins (Ishov et al. 1999; Shen et al. 2006; Zhong et al. 2000). HAdV E2A is a target of the SUMO conjugation machinery (4.1.1) and the virus benefits from this E2A PTM (4.2.1). Therefore, it was investigated whether E2A interacts with PML and if E2A SUMOylation plays a role in in the positioning of PML tracks in proximity to viral RCs. Additionally, the influence of E2A SUMO PTM on the ability of the virus to simultaneously counteract antiviral activity of PML-NBs and exploit their transcription activating components was also examined.

4.3.1 Interaction of HAdV E2A with PML

4.3.1.1 Transfected E2A binds PML independently on E2A SUMOylation

SUMOylation regulates the protein/protein interactions of its substrates in cells (Dohmen 2004; Hendriks and Vertegaal 2016). As the scaffold protein of PML-NBs, PML preferentially recruits SUMO modified proteins through SUMO/SIM interactions (Van Damme et al. 2010). Therefore, it was examined if E2A interacts with PML and whether SUMOylation of E2A affects this interaction independently of any other viral component (Fig. 26).

HepaRG cells were transfected with E2A encoding plasmid pE2A-wt and pE2A-SCM and subjected to immunoprecipitation analysis with PML-specific antibody (Fig. 26 A, right panel, lanes 3 and 4). The interaction between E2A and PML, without the viral background, that was not dependent on E2A SUMOylation was detected after examining PML bound proteins (Fig. 26 A, B).

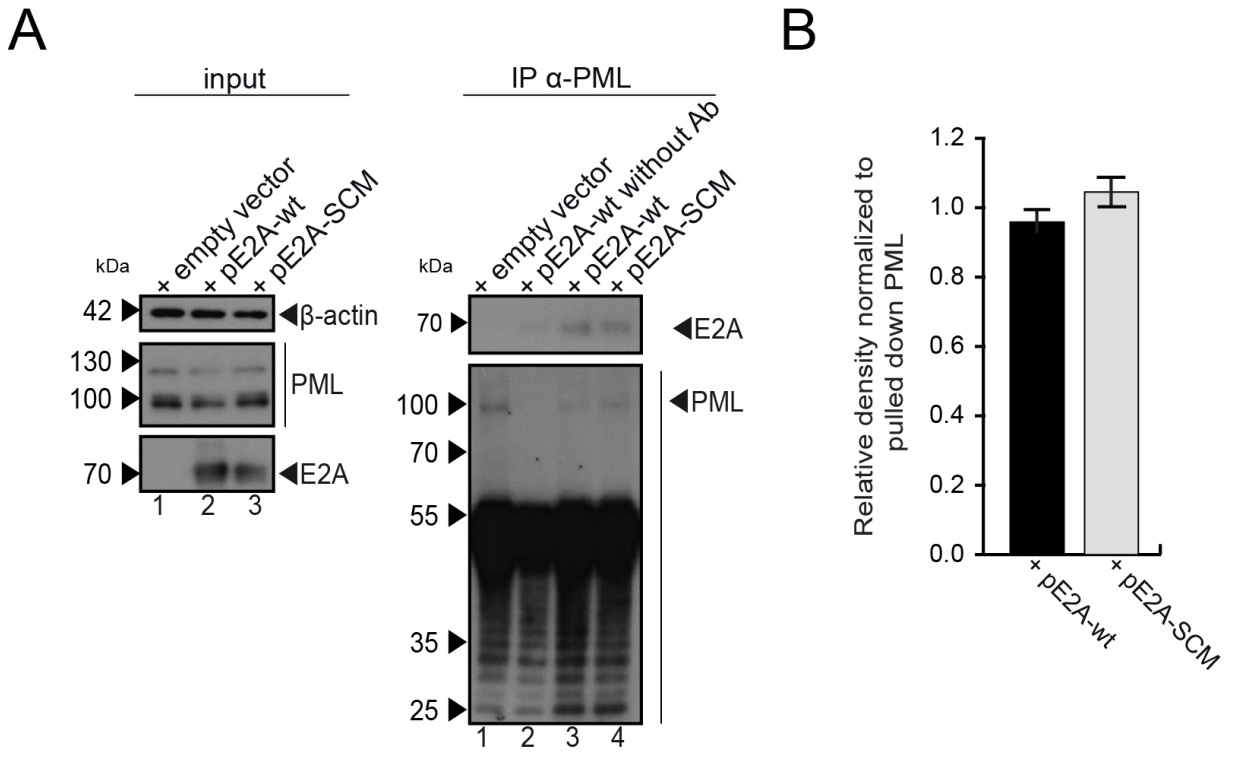

Figure 26: E2A SUMOylation does not affect E2A/PML binding transient transfection. (A) HepaRG cells were transfected with 5 µg of pE2A-wt (lane 2) and pE2A-SCM (lane 3) and harvested 30 h after transfection. Total cell lysates were prepared and subjected to immunoprecipitation of PML using polyclonal rabbit antibody raised against PML protein pAb NB100-59787 (α-PML). Proteins were resolved by SDS-PAGE and visualized by immunoblotting. Input levels of total-cell lysates and coprecipitated proteins were detected using mAb B6-8 (α-E2A), pAb NB100-59787 (α-PML) and mAb AC-15 (α-β-actin). Molecular weights in kDa are indicated on the left, relevant proteins on the right. **(B)** Densitometric analyses of E2A immunoprecipitated with PML in panel A (lanes 3 and 4) quantified with ImageJ (version 1.45s) software, normalized to respective levels of immunoprecipitated PML in pE2A-wt and pE2A-SCM transfected cells. Bar plot represents average values and standard deviations calculated based on data obtained in three independent experiments.

4.3.1.2 SUMOylated E2A binds PML during HAdV infection

E2A is termed as marker protein HAdV RCs (Puvion-Dutilleul, Pedron, and Cajean-Feroldi 1984), located next to PML-NBs which are reorganized into tracks during HAdV infection (Doucas et al. 1996; Everett 2001; Ishov and Maul 1996; Jul-Larsen et al. 2004; Maul 1998; Maul, Ishov, and Everett 1996). It is known that PML-NBs interact with SUMOylated proteins (Ishov et

al. 1999; Shen et al. 2006; Zhong et al. 2000). However, the data described above (4.3.1.1), showed that E2A interacts with PML, independently on E2A SUMO conjugation in the absence of other viral components.

To investigate the influence of E2A SUMOylation on E2A/PML interaction during HAdV infection and to ascertain any difference in E2A/PML binding capacity due to E4orf3-mediated loss of PML-NB integrity, immunoprecipitation of PML from cells infected with HAdV wt, HAdV E2A SCM or HAdV ΔE4orf3 viruses was performed (Fig. 27). Immunoblot analysis revealed that E2A interaction with PML during infection depends on E2A SUMO PTM (Fig. 27 A, right panel, lanes 3 and 4 and Fig. 27 B). E2A binding to PML was decreased by 71.8% during infection with E2A SCM mutant virus, when compared to HAdV wt infection (Fig. 27 B). Additionally, immunoprecipitation analysis of the cells infected with a virus mutant lacking E4orf3 showed no effect of this viral factor on E2A/PML binding (Fig. 27 A, right panel, lane 5 and Fig. 27 B). In sum, these data suggest that E2A SUMOylation regulates E2A/PML interaction during HAdV infection, independently on E4orf3.

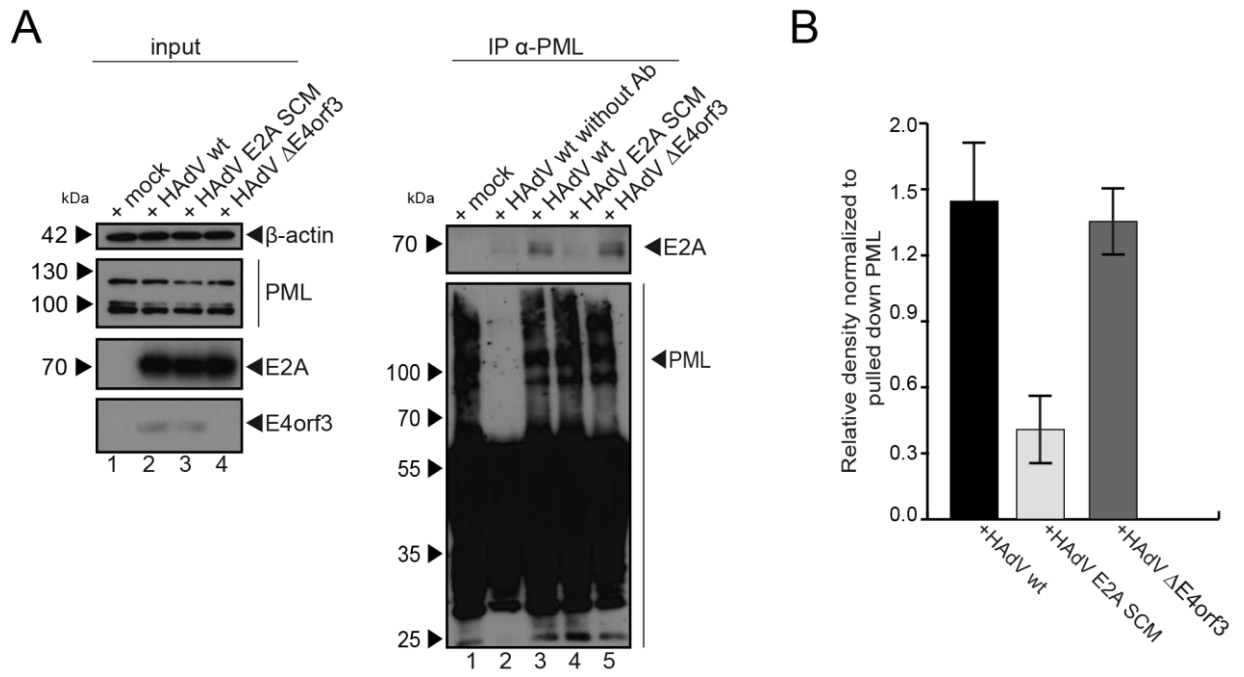

Figure 27: E2A SUMOylation controls PML binding to the viral factor in infected cells. (A) HepaRG cells were infected with HAdV wt (left panel lane 2, right panel lane 2 and 3), HAdV E2A SCM mutant (left panel lane 3, right panel lane 4) and HAdV **Δ**E4orf3 mutant (left panel lane 4, right panel lane 5) at a multiplicity of 20 FFU/cell. Cells were harvested cells 24 h after infection and total cell lysates were prepared. After immunoprecipitation by PML using polyclonal rabbit Ab raised against PML protein NB100-59787 (α-PML), proteins were subjected to immunoblot analyses. Input levels of total-cell lysates and coprecipitated proteins were detected using mAb B6-8 (α-E2A), pAb NB100-59787 (α-PML), mAb AC-15 (α-β-actin) and mAb 6A11 (α-E4orf3). Molecular weights in kDa are indicated on the left, relevant proteins on the right. **(B)** Densitometric

analyses of E2A coimmunoprecipitated with PML in panel A (right panel, lanes 3 and 5), quantified with ImageJ (version 1.45s) software, normalized to respective levels of immunoprecipitated PML in HAdV wt and HAdV E2A SCM infected cells. Average values and standard deviations represented on bar plot were calculated based on three independent experiments.

4.3.2 E2A SUMOylation controls formation and localization of PML tracks next to HAdV RCs

4.3.2.1 Abundance of HAdV RCs and PML-NBs depends on E2A SUMOylation

E2A SCM mutations lowered the production of HAdV progeny viruses (4.2.1) as well as the expression viral late mRNAs (4.2.5) and amount of various viral proteins (4.2.4), including E4orf3 in charged for PML tracks formation (Doucas et al. 1996; Everett 2001; Ishov and Maul 1996; Jul-Larsen et al. 2004; Maul 1998; Maul, Ishov, and Everett 1996). To examine effects of E2A SUMOylation on the organization of HAdV RCs and PML-NBs during infection, morphology and abundance of these two structures in the cells infected with HAdV wt and HAdV E2A SCM was analyzed by immunofluorescence microscopy (Fig. 28).

Although the data described in previous sections showed deficiency in viral progeny production (4.2.1) and lower levels of E4orf3 protein during infection with E2A SUMO conjugation deficient virus (4.2.4), replication centers and PML tracks were still formed (Fig. 28 A). However, the 26.9% reduction of the number of HAdV RCs per infected cell during HAdV E2A SCM infection compared to HAdV wt infection was observed (Fig. 28 B). Furthermore, the number of PML-NBs was reduced by 17.7% compared to HAdV wt infection (Fig. 28 C). Interestingly, the mutual relationship between the number of HAdV RCs and PML tracks showed a positive correlation between amounts of these two structures in cells infected with both viruses (Fig. 28 D).

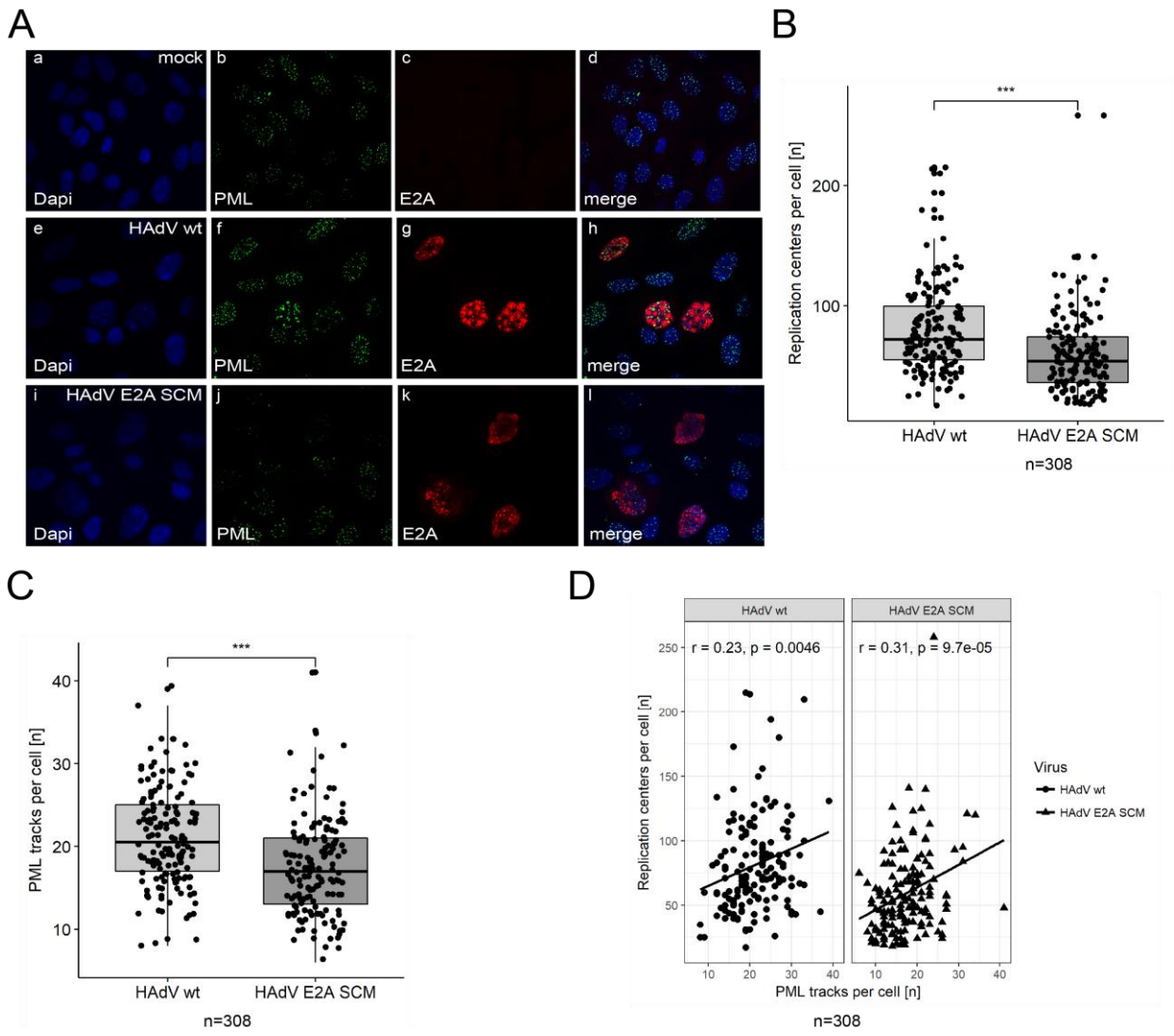

Figure 28: E2A SCM mutations reduce the numbers of HAdV RCs and PML-NBs. (A) HepaRG cells infected with HAdV wt or HAdV E2A SCM at a multiplicity of 50 FFU/cell were fixed with methanol 24 h p.i. and double labeled with mAb B6-8 (α-E2A) and pAb NB100-59787 (α-PML). Primary Abs were detected with Alexa647 (E2A, red) and Alexa488 (PML, green) conjugated secondary Abs. Dapi was used for nuclear staining. Representative E2A (c, g, k) and PML (b, f, j) staining patterns of n=308 cells evaluated are shown (50:50; HAdV wt: HAdV E2A SCM virus infected cells). Overlays of single images (merge) are shown in d, h, l. To avoid differences in staining intensity and extent of bleaching all cells were permeabilized, stained and analyzed together **(B)(C)(D)** RCs and PML-NBs detected by immunofluorescence microscopy were counted per cell during infection with HAdV wt and HAdV E2A SCM using Volocity software. **(B)** Numbers of replication centers and **(C)** PML-NBs per cell were plotted in box plots. P values were calculated using a two-sided Mann-Whitey test. **(D)** Scatter plots represent correlations between numbers of RCs and PML-NBs per infected cell. Correlation coefficients and statistical significances were computed using Spearman's correlation.

4.3.2.2 E2A SUMOylation determines localization of PML tracks during HAdV infection

The results demonstrating E2A SUMOylation-dependent E2A/PML interaction (4.3.1.2) during infection indicate a novel interplay between E2A SUMOylation and PML track

localization. This can be further supported by previous reports showing that tracks are found in the vicinity of E2A marked HAdV RCs, even in the absence of the E4orf3 protein (Doucas et al. 1996; Everett 2001; Ishov and Maul 1996).

To investigate the possibility of E2A SUMO conjugation serving as the molecular mechanism underlying juxtaposed recruitment of PML tracks to HAdV RCs, immunofluorescence studies in cells infected with ether HAdV wt or HAdV E2A SCM mutant virus were performed (Fig. 29). This data substantiated the previous findings that virus induced PML tracks are localized juxtaposed to established HAdV RCs (Fig. 29 A, panels f, g, h). However, during infection with HAdV E2A SCM virus, PML tracks were not associated with HAdV RCs, but displayed predominantly random distribution in the cell nuclei (Fig. 29 A, panels j, k, l). To further confirm the immunofluorescence data, distances between HAdV RCs and PML tracks were measured. Average minimal distances of PML tracks from HAdV RCs significantly increased by 21% during infection with HAdV E2A SCM virus (Fig. 29 B).

As the E2A SUMOylation affects the number of HAdV RCs and PML tracks (4.3.2.1), it was examined how the distances between these two structures depend on their quantity Fig. 29 C, D). A positive correlation between the increasing number of HAdV RCs and their distance from PML tracks during HAdV wt and E2A SCM mutant virus infection was observed (Fig. 29 C). On the other hand, increasing numbers of PML tracks led to reduction of distances from HAdV RCs in wt and HAdV E2A SCM infection (Fig. 29 D). These correlations led to the conclusion that a meaningful comparison of average minimal distances between PML tracks and RCs, shown in Fig. 29 B, requires the comparison of cells with similar amounts of these structures. Therefore, the cells were matched for similar numbers of these structures, to exclude the possibility that the concentration of PML tracks and RCs confound the distance measurements. The replotted data revealed a highly significant 48.8% increase in the median distance between PML tracks and HAdV RCs during infection with HAdV E2A SCM virus (Fig. 29 E). Taken together, this data shows that E2A SUMOylation serves as a connection between PML tracks and HAdV RCs, mediating their juxtaposing subcellular localization during HAdV infection.

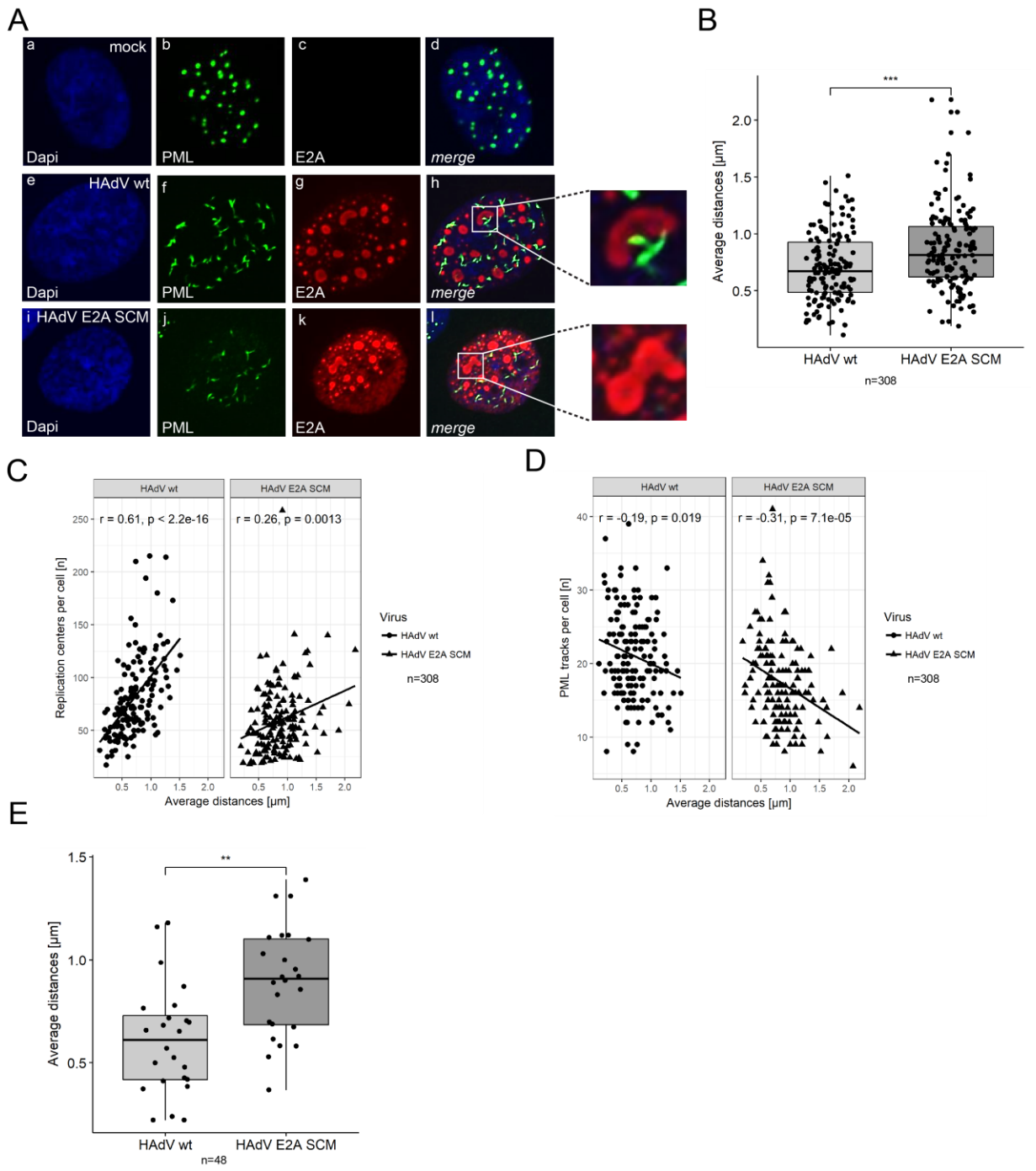

Figure 29: E2A SUMOylation regulates localization of PML tracks next to HAdV RCs. (A) HepaRG cells infected with HAdV wt or HAdV E2A SCM at a multiplicity of 50 FFU/cell were fixed with methanol 24 h p.i. and double labeled with mAb B6-8 (α-E2A) and pAb NB100-59787 (α-PML). Primary Abs were detected with Alexa647 (E2A, red) and Alexa488 (PML, green) conjugated secondary Abs. Nuclear staining was performed using Dapi. Representative E2A (c, g, k) and PML (b, f, j) staining patterns of n=308 cells analyzed are shown (50:50; HAdV wt: HAdV E2A SCM virus infected cells). Overlays of single images (merge) are shown in d, h, l. To avoid differences in staining intensity and extent of bleaching all cells were permeabilized, stained and analyzed together. **(B)** Distances between replication centers and PML tracks per cell were measured using Volocity software in n=308 cells in 2D (50:50; HAdV wt: HAdV E2A SCM virus infected cells) and represented

in box plots. P values were calculated employing a two-sided Mann-Whitey test. Bonferroni correction was used to adjust for multiple comparisons. **(C), (D)** Scatter plots represent correlations between numbers of replication centers **(C)** and PML tracks **(D)** and their distances per infected cell. Correlation coefficients and statistical significances were computed using Spearman's correlation. **(E)** Cells were matched according to the number of PML-NBs and RCs, to prevent concentrations of each component confounding the correlation, before representing distances in box plots. P values were calculated by Mann-Whitney tests. Bonferroni correction was used to adjust for multiple comparisons.

4.3.3 Interaction of HAdV E2A with Sp100A

HAdV protein E2A can target and relocalize one of the major constitutive components of PML-NBs, Sp100 independently on other viral factors (Komatsu, Nagata, and Wodrich 2016). HAdV infection causes reorganization of PML-NBs into PML tracks and redistribution of Sp100 isoforms (Berscheminski et al. 2014). Sp100 isoform, Sp100A promotes chromatin decondensation (Newhart et al. 2013). During HAdV infection, Sp100A is kept in PML tracks to amplify HAdV gene expression (Berscheminski et al. 2014). PML tracks do not localize next to HAdV RC in the absence of E2A SUMOylation (4.3.2.2). The data described in previous sections also revealed the need for E2A SUMOylation for efficient HAdV progeny production (4.2.1), protein (4.2.4) and late mRNA synthesis (4.2.5). These facts prompted the investigation of the mutual relationship between E2A and Sp100A, as well as possible implication of E2A SUMO PTM in the interaction between these two proteins during HAdV infection.

4.3.3.1 E2A SUMOylation does not affect Sp100A sequestration into PML tracks

Sp100A localizes to PML tracks and promotes HAdV gene expression (Berscheminski et al. 2014). As E2A SUMOylation promotes HAdV infection (4.2.4) and represents the molecular mechanism behind subcellular localization of PML tracks next to HAdV RCs (4.3.2.2), the role of E2A SUMOylation in Sp100A positioning in PML-NBs was assessed.

HepaRG cells were transfected with pYFP-Sp100A prior to infection with HAdV wt and HAdV E2A SCM. Immunofluorescence analysis confirmed previously reported observations that Sp100A localizes in PML tracks during HAdV wt infection (Fig. 30 A, panels g and h). Analysis of cells infected with HAdV E2A SCM virus showed that Sp100A remains localized in PML tracks randomly distributed in cell nuclei (Fig. 30 A, panels l and m). There was no change in Sp100A localization during HAdV E2A SCM infection compared to HAdV wt infection (Fig. 30 B). This can be further supported by result demonstrating no difference in Pearson's correlation between Sp100A and PML (Fig. 30 C).

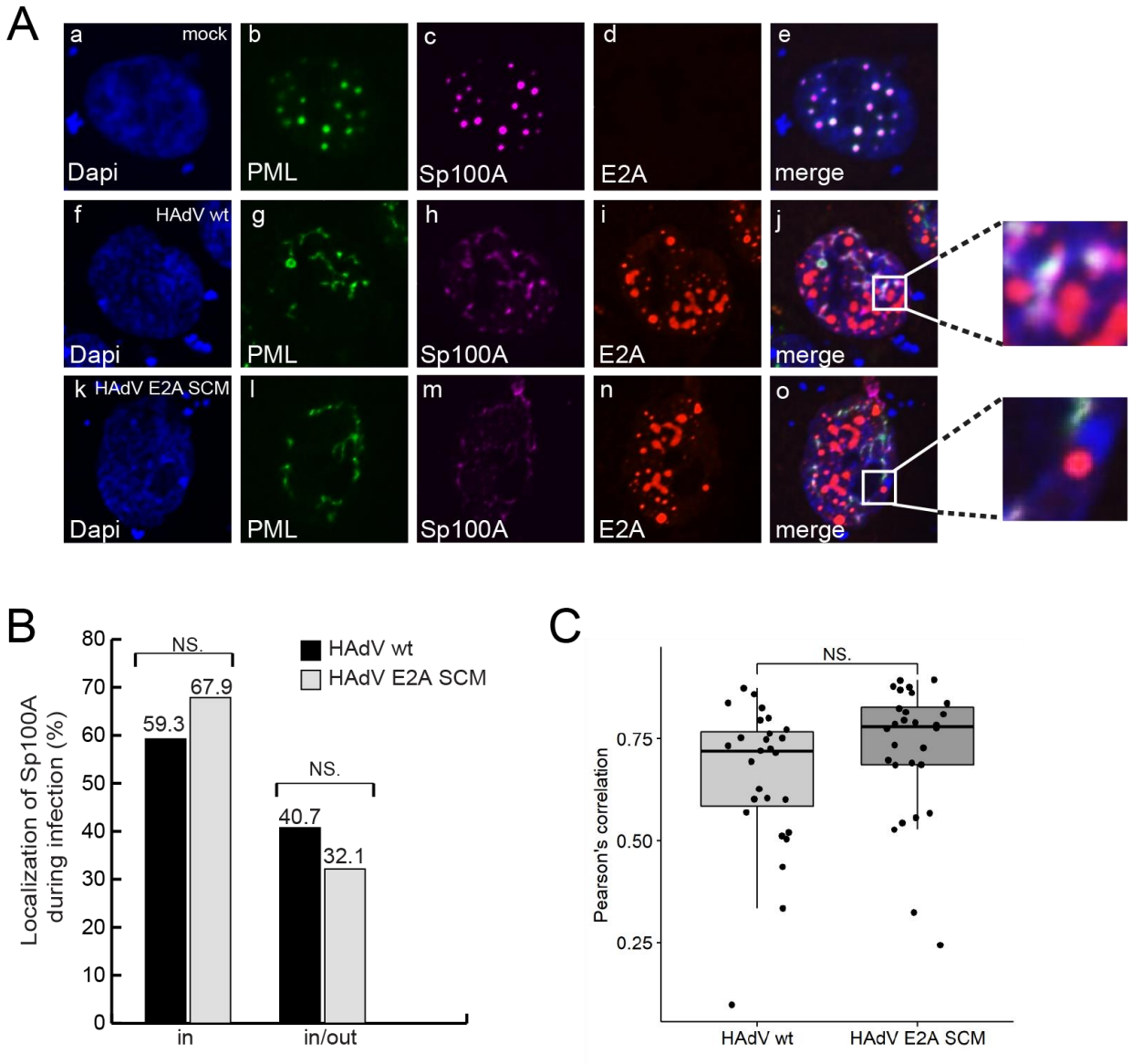

Figure 30: E2A SUMOylation does not alter Sp100A PML tracks localization. (A) HepaRG cells transfected with 3 µg of pYFP-Sp100A and superinfected with HAdV wt or HAdV E2A SCM mutant at a multiplicity of 50 FFU/cell, 4 h post transfection, were fixed with 4% PFA 30 h after infection and double labeled with mAb rb (α-E2A) and pAb m (α-PML). Sp100A was not labeled, but detected via YFP fluorescence (Sp100A, magenta). Primary Abs were detected with Alexa568 (E2A, red), Alexa647 (PML, green) conjugated secondary Abs. Nuclei were stained by Dapi. Anti-PML (green; panels b, g, l) and anti-YFP (magenta; panels c, h, m), staining patterns were analyzed in at least 50 cells. Overlays of the single images (merge) are shown in panels e, j, o. **(B)** Cells were classified according to intracellular YFP-Sp100A localization in PML-NBs, and the counting data is shown in a bar plot. Statistical significance was calculated using a Fisher's exact test, p>0.05. **(C)** Pearson's correlation coefficient for YFP-Sp100A signals and PML stained by PML mouse Ab (α-PML) in cells infected with HAdV wt or HAdV E2A SCM was determined using the Volocity software. For each cell, Pearson's correlation was calculated for colocalization of PML with YFP-Sp100A. The distributions of the respective correlation coefficients are displayed in a box plot. Values above 0.5 are considered colocalization.

4.3.3.2 SUMOylated E2A interacts with Sp100A during HAdV infection

PML tracks localization next to HAdV RCs (4.3.2.2) and E2A/PML interaction (4.3.1.2) depend on E2A SUMOylation. Sp100A associates with PML tracks during wt HAdV infection (Berscheminski et al. 2014), independently on the E2A SUMO conjugation status (4.3.3.1). Based on this data, it could be expected that if E2A and Sp100A interact during infection, that interaction would be E2A SUMOylation-dependent.

To investigate possible E2A interaction with Sp100A and the involvement of E2A SUMO PTM in this binding, human cells were transfected with pYFP-Sp100A and subsequently infected with wt HAdV or E2A SCM virus mutant (Fig. 31). Immunoprecipitation of YFP and staining for E2A revealed an interaction between these two proteins (Fig. 31 A, right panel, lane 4, Fig. 31 B). The amount of E2A protein detected was reduced to 21%, when Sp100A binding was monitored during HAdV E2A SCM infection, confirming an E2A SUMO-dependent interaction between the viral factor and the host transcription factor (Fig. 31 A, right panel, lane 6; Fig. 31 B). Interestingly, HAdV wt infection increased Sp100A protein levels (Fig. 31 A, left panel, lane 4) compared to HAdV E2A SCM infections (Fig. 31 A, left panel, lane 6).

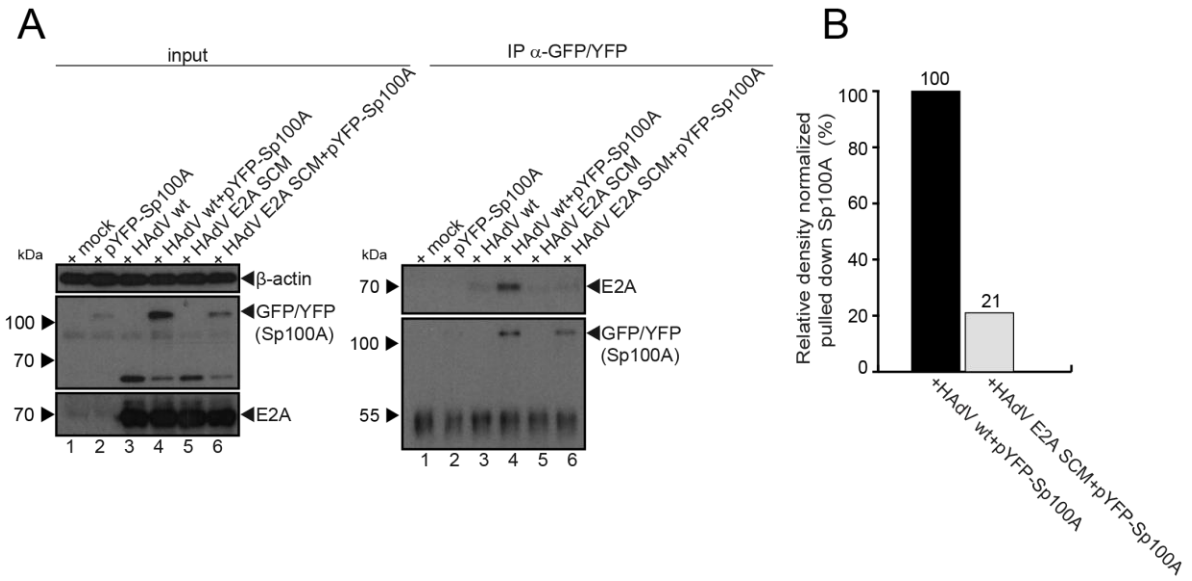

Figure 31: E2A SUMOylation promotes Sp100A/E2A interaction. (A) HepaRG cells were transfected with pYFP-Sp100A (lane 2) and superinfected with HAdV wt (lane 4) and HAdV E2A SCM mutant (lane 6) at a multiplicity of 50 FFU/cell. The cells were harvested 24 h p.i., whole-cell lysates were prepared, and immunoprecipitation analysis was performed using polyclonal rabbit antibody against GFP pAb260 (α-GFP/YFP). Proteins were subjected to immunoblot analyses. Input levels of total-cell lysates and coprecipitated proteins were detected using mAb B6-8 (α-E2A), pAb260 (α-GFP/YFP) and mAb AC-15 (α-β-actin). Molecular weights in kDa are indicated on the left, relevant proteins on the right. **(B)** Densitometric analysis of E2A interaction with Sp100A in panel A (lanes 4 and 6), quantified with ImageJ (version 1.45s) software, normalized to the respective levels of immunoprecipitated YFP Sp100A.

4.3.3.3 HAdV E2A binds Sp100A during infection independently of PML

E2A interacts with PML tracks components PML (4.3.1.2) and Sp100A (4.3.3.2) on an E2A SUMOylation-dependent manner. To investigate if Sp100A/E2A interaction regulates positioning of PML tracks next to HAdV RCs, Sp100A/E2A interaction was examined independently on PML. PML-depleted cells were transfected with pYFP-Sp100A, subsequently infected with wt HAdV or E2A SCM virus mutant and subjected to immunoprecipitation analysis. Immunoprecipitation of YFP and staining for E2A revealed a PML independent interaction between Sp100A and E2A (Fig. 32 A, right panel, lane 4). Taken together, Sp100A/E2A interaction (Fig. 32 A, right panel, lane 6, Fig. 32 B), and Sp100A protein levels (Fig. 32 A, left panel, lane 6) are regulated by E2A SUMOylation also in the absence of PML. This result highlights a novel role for the viral E2A factor regulated by its own SUMO PTM to promote efficient HAdV infection.

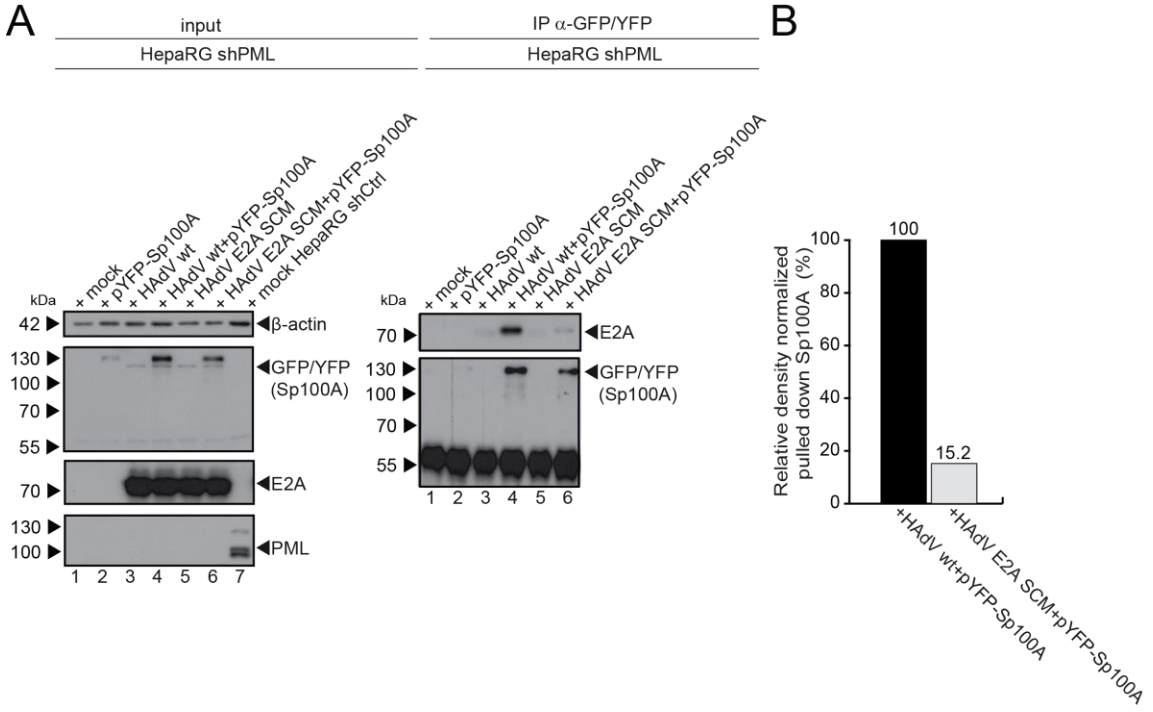

Figure 32: E2A/Sp100A interaction during HAdV infection is PML independent. (A) HepaRG shPML cells were transfected with pYFP-Sp100A (lane 2) and subsequently infected with HAdV wt (lane 4) and HAdV E2A SCM mutant (lane 6) at a multiplicity of 50 FFU/cell. The cells were harvested 24 h p.i. and whole-cell lysates were prepared. HepaRG shCtrl cells were used to verify PML depletion in HepaRG sh PML cells (left panel, lane 7). Immunoprecipitation analysis was performed using polyclonal rabbit antibody against GFP/YFP pAb260 (α-GFP/YFP). After immunoblotting input levels of total-cell lysates and coprecipitated proteins were detected using mAb B6-8 (α-E2A), pAb260 (α-GFP/YFP), pAb NB100-59787 (α-PML) and mAb AC-15 (α-β-actin). Molecular weights in kDa are indicated on the left, relevant proteins on the right. **(B)** Densitometric analysis of E2A interaction with Sp100A in panel A (lanes 4 and 6), quantified with ImageJ (version 1.45s) software, normalized to the respective levels of immunoprecipitated YFP-Sp100A.

4.3.4 Interaction of HAdV E2A with Sp100HMG

After reorganization of PML-NBs into tracks (Carvalho et al. 1995; Doucas et al. 1996; Vink et al. 2015) negative factors for viral replication, previously localized in these domains, are ether degraded by HAdV E3 ubiquitin ligase complex or sequestered into HAdV RCs (Schreiner, Kinkley, et al. 2013; Schreiner, Wimmer, and Dobner 2012). Sp100 isoforms B, -C and -HMG, involved in chromatin condensation, are inactivated by translocation into HAdV replication centers (Berscheminski et al. 2014). The data described in previous sections showed deficiency in HAdV progeny production (4.2.1), protein (4.2.4) and late mRNA synthesis (4.2.5) in the absence of E2A SUMOylation. Moreover, E2A interacts with Sp100A on an E2A SUMOylation-dependent manner (4.3.3.2). Therefore, a possible connection between E2A SUMOylation and HAdV-mediated inactivation of inhibiting properties of Sp100 isoform HMG was investigated.

4.3.4.1 E2A interacts with Sp100HMG on E2A SUMOylation-dependent manner

Sp100HMG localizes in HAdV RCs marked by E2A (Puvion-Dutilleul, Pedron, and Cajean-Feroldi 1984). Moreover, E2A SUMOylation promotes the interaction between E2A and Sp100A isoform (4.3.3.2). Therefore, it was investigated if E2A interacts with Sp100HMG and whether E2A SUMO PTM affects this binding.

Human cells were transfected with pYFP-Sp100HMG and subsequently infected with wt HAdV or E2A SCM virus mutant (Fig. 33). Immunoprecipitation of YFP and staining for E2A revealed an interaction between the two investigated proteins (Fig. 33 A, right panel, lane 4; Fig. 33 B). When Sp100HMG binding was monitored during HAdV E2A SCM infection, the amount of E2A protein was reduced to 13% when compared to HAdV wt infection, confirming an E2A SUMO-dependent interaction between the viral factor and the host chromatin condensing factor (Fig. 33 A, right panel, lane 5; Fig. 33 B). Interestingly, an increase in Sp100HMG protein expression was detected during HAdV infection independently on E2A SUMOylation (Fig. 33, left panel, lanes 4 and 5).

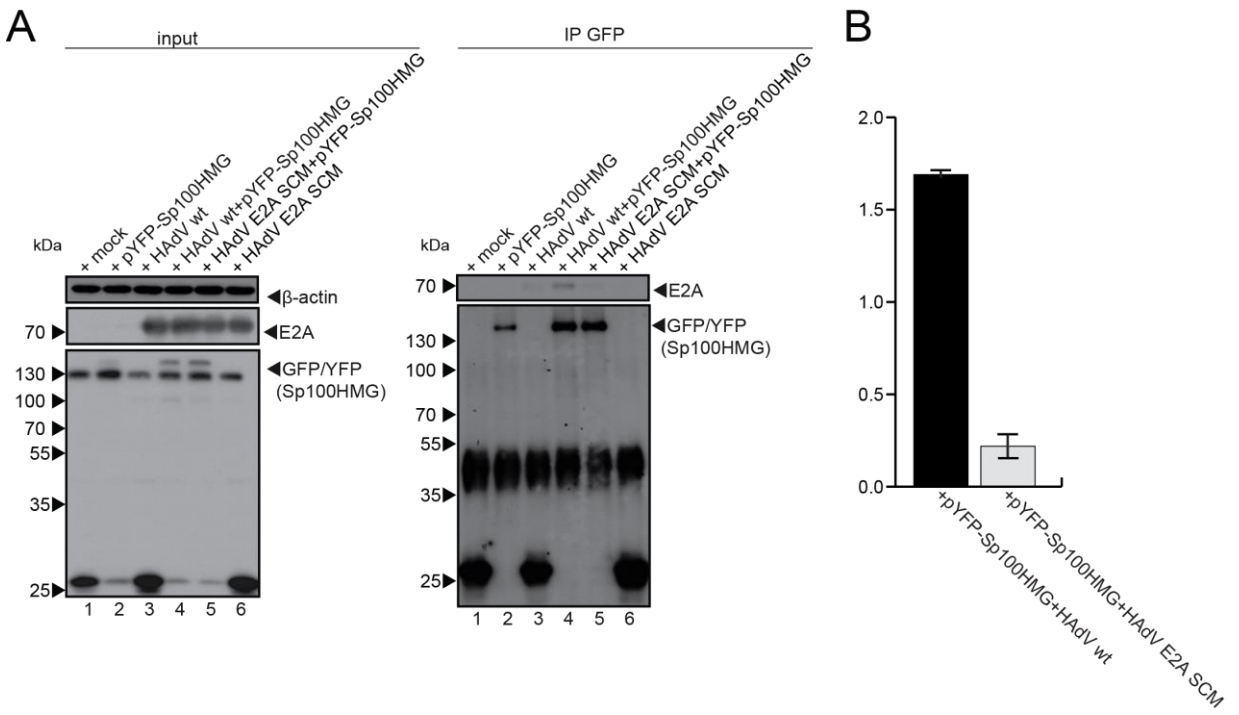

Figure 33: E2A SUMOylation promotes E2A/Sp100HMG interaction. (A) HepaRG cells were transfected with pYFP-Sp100HMG (lane 2) and subsequently infected with HAdV wt (lane 4) and HAdV E2A SCM mutant (lane 6) at a multiplicity of 50 FFU/cell. The cells were harvested 24 h p.i., whole-cell lysates were prepared, and immunoprecipitation analysis was performed using polyclonal rabbit antibody against GFP pAb260 (α-GFP/YFP). Proteins were subjected to immunoblot analyses. Input levels of total-cell lysates and coprecipitated proteins were detected using mAb B6-8 (α-E2A), pAb260 (α-GFP/YFP) and mAb AC-15 (α-β-actin). Molecular weights in kDa are indicated on the left, relevant proteins on the right. **(B)** Densitometric analysis of E2A interaction with Sp100HMG in panel A (lanes 4 and 6), quantified with ImageJ (version 1.45s) software, normalized to the respective levels of immunoprecipitated YFP-Sp100HMG.

4.3.4.2 E2A SUMOylation promotes Sp100HMG localization in HAdV replication centers

Immunoprecipitation studies shown in previous section, emphasized the requirement of E2A SUMOylation for interaction with Sp100HMG. Additionally, Sp100HMG role in chromatin condensation is known from previous studies (Newhart et al. 2013). To investigate if the E2A SUMO PTM affects Sp100HMG localization in HAdV RCs and Sp100HMG-mediated chromatin condensation, immunofluorescence analysis was performed in cells transfected with pYFP-Sp100HMG and subsequently infected with HAdV wt or HAdV E2A SCM viruses (Fig. 34 A). Sp100HMG localized in HAdV RCs during wt virus infection and chromatin visualized by Dapi was in the relaxed state (Fig. 34 A, panels e, f, g and h). On the contrary, infection with HAdV E2A SCM virus led to the Sp100HMG localization outside of HAdV replication centers followed by condensed chromatin appearance (Fig. 34 A, panels I, j, k and l). To validate our immunofluorescence data indicating Sp100HMG colocalization with chromatin, we determined

the average Pearson's correlation coefficient for Sp100HMG visualized by GFP/YFP staining and chromatin labeled by Dapi (Fig. 34 B). Average Pearson's correlation coefficient in cells transfected with Sp100HMG and infected with HAdV wt was 0,32 showing no colocalization between Dapi and Sp100HMG. However, in cells transfected with pYFP-Sp100HMG and infected with HAdV E2A SCM virus Pearson's correlation was 0,78 indicating clear colocalization of Sp100HMG and chromatin (Fig. 34 B) and thereby confirming our immunofluorescence data shown in (Fig. 34 A).

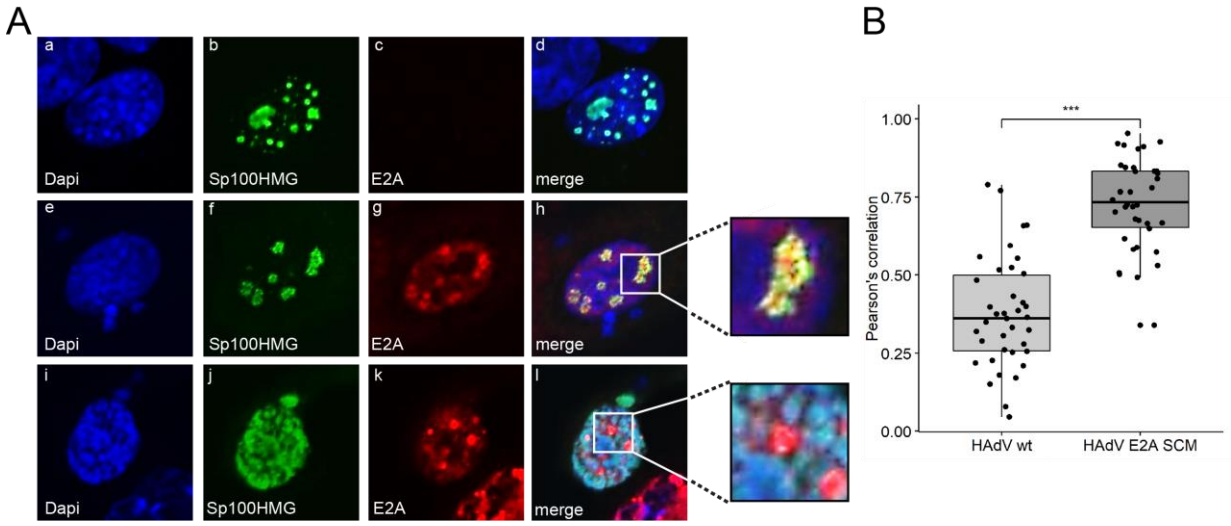

Figure 34: Sp100HMG colocalizes with chromatin during infection with E2A SUMOylation deficient virus. (A) HepaRG cells were transfected with 3 µg of pYFP-Sp100HMG, 4 h prior to infection with HAdV wt or HAdV E2A SCM virus at a multiplicity of 50 FFU/cell. The cells were fixed with methanol 36 h after infection and double labeled with mAb B6-8 (α-E2A), pAb260 (α-GFP/YFP). Primary Abs were detected with Alexa647 (E2A, red) and Alexa488 (α-GFP/YFP, green) conjugated secondary Abs. Nuclear staining was performed using Dapi. Anti-GFP/YFP (green; panels b, f, j) and anti-E2A (red; panels c, g, k), staining patterns representative of at least 50 analyzed cells are shown. Overlays of single images (merge) are shown in panels d, h, l. **(B)** Software Volocity was used to determine Pearson's correlation coefficient for Sp100HMG signal represented by GFP/YFP staining and chromatin stained by Dapi in cells infected with HAdV wt HAdV E2A SCM virus. For each cell, Pearson's correlation was calculated for colocalization of chromatin with Sp100HMG. The distributions of the respective correlation coefficients are displayed in a box plot. Values above 0.5 are considered as colocalized.

4.3.4.3 E2A SUMOylation counteracts Sp100HMG-mediated viral chromatin condensation

Immunofluorescence analyses revealed predominant localization of Sp100HMG in HAdV RCs and chromatin in a relaxed state during infection with that HAdV wt virus. In contrast, infection with the HAdV E2A SCM mutant, which led to Sp100HMG localizing outside of HAdV RCs, was accompanied by condensed chromatin appearance (4.3.4.2).

To validate these observations indicating E2A SUMOylation role in chromatin condensation processes during infection, FAIRE (formaldehyde-assisted isolation of regulatory elements) assays were performed. HepaRG cells were transfected with pYFP-Sp100HMG and 4 h later either mock-infected or infected with HAdV wt or HAdV E2A SCM mutant. Cells were subjected to FAIRE 36 h after infection with primers specific for cellular (RPL30, TUBB, SAT2) and viral (P1, P3, P11) indicator loci. The percentage of output versus input DNA was calculated and revealed that in E2A SCM virus infected cells, significantly more nucleosome-bound viral chromatin was observed compared to wt. Corresponding results were obtained, after monitoring the amount of nucleosome-bound host chromatin in infected compared to mock infected cells, however the E2A SUMO-mediated effect is not as significant as seen for viral loci (Fig. 35 A).

To further relate these findings to cellular (Fig. 35 B) and viral (Fig. 35 C) condensed chromatin states, ChIP analyses was performed at the above shown genomic loci. Repressive H3K9me3 histone mark distribution was analyzed, correlating with transcriptional repression and heterochromatin formation (Barth and Imhof 2010). This data show that there is no significant difference in H3K9me3 on host chromatin when comparing mock-infected versus wt and SCM infected cells (Fig. 35 B). However, 30% more repressive H3K9me3 histone marks was observed on E2A SCM viral chromatin compared to wt, providing evidence that E2A SUMOylation is involved in viral chromatin condensation processes (Fig. 35 C). In summary, this data demonstrates a novel and so far, unknown central role for E2A SUMOylation as a mechanism used by HAdV to counteract host cell antiviral responses by exploiting the cellular SUMO conjugation machinery. Specifically, E2A SUMOylation promotes sequestration of Sp100HMG inside HAdV RCs, and simultaneously reduces chromatin condensation events, which occur during E2A SCM virus infection.

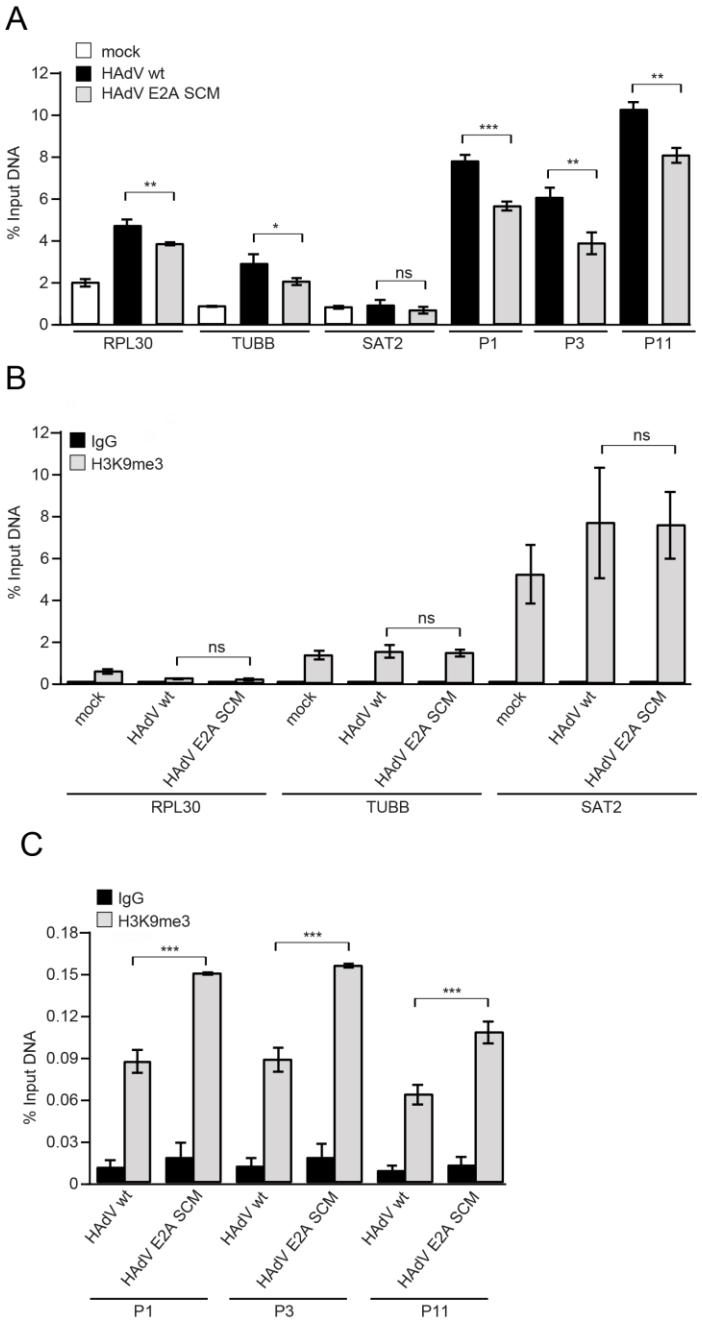

Figure 35: E2A SUMOylation reduces chromatin condensation. (A) HepaRG cells were transfected with pYFP-Sp100HMG and 4 h later either mock-infected or infected with HAdV wt or HAdV E2A SCM mutant at a multiplicity of 20 FFU/cell. At 36 h after infection cells were subjected to FAIRE with primers specific for cellular (RPL30, TUBB, SAT2) and viral (P1, P3, P11) indicator loci. The percentage of output versus input DNA was calculated and values are given as the mean ± standard deviation of three biological replicates. Student t tests were used to determine statistical significance. **(B, C)** HepaRG cells were transfected with pYFP-Sp100HMG and 4 h later either mock-infected or infected with HAdV wt or HAdV E2A SCM mutant at a multiplicity of 20 FFU/cell. At 36 h after infection cells were subjected to ChIP with antibodies to H3K9me3 or normal rabbit IgG and primers specific for cellular (RPL30, TUBB, SAT2) **(B)** and viral indicator loci (P1, P3, P11) **(C)**. The percentage of output versus input DNA was calculated and values are given as the mean ± standard deviation of three biological replicates. Student t tests were used to determine statistical significance.

4.4 Interaction of E2A with the tumor suppressor p53

E1B-55K employs different mechanisms to inhibit p53-dependent transcription. It directly interacts with the tumor suppressor and prevents p53 binding to target genes (Teodoro and Branton 1997; Yew and Berk 1992). E1B-55K interacts with PML-IV and PML-V, SUMOylates p53 and thereby inhibits the p53 transcriptional activity (Pennella et al. 2010; Wimmer et al. 2016). Moreover, E1B-55K interacts with the Sp100A isoform on a SUMOylation-dependent manner. E1B-55K/Sp100A complex recruits p53 and abolishes Sp100A induced activation of p53 transcriptional activity (Berscheminski et al. 2016). The data shown in chapters 4.3.1 and 4.3.3 reveal that E2A also interacts with PML and Sp100A in a E2A SUMOylation-dependent manner. Moreover, E2A has been associated with the HAdV-mediated transformation processes (Rice, Klessig, and Williams 1987). These facts prompted the investigation of a possible connection between E2A and p53.

4.4.1 Influence of E2A SUMOylation on HAdV-mediated inhibition of p53 activity

4.4.1.1 p53 localizes to HAdV replication centers during infection

p53 functions are regulated by its localization (Bosari et al. 1995; Moll et al. 1995; Moll, Riou, and Levine 1992). It has been reported that during HAdV infection E1B-55K relocalizes p53 into E1B-55K containing sites that resemble to HAdV RCs (Cardoso et al. 2008). However, the connection between p53 and HAdV RCs has so far not been fully investigated.

To examine the influence of HAdV infection on p53 subcellular localization, human liver and lung cells were infected and after 24 h subjected to immunofluorescence analysis (Fig. 36). p53 colocalized with the HAdV replication centers in infected HepaRG cells (Fig. 36 A). This observation was confirmed by determination of the Pearson´s correlation coefficient for p53 and E2A, that was 0.71, clearly above the border value for colocalization of 0.5 (Fig. 36 B). In infected A549 cells p53 was found in the region of HAdV RCs but it was more diffusely distributed in comparison to the localization in HepaRG cells, possibly due to faster HAdV life cycle in these cells (Fig. 36 C). However, the colocalization between p53 and E2A was confirmed by Pearson´s correlation coefficient that was 0.57 (Fig. 36 D).

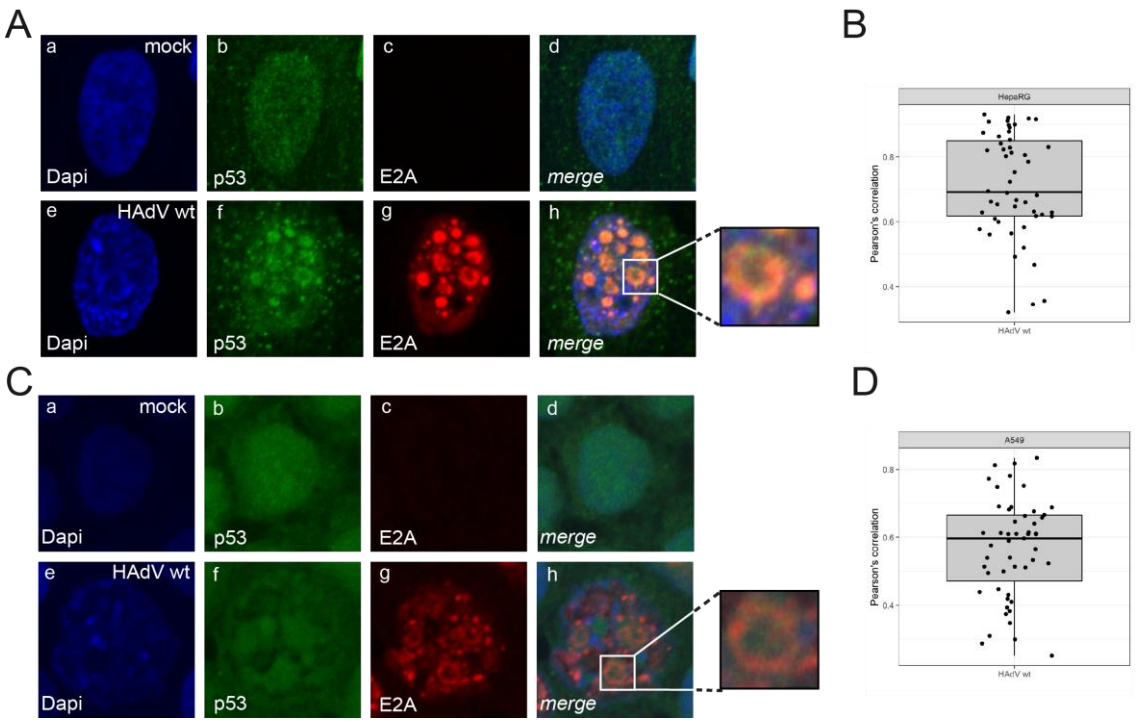

Figure 36: p53 colocalizes with the viral replication centers during HAdV infection. (A, C) HepaRG **(A)** and A549 **(C)** cells were infected with HAdV wt virus at a multiplicity of 20 FFU/cell. The cells were fixed with 2% PFA 24h after infection and double labeled with mAb rb (α-E2A) and mAb DO-1 (α-p53). Primary Abs were detected with Alexa647 (E2A, red) and Alexa488 (α-p53, green) conjugated secondary Abs. Nuclear staining was performed using Dapi. Anti-p53 (green; panels b, f) and anti-E2A (red; panels c, g), staining patterns representative of at least 50 analyzed cells are shown. Overlays of single images (merge) are shown in panels d and h. **(B, D)** Software Volocity was used to determine Pearson's correlation coefficient for p53 and E2A in HepaRG **(B)** and A549 **(D)** cells infected with HAdV wt virus. For each cell, Pearson's correlation was calculated for colocalization of p53 and E2A. The distributions of the respective correlation coefficients are displayed in box plots. Values above 0.5 are considered as colocalized.

4.4.1.2 p53 localizes to HAdV replication centers independently on E1B-55K

During HAdV infection E1B-55K shuttles between cytoplasm and nucleus, localizing both in the nucleus and in perinuclear bodies (Ornelles and Shenk 1991). E1B-55K contains nuclear export signal (NES). Inactivation of NES causes complete redistribution of the E1B-55K protein from the cytoplasm to the nucleus, where it accumulates at the periphery of viral RCs. Inactivation of E1B-55K NES enhances SUMO-1 posttranslational modification of E1B-55K and E1B-55K-mediated transformation (Endter et al. 2005). Interestingly, SUMOylation of E1B-55K is necessary for the E1B-55K nuclear localization (Kindsmuller et al. 2007). The inactivation of E1B-55K SCM completely abrogates its ability to transform cells together with E1A (Endter et al. 2001). E1B-55K primarily performs its pro-tumorigenic functions by modulation of the tumor suppressor p53 (Teodoro and Branton 1997; Yew and Berk 1992; Pennella et al. 2010; Wimmer

et al. 2016). p53 was found in HAdV RCs during HAdV wt infection (4.4.1.1) and it has been reported that E1B-55K has the ability to relocalize p53 during HAdV infection (Cardoso et al. 2008). Therefore, the influence of E1B-55K on the p53 localization in HAdV RCs was monitored by immunofluorescence studies. As E2A represents the marker protein for HAdV RCs (Puvion-Dutilleul, Pedron, and Cajean-Feroldi 1984) and it is SUMOylated (4.1), effect of E2A SUMO PTM on p53 localization during infection was also investigated.

The liver cells were infected with HAdV wt, HAdV E2A SCM, HAdV E1B-, HAdV E1B-55K NES and E1B-55K SCM viruses. Immunofluorescence analysis substantiated the previous findings that E1B-55K shuttles between cytoplasm and nucleus during HAdV wt infection (Fig. 37 A, panels h and j, Fig. 37 C). E1B-55K localization was not affected by E2A SCM mutations (Fig. 37 A, panels m and o, Fig. 37 C). As it has been previously reported, inactivation of E1B-55K NES lead to accumulation of the viral protein in the HAdV RCs and PML tracks (Fig. 37, panels w and y, Fig. 37 C), while the E1B-55K SCM mutation completely abrogated E1B-55K nuclear localization (Fig. 37 A, panels b1 and d1, Fig. 37 C). Interestingly, during HAdV wt infection p53 localized in HAdV RCs as well as in perinuclear bodies together with E1B-55K, independently on E2A SUMOylation (Fig. 37 A, panels g, j and l, o, Fig. 37 C). Infection with the virus lacking E1B-55K expression, HAdV E1B-55K-, led to completely nuclear p53 localization, within the HAdV RCs in the 68% of cells (Fig. 37 A, panels q and t, Fig. 37 C), however the diffuse distribution was also detected in 32% of cells. During HAdV E1B-55K NES virus infection, p53 localized sole in nucleus, within HAdV RCs and PML tracks (Fig. 37 A, panels v and y, Fig. 37 C). E1B-55K SCM mutation leads to p53 localization together with E1B-55K in perinuclear bodies, but in all infected cells p53 also colocalized with HAdV RCs (Fig. 37 A, panels a1 and d1, Fig. 37 C). Data obtained in our immunofluorescence studies were substantiated by Pearson´s correlation coefficients determined for p53 and E2A signals (Fig. 37 B). p53/E2A colocalization was clear in all examined cases. There was no significant difference between Pearson´s correlation coefficients for p53/E2A determined during HAdV E2A SCM virus infection compared to HAdV wt infection. Even though they still colocalized, Pearson´s correlation coefficients for p53/E2A were significantly less during infection with HAdV E1B-55K-, HAdV E1B-55K NES and E1B-55K SCM viruses then during HAdV wt infection (Fig. 37 B).

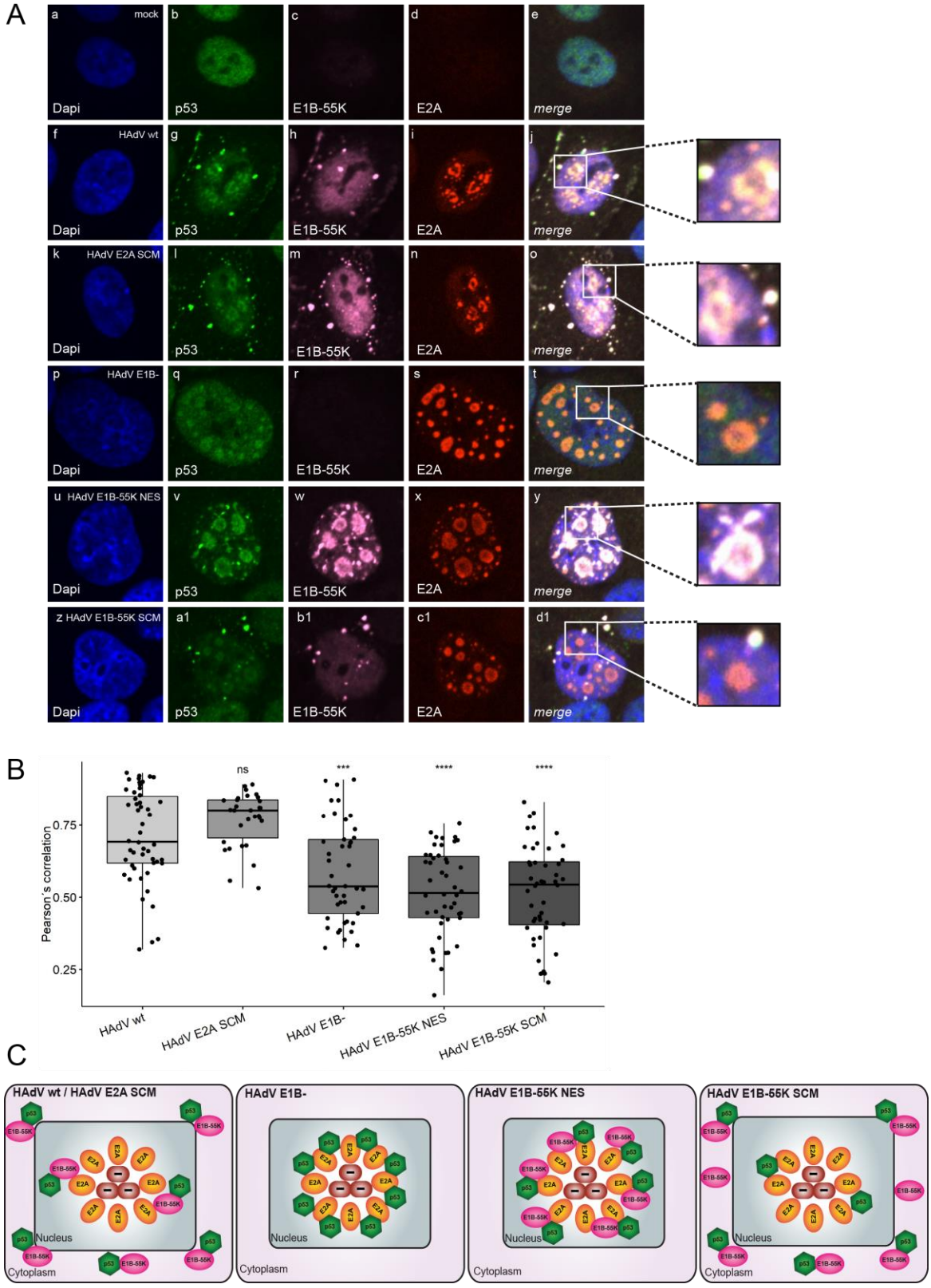

Figure 37: E1B-55K does not affect p53 localization in HAdV replication centers. (A) HepaRG cells were infected with HAdV wt, HAdV E2A SCM, HAdV E1B-, HAdV E1B-55K NES and E1B-55K SCM viruses at a multiplicity of 20 FFU/cell. The cells were fixed with 2 % PFA 24 h after infection and triple labeled with

mAb DO-1 m (α-p53), mAb 4E8 (α-E1B-55K) and mAb rb (α-E2A). Primary Abs were detected with Alexa488 (α-p53, green), Alexa640 (α-E1B-55K, pink) and Alexa568 (α-E2A, red) conjugated secondary Abs. Nuclear staining was performed using Dapi. Anti-p53 (green; panels b, g, l, q, v, a1), anti-E1B-55K (pink; panels c, h, m, r, w, b1) and anti-E2A (red; panels d, i, n, s, x, c1), staining patterns representative of at least 50 analyzed cells are shown. Overlays of single images (merge) are shown in panels e, j, o, t, y, d1. **(B)** Pearson's correlation coefficient for E2A and p53 signals stained by mAb rb (α-E2A) and mAb DO-1 m (α-p53), in cells infected with HAdV wt, HAdV E2A SCM, HAdV E1B-, HAdV E1B-55K NES and E1B-55K SCM viruses was determined using the Volocity software. For each cell, Pearson's correlation was calculated for colocalization of E2A with p53. The distributions of the respective correlation coefficients are displayed in a box plot. Values above 0.5 are considered colocalization. **(C)** Schematic representation of p53 and E1B-55K localization during infection with HAdV wt, HAdV E2A SCM, HAdV E1B-, HAdV E1B-55K NES and E1B-55K SCM viruses.

4.4.1.3 E1B-55K inhibits E2A interaction with p53 during HAdV infection

E1B-55K influences p53 localization during infection, however p53 localized in HAdV RCs independently on this viral protein (4.4.1.2). As E2A marks HAdV RCs, the interaction of E2A with p53 and its dependency on E2A SUMO PTM and E1B-55K was investigated.

Human liver cells were infected with HAdV wt, HAdV E2A SCM, HAdV E1B-, HAdV E1B-55K NES and E1B-55K SCM viruses. Immunoprecipitation analysis of p53 and subsequent staining for E2A did not show interaction between the two investigated proteins during infection with HAdV wt or HAdV E2A SCM virus (Fig. 38 A, right panel, lanes 3 and 4, Fig. 38 B and C). Interestingly, E2A/p53 interaction was present in the cells infected with the virus lacking E1B-55K expression (Fig. 38 A, right panel, lane 5, Fig. 38 B and C). Moreover, inactivation of E1B-55K NES permitted the examined interaction (Fig. 38 A, right panel, lane 6, Fig. 38 B and C). When SCM mutation was introduced in E1B-55K, E2A was also interacting with p53 (Fig. 38 A, right panel, lane 7, Fig. 38 B and C). Densiometric analysis showed similar levels of E2A pulled down with p53 during infection with HAdV E1B- and HAdV E1B-55K NES viruses (Fig. 38 A, right panel, lanes 5 and 6, Fig. 38 B). Even though E2A did interact with p53 in HAdV E1B-55K SCM virus infection, the amount of E2A detected was reduced to 27% when compared to infection with E1B deficient virus (Fig. 38 A, right panel, lane 7, Fig. 38 B). This data indicate that E1B-55K prevents p53 from interacting with E2A, possibly to prevent p53-mediated disruption of E2A functions essential for viral replication.

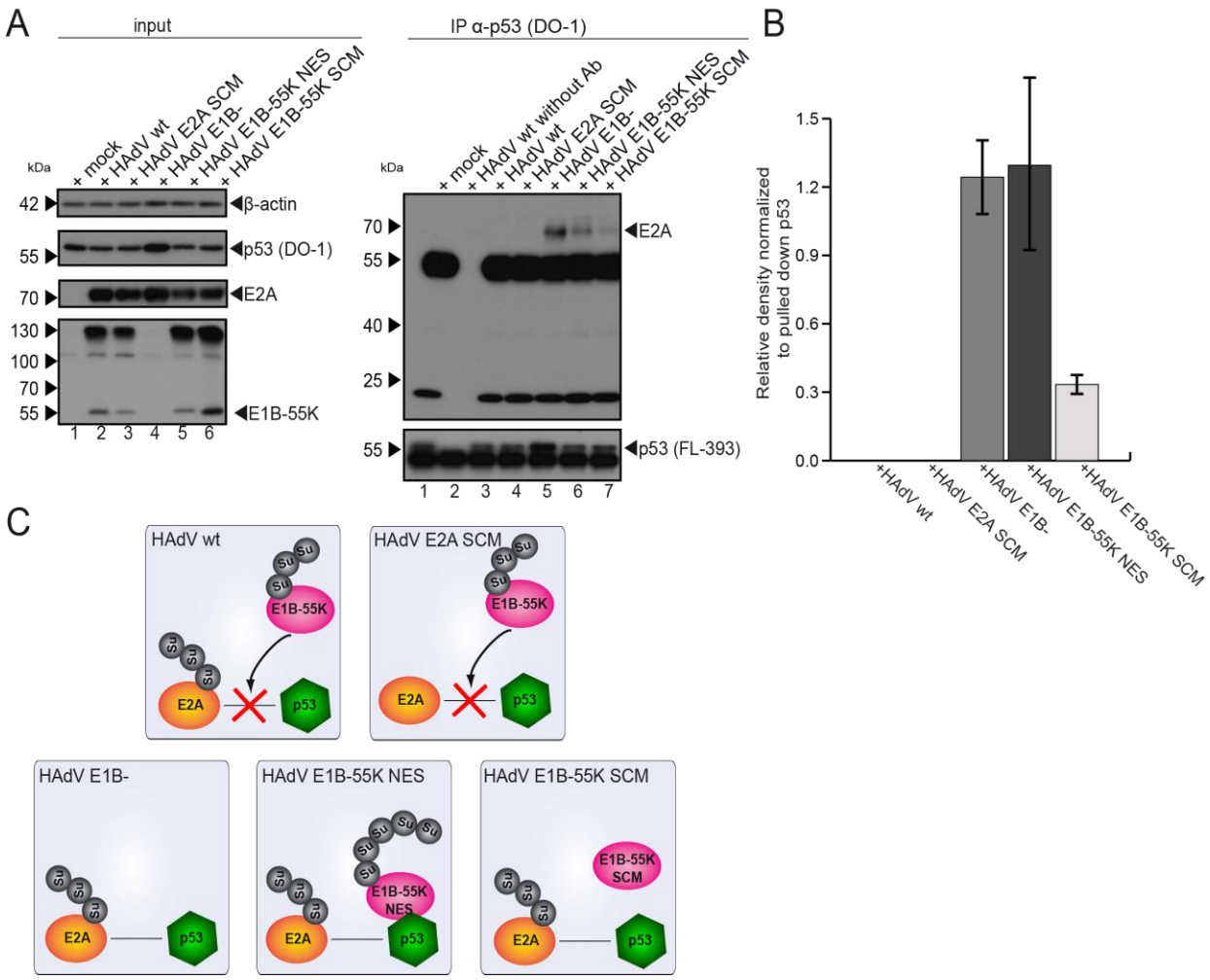

Figure 38: E1B-55K prevents E2A/p53 interaction during HAdV infection. (A) HepaRG cells were infected with HAdV wt (left panel lane 2, right panel lane 3), HAdV E2A SCM mutant (left panel lane 3, right panel lane 4), HAdV E1B- (left panel lane 5, right panel lane 6), HAdV E1B-55K NES (left panel lane 5, right panel lane 6) and HAdV E1B-55K SCM (left panel lane 6, right panel lane 7) at a multiplicity of 20 FFU/cell. The cells were harvested 24 h p.i., whole-cell lysates were prepared, and immunoprecipitation analysis was performed using monoclonal mouse antibody against p53 mAb DO-1 (α-p53). Proteins were subjected to immunoblot analyses. Input levels of total-cell lysates and coprecipitated proteins were detected using mAb DO-1 (α-p53), pAb FL-393 (α-p53), mAb B6-8 (α-E2A), mAb 2A6 (α-E1B-55K) and mAb AC-15 (α-β-actin). Molecular weights in kDa are indicated on the left, relevant proteins on the right. **(B)** Densitometric analysis of E2A/p53 interaction in panel A (lanes 3, 4, 5, 6 and 7), quantified with ImageJ (version 1.45s) software, normalized to the respective levels of immunoprecipitated p53. Average values and standard deviations represented on bar plot were calculated based on three independent experiments. **(C)** Schematic representation of the data shown in panels A and B.

4.4.1.4 E2A SUMOylation promotes HAdV-mediated p53 degradation

E1B-55K associates with the HAdV protein E4orf6 to assemble the E3 ubiquitin ligase complex that degrades negative factors for HAdV infection, including the tumor suppressor p53 (Blanchette et al. 2004; Querido et al. 2001; Schreiner, Wimmer, and Dobner 2012).

To assess the influence of E2A SUMOylation on HAdV-mediated p53 degradation, time course experiments were performed in HepaRG cells. The cells were infected with HAdV wt and HAdV E2A SCM viruses and harvested 24 to 72 h after infection, lysed and subjected to immunoblot analysis. HAdV E1B- and HAdV E4orf6- viruses were included as controls that do not degrade p53 (Fig. 39). As it has been previously reported (Blanchette et al. 2004; Querido et al. 2001; Schreiner, Wimmer, and Dobner 2012), the amount of p53 was reduced compared to mock, during wt virus infection in all examined time points (Fig. 39 A, lanes 2, 7 and 12). Densiometric analysis revealed the reduction of p53 levels in cells infected with HAdV wt of 40.1 % after 24 h, 66.8 % 48 h p.i and 76 % 72 h p.i., when compared to mock (Fig. 39 B). Infection with HAdV E2A SCM virus also led to the reduction of p53 levels compared to the mock infection (Fig. 39 A, lanes 3, 8 and 13). However, densiometric analysis showed lower reduction of p53 amount during infection with HAdV E2A SCM virus compared to HAdV wt infection, especially at 72 h p.i. The reduction of p53 in cells infected with HAdV E2A SCM was 28 % after 24 h, 50.2 % after 48 h and 45.7 % after 72 h when compared to mock infected cells (Fig. 39 B). Interestingly, 48 and 72 h p.i. higher migrating bands indicating possible posttranslational modification were observed above the p53 signals in samples infected with HAdV wt and HAdV E2A SCM viruses. The signal strength of the observed bands was weaker during infection with the E2A SCM mutant virus (Fig. 39 A, lanes 2, 3, 7, 8, 12 and 13). As expected, degradation of p53 was not detected in cells infected with HAdV E1B- and HAdV E4orf6- viruses (Fig. 39 A, lanes 4, 5, 9, 10, 14 and 15).

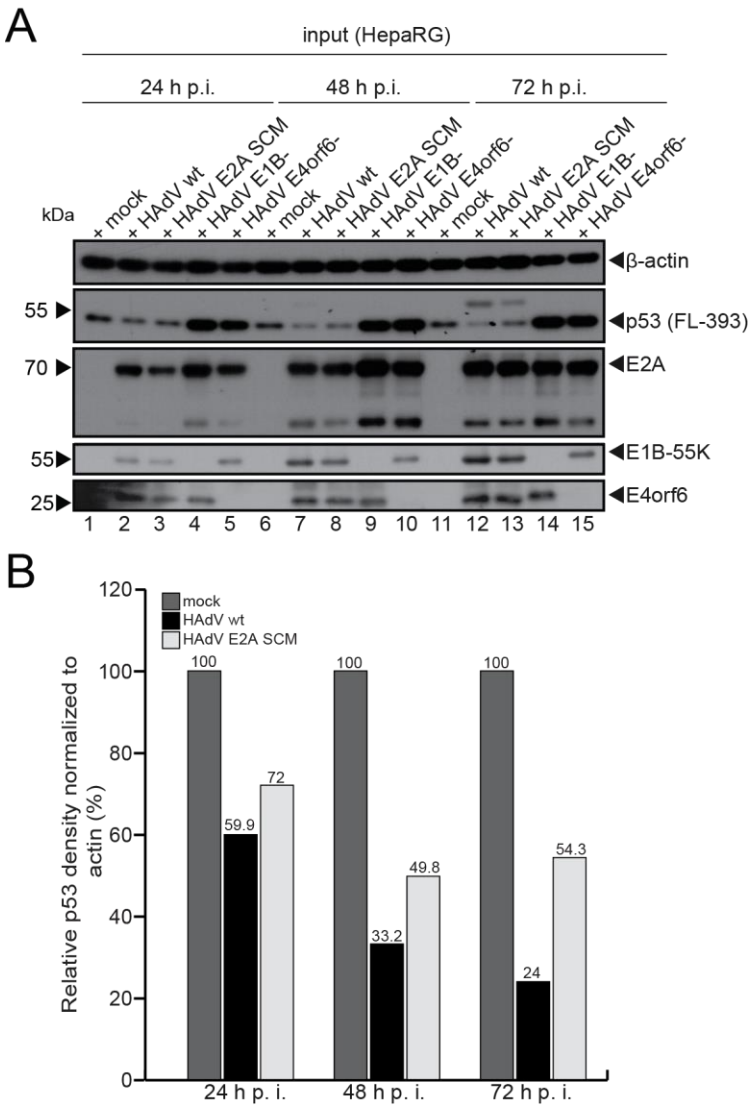

Figure 39: E2A SUMOylation stimulates p53 degradation during HAdV infection. (A) HepaRG cells were infected with HAdV wt (lanes 2, 7 and 12), HAdV E2A SCM (lanes 3, 8 and 13), HAdV E1B- (lanes 4, 9 and 14) and HAdV E4orf6- (lanes 5, 10 and 15) viruses at a multiplicity of 50 FFU/cell. The cells were harvested 24, 48 and 72 h after infection. Total cell lysates were prepared and separated by SDS-PAGE. Immunoblotting was performed using following antibodies: pAb FL-393 (α-p53), mAb B6-8 (α-E2A), mAb 2A6 (α-E1B-55K), mAb RSA3 (α-E4orf6) and mAb AC-15 (α-β-actin). Molecular weights in kDa are indicated on the left, relevant proteins on the right. **(B)** Densitometric analysis of p53 amounts in panel A (lanes 1, 2, 3, 6, 7, 8, 11, 12 and 13), quantified with ImageJ (version 1.45s) software, normalized to the respective levels of β-actin.

4.4.1.5 E2A SUMOylation promotes HAdV-mediated p53 SUMOylation

One of the modes of HAdV-mediated p53 inhibition is E1B-55K-mediated p53 SUMOylation (Pennella et al. 2010; Wimmer et al. 2016). Data shown in the previous section revealed that E2A SUMO PTM promotes p53 degradation. Moreover, immunoblot analysis revealed the higher migrating band in p53-stained blot, indicating possible posttranslational

modification of the tumor suppressor. Therefore, dependency of HAdV-mediated p53 SUMO PTM on E2A SUMOylation was investigated via Ni-NTA assay (Fig. 40).

Ni-NTA analysis was performed in HepaRG His/HA SUMO-2 cells infected with the HAdV wt and HAdV E2A SCM viruses at an MOI of 20 and harvested after 24 h. The MOI of 20 was used because it is not high enough to cause the strong p53 degradation HepaRG cells after 24 h. Immunoblotting confirmed previous finding indicating that HAdV infection leads to the increase in p53 SUMOylation (Fig. 40 A, right panel, lane 2). p53 SUMO levels were increased by 197% in cells infected with the wt virus when compared to the mock infected cells (Fig. 40 B). Interestingly, the upregulation of p53 SUMOylation was substantially lower in cells infected with the E2A SUMOylation deficient virus (Fig. 40 A, right panel, lane 3). Densiometric analysis, revealed only 21% increase in p53 SUMO PTM during infection with HAdV E2A SCM virus when compared to the mock infection (Fig. 40 B). This data highlights the novel E2A role in control of HAdV-mediated p53 SUMOylation, dependent on the E2A SUMO PTM.

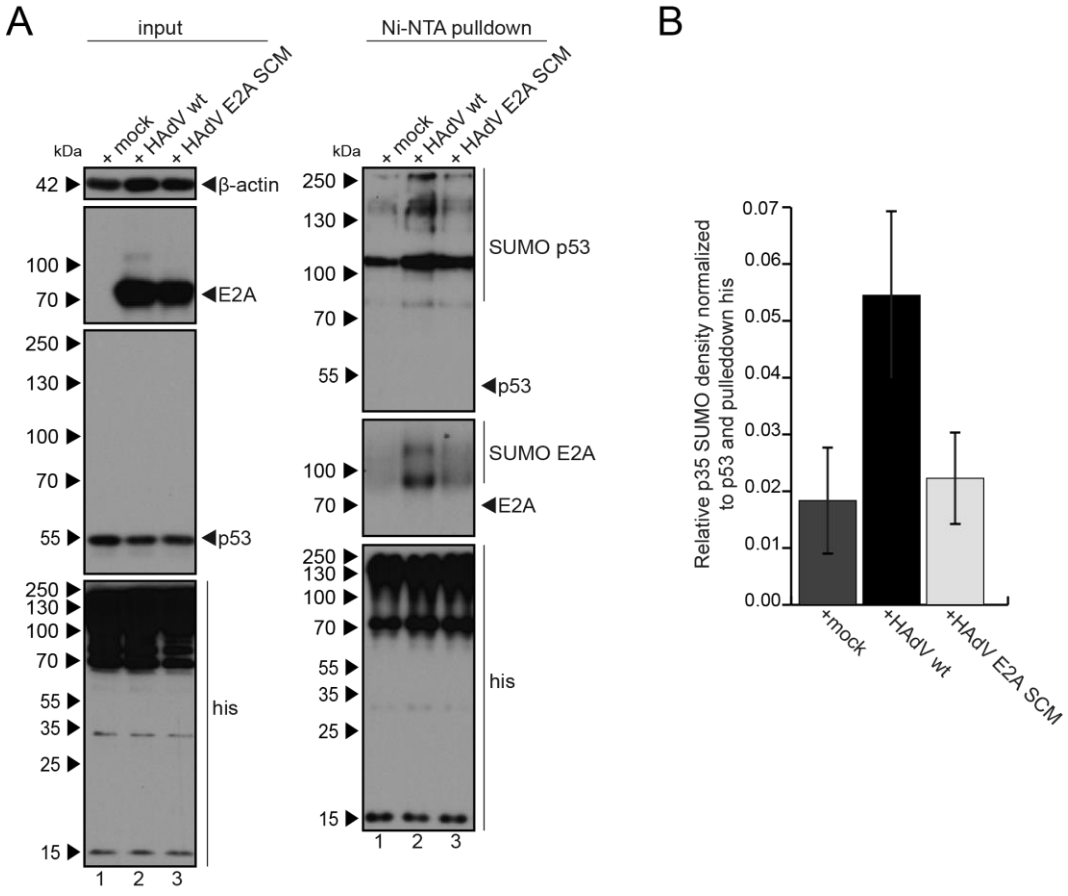

Figure 40: HAdV-mediated p53 SUMOylation depends on the E2A SUMO PTM. (A) HepaRG cells stably expressing His/HA-SUMO-2 were infected with HAdV wt or HAdV E2A SCM viruses at a multiplicity of 20 FFU/cell. The cells were harvested 24 h after infection, whole-cell lysates were prepared with guanidinium

chloride buffer, subjected to Ni-NTA purification of 6xHis-SUMO conjugates and separated by SDS-PAGE. Input levels of total-cell lysates and Ni-NTA purified conjugates were detected with mAb B6-8 (α-E2A), pAb FL-393 (α-p53), mAb 6-His (α-6xHis-tag) and mAb AC-15 (α-β-actin). Molecular weights in kDa are indicated on the left, relevant proteins on the right. **(B)** Densitometric analysis of p53 SUMOylation levels in panel A (lanes 1, 2 and 3), quantified with ImageJ (version 1.45s) software, normalized to the respective levels of p53 and pulled down his. Bar plot represents average values and standard deviations calculated based on data obtained in three independent experiments.

4.4.1.6 E2A SUMOylation promotes E1B-55K/PML-V binding during HAdV infection

E1B-55K SUMOylates and thereby inactivates p53 through its interaction with PML isoforms -IV and -V (Pennella et al. 2010; Wimmer et al. 2016). Data shown in previous section demonstrate that E2A SUMO PTM promotes p53 SUMOylation during infection. As it has been previously shown that E1B-55K does not interact with PML-IV during infection (Wimmer et al. 2010), the influence of E2A SUMOylation on E1B-55K interaction with PML-V was investigated.

Human cells were transfected with pYFP-PML-V and subsequently infected with wt HAdV or E2A SCM virus mutant (Fig. 41). Immunoprecipitation of GFP/YFP and staining for E1B-55K revealed previously shown interaction between the two investigated proteins during HAdV wt infection (Fig. 41 A, right panel, lane 4). However, when PML-V binding was monitored during HAdV E2A SCM infection, the amount of bound E1B-55K protein was reduced to 37.7% compared to HAdV wt infection, showing an E2A SUMO-dependent interaction between E1B-55K and PML isoform -V (Fig. 41 A, right panel, lane 6, Fig. 41 B).

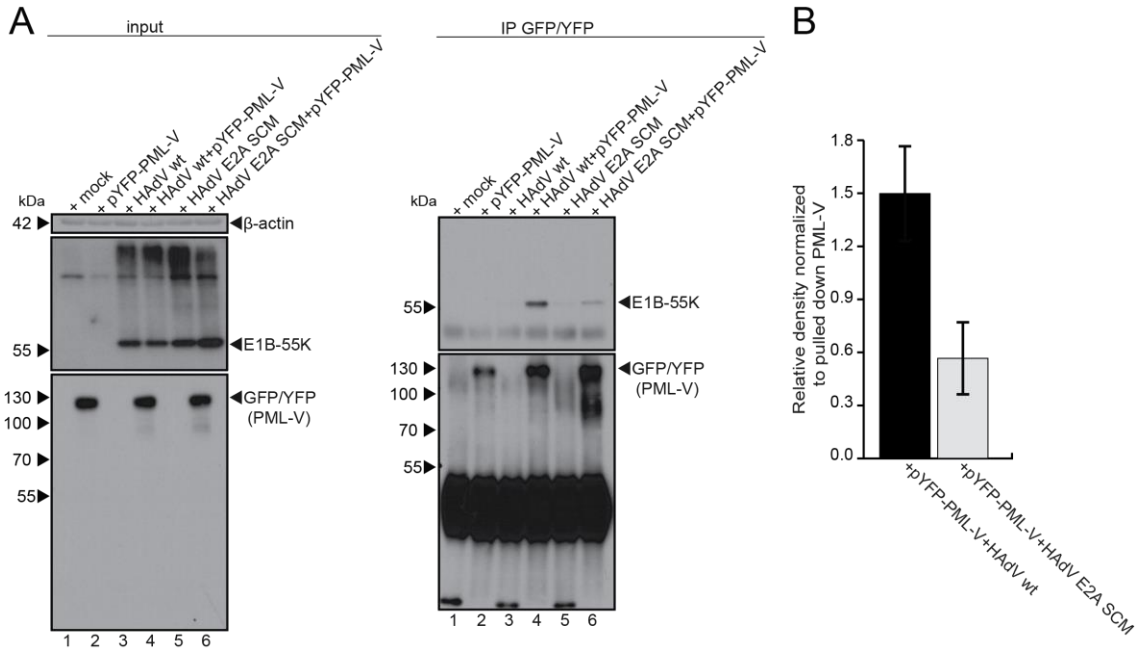

Figure 41: E2A SUMOylation promotes E1B-55K/PML-V interaction. (A) HepaRG cells were transfected with pYFP-PML-V (lane 2) and subsequently infected with HAdV wt (lane 4) and HAdV E2A SCM mutant

(lane 6) at a multiplicity of 20 FFU/cell. The cells were harvested 24 h p.i., whole-cell lysates were prepared, and immunoprecipitation analysis was performed using polyclonal rabbit antibody against GFP pAb260 (α-GFP/YFP). Proteins were subjected to immunoblot analyses. Input levels of total-cell lysates and coprecipitated proteins were detected using mAb 2A6 (α-E1B-55K), pAb260 (α-GFP/YFP) and mAb AC-15 (α-β-actin). Molecular weights in kDa are indicated on the left, relevant proteins on the right. **(B)** Densitometric analysis of E1B-55K interaction with PML-V in panel A (lanes 4 and 6), quantified with ImageJ (version 1.45s) software, normalized to the respective levels of immunoprecipitated YFP-PML-V. Bar plot represents average values and standard deviations calculated based on data obtained in three independent experiments.

4.4.1.7 E2A SUMOylation is required for E1B-55K colocalization with PML-V

During infection E1B-55K localizes predominantly in nucleus where it initially associates with PML tracks (Doucas et al. 1996; Leppard and Everett 1999). Therefore, immunofluorescence studies were performed to substantiate the data showing the lack of interaction between E1B-55K and PML-V during infection with E2A SUMOylation deficient virus, represented in the previous section.

HepaRG cells were transfected with pYFP-PML-V prior to infection with HAdV wt and HAdV E2A SCM. To visualize E1B-55K localized only in nuclear matrix fraction, the cells were treated with CSK buffer before immunostaining to decrease soluble cytoplasmic and loosely held nuclear proteins as described in section 3.6.8. Immunofluorescence analysis confirmed already reported finding that E1B-55K colocalizes with PML-V during HAdV wt infection (Fig. 42 A, panels g and h). On the other hand, the analysis of cells infected with the HAdV E2A SCM virus showed that E1B-55K does not colocalize with the PML-V isoform in the absence of the E2A SUMO PTM (Fig. 42 A, panels k and l). This finding can be further supported by Pearson's correlation coefficient for E1B-55K and PML-V with median value of 0.51 confirming colocalization between the two proteins during HAdV wt infection that was not detected during HAdV E2A SCM virus infection as Pearson correlation coefficient for E1B-55K and PML-V was 0.24 (Fig. 42).

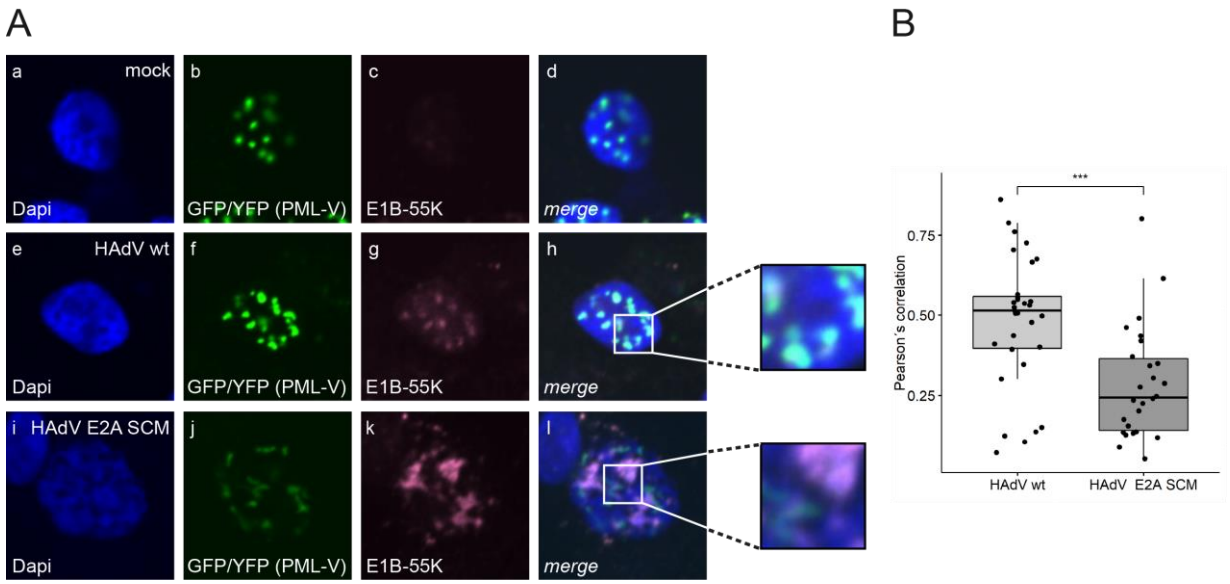

Figure 42: E1B-55K colocalizes with PML-V on an E2A SUMOylation-dependent manner. (A) HepaRG cells were transfected with 3 µg of pYFP-PML-V and superinfected with HAdV wt or HAdV E2A SCM mutant at a multiplicity of 20 FFU/cell, 4 h post transfection. Prior to fixation with 4% PFA, 24 h after infection, the cells were treated with CSK buffer as it has been described in chapter 3.6.8. Fixed cells were double labeled with pAb260 (α-GFP/YFP) and mAb 2A6 (α-E1B-55K). Primary Abs were detected with Alexa488 (GFP/YFP, green) and Alexa647 (E1B-55K, pink) conjugated secondary Abs. Nuclei were stained by Dapi. Anti- GFP/YFP (green; panels b, f, j) and E1B-55K (pink; panels c, g, k), staining patterns were analyzed in at least 30 cells. Overlays of the single images (merge) are shown in panels d, h, l. **(B)** Pearson's correlation coefficient for YFP-PML-V stained by pAb260 (α-GFP/YFP) antibody and E1B-55K stained by mAb 2A6 (α-E1B-55K) antibody in cells infected with HAdV wt or HAdV E2A SCM was determined using the Volocity software. For each cell, Pearson's correlation was calculated for colocalization of YFP-PML-V with E1B-55K. The distributions of the respective correlation coefficients are displayed in a box plot. Values above 0.5 are considered colocalization.

4.4.1.8 E2A SUMOylation inhibits p53-mediated transcription during HAdV infection

To study the influence of E2A SUMOylation on HAdV-mediated modulation of p53-dependent transcriptional activation, the effect of E2A SCM mutations on HAdV infection induced transcriptome changes was evaluated in a previously reported subset of high-confidence p53 target genes (Fischer 2017). Therefore, sequencing libraries were prepared in triplicates for cells infected with HAdV wt and HAdV E2A SCM viruses and analyzed comparing the respective infected cell lines and non-infected cells 24 h after infection. Among the 343 high-confidence p53 target genes (Fischer 2017), 186 genes were differentially expressed comparing HAdV wt infection with non-infected cells. 64 genes were exclusively differentially expressed comparing HAdV wt infection to non-infected cells. 98 genes were solely differentially expressed comparing mock with both, HAdV wt and HAdV E2A SCM infected cells. Moreover, 21 genes that were differentially expressed during HAdV wt infection compared to mock infected cells were also differentially expressed in HAdV E2A SCM mutant infected cells compared to HAdV wt infection. In addition,

four genes were differentially expressed during HAdV E2A SCM infection compared to HAdV wt infection and three more genes were differentially expressed among all three investigated conditions (Fig. 43 A). Comparing HAdV E2A SCM to HAdV wt infection, significant differential expression was observed in a total of 28 genes.These genes were further analyzed. Normalized transcript counts of the most significantly differentially expressed transcript for these genes for all three examined conditions are represented in a bar plot. Nearly all transcripts were downregulated in HAdV wt infected cells compared to mock, while that was not the case in HAdV E2A SCM mutant infected cells. The only exception is the RNF19B transcript, which was downregulated in HAdV E2A SCM infected cells compared to HAdV wt infected cells (Fig. 43 B). Clustering analysis of differentially expressed genes showed that multiple transcripts of p53 target genes were differentially expressed in HAdV wt and HAdV E2A SCM infection. 59 transcripts from the 28 investigated genes were differentially expressed during HAdV E2A SCM infection compared to HAdV wt infection. Most transcripts were upregulated in HAdV E2A SCM infected cells compared to HAdV wt infected cells. However, in some genes (i.e., BAX, CAV1, CCDC51, CES2, DDR1 GAD45A and LARP1), transcript level expression was heterogeneous with both, up- and down regulated expression comparing HAdV wt infection to HAdV E2A SCM infection (Fig. 43 C).

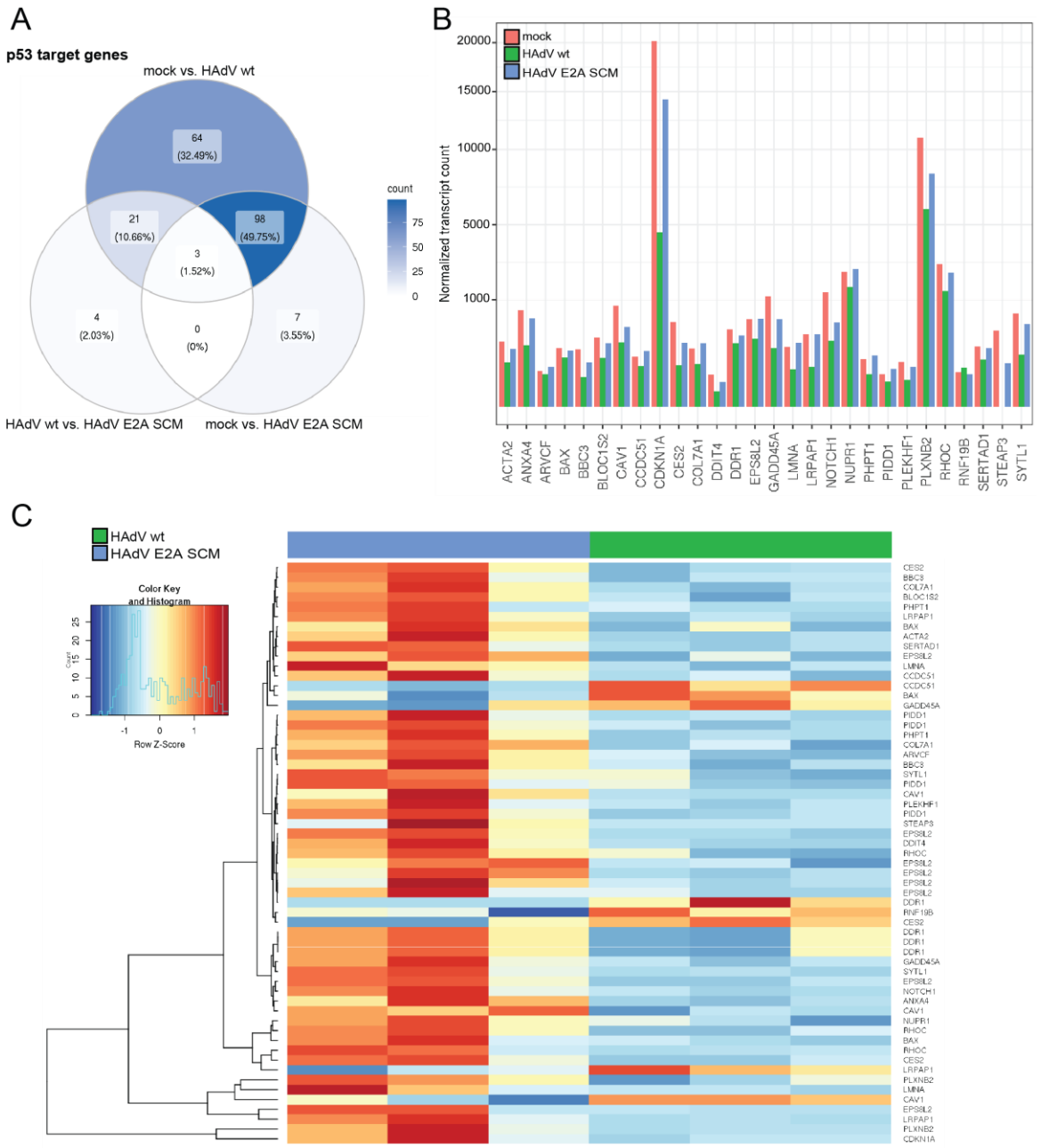

Figure 43: HAdV inhibits expression of specific p53 target genes on an E2A SUMOylation-dependent manner. HepaRG cells were mock infected or infected either with HAdV wt or HAdV E2A SCM virus at a multiplicity of 20 FFU/cell and harvested 24 h p.i. Total RNA was extracted and subjected to RNA sequencing analysis. Differential expression was computed for p53 target genes. P values were corrected for multiple comparisons using a cutoff of $q < 0.1$. **(A)** Venn diagram showing RNA-seq differentially expressed p53 target genes in HAdV wt infected cells in comparison to mock infected cells (mock vs. HAdV wt), compared to differentially expressed p53 target genes in HAdV E2A SCM infected cells in comparison to mock infected cells (mock vs. HAdV E2A SCM) and differentially expressed p53 target genes in HAdV E2A SCM infected cells in comparison to HAdV wt infected cells (HAdV wt vs. HAdV E2A SCM). **(B)** Bar plot represents normalized transcript counts of the most significantly differentially expressed transcript for each significantly differentially expressed gene in mock, HAdV wt and HAdV E2A SCM infected cells. The y axis was transformed using a square root transformation. **(C)** Heat map of RNA-Seq transcriptome analysis for 28 significantly differentially expressed p53 target genes in HAdV E2A SCM infected cells compared to HAdV wt infected cells.

4.4.2 E2A-mediated modulation of p53

4.4.2.1 E2A relocalizes p53 independently on HAdV infection

It has been reported that E2A localizes in the shape of sphere-like structures in the cell nuclei in the absence of other viral factors (Komatsu, Nagata, and Wodrich 2016). The data shown in section 4.4.1.2 revealed E1B-55K independent p53 localization in HAdV RCs marked by E2A (Puvion-Dutilleul, Pedron, and Cajean-Feroldi 1984). Therefore, the influence of E2A on p53 localization in transiently transfected cells was investigated.

Human liver and lung cells were transfected with E2A and subjected to immunofluorescence analysis (Fig. 44). As expected, E2A was detected in sphere-like structures in both examined cell lines (Fig. 44 A panels g and h and Fig. 44 C panels g and h). Previously diffusely distributed p53 was sequestered into the E2A containing spheres in HepaRG (Fig. 44 A panels f and h) and A549 cells (Fig. 44 C panels f and h). Pearson's correlation coefficient for E2A and p53 signals was 0.73 in HepaRG cells (Fig. 44 B) and 0.78 in A549 cells (Fig. 44 D), therefore confirming the data shown in panels A and C.

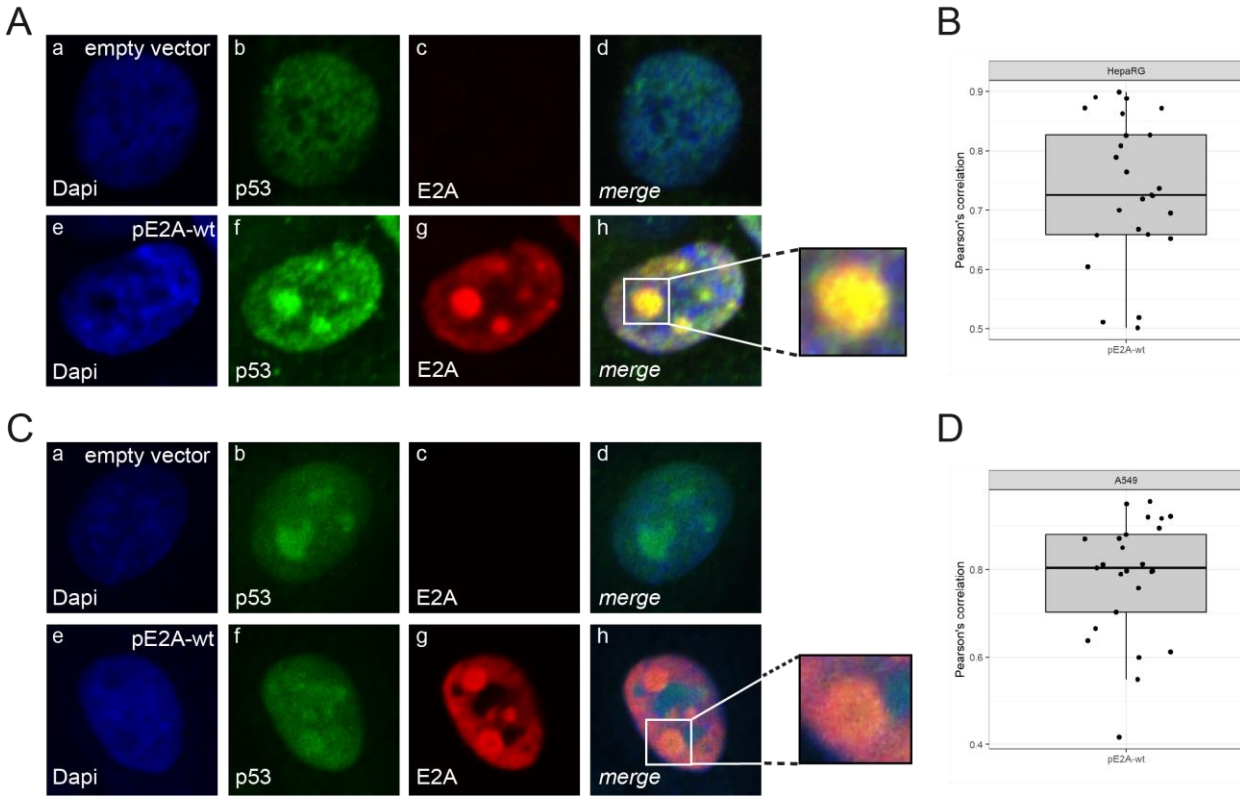

Figure 44: E2A changes p53 localization in transiently transfected cells. (A, C) HepaRG **(A)** and A549 **(C)** cells were transfected with pE2A-wt plasmid. The cells were fixed with 2% PFA 30 h after transfection and double labeled with mAb rb (α-E2A) and mAb DO-1 (α-p53). Primary Abs were detected with Alexa647 (E2A,

red) and Alexa488 (α-p53, green) conjugated secondary Abs. Nuclear staining was performed using Dapi. Anti-p53 (green; panels b, f) and anti-E2A (red; panels c, g), staining patterns representative of 25 analyzed cells are shown. Overlays of single images (merge) are shown in panels d and h. **(B, D)** Software Volocity was used to determine Pearson's correlation coefficient for p53 and E2A signals in HepaRG **(B)** and A549 **(D)** cells transfected with pE2A-wt plasmid. For each cell, Pearson's correlation was calculated for colocalization of p53 with E2A. The distributions of the respective correlation coefficient are displayed in a box plot. Values above 0.5 are considered as colocalized.

4.4.2.2 E2A relocalizes p53 on an E2A SUMOylation independent manner

To investigate the influence of E2A SUMOylation on p53 reorganization in cells transiently transfected with E2A, immunofluorescence analysis was performed. HepaRG cells were transfected with pE2A-wt and pE2A-SCM plasmids. E2A SCM did not affect the organization of E2A in sphere like structures (Fig. 45 A, panels g and k). Moreover, p53 was found in E2A containing regions in cells transfected both with pE2A-wt, as well as pE2A-SCM (Fig. 45 A, panels f, h and j, l). This observation was confirmed by Pearson's correlation coefficients for p53 and E2A of 0.72 in cells transfected with pE2A-wt and 0.74 in cells transfected with pE2A-SCM plasmid (Fig. 45 B). This data substantiated the finding that E2A SUMOylation does not affect p53 localization tin HAdV RCs, shown in section 4.4.1.2.

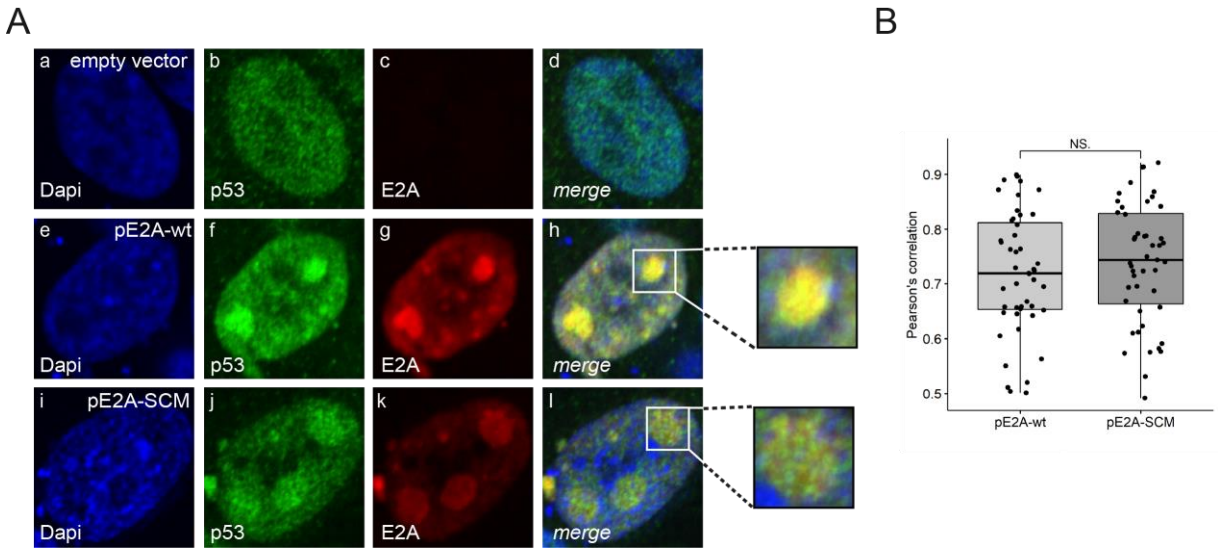

Figure 45: E2A changes p53 subcellular localization independently on E2A SUMO PTM. (A) HepaRG cells were transfected with pE2A-wt or pE2A-SCM plasmids. The cells were fixed with 2% PFA 30 h after transfection and double labeled with mAb rb (α-E2A) and mAb DO-1 (α-p53). Primary Abs were detected with Alexa647 (E2A, red) and Alexa488 (α-p53, green) conjugated secondary Abs. Nuclear staining was performed using Dapi. Anti-p53 (green; panels b, f and j) and anti-E2A (red; panels c, g and k), staining patterns representative of 50 analyzed cells are shown. Overlays of single images (merge) are shown in panels d, h, l. **(B)** Software Volocity was used to determine Pearson's correlation coefficient for p53 and E2A signals in cells transfected with pE2A-wt and pE2A-SCM plasmids. For each cell, Pearson's correlation was calculated for colocalization of p53 with E2A. The distributions of the respective correlation coefficient are displayed in a box plot. Values above 0.5 are considered as colocalized.

4.4.2.3 E2A SUMOylation prevents E2A/p53 interaction in transient transfection assays

E2A interaction with the tumor suppressor p53 was not detected during HAdV infection. However, E2A/p53 binding was observed during infection with HAdV E1B- virus, or when E1B-55K NES or SCM were inactivated by specific mutations (4.4.1.3). To examine if this interaction occurs in the absence of other viral components immunoprecipitation analysis was performed. As SUMOylation affects the protein-protein interactions of its substrates (Hendriks and Vertegaal 2016), E2A SUMO conjugation mutant was also included in the analysis.

HepaRG cells were transfected with p53 together with pE2A-wt or pE2A-SCM plasmid containing mutations in E2A SCMs (Fig. 46). Immunoblot analysis of the proteins bound to E2A did not reveal an interaction between E2A and the cellular tumor suppressor (Fig. 46 A, right panel, lane 3). However, E2A binding to p53 was detected in cells transfected with pE2A-SCM, barring mutations in E2A SCMs (Fig. 46 A, right panel, lane 4). This data was confirmed by densiometric analysis showing that 91.4 % less E2A was immunoprecipitated with p53 in cells transfected with pE2A-wt compared to pE2A-SCM transfected cells (Fig. 46 B).

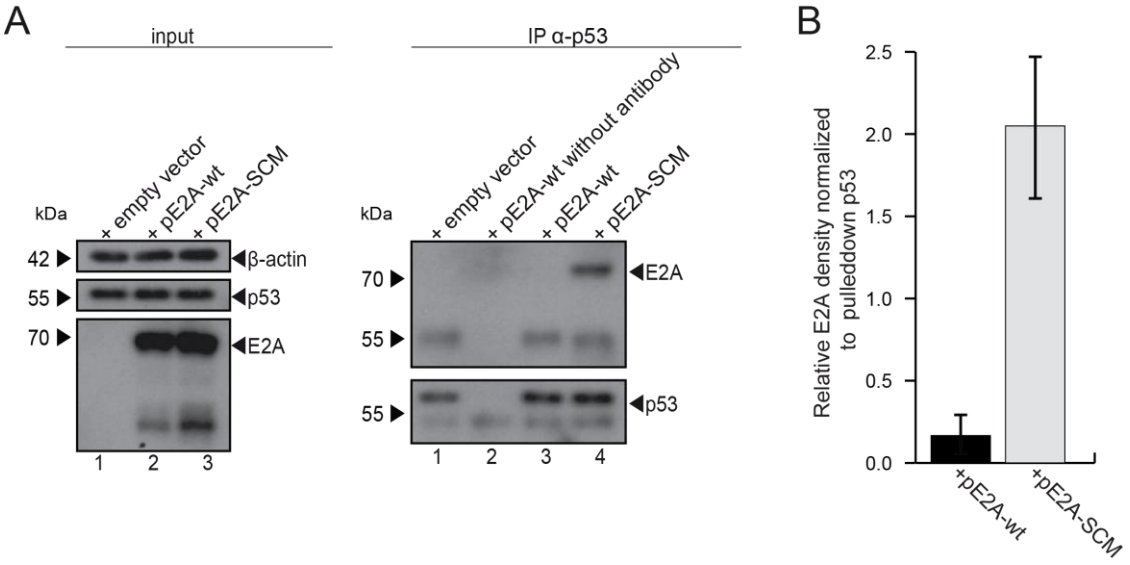

Figure 46: E2A SUMO PTM inhibits E2A/p53 binding during transient transfection. (A) HepaRG cells were transfected with pE2A-wt (lane 2, left panel; lanes 2 and 3, right panel) or pE2A-SCM (lane 3, left panel; lane 4, right panel) plasmid, and harvested 30 h after transfection. Total cell lysates were prepared and subjected to immunoprecipitation of p53 using monoclonal mouse antibody raised against p53 protein mAb DO-1 (α-p53). Proteins were resolved by SDS-PAGE and visualized by immunoblotting. Input levels of total-cell lysates and coprecipitated proteins were detected using using mAb B6-8 (α-E2A), pAb FL-393 (α-p53) and mAb AC-15 (α-β-actin). Molecular weights in kDa are indicated on the left, relevant proteins on the right. **(B)** Densitometric analyses of E2A immunoprecipitated with p53 in panel A (right panel, lanes 3 and 4) quantified with ImageJ (version 1.45s) software, respective levels of immunoprecipitated p53 in pE2A-wt and pE2A-SCM transfected cells. Bar plot represents average values and standard deviations calculated based on data obtained in three independent experiments.

4.4.2.4 E1B-55K prevents E2A/p53 interaction in transient transfection

E2A interaction with the tumor suppressor p53 is present only in the absence of E1B expression or when E1B-55K NES or SCM are inactivated by specific mutations (4.4.1.3). Moreover, non-SUMOylated E2A interacts with p53 during transient transfection (4.4.2.3). To ascertain that E1B-55K prevents E2A/p53 interaction independently on other viral factors, immunoprecipitation analysis was performed in cells transfected with pE2A-SCM and pE1B-55K. Immunoblotting revealed that E1B-55K abrogated E2A SCM interaction with p53 (Fig. 47 A, right panel, lanes 5 and 6 and Fig. 47 B). The amount of E2A SCM precipitated with p53 was 86.6% less when pE1B-55K was cotransfected with pE2A-SCM, compared to pE2A-SCM transfection alone (Fig. 47 B). As it was shown in 4.4.2.3, E2A SUMOylation prevents E2A from interacting with p53, and E1B-55K co-expression did not change this fact (Fig. 47 A, right panel, lanes 3 and 4; Fig. 47 B). Interestingly, E2A expression reduced the amount of E1B-55K to 63% when compared to E1B-55K expression alone (Fig. 47 A, left panel, lanes 2 and 4; Fig. 47 C), while the expression of E2A SCM reduced E1B-55K levels to 69% (Fig. 47 A, left panel, lanes 2 and 6; Fig. 47 C).

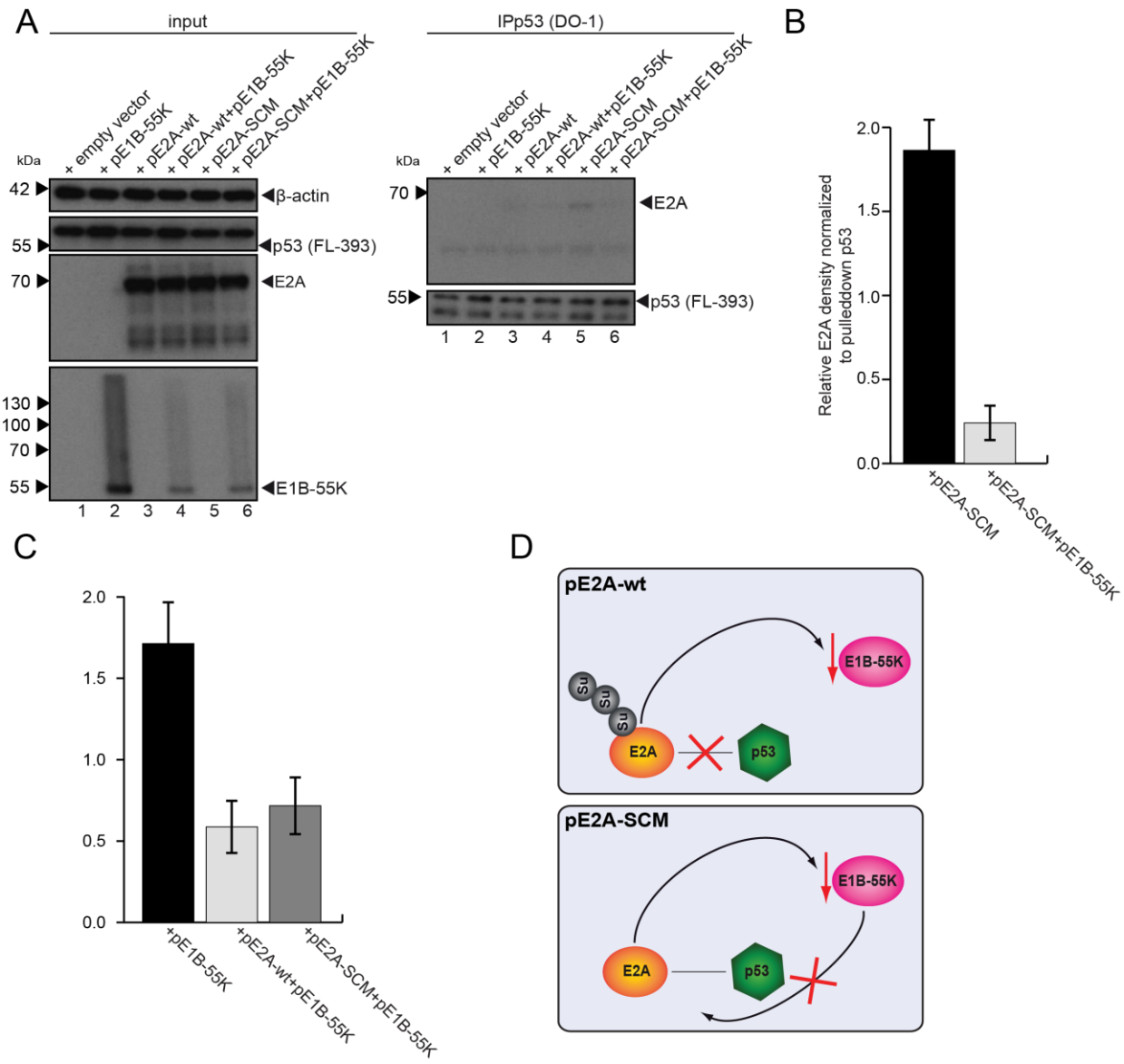

Figure 47: E1B-55K inhibits E2A/p53 interaction during transient transfection. (A) HepaRG cells were transfected with 5 µg of pE1B-55K (lane 2), pE2A-wt (lane 3), pE1B-55K and pE2A-wt (lane 4), pE2A-SCM (lane 5) and pE1B-55K and pE2A-SCM (lane 6) and harvested 30 h after transfection. Total cell lysates were prepared and subjected to immunoprecipitation of p53 using monoclonal mouse antibody raised against p53 protein mAb DO-1 (α-p53). Proteins were resolved by SDS-PAGE and visualized by immunoblotting. Input levels of total-cell lysates and coprecipitated proteins were detected using mAb B6-8 (α-E2A), mAb 2A6 (α-E1B-55K), pAb FL-393 (α-p53) and mAb AC-15 (α-β-actin). Molecular weights in kDa are indicated on the left, relevant proteins on the right. **(B)** Densitometric analyses of E2A immunoprecipitated with p53 in panel A (lanes 5 and 6) quantified with ImageJ (version 1.45s) software, normalized to respective levels of immunoprecipitated p53 in pE2A SCM and pE2A SCM and E1B-55K transfected cells. Bar plot represents average values and standard deviations calculated based on data obtained in three independent experiments. **(C)** Densitometric analyses of E1B-55K levels shown in panel A (lanes 2, 4 and 6) quantified with ImageJ (version 1.45s) software, normalized to respective levels of β-actin. Bar plot represents average values and standard deviations calculated based on data obtained in three independent experiments. (D) Schematic representation of the data shown in panels A, B and C

4.4.2.5 E2A changes E1B-55K and p53 subcellular localization

It has been reported that E1B-55K changes p53 distribution by sequestering it to the perinuclear bodies (Liu et al. 2005). E2A SUMOylation prevents E2A/p53 binding (4.4.2.3), while E2A recruits p53 to E2A containing domains independently on E2A SUMO status (4.4.2.2) in transiently transfected cells. E1B-55K abrogated E2A/p53 interaction both in infected and transfected cell (4.4.1.3 and 4.4.2.4). These findings prompted investigation of joint influence of E2A and E1B-55K on p53 subcellular localization.

HepaRG cells were transfected with pHA-E1B-55K, pHA-pE1B-55K combined with pE2A-wt or pE2A-SCM and immunofluorescence analysis was performed (Fig. 48). As it has been previously reported, transfection of E1B-55K led to p53 redistribution to the perinuclear bodies, together with the viral protein (Fig. 48 A, panels b and e). E1B-55K expression did not affect E2A localization in sphere-like nuclear structures (Fig. 48 A, panels i, j and n, o). However, the expression of E2A was sufficient to translocate E1B-55K into the nucleus where it localized in E2A-containing domains, even though perinuclear bodies distribution of E1B-55K was still detectable (Fig. 48 A, panels h and j). Moreover, E2A ability to promote E1B-55K nuclear import was independent on E2A SUMO PTM (Fig. 48 A, panels m and o). Additionally, Pearson's correlation coefficient of 0.51 for E2A-wt and E1B-55K and 0.53 for E2A SCM and E1B-55K, showing E2A SUMOylation independent colocalization of these two proteins, further supported these findings (Fig. 48 B). Interestingly, p53 localized both in E1B-55K containing perinuclear bodies and in E2A containing domains together with E1B-55K, independently on E2A SUMOylation (Fig. 48 A, panels g, j and l, o). Pearson's correlation coefficient for E2A-wt and p53 of 0.63, and 0.64 for E2A SCM and p53, in cells co-transfected with E1B-55K and E2A variants, showed that E1B-55K does not affect p53/E2A colocalization (Fig. 48 C). Moreover, Pearson's correlation coefficient for E1B-55K and p53 during co-expression of E2A-wt of 0.77 and 0.73 when E2A SCM was co-expressed, demonstrated clear E1B-55K/p53 colocalization that was independent of the E2A (Fig. 48 D). This p53 distribution showed striking resemblance to p53 localization during HAdV infection shown in section 4.4.1.2.

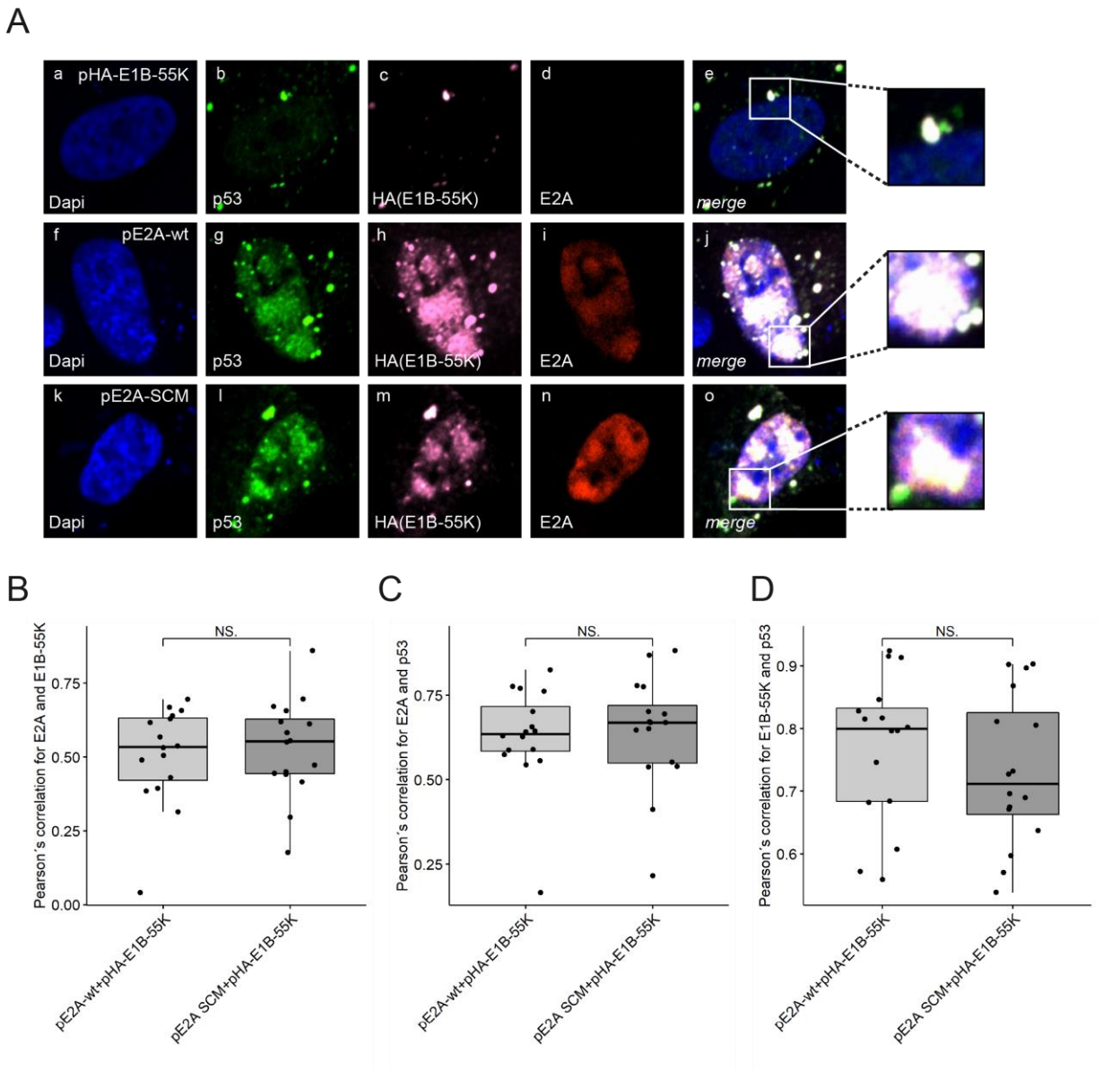

Figure 48: E2A recruits E1B-55K and p53 to the E2A containing domains in the cell nuclei. (A) HepaRG cells were transfected with pHA-E1B-55K (panels a, b, c, d, e) and pHA-E1B-55K with pE2A-wt (panels f, g, h, i, j) or pE2A-SCM (panels k, l, m, n, o) plasmids. The cells were fixed with 2% PFA 30 h after transfection and triple labeled with mAb DO-1 (α-p53), mAb rb (α-E2A) and Ab 3F10 (α-HA). Primary Abs were detected with Alexa488 (α-p53, green), Alexa647 (HA, pink) and Alexa568 (α-E2A, red) conjugated secondary Abs. Nuclear staining was performed using Dapi. Anti-p53 (green; panels b, g and l), Anti-HA (pink; panels c, h and m) and anti-E2A (red; panels d, i and n), staining patterns representative of 30 analyzed cells are shown. Overlays of single images (merge) are shown in panels e, j, o. **(B, C, D)** Software Volocity was used to determine Pearson's correlation coefficient for E2A and E1B-55K **(B)**, E2A and p53 **(C)** and E1B-55K and p53 **(D)** signals in cells transfected with pHA-E1B-55K and pE2A-wt or pE2A-SCM plasmids. For each cell, Pearson's correlation was calculated for colocalization of E2A with E1B-55K **(B)**, E2A with p53 **(C)** and E1B-55K with p53 **(D)**. The distributions of the respective correlation coefficient are displayed in a box plot. Values above 0.5 are considered as colocalized.

4.4.2.6 E2A counteracts E1B-55K-dependent p53 SUMOylation

E1B-55K SUMOylates p53 causing the inhibition of p53 transcriptional activity (Pennella et al. 2010; Wimmer et al. 2016). E2A recruits E1B-55K and p53 to E2A containing domains in the cell nuclei (4.4.2.5) and promotes HAdV-mediated p53 SUMOylation (4.4.1.5). Therefore, the influence of E2A on E1B-55K-mediated p53 SUMOylation was investigated.

Analyses of Ni-NTA purified samples from transfected HepaRG His/HA SUMO-2 cells revealed the previously reported increase in p53 SUMOylation-mediated by E1B-55K by 38-fold (Fig. 49 A, right panel, lane 3 and Fig. 49 B). Interestingly, SUMO conjugation to p53 was reduced when p53 was cotransfected with pE1B-55K and pE2A-wt to 14-fold when compared to E1B-55K expression alone (Fig. 49 A, right panel, lane 4, Fig. 49 B). The reduction of E1B-55K-mediated p53 SUMOylation was independent on E2A SUMO PTM as it was 13-fold compared to E1B-55K expression alone (Fig. 49 A, right panel, lane 5, Fig. 49 B). Moreover, E2A expression reduced E1B-55K levels to 66.6% (Fig. 49 A, left panel, lane 4, Fig. 49 C) and SUMOylation to 66.1% (Fig. 49 A, right panel, lane 4, Fig. 49 D). The reduction of E1B-55K levels and SUMOylation was independent on E2A SUMO PTM, as E2A SCM expression reduced E1B-55K levels to 52.8% (Fig. 49 A, left panel, lane 5, Fig. 49 C) and SUMOylation to 55.6% (Fig. 49 A, right panel, lane 5, Fig. 49 D), offering possible explanation for E2A effects on E1B-55K-mediated p53 SUMOylation.

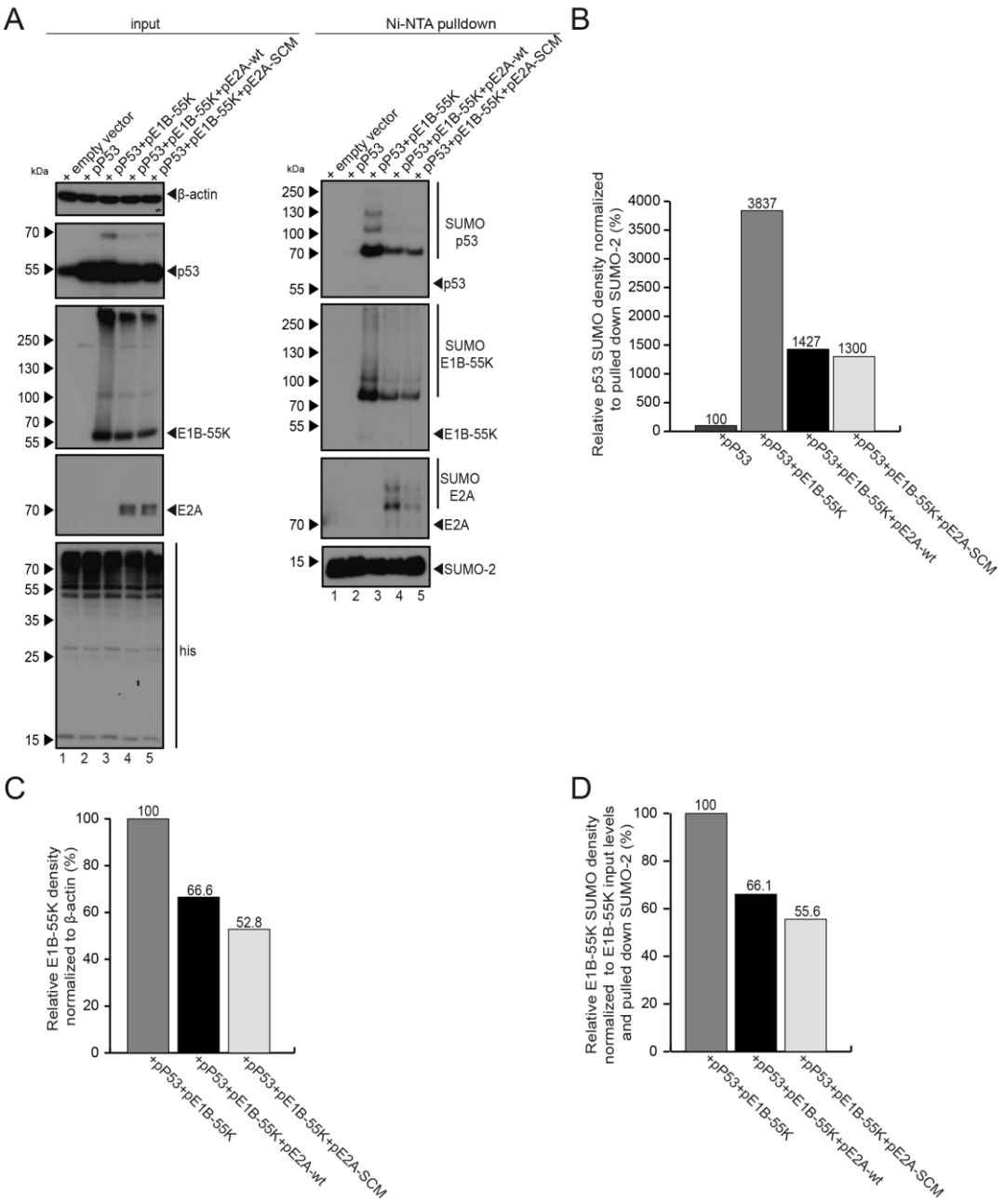

Figure 49: E2A reduces E1B-55K-dependent p53 SUMOylation. (A) HepaRG cells stably expressing His/HA-SUMO-2 were transfected with 0.5 µg of pP53 (lane 2), pP53 and E1B-55K (lane 3), and pP53 and p-E1B-55K with pE2A-wt (lane 4) or pE2A-SCM (lane 5) plasmids. The cells were harvested 30 h after transfection, whole-cell lysates were prepared with guanidinium chloride buffer, subjected to Ni-NTA purification of 6xHis-SUMO conjugates and separated by SDS-PAGE. Input levels of total-cell lysates and Ni-NTA purified conjugates were detected with mAb B6-8 (α-E2A), mAb 2A6 (α-E1B-55K), mAb DO-1 (α-p53), mAb 6-His (α-6xHis-tag), mAb 8A2 (α-SUMO-2/3) and mAb AC- 15 (α-β-actin). Molecular weights in kDa are indicated on the left, relevant proteins on the right. **(B)** Densitometric analysis of p53 SUMOylation levels in panel A (lanes 2, 3, 4 and 5), quantified with ImageJ (version 1.45s) software, normalized to the respective levels of pulled down SUMO-2. **(C)** Densitometric analysis of E1B-55K expression in panel A (lanes 3, 4 and 5), quantified with ImageJ (version 1.45s) software, normalized to the respective β-actin levels. **(D)** Densitometric analysis of E1B-55K SUMOylation levels in panel A (lanes 3, 4 and 5), quantified with ImageJ (version 1.45s) software, normalized to the respective levels of E1B-55K and pulled down SUMO-2.

4.4.2.7 E2A relocalizes Ubc9 on an E2A SUMOylation independent manner

Ubc9 directly interacts with p53 leading to SUMOylation of the tumor suppressor (Lin, Ohshima, and Shimotohno 2004). E2A interacts with Ubc9 on an E2A SCM-dependent manner (4.1.3) and recruits p53 to the E2A containing domains in cell nuclei (4.4.2.2). Immunofluorescence analysis was performed to examine if E2A also sequesters Ubc9 into the E2A domains (Fig. 50). Analysis of cells transfected with pE2A-wt showed E2A-mediated redistribution of Ubc9 into the E2A sphere-like structures in the cell nuclei (Fig. 50 A, panels f and h). Ubc9 also localized together with E2A in the absence of E2A SUMO PTM (Fig. 50 A, panels j and l). This can be further supported by Pearson's correlations of 0.84 for E2A and Ubc9 and 0.71 for E2A SCM and Ubc9. Interestingly, even though both E2A and E2A SCM colocalized with Ubc9, statistically significant difference between Pearson's correlation coefficients for Ubc9 and the two E2A variants was observed (Fig. 50 B).

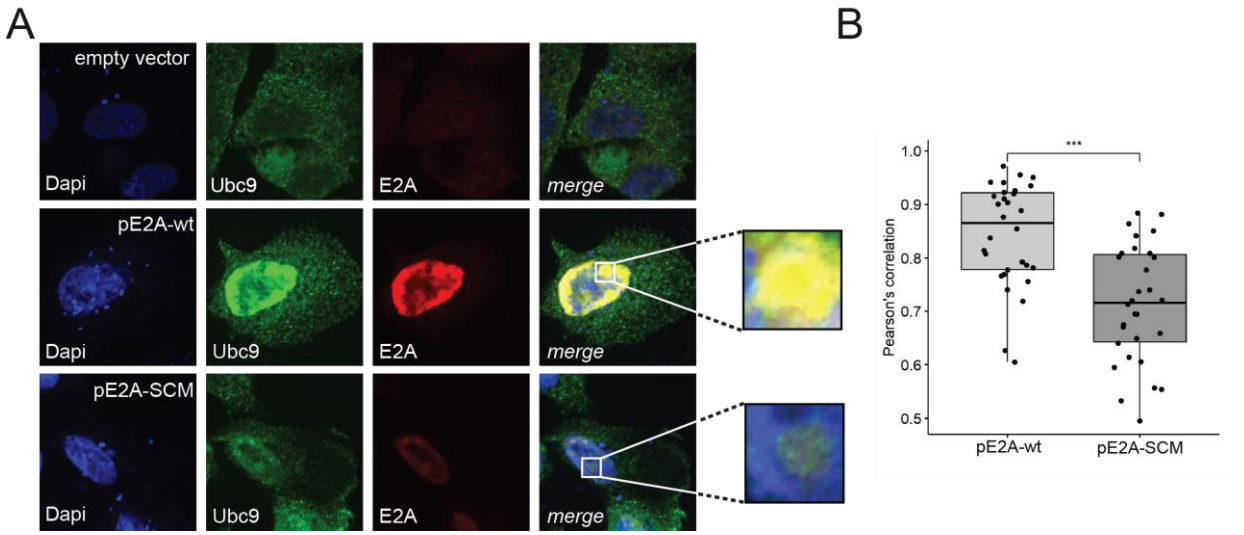

Figure 50: E2A recruits Ubc9 to the E2A containing domains in cell nuclei. (A) HepaRG cells were transfected with pE2A-wt or pE2A-SCM plasmids. The cells were fixed with 2% PFA 30 h after transfection and double labeled with mAb rb (α-E2A) and mAb C-12 (α-Ubc9). Primary Abs were detected with Alexa488 (α-Ubc9, green) and Alexa647 (E2A, red) conjugated secondary Abs. Nuclear staining was performed using Dapi. Anti-Ubc9 (green; panels b, f and j) and anti-E2A (red; panels c, g and k), staining patterns representative of 30 analyzed cells are shown. Overlays of single images (merge) are shown in panels d, h, l. **(B)** Software Volocity was used to determine Pearson's correlation coefficient for Ubc9 and E2A in cells transfected with pE2A-wt and pE2A-SCM plasmids. For each cell, Pearson's correlation was calculated for colocalization of Ubc9 with E2A. The distributions of the respective correlation coefficient are displayed in a box plot. Values above 0.5 are considered as colocalized.

4.4.2.8 SUMO modified E2A inhibits p53 SUMOylation

p53 can be SUMO modified on a lysine residue K386 both with SUMO-1 and SUMO-2/3 (Gostissa et al. 1999). E2A SUMOylation prevents E2A/p53 interaction (4.4.2.3). Moreover, E2A reduces E1B-55K-mediated p53 SUMOylation independently on E2A SUMO status (4.4.2.6). Ubc9 directly interacts with p53 leading to SUMO conjugation to p53 (Lin, Ohshima, and Shimotohno 2004). E2A interacts with the p53 SUMO conjugating enzyme Ubc9 on an E2A SUMOylation-dependent manner (4.1.3). These facts prompted the investigation of E2A influence on p53 SUMOylation in the absence of other viral components.

Immunoblot analysis of Ni-NTA purified samples from transfected HepaRG His/HA SUMO-2 cells showed E2A-mediated reduction of p53 SUMOylation (Fig. 51, right panel, lane 4). Moreover, E2A with inactivated SCMs failed to reduce the p53 SUMO PTM (Fig. 51, right panel, lane 6). Densiometric analysis supported this data showing 60.7 % reduction of p53 SUMOylation during expression of E2A, while p53 SUMO PTM levels were not affected by E2A SCM expression (Fig. 51 B).

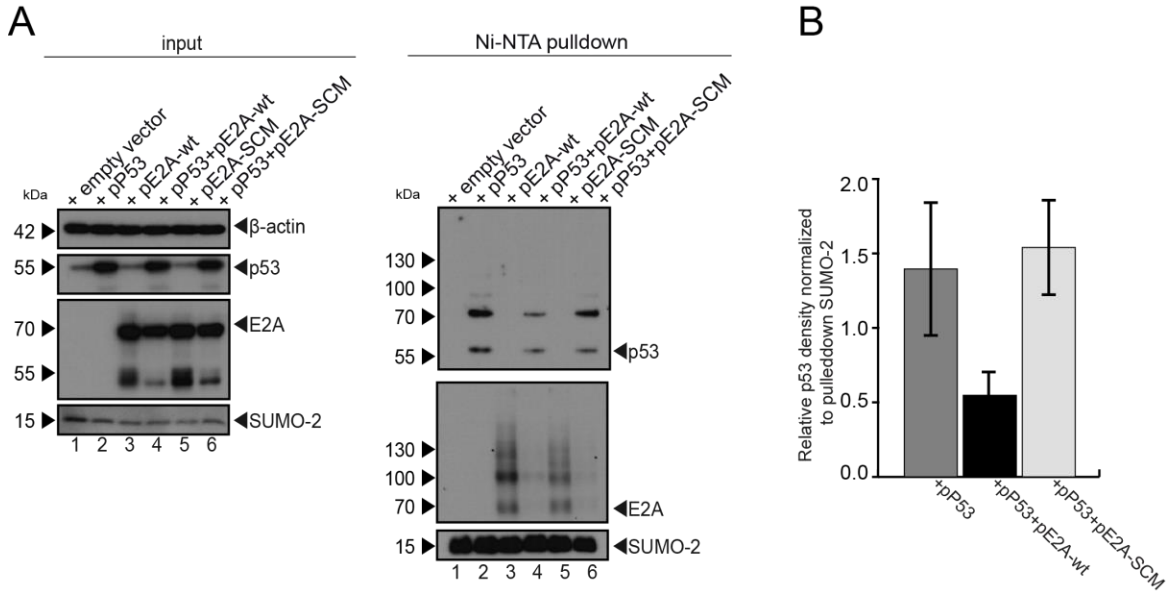

Figure 51: E2A negatively influences p53 SUMOylation. (A) HepaRG cells stably expressing His/HA-SUMO-2 were transfected with 0.5 µg of pP53 (lane 2), p-p53 and pE2A-wt (lane 4), and pP53 and p-E2A-SCM (lane 6) plasmids. The cells were harvested 30 h after transfection, whole-cell lysates were prepared with guanidinium chloride buffer, subjected to Ni-NTA purification of 6xHis-SUMO conjugates, and separated by SDS-PAGE. Input levels of total-cell lysates and Ni-NTA purified conjugates were detected with mAb B6-8 (α-E2A), mAb DO-1 (α-p53), mAb 8A2 (α-SUMO-2/3) and mAb AC-15 (α-β-actin). Molecular weights in kDa are indicated on the left, relevant proteins on the right. **(B)** Densitometric analysis of p53 SUMOylation levels in panel A (lanes 2, 4 and 6), quantified with ImageJ (version 1.45s) software, normalized to the respective levels of pulled down his. Bar plots represents average values and standard deviations calculated based on three separate experiments.

5 Discussion

5.1 E2A SUMOylation is beneficial for HAdV infection

Posttranslational modifications of proteins are fast, energetically inexpensive mechanisms that reversibly alter protein function, enabling the cell to vastly extend the functional repertoire of modified proteins. PTMs regulate the activity, stability, subcellular localization and protein-protein interactions of their substrates (Dohmen 2004). These processes also influence the interplay between viruses and host cells. One of the crucial PTMs regulating the virus-host interactions is SUMOylation. Therefore, it is not surprising that both RNA and DNA viruses developed sophisticated mechanisms to exploit this cellular pathway (Everett, Boutell, and Hale 2013). Adenoviruses use the host SUMOylation machinery as a tool to promote the viral replication and inhibit cellular immune responses (Wimmer and Schreiner 2015). PML-NBs are hot spots for SUMOylation processes (Ishov et al. 1999; Shen et al. 2006; Zhong et al. 2000). Viral RCs marked by HAdV protein E2A are located juxtaposed to these structures during HAdV infection (Puvion-Dutilleul, Pedron, and Cajean-Feroldi 1984). HAdV proteins E1B-55K and pV are so far the only two adenoviral proteins known to be directly targeted by the SUMO PTM (Wimmer et al. 2013; Endter et al. 2001; Freudenberger et al. 2018). This study revealed that E2A also represents a target of host SUMOylation machinery (4.1.1). E2A harbors three SUMO conjugation motifs that, interestingly, do not correspond to classical SUMO consensus motif (4.1.2). This can be explained by the fact that SUMO can also attach to non-canonical motifs especially in the stress conditions, such as viral infection (Hendriks and Vertegaal 2016; Pichler et al. 2017). Ubc9 is the main SUMO conjugating enzyme of the SUMOylation pathway that enables direct SUMO attachment to the SCMs within the target proteins (Desterro, Thomson, and Hay 1997; Okuma et al. 1999). HAdV proteins employ different mechanisms to manipulate the Ubc9 function to establish suitable environment for viral replication. HAdV proteins E1A and E4orf3 are not directly SUMO modified but they interact with Ubc9 (Yousef et al. 2010; Sohn and Hearing 2019; Hateboer et al. 1996). Another viral interaction partner of Ubc9 is E1B-55K, a protein that binds to the cellular SUMO conjugating enzyme on a SUMOylation-independent way (Wimmer et al. 2013). The data showing E2A as a target of the cellular SUMO conjugation machinery was supported by the observation that Ubc9 also interacts with E2A. However, contrary to E1B-55K, intact E2A SCMs are crucial for E2A interaction with Ubc9 (4.1.3). SUMOylation

and Ubiquitinylation use similar three-step enzymatic cascade. SUMO and ubiquitin often compete for the same lysine residues within the conjugation motifs (Hay 2007; Johnson 2004). The possibility that E2A SCM mutations disrupt the Ubiquitin PTM was excluded (4.1.4), however further studies would have to be conducted to investigate the influence of E2A SCMs disruption on other E2A PTMs such as acetylation or phosphorylation.

E2A SCM mutations reduced the viral progeny production, revealing the beneficial role of E2A SUMO PTM in HAdV infection cycle (4.2.1). This data concorded with the infection promoting effects of E1B-55K SUMOylation. However, the previously reported inhibitory function of pV SUMOylation was not in accordance with this data, demonstrating complexity of HAdV interactions with the host SUMOylation pathway (Freudenberger et al. 2018).

The major function contributed to E2A is in viral DNA replication (Hay et al. 1995; Schilling, Weingartner, and Winnacker 1975; van Breukelen et al. 2003; van Breukelen et al. 2000). This lead to designating the E2A as marker protein for viral replication centers (Puvion-Dutilleul, Pedron, and Cajean-Feroldi 1984). E2A performs its function in replication via interaction with single-stranded DNA (van der Vliet and Levine 1973), double-stranded DNA (Fowlkes et al. 1979) and RNA (Cleghon and Klessig 1986) on a sequence unspecific manner. SUMOylation can affect various properties of its protein substrates, thereby altering their functions (Hendriks and Vertegaal 2016). Based on these facts and the above-mentioned finding showing the importance of E2A SUMOylation for efficient progeny production (4.2.1), it would be expected that the lack of functional SCMs in E2A disrupted its role in viral DNA replication. The reduction in levels of the viral DNA polymerase, pTP and TP (4.2.4), proteins also involved in HAdV DNA replication (Shenk 2001), supported this hypothesis. However, both viral DNA synthesis and E2A DNA binding ability were not impaired by E2A SCM mutations (4.2.3 and 4.2.2).

E1A induces the cell cycle progression by leading the cells to the S-phase to establish optimal environment for virus replication entry (Bagchi, Raychaudhuri, and Nevins 1990; Bandara and La Thangue 1991; Blais and Dynlacht 2004; Ghosh and Harter 2003; Ip and Dobner 2020). Therefore, the reduction in the levels of all E1A isoforms during infection with E2A SUMOylation deficient virus (4.2.4), could offer at least partial explanation for the observed impaired viral progeny production. Moreover, as E1A is the major adenoviral transcription factor that induces transcription of other early genes E1B to E4 (Avvakumov, Sahbegovic, et al. 2002; Avvakumov,

Wheeler, et al. 2002; Moran et al. 1986), it was logical to assume that the expression of other viral proteins could be affected by impaired E2A SCMs.

E1B-55K and E4orf6 assemble the viral E3 ubiquitin ligase complex (Blanchette et al. 2004; Querido et al. 2001; Schreiner, Wimmer, and Dobner 2012). Even though the levels of the two proteins were unaffected by E2A SCMs, their splice forms E1B-156R, E1B-93R, E1B-84R and E4orf6/7 were less expressed (4.2.4). The observed effect can be explained by previously discussed reduction of levels of all E1A isoforms. As E4orf6/7 enchases transcription from E2 genes, it can be assumed that the decrease in steady state levels of the mentioned viral protein, caused by E2A SCM mutations leads to the reduction of the levels of the viral DNA polymerase, pTP and TP (4.2.4). Intriguingly, the decreased expression of these proteins with essential roles in HAdV DNA replication did not affect this process (4.2.3).

Another protein encoded by the E4 region, affected by E2A SCM mutations, is E4orf3 (4.2.4). As E4orf3 reorganizes PML-NBs into track like structures (Carvalho et al. 1995; Doucas et al. 1996; Vink et al. 2015), it would be expected that the reduction in levels of E4orf3 impaired this process. However, as it will be discussed in the following chapter, PML tracks were still formed, despite the mutations in E2A SCMs. The reduction of E4orf3 levels could impair its function in the HAdV-mediated inhibition of p53-dependent transcription (Soria et al. 2010). Therefore, it would be interesting to investigate if HAdV E2A SCM infection prevents p53/DNA binding with the same efficiency as the HAdV wt infection. If this would be truly the case, the lack of recruitment of the histone methyltransferases SUV38H1 and SUVH2 to p53 responsive elements during HAdV E2A SCM infection would indicate that the reduction of E4orf3 levels led to the supposed reduction of the p53/DNA binding (Soria et al. 2010).

Ahi and coworkers reported that E2A, IVa2 and L4-33K form a complex on viral capsids and cooperate in genome packaging (Ahi, Vemula, and Mittal 2013). E2A and IVa2 protein levels were not affected by E2A SCM mutations, while moderate reduction of L4-33K levels was accompanied with the lower expression of the higher migrating band indicating possible PTM of the viral protein. (4.2.4). This data suggests possible E2A SCM-dependent influence on L4-33K PTM, most presumably SUMOylation. Moreover, based on the studies showing that SUMOylation regulates the protein/protein interactions of its substrates (Dohmen 2004; Hendriks and Vertegaal 2016) it would be logical to assume that E2A SCM mutant cannot properly form complex with IVa2 and L4-33K, thus causing the defect in genome packaging, leading to the impaired progeny

production. This assumption can be further supported by the work of Nicolas and coworkers demonstrating that temperature sensitive mutant of HAdV with point mutations in E2A coding region was found to be defective for capsid assembly (Nicolas et al. 1983). Nevertheless, further studies, involving immunoprecipitation analysis, immunofluorescence and electron microscopy are necessary to fully prove this hypothesis.

Besides the possible inability of the E2A SCM mutant virus to form the fully functional viral DNA packaging complex, it seems that E2A SCM mutations also impair the formation of viral capsids. Namely, the capsid protein expression was also reduced in the absence of E2A SUMOylation (4.2.4), consistently with the virus yield data (4.2.1). Similar results were obtained monitoring the viral Hexon mRNA synthesis in infected cells (4.2.5) and go in line with the reports that SUMOylation can also increase the transcriptional activation mediated by its substrates, even though the SUMO attachment to transcription factors often results in repression (Johnson 2004).

L4-33K plays an important role in early to late phase switch together with L4-100K, regulatory phosphoprotein transcribed from the adenovirus major late transcription unit (Farley, Brown, and Leppard 2004). L4-100K alters cellular machinery in favor of translation of large amounts of viral products, leading to their accumulation in the nucleus for capsid assembly. It promotes the viral mRNA translation by interacting with late viral transcripts and the scaffolding element of the cap-dependent translation initiation complex, eIF4G (Riley and Flint 1993; Cuesta, Xi, and Schneider 2004). Binding of L4-100K to eIF4G inhibits its phosphorylation necessary for eukaryotic cell translation, hence causing the inhibition of host cell translation, also called the *host shut-off*. L4-100K levels were reduced during E2A SCM virus infection, thus one could expect consequential defects in in *host shut-off* mechanism and viral translation. Furthermore, L4-100K functions as a chaperone for the formation of hexon trimmers (Hong et al. 2005; Cepko and Sharp 1983, 1982), which would otherwise be unstable and also supports their transport and capsid assembly (Morin and Boulanger 1986). Reduction in levels of L4-100K caused by E2A SCM mutations observed in this study could disrupt proper hexon trimerization, which in turn could lead to the impaired viral particle formation. If this hypothesis were true, it could explain the decrease in adenovirus capsid protein synthesis (4.2.4), as well as the defect in HAdV progeny production (4.2.1).

In summary, E2A is modified by the cellular SUMO PTM. E2A SUMOylation is beneficial for HAdV infection, even though it does not control the main E2A function in viral DNA

replication. E2A SUMOylation promotes HAdV progeny production by the control of HAdV protein synthesis with possible implications on HAdV gene splicing and packaging of the viral genome. As discussed in following sections, further studies were performed to unravel more detailed mechanisms underlying these events.

5.2 E2A SUMOylation underlies PML tracks localization next to HAdV replication centers

PML-NBs are mostly regarded as a component of the intracellular anti-viral defense mechanism (Everett and Chelbi-Alix 2007; Tavalai and Stamminger 2008). PML and PML-NBs associated protein genes are stimulated by interferon and they efficiently inhibit the virus replication (Chelbi-Alix et al. 1998; Regad and Chelbi-Alix 2001). To establish the most optimal environment for viral infection, viruses have evolved diverse mechanisms to counteract antiviral activities mediated by PML-NBs (Everett 2001; Everett and Chelbi-Alix 2007; Tavalai and Stamminger 2008). One example is the HSV-1 infection, where the immediate early protein ICP0 localizes to PML-NBs leading to their complete disruption. Subsequently, ICP0 causes proteasomal degradation of PML that results in disintegration of PML-NBs (Everett et al. 2006). During HAdV infection, PML-NBs are reorganized in into track-like structures, via direct interaction of the HAdV protein E4orf3 with PML (Carvalho et al. 1995; Doucas et al. 1996; Vink et al. 2015). Contrary to HSV-1, adenoviruses do not completely disrupt PML-NBs by targeting their main components for degradation, but rather keep the PML tracks until the late stages of infection. Even though PML-NBs represent antiviral compartments of the cell, many DNA viruses position their genomes juxtaposed to PML-NBs by so far unknown mechanism (Doucas et al. 1996; Everett 2001; Ishov and Maul 1996; Jul-Larsen et al. 2004; Maul 1998; Maul, Ishov, and Everett 1996; Sourvinos and Everett 2002). This is also the case during HAdV infection, where the HAdV RCs, marked by the viral protein E2A (Puvion-Dutilleul, Pedron, and Cajean-Feroldi 1984), localize juxtaposed to PML tracks (Doucas et al. 1996). PML-NBs are regarded as the hotspots for SUMOylation processes (Van Damme et al. 2010) and PML interacts with SUMOylated proteins (Ishov et al. 1999; Shen et al. 2006; Zhong et al. 2000). As it is known that SUMOylation affects protein/protein interactions and subcellular localization of its substrates (Hendriks and Vertegaal 2016) and this work revealed that SUMO conjugation machinery targets the HAdV E2A (4.1.1), it was assumed that E2A SUMOylation represents the molecular

mechanism underlying the localization of HAdV RCs next to PML tracks. This hypothesis was confirmed by the data showing increased distances between HAdV RCs an PML tracks in the absence of E2A SUMO PTM (4.3.2.2). This can be further substantiated by the finding that E2A indeed interacts with PML during HAdV infection and that this binding depends on E2A SUMOylation (4.3.1.2). Interestingly, E2A also interacted with PML during transient transfection, but contrary to the infection experiments this interaction did not require intact E2A SCMs (4.3.1.1). The explanation for this observation could be that during infection, majority of E2A will be bound to HAdV DNA, masking its DNA binding domain and potentially also other surfaces that might mediate direct interactions with PML, so only SUMO-SIM interactions remain. Another reason could be the organization of E2A in RCs together with different SUMO proteins in infection. It was recently reported that during infection SUMO-1 localizes outside of RC, while SUMO-2 and SUMO-3 mainly localize inside RCs (Hidalgo et al. 2016). This infection-mediated localization of SUMO proteins involved in the E2A/PML interaction, could offer a plausible explanation for the change in binding capacity. The E2A/PML interaction during infection was still observed in the absence of E4orf3 (4.3.1.2). Furthermore, it was reported that even when PML is not redistributed to tracks, as in the case of an E4orf3 depleted virus, RCs still form juxtaposing to PML-NBs (Ishov and Maul 1996). Therefore, the reorganization of PML-NBs in tracks by E4orf3 is not involved in the E2A/PML interaction or the RCs localization next to PML tracks.

The reason why different viruses localize their replication machineries in the vicinity of PML-NBs that exhibit antiviral function, lays in the fact that those cellular structures also contain beneficial components for viral infection. Therefore, different viruses, particularly the group of DNA viruses, have developed refined mechanisms to simultaneously counteract antiviral activity of PML-NBs and exploit their infection promoting components. Viral DNA replication and transcription of DNA viruses often takes place in the proximity of these cellular structures. For example, genome transcription of human cytomegalovirus (HCMV) and human herpes simplex virus type 1 (HSV-1) occurs specifically at PML-NBs (Ishov, Stenberg, and Maul 1997; Ishov and Maul 1996; Maul, Ishov, and Everett 1996). SV40 and human polyomaviruses (HPyV) replication favors the proximity of PML-NBs (Shishido-Hara et al. 2008; Tang et al. 2000). Moreover, PML expression promotes the human papillomavirus (HPV) infection (Day et al. 2004). PML-specifically the PML II isoform, promotes HAdV infection through the interaction with E1A-13S, enhancing its trans activating capacity towards adenoviral genes (Berscheminski et al. 2013).

Additionally, Sp100A isoform is kept in PML tracks during HAdV infection to support efficient expression of adenoviral genes (Berscheminski et al. 2014). During infection with E2A SUMOylation deficient virus, localization of PML tracks was displaced from the HAdV RCs (4.3.2.2). This might prevent the virus from using beneficial PML components localized in virus-induced tracks by eliminating contact of PML tracks and newly synthesized HAdV mRNA. As PML tracks are the sites of active viral transcription (Doucas et al. 1996; Hidalgo et al. 2016), it is not surprising that the infection with E2A SCM mutant virus resulted in decreased replication efficacy (4.2.1). Furthermore, defect in splicing of certain HAdV proteins (4.2.4), that also contributes to impaired viral progeny production in the absence of the E2A SUMOylation, could indicate the miss localization of the interchromatin granules region, where the splicing events take place (Hidalgo et al. 2016). It has been proposed that HAdV modulates the Sp100A activity to benefit the infection through the interaction with E1B-55K and reduction of SUMOylation of the cellular factor (Berscheminski et al. 2016; Berscheminski et al. 2014). Interestingly, the data described in section 4.3.3.2 clearly demonstrate that SUMOylated E2A also binds the Sp100A. This data leads to the assumption that the Sp100A-mediated activation of HAdV gene expression is promoted by the increase in the Sp100A quantity during wt HAdV infection. This was not detected in cells infected with the E2A SUMOylation deficient virus, thus SUMOylation and the interaction with E2A might be involved. Ubc9 is the main SUMO conjugating enzyme also involved in Sp100 SUMOylation (Seeler et al. 2001). Therefore, the inability of E2A with impaired SCMs to bind Ubc9 might prevent the HAdV-mediated reduction of Sp100A SUMOylation and thus block its transcription activating properties (Berscheminski et al. 2016). Lower Sp100A protein levels and altered PML-track localization during E2A SCM infection might in sum prevent the virus from exploiting beneficial Sp100A capability. Furthermore, the interaction between E2A and Sp100A was E2A SUMOylation-dependent, but it did not depend on PML (4.3.3.3). Therefore, it is tempting to speculate that Sp100A represents the unknown factor bridging RCs to PML tracks.

5.3 E2A SUMOylation counteracts the host antiviral response

HAdV-mediated redistribution of PML-NBs into track-like structures enables the virus to gain access to the factors beneficial for infection but in the same time repressive factors become accessible for targeting by the viral proteins involved in the inhibition of the host antiviral

response. HAdV counteracts the repressive factors by direct interaction, targeting for degradation, relocalization and change of posttranslational modification. For example, constitutive PML-NB factor Daxx inhibits HAdV infection. This inhibition is counteracted by pVI-mediated relocalization from PML-NBs and subsequent proteasomal degradation dependent on E1B-55K (Schreiner et al. 2010; Schreiner et al. 2012). Moreover, certain antiviral factors such as SPOC1 and BLM localize at the HAdV RCs early during infection but get degraded in later infection stages (Orazio et al. 2011; Schreiner, Kinkley, et al. 2013). Therefore, it appears that some seemingly negative factors might have a beneficial effect in the early phases of HAdV life cycle, whereas they are no longer needed in the later phases when they are targeted for degradation by E3 ubiquitin ligase complex assembled by HAdV proteins E1B-55K and E4orf6 (Baker et al. 2007a; Blanchette et al. 2004; Gupta et al. 2013; Orazio et al. 2011; Schreiner, Burck, et al. 2013; Schreiner, Kinkley, et al. 2013; Stracker, Carson, and Weitzman 2002; Yondola and Hearing 2007; Dallaire et al. 2009). However, certain data also points out the possibility that HAdVs sequester some inhibitory factors to HAdV RCs to prevent their contact with sites of active viral replication/transcription (Turnell and Grand 2012). One example is the cellular factor Sp100. The depletion of Sp100 promotes HAdV infection and it is assumed that this is due to the lack of chromatin condensing isoforms -B, -C and -HMG, as it is known that Sp100A isoform has viral gene expression promoting properties, while the Sp100B inhibits viral promotors (Berscheminski et al. 2016; Berscheminski et al. 2014). It has been shown that Sp100 depletion also promotes HCMV infection (Kim et al. 2011). The idea that chromatin condensing Sp100 isoforms inhibit HAdV infection is further supported by the data by Maul and coworkers showing that specifically Sp100 isoforms -B, -C and -HMG suppress HSV-1 infection (Negorev et al. 2006). During HAdV infection, Sp100 isoforms -B, -C and -HMG are sequestered to the HAdV RCs. It has been proposed that this is the mechanism used by the virus to inactivate their repressive properties (Berscheminski et al. 2014). Interestingly, this work shows that the relocalization of Sp100 isoform HMG to RCs depends on the E2A SUMO PTM (4.3.4.2). This finding indicates a novel E2A role in inhibition of the host cellular antiviral response, based on the E2A SUMOylation. As discussed in the previous chapter, E2A binds Sp100A on SUMOylation-dependent manner (4.3.3.2). E1B-55K interacts specifically with Sp100A (Berscheminski et al. 2016). However, even though the stability of the higher molecular weight Sp100 isoforms depends on E1B-55K and E4orf6 in infection, E1B-55K does not bind Sp100 B, -C and -HMG. This indicates that some other viral proteins contribute to the

loss of high molecular weight Sp100 isoforms (Berscheminski et al. 2014). Interestingly, the data from this work show that E2A interacts with Sp100HMG during HAdV infection. Moreover, this interaction is E2A SUMO PTM-dependent (4.3.4.1). Therefore, it can be assumed that HAdVs sequester Sp100HMG to the RCs through the E2A SUMO-dependent interaction. It is tempting to speculate that E2A SUMOylation might be necessary for the reduction of high molecular weight Sp100 isoforms via so far unknown mechanism. Furthermore, it is known that polySUMO-2/3 chains protrude into the interior of HAdV RCs, while SUMO-1 localizes to the periphery of RCs (Hidalgo et al. 2016). Therefore, it might be possible that E2A interaction with Sp100HMG and other factors localized in HAdV RCs is SUMO-2/3-dependent, while the interaction with factors localized outside of HAdV RCs such as Sp100A depends on the SUMO-1 conjugation. However, further studies would have to be performed to confirm these ideas. Sp100HMG interacts with HP1α forming a chromatin-associated complex involved in repression of gene expression by inducing chromatin condensation (Newhart et al. 2013; Seeler et al. 1998). Consequently, the observed inability of E2A SUMOylation depleted HAdV to displace the Sp100HMG isoform into HAdV RCs led to a condensed chromatin state (4.3.4.3) and could be the cause of the impaired viral replication. It has been reported that HAdV infection leads to the reduction of Sp100 SUMOylation (Berscheminski et al. 2016; Berscheminski et al. 2014). As it is known that Sp100 SUMOylation stabilize its interaction with HP1α (Seeler et al. 2001), it can be assumed that HAdV sequesters Sp100HMG to RCs on an E2A SUMOylation-dependent manner, preventing SUMOylation of Sp100HMG, and hence its interaction with HP1α. Furthermore, Ubc9 represents the main SUMO conjugating enzyme also involved in Sp100 SUMOylation (Seeler et al. 2001). Therefore, it is also possible that the inability of E2A SCM to interact with Ubc9 prevents the virus from decreasing SUMOylation of Sp100 and its isoforms -A and -HMG. This could lead to the inability of HAdV to support Sp100A deSUMOylation and sequester SUMOylated Sp100HMG into viral RCs to prevent the repressive properties.

Taken together, E2A is targeted by the host SUMOylation machinery. HAdV benefits from the E2A SUMO PTM. Even though the inactivation of E2A SCMs repressed the viral replication properties, the E2A function in DNA replication was not affected by the SUMO PTM of this viral factor. This work clearly illustrates the influence of E2A SUMOylation on PML-NBs subcellular localization and PML interaction. The Sp100A and PML interactions enable the virus to position PML tracks juxtaposing to HAdV replication centers where it can utilize their transcription

activating capacities. Furthermore, E2A SUMOylation supports efficient splicing of certain HAdV proteins, indicating possible effect on the localization of the interchromatin granules region. In contrast, SUMOylated E2A prevents the condensation of viral chromatin, by active displacement of the repressive factor Sp100HMG into HAdV replication centers. E2A SUMOylation is invaluable for HAdV to both exploit beneficial cellular components and to counteract host cell antiviral response. In sum, E2A SUMOylation is highly beneficial for HAdV life cycle and therefore can be used as a target for future antiviral strategies.

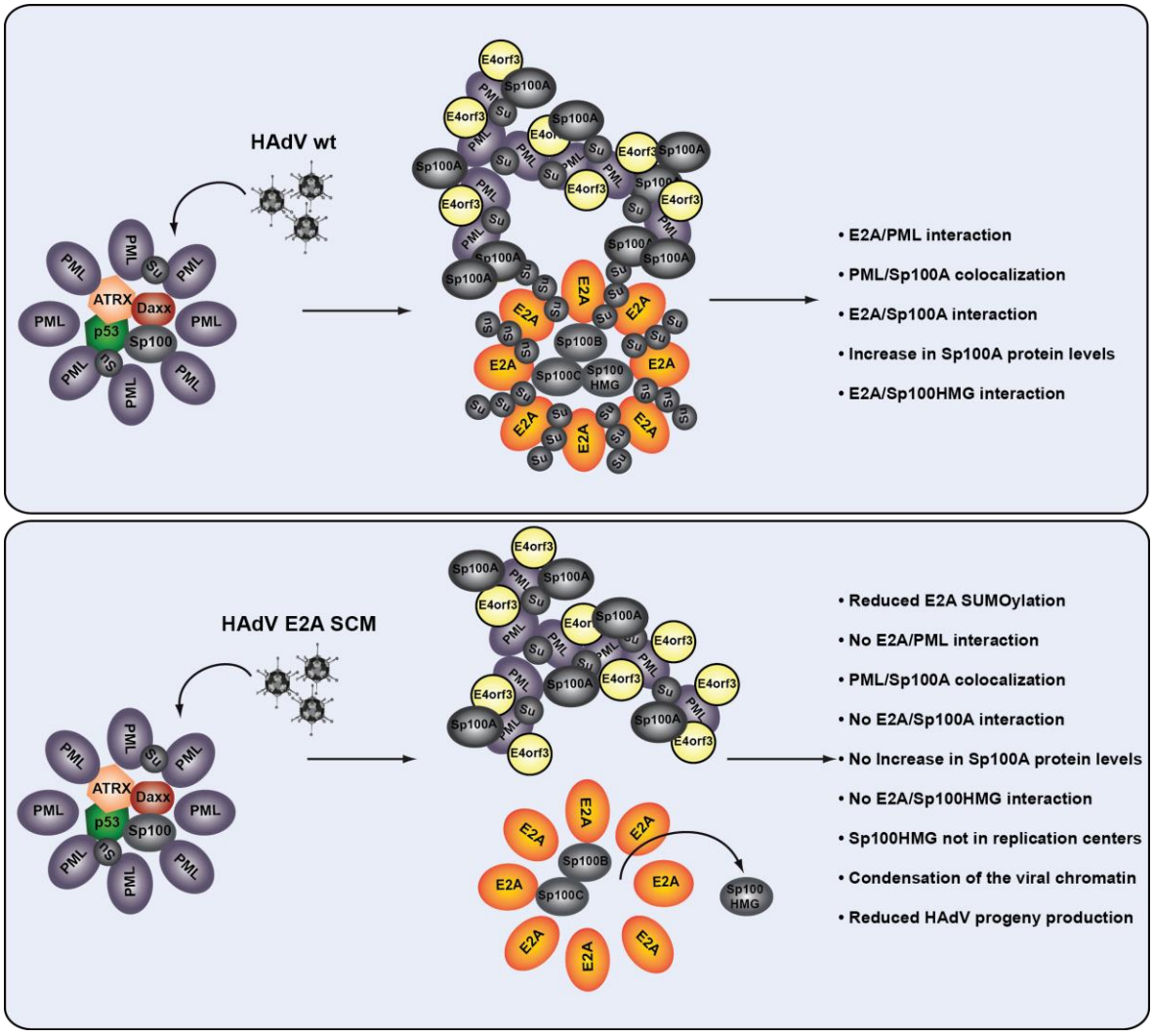

Figure 52: Schematic representation of the E2A SUMOylation-mediated manipulation of the host antiviral response. Proposed model links E2A SUMOylation with the subcellular localization of PML-NBs and Sp100HMG during HAdV infection. The model shows the influence of E2A SUMO PTM on PML-NBs localization adjacent to HAdV RC by E2A SUMOylation-dependent E2A/PML and E2A/Sp100A interactions. E2A SUMO PTM promotes the localization of Sp100HMG in HAdV RCs during infection by E2A SUMOylation-dependent E2A/Sp100HMG interaction. E2A SCM mutations prevent the virus to use beneficial components from PML-NBs and simultaneously counteract inhibitory function of the Sp100HMG isoform, leading to a defect in virus gene expression and progeny production.

5.4 E2A SUMOylation promotes HAdV-mediated inhibition of the tumor suppressor p53

In addition to its key function in tumor suppression, p53 is also participates in antiviral innate immunity by both induction of apoptosis and the type I interferon response (Rivas, Aaronson, and Munoz-Fontela 2010). Consequently, various viruses use complex mechanisms to counteract its activity. For example, HCMV infection suppresses p53 activity (Speir et al. 1994; Casavant et al. 2006), and Human immunodeficiency virus-1 (HIV-1) triggers p53 degradation (Izumi et al. 2010). Intriguingly, p53 is both as positive and negative factor for HSV-1 infection p53 (Maruzuru et al. 2013), while p53 functions promote Influenza A infection (Wang et al. 2018). HAdV and SV-40 infections lead cells to the S-phase, causing the p53 accumulation. This leads to apoptosis without the inhibition of p53 activity (Whyte et al. 1988; DeCaprio et al. 1988; Sarnow et al. 1982). Therefore, both viruses use distinct approaches to inhibit p53 and assure efficient viral replication (Hermannstädter et al. 2009; Ip and Dobner 2020; Liu and Marmorstein 2006; Zhu et al. 1991).

Localization of the tumor suppressor protein p53 is one of the main qualities regulating its activity (Bosari et al. 1995; Moll et al. 1995; Moll, Riou, and Levine 1992). HAdV early protein E1B-55K shuttles between the cytoplasm and nucleus during infection, and it can be found both in the nucleus and in perinuclear bodies (Ornelles and Shenk 1991). It has been reported that E1B-55K actively translocates p53 into perinuclear bodies but during HAdV infection, p53 can also be found in E1B-55K containing sites that resemble to HAdV RCs (Cardoso et al. 2008). Nonetheless, a clear association of p53 with HAdV RCs has so far not been established. This study undoubtedly showed that p53 localizes to HAdV RCs (4.4.1.1). E1B-55K employs several mechanisms to inhibit the p53 activity (Teodoro and Branton 1997; Yew and Berk 1992; Pennella et al. 2010; Wimmer et al. 2016). The ability of E1B-55K to inhibit p53 and consequently transform cells depends on its nuclear localization signal (NES) and SUMO conjugation motif (SCM). Inactive NES leads to complete nuclear localization of E1B-55K protein, where it accumulates at PML-NBs and the periphery of viral RCs. E1B-55K with nonfunctional NES is highly SUMOylated by the SUMO-1, which leads to the enhanced E1B-55K-mediated transformation (Endter et al. 2005). Moreover, SUMOylation of E1B-55K is necessary for the E1B-55K nuclear localization (Kindsmuller et al. 2007). E1B-55K without functional SCM is unable to transform cells (Endter et al. 2001). Intriguingly, localization of p53 in HAdV RCs was shown to be independent on E1B-

55K NES, E1B-55K SCM or E1B-55K itself (4.4.1.2). As E2A represents the marker protein for HAdV RCs (Puvion-Dutilleul, Pedron, and Cajean-Feroldi 1984) it can be hypothesized that E2A recruits p53 to RCs and that this occurs on an E2A SUMOylation independent way. However, the interaction between the HAdV DNA binding protein and p53 has not been detected during infection. Interestingly, E2A did interact with p53 in the absence of E1B-55K or when E1B-55K was lacking the NES or SCM motif (4.4.1.3). This data shows the ability of E1B-55K to prevent the interaction between p53 and E2A, and thereby possibly protect the HAdV RCs from negative effects of p53. This can be further explained by reports showing direct E1B-55K interaction with the tumor suppressor (Teodoro and Branton 1997; Yew and Berk 1992). In the absence of E1B-55K there is no barrier for the interaction between E2A and p53. In the case of E1B-55K NES mutant virus the presence of this interaction can be explained by the fact that E1B-55K and p53 localize exclusively in the nucleus so the portion of p53 that would be in cytoplasmic inclusions in wt infection can target HAdV RCs. E1B-55K SCM mutation prevents E1B-55K nuclear localization, and thus the barrier between p53 localized in RCs and E2A (4.4.1.2 and 4.4.1.3).

Even though E2A does not interact with p53 during HAdV infection, E1B-55K/E4orf6-mediated p53 degradation (Blanchette et al. 2004; Querido et al. 2001; Schreiner, Wimmer, and Dobner 2012) was slowed down by the introduction of SCM mutations in E2A (4.4.1.4). Based on this data, it can be concluded that E2A SUMO PTM promotes the inhibition of p53-mediated by the HAdV E3 ubiquitin ligase complex. It can be further hypothesized that E2A SUMO PTM underlays the efficient activity of the HAdV E3 ubiquitin ligase complex and thereby the degradation of all factors targeted for degradation. However, further studies are needed to substantiate this claim. Furthermore, western blot analysis revealed the reduced expression of the band migrating above the p53 signal in cells infected with HAdV E2A SCM virus, that could indicate the posttranslational modification of the tumor suppressor (4.4.1.4). This observation was substantiated by data showing the increase of p53 SUMO PTM during wt infection, as it has been expected based on previous reports (Pennella et al. 2010; Wimmer et al. 2016), that was not as pronounced in cells infected with the E2A SUMOylation deficient virus (4.4.1.5). E1B-55K inhibits the p53 transcriptional activity by induction of the p53 SUMOylation through its interaction with PML-IV and PML-V (Pennella et al. 2010; Wimmer et al. 2016). Therefore, the observed lack of p53 SUMOylation during infection with E2A SCM mutant virus is a consequence of the reduction of E1B-55K interaction and colocalization with PML-V in cells infected with the

E2A SUMOylation deficient virus detected in this study (4.4.1.6, 4.4.1.7). It can be hypothesized that E2A SUMOylation-dependent E2A/PML interaction and PML tracks localization next to HAdV RCs (4.3.1.2, 4.3.2.2) are required for E1B-55K/PML-V colocalization and interaction. As the transforming activity of E1B-55K highly depends on its localization in PML-NBs (Wimmer et al. 2016) it is possible that the infection with E2A SUMOylation deficient virus would have impaired transforming potential in primary rodent cells.

The influence of E2A SUMOylation on E1B-55K interaction with PML-IV has not been investigated due to previous reports showing that E1B-55K interacts with PML-IV only in transfection settings, while during infection E1B-55K preference for specific PML isoforms changes and the interaction with PML-IV is no longer detected (Wimmer et al. 2010). However, it would be interesting to perform future studies investigating the influence of E2A SUMOylation on E1B-55K interaction with PML isoforms -I and -VI that were also reported to interact with E1B-55K during HAdV infection (Wimmer et al. 2010).

The finding that E2A SUMOylation promotes p53 degradation, SUMOylation and E1B-55K/PML-V interaction indicate a novel role of E2A in the inhibition of p53-mediated transcription. This hypothesis can be further supported by reports, dating decades ago, connecting E2A with HAdV-mediated cell transformation (Rice, Klessig, and Williams 1987). Indeed, transcriptome analysis of p53 target genes during infection performed in this study, revealed a subset of p53-dependent transcripts that were downregulated during infection with HAdV wt virus but not during infection with the E2A SUMOylation deficient virus (4.4.1.8). However, E2A SUMOylation was not necessary for downregulation of all p53-dependent transcripts observed during HAdV wt infection. Therefore, it could be assumed that the virus uses the E2A SUMO PTM to inhibit only specific p53 functions. The failure to efficiently inhibit p53 activity offers an additional explanation for the impaired HAdV progeny production during infection with the E2A SUMOylation deficient virus, observed in this study (4.2.1).

E1B-55K employs additional mechanism to inhibit p53 activity leading to adenovirus-mediated transformation. E1B-55K interacts with Sp100A, SUMOylates it and sequesters it into the insoluble matrix of the nucleus or into cytoplasmic inclusions where the E1B-55K/Sp100A complex recruits p53 inhibiting its transcription activating properties (Berscheminski et al. 2016). Both interaction of E1B-55K with PML and Sp100A are E1B-55K SUMOylation-dependent (Berscheminski et al. 2016; Wimmer et al. 2010). Data described in previous chapters showed the

interaction of E2A with these two cellular factors that was also dependent on the E2A SUMO PTM (4.3.1.2 and 4.3.3.2). Based on these findings and previous studies connecting E2A with HAdV-mediated cell transformation (Rice, Klessig, and Williams 1987), it would be tempting to hypothesize that E2A employs the mechanism independent on E1B-55K, to inhibit p53 thorough Sp100A and PML interaction. On the other hand, E2A SUMOylation could also be the prerequisite for E1B-55K interaction with Sp100A leading to the p53 inhibition. However, further studies are necessary to substantiate these concepts.

In sum, p53 localizes to HAdV RCs independently on E1B-55K and E2A SUMO PTM. E1B-55K prevents E2A/p53 binding. E2A SUMOylation promotes HAdV-mediated inhibition of p53-dependent transcription by supporting p53 degradation and E1B-55K interaction with PML-V that leads to p53 SUMOylation and subsequent inhibition of the tumor suppressor activity. Taken together, this data unravels a novel mechanism by which HAdV inhibits p53-mediated transcriptional activation using HAdV DNA-binding protein E2A.

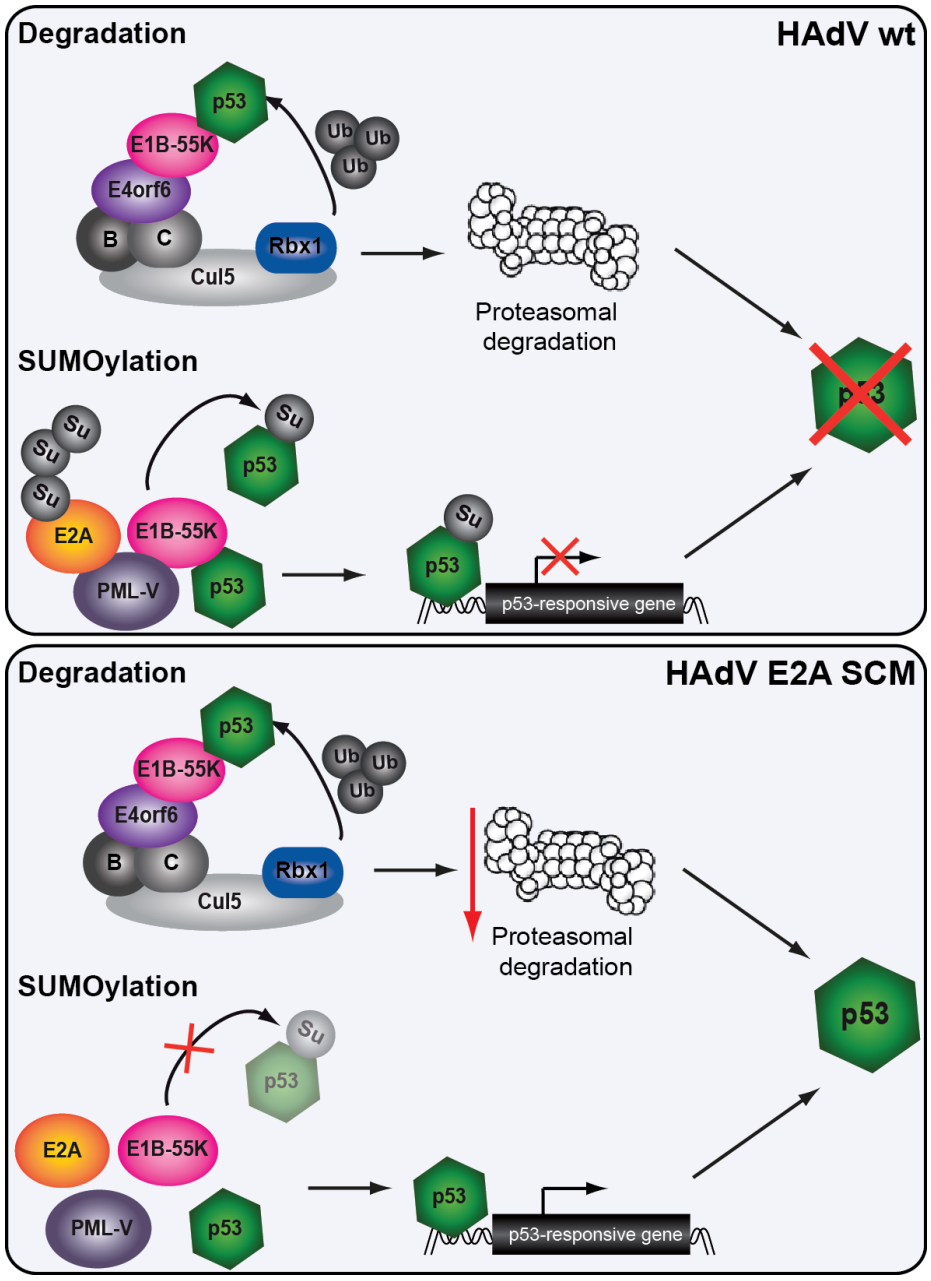

Figure 53: Schematic representation of the E2A SUMOylation-mediated inhibition of p53 activity. Proposed model links E2A SUMOylation with the inhibition of the p53 activity during HAdV infection. The model shows the role of E2A SUMO PTM in proteasomal degradation and inhibition of p53. E2A SUMOylation promotes E2A/PML binding and E1B-55K interaction and colocalization with PML-V thereby causing the increase in p53 SUMOylation and subsequent inhibition of the p53-mediated transcriptional activation.

5.5 E2A affects localization and SUMOylation of p53

HAdVs use diverse of mechanisms to modulate p53 activity to their benefit. After the E1A-mediated p53 stabilization in the early stages of the infection, necessary to establish optimal conditions for viral replication (Ait-Si-Ali et al. 1998; Ip and Dobner 2020), HAdV inhibits p53

activity to prevent apoptosis. It is known that E1B-55K translocates p53 into the perinuclear bodies (Liu et al. 2005), however as it has been described in previous section, p53 also localizes in HAdV RCs during infection on an E1B-55K independent manner (4.4.1.2). As E2A represents a marker protein for HAdV RCs (Puvion-Dutilleul, Pedron, and Cajean-Feroldi 1984), it was reasonable to assume that E2A might be able to recruit p53 independently on other viral factors. Indeed, the data shown in chapters 4.4.2.1 and 4.4.2.2 clearly demonstrate that E2A alone can sequester p53 on an E2A SUMOylation independent manner. Sphere like organization of E2A is known from previous reports that showed the ability of E2A to sequester PML component Sp100 into these structures (Komatsu, Nagata, and Wodrich 2016). This data, together with the observation that p53 also colocalizes with the E2A spheres, indicate more complex mechanism used by E2A to modulate and possibly inhibit cellular antiviral and tumor suppression machinery. E1B-55K and E4orf6 both use distinct mechanisms to inhibit p53 activity that include their direct interaction with the tumor suppressor genes (Teodoro and Branton 1997; Yew and Berk 1992; Dobner et al. 1996). E2A interacts with p53 during infection, but only in the absence of E1B-55K or when the function of E1B-55K is mutationally impaired (4.4.1.3). Therefore, it was not surprising that the E2A interaction with p53 was detected in transfection settings. However, in contrast to E1B-55K (Endter et al. 2001), E2A SUMO PTM completely abolished this binding (4.4.2.3). Transfection experiments confirmed the data obtained in the infection studies, showing that E1B-55K prevents E2A SCM from interacting with p53 (4.4.2.4). The reasoning behind this observation, besides the simple competition for the same target, might be that E1B-55K protects the replication compartments from the negative p53 influence. It appears that the virus uses both E2A SUMOylation and E1B-55K to prevent p53 binding to the replication centers marker protein, E2A. It is possible that the virus uses E2A SUMO PTM to prevent E2A/p53 interaction in very early stages of infection, before the E1B-55K expression starts. However, as shown in section 4.4.1.3, E2A SUMOylation alone is not sufficient to inhibit this binding in later stages of the viral life cycle. Furthermore, the reduction of E1B-55K levels and SUMOylation by E2A indicates the need for precise regulation of E1B-55K activity during infection. It could be that E2A leads to downregulation of E1B-55K levels in the beginning of the infection in order to support the stabilization of p53 needed for the transition from G1 to S phase of cell cycle. However, based on the finding that E2A SUMO PTM promotes p53 inhibition during infection, one could hypothesize that even though E2A downregulates E1B-55K to possibly help p53 stabilization, to prevent

apoptosis E2A inhibits p53 via specific mechanism before the onset of E1B-55K-mediated p53 inhibition.

E1B-55K can be found both in the nucleus and in perinuclear bodies during HAdV infection as E4orf6 promotes E1B-55K nuclear localization (Ornelles and Shenk 1991; Stracker et al. 2005). In addition, it was reported that E4orf3 expression in transfection settings leads to E1B-55K colocalization with PML-NBs (Stracker et al. 2005). Interestingly, this study showed that E2A can also translocate E1B-55K into the nucleus in the absence of other viral proteins and that this happens on an E2A SUMOylation independent way. In the presence of E2A, similarly as in the infection experiments described in the section 4.4.1.2, E1B-55K and p53 localize together both in perinuclear bodies and in the E2A spheres (4.4.2.5). Therefore, it can be assumed that E1B-55K prevents the E2A SCM/p53 interaction by directly binding the tumor suppressor, exporting it to perinuclear bodies and by forming a physical barrier between the two proteins by localizing in E2A domains. Immunoprecipitation studies performed in the infection settings showing E2A/p53 interaction in the absence of fully functional E1B-55K (4.4.1.3) further support this hypothesis.

Besides by the direct interaction, E1B-55K inhibits p53 transcriptional activity by interacting with PML-IV and PML-V causing the SUMO conjugation to p53 (Pennella et al. 2010; Wimmer et al. 2016). E2A also interacts with PML and likewise to E1B-55K, this interaction is E2A SUMO PTM-dependent during infection (4.3.1.2). Interestingly, both E2A and E2A SCM expression led to the reduction of E1B-55K-mediated p53 SUMOylation (4.4.2.6). The reason for that could be that E2A interaction with PML does not depend on its SUMO PTM in transfection conditions (4.3.1.1), so it could be that E2A and E2A SCM prevent E1B-55K interaction with PML-IV and PML-V, therefore inhibiting E1B-55K-mediated increase of p53 SUMOylation. Additionally, the reduction of E1B-55K levels and SUMOylation by E2A could singlehandedly explain the inhibitory effect on the E1B-55K-mediated p53 SUMOylation. Based on these findings, it would be logical to assume that E2A promotes p53 activity. However, the results obtained in infection studies showing the need for E2A SUMO PTM for efficient p53 inhibition and the study by Rice and coworkers (Rice, Klessig, and Williams 1987) connecting E2A with HAdV-mediated cell transformation, suggest otherwise. Furthermore, this study showed that E2A expression leads to the reduction of p53 SUMOylation on an E2A SUMO PTM-dependent manner (4.4.2.8). It is known that the increase of p53 SUMOylation by E1B-55K leads to the inhibition of p53 (Pennella et al. 2010; Wimmer et al. 2016). However, various publications have shown that

p53 SUMOylation can have both activating and inhibiting properties (Gostissa et al. 1999; Kwek et al. 2001; Rodriguez et al. 1999; Schmidt and Muller 2002; Chang et al. 2010; Li et al. 2006; Stindt et al. 2011). It is possible that p53 requires specific level of SUMOylation in order to be fully functional. Therefore, as hyper SUMOylation by E1B-55K leads to the p53 inhibition, it can very well be that downregulation of p53 SUMO PTM in the presence of E2A also inhibits p53 activity. Furthermore, E2A interacts with Ubc9 on an E2A SCM-dependent manner (4.1.3). Like in the case of p53, E2A recruits Ubc9 to the E2A sphere like structures (4.4.2.74.1.3). As Ubc9 is also SUMO conjugating enzyme for p53 (Lin, Ohshima, and Shimotohno 2004), it can be hypothesized that E2A leads to the reduction of the p53 SUMOylation by preventing the Ubc9 interaction with p53. Contrary to the transfection conditions, during infection E2A supports p53 SUMOylation (4.4.1.5). Therefore, one could assume that E2A employs different mechanisms to modulate p53 activity. One mechanism that presumably takes place at the start of the viral replication cycle, would be the p53 stabilization via downregulation of E1B-55K levels and SUMOylation followed by reduction of p53 SUMOylation that might lead to the inhibition of specific p53 functions. On the other hand, in the later stages of infection E2A promotes E1B-55K interaction with PML isoform V leading to SUMOylation and subsequent inhibition of p53. Both mechanisms are E2A SUMOylation-dependent. As it has been previously shown, E2A recruits Sp100 to the E2A spere like structures. Furthermore, SUMOylated E2A interacts with Sp100A during infection (4.3.3.2). As E1B-55K specifically interacts with the Sp100A isoform and inhibits p53 transcriptional activity by promoting generation of the p53/Sp100A complex (Berscheminski et al. 2016), it would be interesting to investigate if E2A behaves on the similar manner.

Taken together, E2A sequesters p53 and Ubc9 into E2A containing domains independently on the other viral components and E2A SUMO PTM. SUMOylation deficient E2A interacts with p53 in transfection settings, however, this interaction can be disrupted by E1B-55K. Interestingly, E2A reduces E1B-55K-mediated p53 SUMOylation independently on E2A SUMO PTM but the infection independent expression of E2A only with intact SCM motifs leads to the reduction of p53 SUMOylation indicating the possible existence of an additional mechanism used by HAdV to modulate p53 activity through the action of E2A.

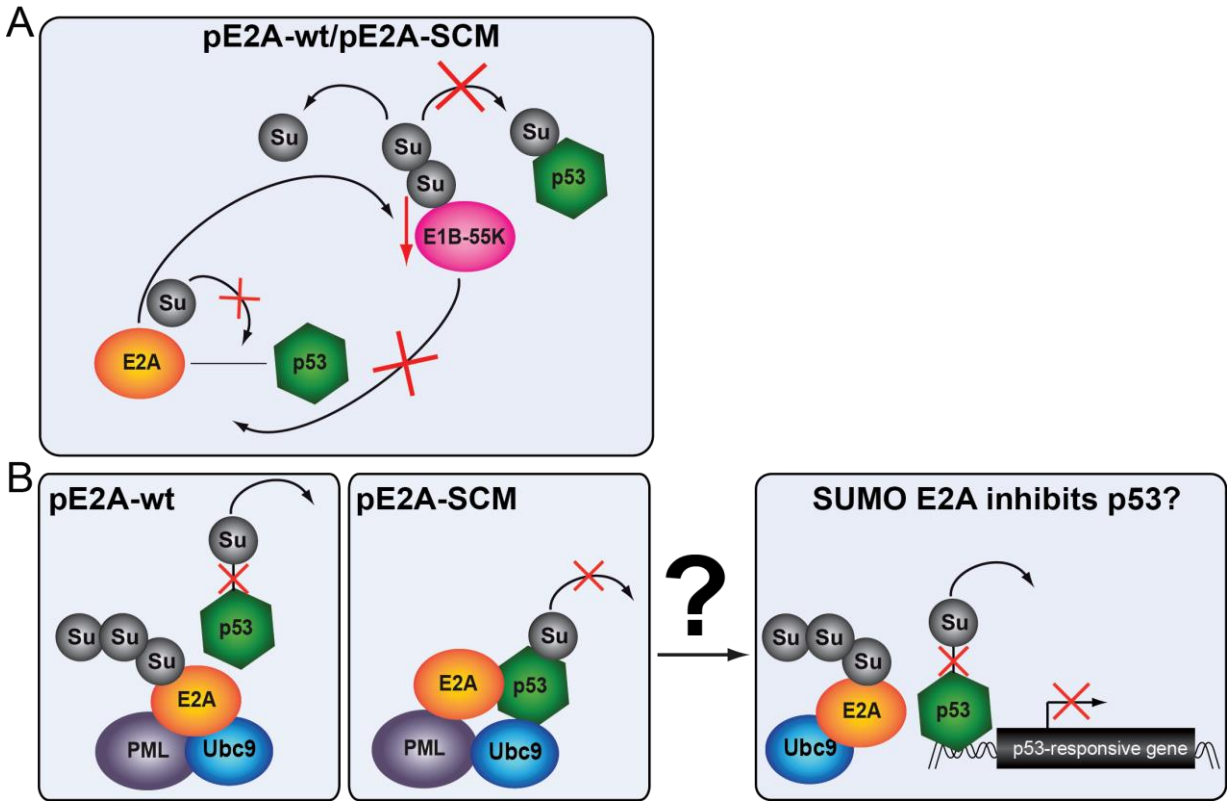

Figure 54: Schematic representation of the p53 modulation by SUMOylated E2A. Proposed model links E2A SUMOylation with the inhibition of the p53 activity in transfection settings. The model shows the role of E2A SUMO PTM in the reduction of p53 SUMOylation. **(A)** E2A SUMOylation and E1B-55K disrupt E2A binding to p53. E2A reduces E1B-55K SUMOylation and steady state levels on an E2A SUMOylation independent manner, leading to the inhibition of E1B-55K-mediated p53 SUMOylation. **(B)** E2A interacts with PML and recruits p53 and Ubc9 into E2A containing domains independently on E2A SUMOylation. Even though SUMOylated E2A does not interact with p53, it binds Ubc9 leading to the reduction of p53 SUMOylation that could cause the inhibition of the p53-mediated transcriptional activation.

5.6 Clinical relevance of the study

HAdV infection is often lethal in immunocompromised patients (Berciaud et al. 2012; Krilov 2005; Lion 2014), but specific treatment is currently not available. Small-molecule inhibitor antivirals target different stages of the viral life cycle through the interaction with virus or host proteins essential for virus replication (De Clercq and Li 2016). As this approach effectively targets both the extracellular and the intracellular proteins, it enables therapeutic targeting of the SUMOylation pathway. This strategy is already in use as a cancer treatment (Kroonen and Vertegaal 2021) and shows promising results in development of antivirals against HIV (Madu et al. 2015) and EBV (Garcia et al. 2021) infections. This work demonstrates the importance of E2A SUMO PTM for efficient HAdV infection, rendering it as a target for development of antiviral therapeutics. Therefore, the generation of small-molecule inhibitors targeting the E2A-SUMO

binding or the use of more broad inhibitors targeting cellular SUMOylation pathway are possible strategies for development of anti-adenoviral therapeutics.

Even though the DNA of several HAdV types has been found in different human tumors (Kosulin et al. 2007; Kosulin et al. 2013), HAdV infection has so far not been associated with oncogenicity in humans. Nevertheless, HAdV-5 E1A/E1B oncogenes are capable of causing transformation of human mesenchymal stem/stroma cells (hMSCs) in tissue culture (Speiseder et al. 2017). Although the virus-host interplay during HAdV infection is not fully understood, and it is completely unknown for various serotypes, HAdVs are thoroughly researched in context of their therapeutic potential. Adenoviral vectors are the most frequent vectors in the field of gene therapy (Lee et al. 2017; St George 2003) and oncolytic adenoviruses are used as anticancer agents (Ganly et al. 2000; Goradel et al. 2019). Furthermore, adenoviruses are studied and used as vaccine vectors (Ewer et al. 2017; Tatsis and Ertl 2004) against pathogens such as Ebola (Ledgerwood et al. 2017), HIV (Catanzaro et al. 2006) or currently emerging SARS-CoV-2 (Folegatti et al. 2020; Hassan et al. 2020; Mercado et al. 2020). This study showed so far unknown role of E2A SUMOylation in HAdV-mediated inhibition of p53 activity, indicating the possible oncogenic potential of E2A. Introduction of E2A SCM mutations into adenoviral vectors used as therapeutics should therefore be explored as a viable option to improve their safety and efficacy. Further studies are currently ongoing to determine whether E2A, independently on HAdV infection, possess the properties ascribed to oncogenic proteins. Oncolytic adenovirus therapy approaches exploit the ability of the virus to cause the cell lysis and engineered tumor selectivity is based on the knowledge on HAdV-mediated inhibition of DNA damage response and apoptosis. Tumor selectivity can be achieved by deleting parts of viral genes (Abudoureyimu et al. 2019). E1B-55K deleted virus, dl1520/ONYX-015, was shown to induce high p53 levels, expected to restrict viral replication in normal cells but not in p53 mutant tumor cells (Bischoff et al. 1996). However, high p53 levels in dl1520/ONYX-015 infected human cells do not lead to activation of all p53 transcriptional targets (Soria et al. 2010). As this limits the treatment success, it was proposed that the deletion other adenoviral protein that inhibits p53 independently on E1B-55K such as E4orf3 or E4orf6, could improve the outcome (Soria et al. 2010; Yanagawa-Matsuda et al. 2019). In line with these findings, this study indicates that the introduction of SCM mutations into E2A, without the need for complete E2A deletion, could further improve the selectivity and efficacy of p53 selective oncolytic adenoviruses.

In summary, this study changes the longstanding definition of how adenovirus infection inactivates the host antiviral and DNA damage responses. These findings offer crucial insights that could enable the development anti-adenoviral therapeutics on the one hand and improve the p53 selective oncolytic virus therapies and adenoviral vectors, on the other.

6 Literature

Abudoureyimu, Mubalake, Yongting Lai, Chuan Tian, Ting Wang, Rui Wang, and Xiaoyuan Chu. 2019. "Oncolytic Adenovirus—A Nova for Gene-Targeted Oncolytic Viral Therapy in HCC." *Frontiers in Oncology* 9 (1182). doi: 10.3389/fonc.2019.01182.

Ahi, Y. S., S. V. Vemula, and S. K. Mittal. 2013. "Adenoviral E2 IVa2 protein interacts with L4 33K protein and E2 DNA-binding protein." *J Gen Virol* 94 (Pt 6):1325-34. doi: 10.1099/vir.0.049346-0.

Ait-Si-Ali, S., S. Ramirez, F. X. Barre, F. Dkhissi, L. Magnaghi-Jaulin, J. A. Girault, P. Robin, M. Knibiehler, L. L. Pritchard, B. Ducommun, D. Trouche, and A. Harel-Bellan. 1998. "Histone acetyltransferase activity of CBP is controlled by cycle-dependent kinases and oncoprotein E1A." *Nature* 396 (6707):184-6. doi: 10.1038/24190.

Ali, H., G. LeRoy, G. Bridge, and S. J. Flint. 2007. "The adenovirus L4 33-kilodalton protein binds to intragenic sequences of the major late promoter required for late phase-specific stimulation of transcription." *J Virol* 81 (3):1327-38. doi: 10.1128/jvi.01584-06.

Allen, M. A., Z. Andrysik, V. L. Dengler, H. S. Mellert, A. Guarnieri, J. A. Freeman, K. D. Sullivan, M. D. Galbraith, X. Luo, W. L. Kraus, R. D. Dowell, and J. M. Espinosa. 2014. "Global analysis of p53-regulated transcription identifies its direct targets and unexpected regulatory mechanisms." *Elife* 3:e02200. doi: 10.7554/eLife.02200.

Ampuero, J. S., V. Ocana, J. Gomez, M. E. Gamero, J. Garcia, E. S. Halsey, and V. A. Laguna-Torres. 2012. "Adenovirus respiratory tract infections in Peru." *PLoS One* 7 (10):e46898. doi: 10.1371/journal.pone.0046898.

An, W., J. Kim, and R. G. Roeder. 2004. "Ordered cooperative functions of PRMT1, p300, and CARM1 in transcriptional activation by p53." *Cell* 117 (6):735-48. doi: 10.1016/j.cell.2004.05.009.

Anderson, C. W. 1981. "Spontaneous mutants of the adenovirus-simian virus 40 hybrid, Ad2+ND3, that grow efficiently in monkey cells." *Virology* 111 (1):263-9. doi: 10.1016/0042-6822(81)90670-x.

Anderson, K. P., and D. F. Klessig. 1984. "Altered mRNA splicing in monkey cells abortively infected with human adenovirus may be responsible for inefficient synthesis of the virion fiber polypeptide." *Proc Natl Acad Sci U S A* 81 (13):4023-7. doi: 10.1073/pnas.81.13.4023.

Anderson, M. E., B. Woelker, M. Reed, P. Wang, and P. Tegtmeyer. 1997. "Reciprocal interference between the sequence-specific core and nonspecific C-terminal DNA binding domains of p53: implications for regulation." *Mol Cell Biol* 17 (11):6255-64. doi: 10.1128/mcb.17.11.6255.

Appella, E., and C. W. Anderson. 2001. "Post-translational modifications and activation of p53 by genotoxic stresses." *Eur J Biochem* 268 (10):2764-72. doi: 10.1046/j.1432-1327.2001.02225.x.

Araujo, F. D., T. H. Stracker, C. T. Carson, D. V. Lee, and M. D. Weitzman. 2005. "Adenovirus type 5 E4orf3 protein targets the Mre11 complex to cytoplasmic aggresomes." *J Virol* 79 (17):11382-91. doi: 10.1128/jvi.79.17.11382-11391.2005.

Ariga, H., H. Klein, A. J. Levine, and M. S. Horwitz. 1980. "A cleavage product of the adenovirus DNA binding protein is active in DNA replication in vitro." *Virology* 101 (1):307-10. doi: 10.1016/0042-6822(80)90510-3.

Ascoli, C. A., and G. G. Maul. 1991. "Identification of a novel nuclear domain." *J Cell Biol* 112 (5):785-95. doi: 10.1083/jcb.112.5.785.

Avvakumov, N., M. Sahbegovic, Z. Zhang, M. Shuen, and J. S. Mymryk. 2002. "Analysis of DNA binding by the adenovirus type 5 E1A oncoprotein." *J Gen Virol* 83 (Pt 3):517-24. doi: 10.1099/0022-1317-83-3-517.

Avvakumov, N., R. Wheeler, J. C. D'Halluin, and J. S. Mymryk. 2002. "Comparative sequence analysis of the largest E1A proteins of human and simian adenoviruses." *J Virol* 76 (16):7968-75. doi: 10.1128/jvi.76.16.7968-7975.2002.

Axelrod, N. 1978. "Phosphoproteins of adenovirus 2." *Virology* 87 (2):366-83. doi: 10.1016/0042-6822(78)90141-1.

Babich, A., and J. R. Nevins. 1981. "The stability of early adenovirus mRNA is controlled by the viral 72 kd DNA-binding protein." *Cell* 26 (3 Pt 1):371-9. doi: 10.1016/0092-8674(81)90206-3.

Bagchi, S., P. Raychaudhuri, and J. R. Nevins. 1990. "Adenovirus E1A proteins can dissociate heteromeric complexes involving the E2F transcription factor: a novel mechanism for E1A trans-activation." *Cell* 62 (4):659-69. doi: 10.1016/0092-8674(90)90112-r.

Bailey, A., and V. Mautner. 1994. "Phylogenetic relationships among adenovirus serotypes." *Virology* 205 (2):438-52. doi: 10.1006/viro.1994.1664.

Baker, A., K. J. Rohleder, L. A. Hanakahi, and G. Ketner. 2007a. "Adenovirus E4 34k and E1b 55k oncoproteins target host DNA ligase IV for proteasomal degradation." *J Virol* 81 (13):7034-40. doi: 10.1128/jvi.00029-07.

Baker, Amy, Kent J. Rohleder, Les A. Hanakahi, and Gary Ketner. 2007b. "Adenovirus E4 34k and E1b 55k Oncoproteins Target Host DNA Ligase IV for Proteasomal Degradation." *Journal of Virology* 81 (13):7034-7040. doi: 10.1128/jvi.00029-07.

Baker, L. A., C. D. Allis, and G. G. Wang. 2008. "PHD fingers in human diseases: disorders arising from misinterpreting epigenetic marks." *Mutat Res* 647 (1-2):3-12. doi: 10.1016/j.mrfmmm.2008.07.004.

Bandara, L. R., and N. B. La Thangue. 1991. "Adenovirus E1a prevents the retinoblastoma gene product from complexing with a cellular transcription factor." *Nature* 351 (6326):494-7. doi: 10.1038/351494a0.

Barak, Y., T. Juven, R. Haffner, and M. Oren. 1993. "mdm2 expression is induced by wild type p53 activity." *Embo j* 12 (2):461-8.

Barlev, N. A., L. Liu, N. H. Chehab, K. Mansfield, K. G. Harris, T. D. Halazonetis, and S. L. Berger. 2001. "Acetylation of p53 activates transcription through recruitment of coactivators/histone acetyltransferases." *Mol Cell* 8 (6):1243-54. doi: 10.1016/s1097-2765(01)00414-2.

Barth, T. K., and A. Imhof. 2010. "Fast signals and slow marks: the dynamics of histone modifications." *Trends Biochem Sci* 35 (11):618-26. doi: 10.1016/j.tibs.2010.05.006.

Beltz, G. A., and S. J. Flint. 1979. "Inhibition of HeLa cell protein synthesis during adenovirus infection. Restriction of cellular messenger RNA sequences to the nucleus." *J Mol Biol* 131 (2):353-73. doi: 10.1016/0022-2836(79)90081-0.

Benkő, M., K. Aoki, N. Arnberg, A. J. Davison, M. Echavarría, M. Hess, M. S. Jones, G. L. Kaján, A. E. Kajon, S. K. Mittal, Podgorski, II, C. San Martín, G. Wadell, H. Watanabe, B. Harrach, and Consortium Ictv Report. 2022. "ICTV Virus Taxonomy Profile: Adenoviridae 2022." *J Gen Virol* 103 (3). doi: 10.1099/jgv.0.001721.

Berciaud, S., F. Rayne, S. Kassab, C. Jubert, M. Faure-Della Corte, F. Salin, H. Wodrich, and M. E. Lafon. 2012. "Adenovirus infections in Bordeaux University Hospital 2008-2010: clinical and virological features." *J Clin Virol* 54 (4):302-7. doi: 10.1016/j.jcv.2012.04.009.

Bergamaschi, D., Y. Samuels, B. Jin, S. Duraisingham, T. Crook, and X. Lu. 2004. "ASPP1 and ASPP2: common activators of p53 family members." *Mol Cell Biol* 24 (3):1341-50. doi: 10.1128/mcb.24.3.1341-1350.2004.

Bergelson, J. M., J. A. Cunningham, G. Droguett, E. A. Kurt-Jones, A. Krithivas, J. S. Hong, M. S. Horwitz, R. L. Crowell, and R. W. Finberg. 1997. "Isolation of a common receptor for Coxsackie B viruses and adenoviruses 2 and 5." *Science* 275 (5304):1320-3. doi: 10.1126/science.275.5304.1320.

Berk, A. J. 1986a. "Adenovirus promoters and E1A transactivation." *Annu Rev Genet* 20:45-79. doi: 10.1146/annurev.ge.20.120186.000401.

Berk, A. J. 1986b. "Functions of adenovirus E1A." *Cancer Surv* 5 (2):367-87.

Berk, AJ. 2007. "Adenoviridae: the viruses and their replication." *Fields virology* 5:2355-2394.

Bernardi, R., and P. P. Pandolfi. 2007. "Structure, dynamics and functions of promyelocytic leukaemia nuclear bodies." *Nat Rev Mol Cell Biol* 8 (12):1006-16. doi: 10.1038/nrm2277.

Bernardi, R., and P. P. Pandolfi. 2014. "A Dialog on the First 20 Years of PML Research and the Next 20 Ahead." *Front Oncol* 4:23. doi: 10.3389/fonc.2014.00023.

Bernier-Villamor, V., D. A. Sampson, M. J. Matunis, and C. D. Lima. 2002. "Structural basis for E2-mediated SUMO conjugation revealed by a complex between ubiquitin-conjugating enzyme Ubc9 and RanGAP1." *Cell* 108 (3):345-56. doi: 10.1016/s0092-8674(02)00630-x.

Berscheminski, J., J. Brun, T. Speiseder, P. Wimmer, W. H. Ip, M. Terzic, T. Dobner, and S. Schreiner. 2016. "Sp100A is a tumor suppressor that activates p53-dependent transcription and counteracts E1A/E1B-55K-mediated transformation." *Oncogene* 35 (24):3178-89. doi: 10.1038/onc.2015.378.

Berscheminski, J., P. Groitl, T. Dobner, P. Wimmer, and S. Schreiner. 2013. "The adenoviral oncogene E1A-13S interacts with a specific isoform of the tumor suppressor PML to enhance viral transcription." *J Virol* 87 (2):965-77. doi: 10.1128/jvi.02023-12.

Berscheminski, J., P. Wimmer, J. Brun, W. H. Ip, P. Groitl, T. Horlacher, E. Jaffray, R. T. Hay, T. Dobner, and S. Schreiner. 2014. "Sp100 isoform-specific regulation of human adenovirus 5 gene expression." *J Virol* 88 (11):6076-92. doi: 10.1128/jvi.00469-14.

Besse, S., and F. Puvion-Dutilleul. 1995. "Anchorage of adenoviral RNAs to clusters of interchromatin granules." *Gene Expr* 5 (2):79-92.

Bischof, O., K. Schwamborn, N. Martin, A. Werner, C. Sustmann, R. Grosschedl, and A. Dejean. 2006. "The E3 SUMO ligase PIASy is a regulator of cellular senescence and apoptosis." *Mol Cell* 22 (6):783-94. doi: 10.1016/j.molcel.2006.05.016.

Bischoff, J. R., D. H. Kirn, A. Williams, C. Heise, S. Horn, M. Muna, L. Ng, J. A. Nye, A. Sampson-Johannes, A. Fattaey, and F. McCormick. 1996. "An adenovirus mutant that replicates selectively in p53-deficient human tumor cells." *Science* 274 (5286):373-6. doi: 10.1126/science.274.5286.373.

Blais, A., and B. D. Dynlacht. 2004. "Hitting their targets: an emerging picture of E2F and cell cycle control." *Curr Opin Genet Dev* 14 (5):527-32. doi: 10.1016/j.gde.2004.07.003.

Blanchette, P., C. Y. Cheng, Q. Yan, G. Ketner, D. A. Ornelles, T. Dobner, R. C. Conaway, J. W. Conaway, and P. E. Branton. 2004. "Both BC-box motifs of adenovirus protein E4orf6 are

required to efficiently assemble an E3 ligase complex that degrades p53." *Mol Cell Biol* 24 (21):9619-29. doi: 10.1128/mcb.24.21.9619-9629.2004.

Bohren, K. M., V. Nadkarni, J. H. Song, K. H. Gabbay, and D. Owerbach. 2004. "A M55V polymorphism in a novel SUMO gene (SUMO-4) differentially activates heat shock transcription factors and is associated with susceptibility to type I diabetes mellitus." *J Biol Chem* 279 (26):27233-8. doi: 10.1074/jbc.M402273200.

Boisvert, F. M., M. J. Hendzel, and D. P. Bazett-Jones. 2000. "Promyelocytic leukemia (PML) nuclear bodies are protein structures that do not accumulate RNA." *J Cell Biol* 148 (2):283-92. doi: 10.1083/jcb.148.2.283.

Borrow, J., A. D. Goddard, B. Gibbons, F. Katz, D. Swirsky, T. Fioretos, I. Dube, D. A. Winfield, J. Kingston, A. Hagemeijer, and et al. 1992. "Diagnosis of acute promyelocytic leukaemia by RT-PCR: detection of PML-RARA and RARA-PML fusion transcripts." *Br J Haematol* 82 (3):529-40. doi: 10.1111/j.1365-2141.1992.tb06463.x.

Bosari, S., G. Viale, M. Roncalli, D. Graziani, G. Borsani, A. K. Lee, and G. Coggi. 1995. "p53 gene mutations, p53 protein accumulation and compartmentalization in colorectal adenocarcinoma." *Am J Pathol* 147 (3):790-8.

Bosher, J., A. Dawson, and R. T. Hay. 1992. "Nuclear factor I is specifically targeted to discrete subnuclear sites in adenovirus type 2-infected cells." *J Virol* 66 (5):3140-50.

Bossis, G., and F. Melchior. 2006. "SUMO: regulating the regulator." *Cell Div* 1:13. doi: 10.1186/1747-1028-1-13.

Bottomley, M. J., M. W. Collard, J. I. Huggenvik, Z. Liu, T. J. Gibson, and M. Sattler. 2001. "The SAND domain structure defines a novel DNA-binding fold in transcriptional regulation." *Nat Struct Biol* 8 (7):626-33. doi: 10.1038/89675.

Boyer, G. S., F. W. Denny, Jr., and H. S. Ginsberg. 1959. "Sequential cellular changes produced by types 5 and 7 adenoviruses in HeLa cells and in human amniotic cells; cytological studies aided by fluorescein-labelled antibody." *J Exp Med* 110:827-44. doi: 10.1084/jem.110.5.827.

Bradford, M. M. 1976. "A rapid and sensitive method for the quantitation of microgram quantities of protein utilizing the principle of protein-dye binding." *Anal Biochem* 72:248-54. doi: 10.1006/abio.1976.9999.

Brady, C. A., and L. D. Attardi. 2010. "p53 at a glance." *J Cell Sci* 123 (Pt 15):2527-32. doi: 10.1242/jcs.064501.

Bray, N. L., H. Pimentel, P. Melsted, and L. Pachter. 2016. "Near-optimal probabilistic RNA-seq quantification." *Nat Biotechnol* 34 (5):525-7. doi: 10.1038/nbt.3519.

Bremner, K. H., J. Scherer, J. Yi, M. Vershinin, S. P. Gross, and R. B. Vallee. 2009. "Adenovirus transport via direct interaction of cytoplasmic dynein with the viral capsid hexon subunit." *Cell Host Microbe* 6 (6):523-35. doi: 10.1016/j.chom.2009.11.006.

Bridge, E., D. X. Xia, M. Carmo-Fonseca, B. Cardinali, A. I. Lamond, and U. Pettersson. 1995. "Dynamic organization of splicing factors in adenovirus-infected cells." *J Virol* 69 (1):281-90.

Bridges, R. G., S. Y. Sohn, J. Wright, K. N. Leppard, and P. Hearing. 2016. "The Adenovirus E4-ORF3 Protein Stimulates SUMOylation of General Transcription Factor TFII-I to Direct Proteasomal Degradation." *mBio* 7 (1):e02184-15. doi: 10.1128/mBio.02184-15.

Brosh, R., and V. Rotter. 2009. "When mutants gain new powers: news from the mutant p53 field." *Nat Rev Cancer* 9 (10):701-13. doi: 10.1038/nrc2693.

Burck, C., A. Mund, J. Berscheminski, L. Kieweg, S. Muncheberg, T. Dobner, and S. Schreiner. 2016. "KAP1 Is a Host Restriction Factor That Promotes Human Adenovirus E1B-55K SUMO Modification." *J Virol* 90 (2):930-46. doi: 10.1128/jvi.01836-15.

Burnett, E., J. Christensen, and P. Tattersall. 2001. "A consensus DNA recognition motif for two KDWK transcription factors identifies flexible-length, CpG-methylation sensitive cognate binding sites in the majority of human promoters." *J Mol Biol* 314 (5):1029-39. doi: 10.1006/jmbi.2000.5198.

Butler, J. S., and S. N. Loh. 2006. "Folding and misfolding mechanisms of the p53 DNA binding domain at physiological temperature." *Protein Sci* 15 (11):2457-65. doi: 10.1110/ps.062324206.

Cahilly-Snyder, L., T. Yang-Feng, U. Francke, and D. L. George. 1987. "Molecular analysis and chromosomal mapping of amplified genes isolated from a transformed mouse 3T3 cell line." *Somat Cell Mol Genet* 13 (3):235-44. doi: 10.1007/bf01535205.

Cardoso, F. M., S. E. Kato, W. Huang, S. J. Flint, and R. A. Gonzalez. 2008. "An early function of the adenoviral E1B 55 kDa protein is required for the nuclear relocalization of the cellular p53 protein in adenovirus-infected normal human cells." *Virology* 378 (2):339-46. doi: 10.1016/j.virol.2008.06.016.

Carson, C. T., N. I. Orazio, D. V. Lee, J. Suh, S. Bekker-Jensen, F. D. Araujo, S. S. Lakdawala, C. E. Lilley, J. Bartek, J. Lukas, and M. D. Weitzman. 2009. "Mislocalization of the MRN complex prevents ATR signaling during adenovirus infection." *Embo j* 28 (6):652-62. doi: 10.1038/emboj.2009.15.

Carter, T. H., and R. A. Blanton. 1978. "Possible role of the 72,000 dalton DNA-binding protein in regulation of adenovirus type 5 early gene expression." *J Virol* 25 (2):664-74.

Carvalho, T., J. S. Seeler, K. Ohman, P. Jordan, U. Pettersson, G. Akusjarvi, M. Carmo-Fonseca, and A. Dejean. 1995. "Targeting of adenovirus E1A and E4-ORF3 proteins to nuclear matrix-associated PML bodies." *J Cell Biol* 131 (1):45-56. doi: 10.1083/jcb.131.1.45.

Casavant, N. C., M. H. Luo, K. Rosenke, T. Winegardner, A. Zurawska, and E. A. Fortunato. 2006. "Potential role for p53 in the permissive life cycle of human cytomegalovirus." *J Virol* 80 (17):8390-401. doi: 10.1128/jvi.00505-06.

Catalucci, Daniele, Elisabetta Sporeno, Agostino Cirillo, Gennaro Ciliberto, Alfredo Nicosia, and Stefano Colloca. 2005. "An Adenovirus Type 5 (Ad5) Amplicon-Based Packaging Cell Line for Production of High-Capacity Helper-Independent ΔE1-E2-E3-E4 Ad5 Vectors." *Journal of Virology* 79 (10):6400-6409. doi: 10.1128/jvi.79.10.6400-6409.2005.

Catanzaro, A. T., R. A. Koup, M. Roederer, R. T. Bailer, M. E. Enama, Z. Moodie, L. Gu, J. E. Martin, L. Novik, B. K. Chakrabarti, B. T. Butman, J. G. Gall, C. R. King, C. A. Andrews, R. Sheets, P. L. Gomez, J. R. Mascola, G. J. Nabel, and B. S. Graham. 2006. "Phase 1 safety and immunogenicity evaluation of a multiclade HIV-1 candidate vaccine delivered by a replication-defective recombinant adenovirus vector." *J Infect Dis* 194 (12):1638-49. doi: 10.1086/509258.

Celik, C., M. G. Gozel, H. Turkay, M. Z. Bakici, A. S. Guven, and N. Elaldi. 2015. "Rotavirus and adenovirus gastroenteritis: time series analysis." *Pediatr Int* 57 (4):590-6. doi: 10.1111/ped.12592.

Cepko, C. L., and P. A. Sharp. 1982. "Assembly of adenovirus major capsid protein is mediated by a nonvirion protein." *Cell* 31 (2 Pt 1):407-15.

Cepko, C. L., and P. A. Sharp. 1983. "Analysis of Ad5 hexon and 100K ts mutants using conformation-specific monoclonal antibodies." *Virology* 129 (1):137-54.

Chang, P. C., Y. Izumiya, C. Y. Wu, L. D. Fitzgerald, M. Campbell, T. J. Ellison, K. S. Lam, P. A. Luciw, and H. J. Kung. 2010. "Kaposi's sarcoma-associated herpesvirus (KSHV) encodes a SUMO E3 ligase that is SIM-dependent and SUMO-2/3-specific." *J Biol Chem* 285 (8):5266-73. doi: 10.1074/jbc.M109.088088.

Chelbi-Alix, M. K., F. Quignon, L. Pelicano, M. H. Koken, and H. de The. 1998. "Resistance to virus infection conferred by the interferon-induced promyelocytic leukemia protein." *J Virol* 72 (2):1043-51.

Chen, A., H. Mannen, and S. S. Li. 1998. "Characterization of mouse ubiquitin-like SMT3A and SMT3B cDNAs and gene/pseudogenes." *Biochem Mol Biol Int* 46 (6):1161-74. doi: 10.1080/15216549800204722.

Chen, J., V. Marechal, and A. J. Levine. 1993. "Mapping of the p53 and mdm-2 interaction domains." *Mol Cell Biol* 13 (7):4107-14. doi: 10.1128/mcb.13.7.4107.

Chen, Z., and S. J. Chen. 1992. "RARA and PML genes in acute promyelocytic leukemia." *Leuk Lymphoma* 8 (4-5):253-60. doi: 10.3109/10428199209051004.

Chene, P. 2001. "The role of tetramerization in p53 function." *Oncogene* 20 (21):2611-7. doi: 10.1038/sj.onc.1204373.

Cheng, X., and H. Y. Kao. 2012. "Post-translational modifications of PML: consequences and implications." *Front Oncol* 2:210. doi: 10.3389/fonc.2012.00210.

Chhabra, P., D. C. Payne, P. G. Szilagyi, K. M. Edwards, M. A. Staat, S. H. Shirley, M. Wikswo, W. A. Nix, X. Lu, U. D. Parashar, and J. Vinje. 2013. "Etiology of viral gastroenteritis in children <5 years of age in the United States, 2008-2009." *J Infect Dis* 208 (5):790-800. doi: 10.1093/infdis/jit254.

Chu, Y., and X. Yang. 2011. "SUMO E3 ligase activity of TRIM proteins." *Oncogene* 30 (9):1108-16. doi: 10.1038/onc.2010.462.

Chuikov, S., J. K. Kurash, J. R. Wilson, B. Xiao, N. Justin, G. S. Ivanov, K. McKinney, P. Tempst, C. Prives, S. J. Gamblin, N. A. Barlev, and D. Reinberg. 2004. "Regulation of p53 activity through lysine methylation." *Nature* 432 (7015):353-60. doi: 10.1038/nature03117.

Cleghon, V. G., and D. F. Klessig. 1986. "Association of the adenovirus DNA-binding protein with RNA both in vitro and in vivo." *Proc Natl Acad Sci U S A* 83 (23):8947-51. doi: 10.1073/pnas.83.23.8947.

Cleghon, V., A. Piderit, D. E. Brough, and D. F. Klessig. 1993. "Phosphorylation of the adenovirus DNA-binding protein and epitope mapping of monoclonal antibodies against it." *Virology* 197 (2):564-75. doi: 10.1006/viro.1993.1630.

Cleghon, V., K. Voelkerding, N. Morin, C. Delsert, and D. F. Klessig. 1989. "Isolation and characterization of a viable adenovirus mutant defective in nuclear transport of the DNA-binding protein." *J Virol* 63 (5):2289-99.

Cuesta, R., Q. Xi, and R. J. Schneider. 2004. "Structural basis for competitive inhibition of eIF4G-Mnk1 interaction by the adenovirus 100-kilodalton protein." *J Virol* 78 (14):7707-16. doi: 10.1128/JVI.78.14.7707-7716.2004.

Dales, S., and Y. Chardonnet. 1973. "Early events in the interaction of adenoviruses with HeLa cells. IV. Association with microtubules and the nuclear pore complex during vectorial movement of the inoculum." *Virology* 56 (2):465-83. doi: 10.1016/0042-6822(73)90050-0.

Dallaire, F., P. Blanchette, P. Groitl, T. Dobner, and P. E. Branton. 2009. "Identification of integrin alpha3 as a new substrate of the adenovirus E4orf6/E1B 55-kilodalton E3 ubiquitin ligase complex." *J Virol* 83 (11):5329-38. doi: 10.1128/jvi.00089-09.

Davison, A. J., M. Benko, and B. Harrach. 2003. "Genetic content and evolution of adenoviruses." *J Gen Virol* 84 (Pt 11):2895-908. doi: 10.1099/vir.0.19497-0.

Day, P. M., C. C. Baker, D. R. Lowy, and J. T. Schiller. 2004. "Establishment of papillomavirus infection is enhanced by promyelocytic leukemia protein (PML) expression." *Proc Natl Acad Sci U S A* 101 (39):14252-7. doi: 10.1073/pnas.0404229101.

De Clercq, E., and G. Li. 2016. "Approved Antiviral Drugs over the Past 50 Years." *Clin Microbiol Rev* 29 (3):695-747. doi: 10.1128/cmr.00102-15.

de Jong, R. N., P. C. van der Vliet, and A. B. Brenkman. 2003. "Adenovirus DNA replication: protein priming, jumping back and the role of the DNA binding protein DBP." *Curr Top Microbiol Immunol* 272:187-211. doi: 10.1007/978-3-662-05597-7_7.

de Ory, F., A. Avellon, J. E. Echevarria, M. P. Sanchez-Seco, G. Trallero, M. Cabrerizo, I. Casas, F. Pozo, G. Fedele, D. Vicente, M. J. Pena, A. Moreno, J. Niubo, N. Rabella, G. Rubio, M. Perez-Ruiz, M. Rodriguez-Iglesias, C. Gimeno, J. M. Eiros, S. Melon, M. Blasco, I. Lopez-Miragaya, E. Varela, A. Martinez-Sapina, G. Rodriguez, M. A. Marcos, M. I. Gegundez, G. Cilla, I. Gabilondo, J. M. Navarro, J. Torres, C. Aznar, A. Castellanos, M. E. Guisasola, A. I. Negredo, A. Tenorio, and S. Vazquez-Moron. 2013. "Viral infections of the central nervous system in Spain: a prospective study." *J Med Virol* 85 (3):554-62. doi: 10.1002/jmv.23470.

de Stanchina, E., E. Querido, M. Narita, R. V. Davuluri, P. P. Pandolfi, G. Ferbeyre, and S. W. Lowe. 2004. "PML is a direct p53 target that modulates p53 effector functions." *Mol Cell* 13 (4):523-35. doi: 10.1016/s1097-2765(04)00062-0.

Debbas, M., and E. White. 1993. "Wild-type p53 mediates apoptosis by E1A, which is inhibited by E1B." *Genes Dev* 7 (4):546-54. doi: 10.1101/gad.7.4.546.

DeCaprio, J. A., J. W. Ludlow, J. Figge, J. Y. Shew, C. M. Huang, W. H. Lee, E. Marsilio, E. Paucha, and D. M. Livingston. 1988. "SV40 large tumor antigen forms a specific complex with the product of the retinoblastoma susceptibility gene." *Cell* 54 (2):275-83. doi: 10.1016/0092-8674(88)90559-4.

Dekker, J., P. N. Kanellopoulos, A. K. Loonstra, J. A. van Oosterhout, K. Leonard, P. A. Tucker, and P. C. van der Vliet. 1997. "Multimerization of the adenovirus DNA-binding protein is the driving force for ATP-independent DNA unwinding during strand displacement synthesis." *Embo j* 16 (6):1455-63. doi: 10.1093/emboj/16.6.1455.

Dellaire, G., and D. P. Bazett-Jones. 2004. "PML nuclear bodies: dynamic sensors of DNA damage and cellular stress." *Bioessays* 26 (9):963-77. doi: 10.1002/bies.20089.

Dellaire, G., R. W. Ching, H. Dehghani, Y. Ren, and D. P. Bazett-Jones. 2006. "The number of PML nuclear bodies increases in early S phase by a fission mechanism." *J Cell Sci* 119 (Pt 6):1026-33. doi: 10.1242/jcs.02816.

Dellaire, G., C. H. Eskiw, H. Dehghani, R. W. Ching, and D. P. Bazett-Jones. 2006. "Mitotic accumulations of PML protein contribute to the re-establishment of PML nuclear bodies in G1." *J Cell Sci* 119 (Pt 6):1034-42. doi: 10.1242/jcs.02817.

Deppert, W., A. Walser, and U. Klockmann. 1988. "A subclass of the adenovirus 72K DNA binding protein specifically associating with the cytoskeletal framework of the plasma membrane." *Virology* 165 (2):457-68. doi: 10.1016/0042-6822(88)90589-2.

Desterro, J. M., M. S. Rodriguez, G. D. Kemp, and R. T. Hay. 1999. "Identification of the enzyme required for activation of the small ubiquitin-like protein SUMO-1." *J Biol Chem* 274 (15):10618-24. doi: 10.1074/jbc.274.15.10618.

Desterro, J. M., J. Thomson, and R. T. Hay. 1997. "Ubch9 conjugates SUMO but not ubiquitin." *FEBS Lett* 417 (3):297-300. doi: 10.1016/s0014-5793(97)01305-7.

Detrait, M., S. De Prophetis, J. P. Delville, and M. Komuta. 2015. "Fulminant isolated adenovirus hepatitis 5 months after haplo-identical HSCT for AML." *Clin Case Rep* 3 (10):802-5. doi: 10.1002/ccr3.347.

Dhingra, A., E. Hage, T. Ganzenmueller, S. Bottcher, J. Hofmann, K. Hamprecht, P. Obermeier, B. Rath, F. Hausmann, T. Dobner, and A. Heim. 2019. "Molecular Evolution of Human Adenovirus (HAdV) Species C." *Sci Rep* 9 (1):1039. doi: 10.1038/s41598-018-37249-4.

Di Lello, P., L. M. Jenkins, T. N. Jones, B. D. Nguyen, T. Hara, H. Yamaguchi, J. D. Dikeakos, E. Appella, P. Legault, and J. G. Omichinski. 2006. "Structure of the Tfb1/p53 complex: Insights into the interaction between the p62/Tfb1 subunit of TFIIH and the activation domain of p53." *Mol Cell* 22 (6):731-40. doi: 10.1016/j.molcel.2006.05.007.

Dippold, W. G., G. Jay, A. B. DeLeo, G. Khoury, and L. J. Old. 1981. "p53 transformation-related protein: detection by monoclonal antibody in mouse and human cells." *Proc Natl Acad Sci U S A* 78 (3):1695-9. doi: 10.1073/pnas.78.3.1695.

Dobner, T., N. Horikoshi, S. Rubenwolf, and T. Shenk. 1996. "Blockage by adenovirus E4orf6 of transcriptional activation by the p53 tumor suppressor." *Science* 272 (5267):1470-3. doi: 10.1126/science.272.5267.1470.

Dohmen, R. J. 2004. "SUMO protein modification." *Biochim Biophys Acta* 1695 (1-3):113-31. doi: 10.1016/j.bbamcr.2004.09.021.

Dornan, D., H. Shimizu, N. D. Perkins, and T. R. Hupp. 2003. "DNA-dependent acetylation of p53 by the transcription coactivator p300." *J Biol Chem* 278 (15):13431-41. doi: 10.1074/jbc.M211460200.

Doucas, V., A. M. Ishov, A. Romo, H. Juguilon, M. D. Weitzman, R. M. Evans, and G. G. Maul. 1996. "Adenovirus replication is coupled with the dynamic properties of the PML nuclear structure." *Genes Dev* 10 (2):196-207. doi: 10.1101/gad.10.2.196.

Duprez, E., A. J. Saurin, J. M. Desterro, V. Lallemand-Breitenbach, K. Howe, M. N. Boddy, E. Solomon, H. de The, R. T. Hay, and P. S. Freemont. 1999. "SUMO-1 modification of the acute promyelocytic leukaemia protein PML: implications for nuclear localisation." *J Cell Sci* 112 (Pt 3):381-93.

Dyck, J. A., G. G. Maul, W. H. Miller, Jr., J. D. Chen, A. Kakizuka, and R. M. Evans. 1994. "A novel macromolecular structure is a target of the promyelocyte-retinoic acid receptor oncoprotein." *Cell* 76 (2):333-43. doi: 10.1016/0092-8674(94)90340-9.

Echavarria, M. 2008. "Adenoviruses in immunocompromised hosts." *Clin Microbiol Rev* 21 (4):704-15. doi: 10.1128/cmr.00052-07.

Enders, J. F., J. A. Bell, J. H. Dingle, T. Francis, Jr., M. R. Hilleman, R. J. Huebner, and A. M. Payne. 1956. "Adenoviruses: group name proposed for new respiratory-tract viruses." *Science* 124 (3212):119-20. doi: 10.1126/science.124.3212.119.

Endter, C., B. Hartl, T. Spruss, J. Hauber, and T. Dobner. 2005. "Blockage of CRM1-dependent nuclear export of the adenovirus type 5 early region 1B 55-kDa protein augments oncogenic transformation of primary rat cells." *Oncogene* 24 (1):55-64. doi: 10.1038/sj.onc.1208170.

Endter, C., J. Kzhyshkowska, R. Stauber, and T. Dobner. 2001. "SUMO-1 modification required for transformation by adenovirus type 5 early region 1B 55-kDa oncoprotein." *Proc Natl Acad Sci U S A* 98 (20):11312-7. doi: 10.1073/pnas.191361798.

Epps, J. L., and S. Tanda. 1998. "The Drosophila semushi mutation blocks nuclear import of bicoid during embryogenesis." *Curr Biol* 8 (23):1277-80. doi: 10.1016/s0960-9822(07)00538-6.

Esposito, S., C. Daleno, G. Prunotto, A. Scala, C. Tagliabue, I. Borzani, E. Fossali, C. Pelucchi, and N. Principi. 2013. "Impact of viral infections in children with community-acquired pneumonia: results of a study of 17 respiratory viruses." *Influenza Other Respir Viruses* 7 (1):18-26. doi: 10.1111/j.1750-2659.2012.00340.x.

Evans, J. D., and P. Hearing. 2005. "Relocalization of the Mre11-Rad50-Nbs1 complex by the adenovirus E4 ORF3 protein is required for viral replication." *J Virol* 79 (10):6207-15. doi: 10.1128/jvi.79.10.6207-6215.2005.

Everett, R. D. 2001. "DNA viruses and viral proteins that interact with PML nuclear bodies." *Oncogene* 20 (49):7266-73. doi: 10.1038/sj.onc.1204759.

Everett, R. D., C. Boutell, and B. G. Hale. 2013. "Interplay between viruses and host sumoylation pathways." *Nat Rev Microbiol* 11 (6):400-11. doi: 10.1038/nrmicro3015.

Everett, R. D., and M. K. Chelbi-Alix. 2007. "PML and PML nuclear bodies: implications in antiviral defence." *Biochimie* 89 (6-7):819-30. doi: 10.1016/j.biochi.2007.01.004.

Everett, R. D., S. Rechter, P. Papior, N. Tavalai, T. Stamminger, and A. Orr. 2006. "PML contributes to a cellular mechanism of repression of herpes simplex virus type 1 infection that is inactivated by ICP0." *J Virol* 80 (16):7995-8005. doi: 10.1128/jvi.00734-06.

Everitt, E., L. Lutter, and L. Philipson. 1975. "Structural proteins of adenoviruses. XII. Location and neighbor relationship among proteins of adenovirion type 2 as revealed by enzymatic iodination, immunoprecipitation and chemical cross-linking." *Virology* 67 (1):197-208. doi: 10.1016/0042-6822(75)90417-1.

Ewer, K., S. Sebastian, A. J. Spencer, S. Gilbert, A. V. S. Hill, and T. Lambe. 2017. "Chimpanzee adenoviral vectors as vaccines for outbreak pathogens." *Hum Vaccin Immunother* 13 (12):3020-3032. doi: 10.1080/21645515.2017.1383575.

Farley, D. C., J. L. Brown, and K. N. Leppard. 2004. "Activation of the early-late switch in adenovirus type 5 major late transcription unit expression by L4 gene products." *J Virol* 78 (4):1782-91. doi: 10.1128/jvi.78.4.1782-1791.2004.

Fessler, S. P., and C. S. Young. 1999. "The role of the L4 33K gene in adenovirus infection." *Virology* 263 (2):507-16. doi: 10.1006/viro.1999.9951.

Fischer, M. 2017. "Census and evaluation of p53 target genes." *Oncogene* 36 (28):3943-3956. doi: 10.1038/onc.2016.502.

Fogal, V., N. N. Kartasheva, G. Trigiante, S. Llanos, D. Yap, K. H. Vousden, and X. Lu. 2005. "ASPP1 and ASPP2 are new transcriptional targets of E2F." *Cell Death Differ* 12 (4):369-76. doi: 10.1038/sj.cdd.4401562.

Folegatti, P. M., K. J. Ewer, P. K. Aley, B. Angus, S. Becker, S. Belij-Rammerstorfer, D. Bellamy, S. Bibi, M. Bittaye, E. A. Clutterbuck, C. Dold, S. N. Faust, A. Finn, A. L. Flaxman, B. Hallis, P. Heath, D. Jenkin, R. Lazarus, R. Makinson, A. M. Minassian, K. M. Pollock, M. Ramasamy, H. Robinson, M. Snape, R. Tarrant, M. Voysey, C. Green, A. D. Douglas, A. V. S. Hill, T. Lambe, S. C. Gilbert, and A. J. Pollard. 2020. "Safety and immunogenicity of the ChAdOx1 nCoV-19 vaccine against SARS-CoV-2: a preliminary report of a phase 1/2, single-blind, randomised controlled trial." *Lancet* 396 (10249):467-478. doi: 10.1016/s0140-6736(20)31604-4.

Forrester, N. A., R. N. Patel, T. Speiseder, P. Groitl, G. G. Sedgwick, N. J. Shimwell, R. I. Seed, P. O. Catnaigh, C. J. McCabe, G. S. Stewart, T. Dobner, R. J. Grand, A. Martin, and A. S. Turnell. 2012. "Adenovirus E4orf3 targets transcriptional intermediary factor 1gamma for

proteasome-dependent degradation during infection." *J Virol* 86 (6):3167-79. doi: 10.1128/jvi.06583-11.

Fowlkes, D. M., S. T. Lord, T. Linne, U. Pettersson, and L. Philipson. 1979. "Interaction between the adenovirus DNA-binding protein and double-stranded DNA." *J Mol Biol* 132 (2):163-80. doi: 10.1016/0022-2836(79)90389-9.

Fraser, Andrew G., Ravi S. Kamath, Peder Zipperlen, Maruxa Martinez-Campos, Marc Sohrmann, and Julie Ahringer. 2000. "Functional genomic analysis of C. elegans chromosome I by systematic RNA interference." *Nature* 408 (6810):325-330. doi: 10.1038/35042517.

Freudenberger, N., T. Meyer, P. Groitl, T. Dobner, and S. Schreiner. 2018. "Human Adenovirus Core Protein V Is Targeted by the Host SUMOylation Machinery To Limit Essential Viral Functions." *J Virol* 92 (4). doi: 10.1128/jvi.01451-17.

Friedler, A., D. B. Veprintsev, L. O. Hansson, and A. R. Fersht. 2003. "Kinetic instability of p53 core domain mutants: implications for rescue by small molecules." *J Biol Chem* 278 (26):24108-12. doi: 10.1074/jbc.M302458200.

Furcinitti, P. S., J. van Oostrum, and R. M. Burnett. 1989. "Adenovirus polypeptide IX revealed as capsid cement by difference images from electron microscopy and crystallography." *Embo j* 8 (12):3563-70.

Gaggar, A., D. M. Shayakhmetov, and A. Lieber. 2003. "CD46 is a cellular receptor for group B adenoviruses." *Nat Med* 9 (11):1408-12. doi: 10.1038/nm952.

Ganapathi, L., A. Arnold, S. Jones, A. Patterson, D. Graham, M. Harper, and O. Levy. 2016. "Use of cidofovir in pediatric patients with adenovirus infection." *F1000Res* 5:758. doi: 10.12688/f1000research.8374.2.

Ganly, I., D. Kirn, G. Eckhardt, G. I. Rodriguez, D. S. Soutar, R. Otto, A. G. Robertson, O. Park, M. L. Gulley, C. Heise, D. D. Von Hoff, and S. B. Kaye. 2000. "A phase I study of Onyx-015, an E1B attenuated adenovirus, administered intratumorally to patients with recurrent head and neck cancer." *Clin Cancer Res* 6 (3):798-806.

Garcia, P., A. Harrod, S. Jha, J. Jenkins, A. Barnhill, H. Lee, M. Thompson, J. P. Williams, J. Barefield, A. McKinnon, P. Suarez, A. Shah, A. J. Lowrey, and G. L. Bentz. 2021. "Effects of targeting sumoylation processes during latent and induced Epstein-Barr virus infections using the small molecule inhibitor ML-792." *Antiviral Res* 188:105038. doi: 10.1016/j.antiviral.2021.105038.

Garnett, C. T., G. Talekar, J. A. Mahr, W. Huang, Y. Zhang, D. A. Ornelles, and L. R. Gooding. 2009. "Latent species C adenoviruses in human tonsil tissues." *J Virol* 83 (6):2417-28. doi: 10.1128/jvi.02392-08.

Gavin, P. J., and B. Z. Katz. 2002. "Intravenous ribavirin treatment for severe adenovirus disease in immunocompromised children." *Pediatrics* 110 (1 Pt 1):e9. doi: 10.1542/peds.110.1.e9.

Ghosh, M. K., and M. L. Harter. 2003. "A viral mechanism for remodeling chromatin structure in G0 cells." *Mol Cell* 12 (1):255-60. doi: 10.1016/s1097-2765(03)00225-9.

Giard, D. J., S. A. Aaronson, G. J. Todaro, P. Arnstein, J. H. Kersey, H. Dosik, and W. P. Parks. 1973. "In vitro cultivation of human tumors: establishment of cell lines derived from a series of solid tumors." *J Natl Cancer Inst* 51 (5):1417-23. doi: 10.1093/jnci/51.5.1417.

Goodman, R. H., and S. Smolik. 2000. "CBP/p300 in cell growth, transformation, and development." *Genes Dev* 14 (13):1553-77.

Goradel, N. H., N. Mohajel, Z. V. Malekshahi, S. Jahangiri, M. Najafi, B. Farhood, K. Mortezaee, B. Negahdari, and A. Arashkia. 2019. "Oncolytic adenovirus: A tool for cancer therapy in

combination with other therapeutic approaches." *J Cell Physiol* 234 (6):8636-8646. doi: 10.1002/jcp.27850.

Gorisch, S. M., M. Wachsmuth, C. Ittrich, C. P. Bacher, K. Rippe, and P. Lichter. 2004. "Nuclear body movement is determined by chromatin accessibility and dynamics." *Proc Natl Acad Sci U S A* 101 (36):13221-6. doi: 10.1073/pnas.0402958101.

Gostissa, M., A. Hengstermann, V. Fogal, P. Sandy, S. E. Schwarz, M. Scheffner, and G. Del Sal. 1999. "Activation of p53 by conjugation to the ubiquitin-like protein SUMO-1." *Embo j* 18 (22):6462-71. doi: 10.1093/emboj/18.22.6462.

Graham, F. L., J. Smiley, W. C. Russell, and R. Nairn. 1977. "Characteristics of a human cell line transformed by DNA from human adenovirus type 5." *J Gen Virol* 36 (1):59-74. doi: 10.1099/0022-1317-36-1-59.

Greber, U. F., M. Suomalainen, R. P. Stidwill, K. Boucke, M. W. Ebersold, and A. Helenius. 1997. "The role of the nuclear pore complex in adenovirus DNA entry." *Embo j* 16 (19):5998-6007. doi: 10.1093/emboj/16.19.5998.

Greber, U. F., and M. Way. 2006. "A superhighway to virus infection." *Cell* 124 (4):741-54. doi: 10.1016/j.cell.2006.02.018.

Greber, U. F., M. Willetts, P. Webster, and A. Helenius. 1993. "Stepwise dismantling of adenovirus 2 during entry into cells." *Cell* 75 (3):477-86. doi: 10.1016/0092-8674(93)90382-z.

Groitl, P., and T. Dobner. 2007. "Construction of adenovirus type 5 early region 1 and 4 virus mutants." *Methods Mol Med* 130:29-39. doi: 10.1385/1-59745-166-5:29.

Grotzinger, T., T. Sternsdorf, K. Jensen, and H. Will. 1996. "Interferon-modulated expression of genes encoding the nuclear-dot-associated proteins Sp100 and promyelocytic leukemia protein (PML)." *Eur J Biochem* 238 (2):554-60. doi: 10.1111/j.1432-1033.1996.0554z.x.

Gu, B., and W. G. Zhu. 2012. "Surf the post-translational modification network of p53 regulation." *Int J Biol Sci* 8 (5):672-84. doi: 10.7150/ijbs.4283.

Gu, J., L. Nie, D. Wiederschain, and Z. M. Yuan. 2001. "Identification of p53 sequence elements that are required for MDM2-mediated nuclear export." *Mol Cell Biol* 21 (24):8533-46. doi: 10.1128/mcb.21.24.8533-8546.2001.

Gu, W., and R. G. Roeder. 1997. "Activation of p53 sequence-specific DNA binding by acetylation of the p53 C-terminal domain." *Cell* 90 (4):595-606. doi: 10.1016/s0092-8674(00)80521-8.

Guan, D., and H. Y. Kao. 2015. "The function, regulation and therapeutic implications of the tumor suppressor protein, PML." *Cell Biosci* 5:60. doi: 10.1186/s13578-015-0051-9.

Guldner, H. H., C. Szostecki, P. Schroder, U. Matschl, K. Jensen, C. Luders, H. Will, and T. Sternsdorf. 1999. "Splice variants of the nuclear dot-associated Sp100 protein contain homologies to HMG-1 and a human nuclear phosphoprotein-box motif." *J Cell Sci* 112 (Pt 5):733-47.

Gupta, A., S. Jha, D. A. Engel, D. A. Ornelles, and A. Dutta. 2013. "Tip60 degradation by adenovirus relieves transcriptional repression of viral transcriptional activator EIA." *Oncogene* 32 (42):5017-25. doi: 10.1038/onc.2012.534.

Gustafsson, B., W. Huang, G. Bogdanovic, F. Gauffin, A. Nordgren, G. Talekar, D. A. Ornelles, and L. R. Gooding. 2007. "Adenovirus DNA is detected at increased frequency in Guthrie cards from children who develop acute lymphoblastic leukaemia." *Br J Cancer* 97 (7):992-4. doi: 10.1038/sj.bjc.6603983.

Haack, T. B., R. Kopajtich, P. Freisinger, T. Wieland, J. Rorbach, T. J. Nicholls, E. Baruffini, A. Walther, K. Danhauser, F. A. Zimmermann, R. A. Husain, J. Schum, H. Mundy, I. Ferrero, T. M. Strom, T. Meitinger, R. W. Taylor, M. Minczuk, J. A. Mayr, and H. Prokisch. 2013. "ELAC2 mutations cause a mitochondrial RNA processing defect associated with hypertrophic cardiomyopathy." *Am J Hum Genet* 93 (2):211-23. doi: 10.1016/j.ajhg.2013.06.006.

Hafner, A., M. L. Bulyk, A. Jambhekar, and G. Lahav. 2019. "The multiple mechanisms that regulate p53 activity and cell fate." *Nat Rev Mol Cell Biol* 20 (4):199-210. doi: 10.1038/s41580-019-0110-x.

Hage, E., U. Gerd Liebert, S. Bergs, T. Ganzenmueller, and A. Heim. 2015. "Human mastadenovirus type 70: a novel, multiple recombinant species D mastadenovirus isolated from diarrhoeal faeces of a haematopoietic stem cell transplantation recipient." *J Gen Virol* 96 (9):2734-42. doi: 10.1099/vir.0.000196.

Hanahan, D. 1983. "Studies on transformation of Escherichia coli with plasmids." *J Mol Biol* 166 (4):557-80. doi: 10.1016/s0022-2836(83)80284-8.

Harlow, E., B. R. Franza, Jr., and C. Schley. 1985. "Monoclonal antibodies specific for adenovirus early region 1A proteins: extensive heterogeneity in early region 1A products." *J Virol* 55 (3):533-46.

Harlow, E., P. Whyte, B. R. Franza, Jr., and C. Schley. 1986. "Association of adenovirus early-region 1A proteins with cellular polypeptides." *Mol Cell Biol* 6 (5):1579-89. doi: 10.1128/mcb.6.5.1579.

Harpst, J. A., J. F. Ennever, and W. C. Russell. 1977. "Physical properties of nucleoprotein cores from adenovirus type 5." *Nucleic Acids Res* 4 (2):477-90. doi: 10.1093/nar/4.2.477.

Harrach, B., Benkö, M., Both, G., Brown, M., Davison, A., Echavarria, M., Hess, M., Jones, M.,, and A. Kajon, Lehmkuhl, H. D., Mautner, V., Mittal, S. K. & Wadell, G. . 2012. "Adenoviridae -ninth report of the International Committee on Taxonomy of Viruses. ." In *Virus Taxonomy*, edited by M. J. Adams A. M. Q. King, E. B. Carstens & Lefkowitz Elliot J, 125–141. Oxford: Elsevier.

Hashimoto, S., G. Gonzalez, S. Harada, H. Oosako, N. Hanaoka, R. Hinokuma, and T. Fujimoto. 2018. "Recombinant type Human mastadenovirus D85 associated with epidemic keratoconjunctivitis since 2015 in Japan." *J Med Virol* 90 (5):881-889. doi: 10.1002/jmv.25041.

Hassan, A. O., N. M. Kafai, I. P. Dmitriev, J. M. Fox, B. K. Smith, I. B. Harvey, R. E. Chen, E. S. Winkler, A. W. Wessel, J. B. Case, E. Kashentseva, B. T. McCune, A. L. Bailey, H. Zhao, L. A. VanBlargan, Y. N. Dai, M. Ma, L. J. Adams, S. Shrihari, J. E. Danis, L. E. Gralinski, Y. J. Hou, A. Schäfer, A. S. Kim, S. P. Keeler, D. Weiskopf, R. S. Baric, M. J. Holtzman, D. H. Fremont, D. T. Curiel, and M. S. Diamond. 2020. "A Single-Dose Intranasal ChAd Vaccine Protects Upper and Lower Respiratory Tracts against SARS-CoV-2." *Cell* 183 (1):169-184.e13. doi: 10.1016/j.cell.2020.08.026.

Hateboer, G., E. M. Hijmans, J. B. Nooij, S. Schlenker, S. Jentsch, and R. Bernards. 1996. "mUBC9, a novel adenovirus E1A-interacting protein that complements a yeast cell cycle defect." *J Biol Chem* 271 (42):25906-11. doi: 10.1074/jbc.271.42.25906.

Haupt, Y., R. Maya, A. Kazaz, and M. Oren. 1997. "Mdm2 promotes the rapid degradation of p53." *Nature* 387 (6630):296-9. doi: 10.1038/387296a0.

Hay, R. T. 2005. "SUMO: a history of modification." *Mol Cell* 18 (1):1-12. doi: 10.1016/j.molcel.2005.03.012.

Hay, R. T. 2007. "SUMO-specific proteases: a twist in the tail." *Trends Cell Biol* 17 (8):370-6. doi: 10.1016/j.tcb.2007.08.002.

Hay, R. T., A. Freeman, I. Leith, A. Monaghan, and A. Webster. 1995. "Molecular interactions during adenovirus DNA replication." *Curr Top Microbiol Immunol* 199 (Pt 2):31-48. doi: 10.1007/978-3-642-79499-5_2.

Hendriks, I. A., and A. C. Vertegaal. 2016. "A comprehensive compilation of SUMO proteomics." *Nat Rev Mol Cell Biol* 17 (9):581-95. doi: 10.1038/nrm.2016.81.

Hermannstädter, A., C. Ziegler, M. Kühl, W. Deppert, and G. V. Tolstonog. 2009. "Wild-type p53 enhances efficiency of simian virus 40 large-T-antigen-induced cellular transformation." *J Virol* 83 (19):10106-18. doi: 10.1128/jvi.00174-09.

Hidalgo, P., L. Anzures, A. Hernandez-Mendoza, A. Guerrero, C. D. Wood, M. Valdes, T. Dobner, and R. A. Gonzalez. 2016. "Morphological, Biochemical, and Functional Study of Viral Replication Compartments Isolated from Adenovirus-Infected Cells." *J Virol* 90 (7):3411-27. doi: 10.1128/jvi.00033-16.

Hidalgo, P., and R. A. Gonzalez. 2019. "Formation of adenovirus DNA replication compartments." *FEBS Lett* 593 (24):3518-3530. doi: 10.1002/1873-3468.13672.

Higashino, F., J. M. Pipas, and T. Shenk. 1998. "Adenovirus E4orf6 oncoprotein modulates the function of the p53-related protein, p73." *Proc Natl Acad Sci U S A* 95 (26):15683-7. doi: 10.1073/pnas.95.26.15683.

Hilleman, M. R., and J. H. Werner. 1954. "Recovery of new agent from patients with acute respiratory illness." *Proc Soc Exp Biol Med* 85 (1):183-8. doi: 10.3181/00379727-85-20825.

Hiscox, J. A. 2002. "The nucleolus--a gateway to viral infection?" *Arch Virol* 147 (6):1077-89. doi: 10.1007/s00705-001-0792-0.

Hodges, M., C. Tissot, K. Howe, D. Grimwade, and P. S. Freemont. 1998. "Structure, organization, and dynamics of promyelocytic leukemia protein nuclear bodies." *Am J Hum Genet* 63 (2):297-304. doi: 10.1086/301991.

Hofland, C. A., L. J. Eron, and R. M. Washecka. 2004. "Hemorrhagic adenovirus cystitis after renal transplantation." *Transplant Proc* 36 (10):3025-7. doi: 10.1016/j.transproceed.2004.10.090.

Hofmann, S., J. Mai, S. Masser, P. Groitl, A. Herrmann, T. Sternsdorf, R. Brack-Werner, and S. Schreiner. 2020. "ATO (Arsenic Trioxide) Effects on Promyelocytic Leukemia Nuclear Bodies Reveals Antiviral Intervention Capacity." *Adv Sci (Weinh)* 7 (8):1902130. doi: 10.1002/advs.201902130.

Hong, S. S., E. Szolajska, G. Schoehn, L. Franqueville, S. Myhre, L. Lindholm, R. W. Ruigrok, P. Boulanger, and J. Chroboczek. 2005. "The 100K-chaperone protein from adenovirus serotype 2 (Subgroup C) assists in trimerization and nuclear localization of hexons from subgroups C and B adenoviruses." *J Mol Biol* 352 (1):125-38. doi: 10.1016/j.jmb.2005.06.070.

Horn, H. F., and K. H. Vousden. 2007. "Coping with stress: multiple ways to activate p53." *Oncogene* 26 (9):1306-16. doi: 10.1038/sj.onc.1210263.

Horwitz, M. S., M. D. Scharff, and J. V. Maizel, Jr. 1969. "Synthesis and assembly of adenovirus 2. I. Polypeptide synthesis, assembly of capsomeres, and morphogenesis of the virion." *Virology* 39 (4):682-94. doi: 10.1016/0042-6822(69)90006-3.

Huang, J., J. Dorsey, S. Chuikov, L. Perez-Burgos, X. Zhang, T. Jenuwein, D. Reinberg, and S. L. Berger. 2010. "G9a and Glp methylate lysine 373 in the tumor suppressor p53." *J Biol Chem* 285 (13):9636-41. doi: 10.1074/jbc.M109.062588.

Huang, J., L. Perez-Burgos, B. J. Placek, R. Sengupta, M. Richter, J. A. Dorsey, S. Kubicek, S. Opravil, T. Jenuwein, and S. L. Berger. 2006. "Repression of p53 activity by Smyd2-mediated methylation." *Nature* 444 (7119):629-32. doi: 10.1038/nature05287.

Huang, J., R. Sengupta, A. B. Espejo, M. G. Lee, J. A. Dorsey, M. Richter, S. Opravil, R. Shiekhattar, M. T. Bedford, T. Jenuwein, and S. L. Berger. 2007. "p53 is regulated by the lysine demethylase LSD1." *Nature* 449 (7158):105-8. doi: 10.1038/nature06092.

Ip, W. H., and T. Dobner. 2020. "Cell transformation by the adenovirus oncogenes E1 and E4." *FEBS Lett* 594 (12):1848-1860. doi: 10.1002/1873-3468.13717.

Isaac, A., K. W. Wilcox, and J. L. Taylor. 2006. "SP100B, a repressor of gene expression preferentially binds to DNA with unmethylated CpGs." *J Cell Biochem* 98 (5):1106-22. doi: 10.1002/jcb.20841.

Ishiko, H., Y. Shimada, T. Konno, A. Hayashi, T. Ohguchi, Y. Tagawa, K. Aoki, S. Ohno, and S. Yamazaki. 2008. "Novel human adenovirus causing nosocomial epidemic keratoconjunctivitis." *J Clin Microbiol* 46 (6):2002-8. doi: 10.1128/jcm.01835-07.

Ishov, A. M., and G. G. Maul. 1996. "The periphery of nuclear domain 10 (ND10) as site of DNA virus deposition." *J Cell Biol* 134 (4):815-26. doi: 10.1083/jcb.134.4.815.

Ishov, A. M., A. G. Sotnikov, D. Negorev, O. V. Vladimirova, N. Neff, T. Kamitani, E. T. Yeh, J. F. Strauss, 3rd, and G. G. Maul. 1999. "PML is critical for ND10 formation and recruits the PML-interacting protein daxx to this nuclear structure when modified by SUMO-1." *J Cell Biol* 147 (2):221-34. doi: 10.1083/jcb.147.2.221.

Ishov, A. M., R. M. Stenberg, and G. G. Maul. 1997. "Human cytomegalovirus immediate early interaction with host nuclear structures: definition of an immediate transcript environment." *J Cell Biol* 138 (1):5-16. doi: 10.1083/jcb.138.1.5.

Ismail, A. M., J. S. Lee, J. Y. Lee, G. Singh, D. W. Dyer, D. Seto, J. Chodosh, and J. Rajaiya. 2018. "Adenoviromics: Mining the Human Adenovirus Species D Genome." *Front Microbiol* 9:2178. doi: 10.3389/fmicb.2018.02178.

Izumi, T., K. Io, M. Matsui, K. Shirakawa, M. Shinohara, Y. Nagai, M. Kawahara, M. Kobayashi, H. Kondoh, N. Misawa, Y. Koyanagi, T. Uchiyama, and A. Takaori-Kondo. 2010. "HIV-1 viral infectivity factor interacts with TP53 to induce G2 cell cycle arrest and positively regulate viral replication." *Proc Natl Acad Sci U S A* 107 (48):20798-803. doi: 10.1073/pnas.1008076107.

James, N. J., G. J. Howell, J. H. Walker, and G. E. Blair. 2010. "The role of Cajal bodies in the expression of late phase adenovirus proteins." *Virology* 399 (2):299-311. doi: 10.1016/j.virol.2010.01.013.

Jawetz, E. 1959. "The story of shipyard eye." *Br Med J* 1 (5126):873-6. doi: 10.1136/bmj.1.5126.873.

Jensen, K., C. Shiels, and P. S. Freemont. 2001. "PML protein isoforms and the RBCC/TRIM motif." *Oncogene* 20 (49):7223-33. doi: 10.1038/sj.onc.1204765.

Joanisse, D. R., Y. Inaguma, and R. M. Tanguay. 1998. "Cloning and developmental expression of a nuclear ubiquitin-conjugating enzyme (DmUbc9) that interacts with small heat shock proteins in Drosophila melanogaster." *Biochem Biophys Res Commun* 244 (1):102-9. doi: 10.1006/bbrc.1998.8214.

Johnson, E. S. 2004. "Protein modification by SUMO." *Annu Rev Biochem* 73:355-82. doi: 10.1146/annurev.biochem.73.011303.074118.

Jones, D., E. Crowe, T. A. Stevens, and E. P. Candido. 2002. "Functional and phylogenetic analysis of the ubiquitylation system in Caenorhabditis elegans: ubiquitin-conjugating enzymes, ubiquitin-activating enzymes, and ubiquitin-like proteins." *Genome Biol* 3 (1):Research0002. doi: 10.1186/gb-2001-3-1-research0002.

Joseph, T. W., A. Zaika, and U. M. Moll. 2003. "Nuclear and cytoplasmic degradation of endogenous p53 and HDM2 occurs during down-regulation of the p53 response after multiple types of DNA damage." *Faseb j* 17 (12):1622-30. doi: 10.1096/fj.02-0931com.

Jul-Larsen, A., T. Visted, B. O. Karlsen, C. H. Rinaldo, R. Bjerkvig, P. E. Lonning, and S. O. Boe. 2004. "PML-nuclear bodies accumulate DNA in response to polyomavirus BK and simian virus 40 replication." *Exp Cell Res* 298 (1):58-73. doi: 10.1016/j.yexcr.2004.03.045.

Kamitani, T., K. Kito, H. P. Nguyen, H. Wada, T. Fukuda-Kamitani, and E. T. Yeh. 1998. "Identification of three major sentrinization sites in PML." *J Biol Chem* 273 (41):26675-82. doi: 10.1074/jbc.273.41.26675.

Kanellopoulos, P. N., D. Tsernoglou, P. C. van der Vliet, and P. A. Tucker. 1996. "Alternative arrangements of the protein chain are possible for the adenovirus single-stranded DNA binding protein." *J Mol Biol* 257 (1):1-8. doi: 10.1006/jmbi.1996.0141.

Keiten-Schmitz, J., K. Schunck, and S. Muller. 2019. "SUMO Chains Rule on Chromatin Occupancy." *Front Cell Dev Biol* 7:343. doi: 10.3389/fcell.2019.00343.

Kentsis, A., R. E. Gordon, and K. L. Borden. 2002. "Self-assembly properties of a model RING domain." *Proc Natl Acad Sci U S A* 99 (2):667-72. doi: 10.1073/pnas.012317299.

Kim, Y. E., J. H. Lee, E. T. Kim, H. J. Shin, S. Y. Gu, H. S. Seol, P. D. Ling, C. H. Lee, and J. H. Ahn. 2011. "Human cytomegalovirus infection causes degradation of Sp100 proteins that suppress viral gene expression." *J Virol* 85 (22):11928-37. doi: 10.1128/jvi.00758-11.

Kindsmuller, K., P. Groitl, B. Hartl, P. Blanchette, J. Hauber, and T. Dobner. 2007. "Intranuclear targeting and nuclear export of the adenovirus E1B-55K protein are regulated by SUMO1 conjugation." *Proc Natl Acad Sci U S A* 104 (16):6684-9. doi: 10.1073/pnas.0702158104.

Kindsmuller, K., S. Schreiner, F. Leinenkugel, P. Groitl, E. Kremmer, and T. Dobner. 2009. "A 49-kilodalton isoform of the adenovirus type 5 early region 1B 55-kilodalton protein is sufficient to support virus replication." *J Virol* 83 (18):9045-56. doi: 10.1128/jvi.00728-09.

Kitayner, M., H. Rozenberg, N. Kessler, D. Rabinovich, L. Shaulov, T. E. Haran, and Z. Shakked. 2006. "Structural basis of DNA recognition by p53 tetramers." *Mol Cell* 22 (6):741-53. doi: 10.1016/j.molcel.2006.05.015.

Kitchingman, G. R. 1985. "Sequence of the DNA-binding protein of a human subgroup E adenovirus (type 4): comparisons with subgroup A (type 12), subgroup B (type 7), and subgroup C (type 5)." *Virology* 146 (1):90-101. doi: 10.1016/0042-6822(85)90055-8.

Klein, H., W. Maltzman, and A. J. Levine. 1979. "Structure-function relationships of the adenovirus DNA-binding protein." *J Biol Chem* 254 (21):11051-60.

Knipscheer, P., W. J. van Dijk, J. V. Olsen, M. Mann, and T. K. Sixma. 2007. "Noncovalent interaction between Ubc9 and SUMO promotes SUMO chain formation." *Embo j* 26 (11):2797-807. doi: 10.1038/sj.emboj.7601711.

Koken, M. H., F. Puvion-Dutilleul, M. C. Guillemin, A. Viron, G. Linares-Cruz, N. Stuurman, L. de Jong, C. Szostecki, F. Calvo, C. Chomienne, and et al. 1994. "The t(15;17) translocation alters a nuclear body in a retinoic acid-reversible fashion." *Embo j* 13 (5):1073-83.

Komatsu, T., K. Nagata, and H. Wodrich. 2016. "An Adenovirus DNA Replication Factor, but Not Incoming Genome Complexes, Targets PML Nuclear Bodies." *J Virol* 90 (3):1657-67. doi: 10.1128/jvi.02545-15.

Konig, C., J. Roth, and M. Dobbelstein. 1999. "Adenovirus type 5 E4orf3 protein relieves p53 inhibition by E1B-55-kilodalton protein." *J Virol* 73 (3):2253-62.

Kosulin, K., C. Haberler, J. A. Hainfellner, G. Amann, S. Lang, and T. Lion. 2007. "Investigation of adenovirus occurrence in pediatric tumor entities." *J Virol* 81 (14):7629-35. doi: 10.1128/jvi.00355-07.

Kosulin, K., F. Hoffmann, T. S. Clauditz, W. Wilczak, and T. Dobner. 2013. "Presence of adenovirus species C in infiltrating lymphocytes of human sarcoma." *PLoS One* 8 (5):e63646. doi: 10.1371/journal.pone.0063646.

Kress, M., E. May, R. Cassingena, and P. May. 1979. "Simian virus 40-transformed cells express new species of proteins precipitable by anti-simian virus 40 tumor serum." *J Virol* 31 (2):472-83.

Krilov, L. R. 2005. "Adenovirus infections in the immunocompromised host." *Pediatr Infect Dis J* 24 (6):555-6. doi: 10.1097/01.inf.0000165306.95815.68.

Kroonen, J. S., and A. C. O. Vertegaal. 2021. "Targeting SUMO Signaling to Wrestle Cancer." *Trends Cancer* 7 (6):496-510. doi: 10.1016/j.trecan.2020.11.009.

Kruijer, W., F. M. van Schaik, and J. S. Sussenbach. 1981. "Structure and organization of the gene coding for the DNA binding protein of adenovirus type 5." *Nucleic Acids Res* 9 (18):4439-57. doi: 10.1093/nar/9.18.4439.

Kruse, J. P., and W. Gu. 2009. "Modes of p53 regulation." *Cell* 137 (4):609-22. doi: 10.1016/j.cell.2009.04.050.

Kurepa, J., J. M. Walker, J. Smalle, M. M. Gosink, S. J. Davis, T. L. Durham, D. Y. Sung, and R. D. Vierstra. 2003. "The small ubiquitin-like modifier (SUMO) protein modification system in Arabidopsis. Accumulation of SUMO1 and -2 conjugates is increased by stress." *J Biol Chem* 278 (9):6862-72. doi: 10.1074/jbc.M209694200.

Kwek, S. S., J. Derry, A. L. Tyner, Z. Shen, and A. V. Gudkov. 2001. "Functional analysis and intracellular localization of p53 modified by SUMO-1." *Oncogene* 20 (20):2587-99. doi: 10.1038/sj.onc.1204362.

Kzhyshkowska, J., E. Kremmer, M. Hofmann, H. Wolf, and T. Dobner. 2004. "Protein arginine methylation during lytic adenovirus infection." *Biochem J* 383 (Pt 2):259-65. doi: 10.1042/bj20040210.

Lallemand-Breitenbach, V., and H. de The. 2010. "PML nuclear bodies." *Cold Spring Harb Perspect Biol* 2 (5):a000661. doi: 10.1101/cshperspect.a000661.

Lallemand-Breitenbach, V., M. Jeanne, S. Benhenda, R. Nasr, M. Lei, L. Peres, J. Zhou, J. Zhu, B. Raught, and H. de The. 2008. "Arsenic degrades PML or PML-RARalpha through a SUMO-triggered RNF4/ubiquitin-mediated pathway." *Nat Cell Biol* 10 (5):547-55. doi: 10.1038/ncb1717.

Lallemand-Breitenbach, V., J. Zhu, F. Puvion, M. Koken, N. Honore, A. Doubeikovsky, E. Duprez, P. P. Pandolfi, E. Puvion, P. Freemont, and H. de The. 2001. "Role of promyelocytic leukemia (PML) sumolation in nuclear body formation, 11S proteasome recruitment, and As2O3-induced PML or PML/retinoic acid receptor alpha degradation." *J Exp Med* 193 (12):1361-71. doi: 10.1084/jem.193.12.1361.

Lane, D. P. 1992. "Cancer. p53, guardian of the genome." *Nature* 358 (6381):15-6. doi: 10.1038/358015a0.

Lane, D. P., and L. V. Crawford. 1979. "T antigen is bound to a host protein in SV40-transformed cells." *Nature* 278 (5701):261-3. doi: 10.1038/278261a0.

Laptenko, O., I. Shiff, W. Freed-Pastor, A. Zupnick, M. Mattia, E. Freulich, I. Shamir, N. Kadouri, T. Kahan, J. Manfredi, I. Simon, and C. Prives. 2015. "The p53 C terminus controls site-specific DNA binding and promotes structural changes within the central DNA binding domain." *Mol Cell* 57 (6):1034-1046. doi: 10.1016/j.molcel.2015.02.015.

Ledgerwood, J. E., A. D. DeZure, D. A. Stanley, E. E. Coates, L. Novik, M. E. Enama, N. M. Berkowitz, Z. Hu, G. Joshi, A. Ploquin, S. Sitar, I. J. Gordon, S. A. Plummer, L. A. Holman, C. S. Hendel, G. Yamshchikov, F. Roman, A. Nicosia, S. Colloca, R. Cortese, R. T. Bailer, R. M. Schwartz, M. Roederer, J. R. Mascola, R. A. Koup, N. J. Sullivan, and B. S. Graham. 2017. "Chimpanzee Adenovirus Vector Ebola Vaccine." *N Engl J Med* 376 (10):928-938. doi: 10.1056/NEJMoa1410863.

Ledl, A., D. Schmidt, and S. Muller. 2005. "Viral oncoproteins E1A and E7 and cellular LxCxE proteins repress SUMO modification of the retinoblastoma tumor suppressor." *Oncogene* 24 (23):3810-8. doi: 10.1038/sj.onc.1208539.

Lee, C. S., E. S. Bishop, R. Zhang, X. Yu, E. M. Farina, S. Yan, C. Zhao, Z. Zheng, Y. Shu, X. Wu, J. Lei, Y. Li, W. Zhang, C. Yang, K. Wu, Y. Wu, S. Ho, A. Athiviraham, M. J. Lee, J. M. Wolf, R. R. Reid, and T. C. He. 2017. "Adenovirus-Mediated Gene Delivery: Potential Applications for Gene and Cell-Based Therapies in the New Era of Personalized Medicine." *Genes Dis* 4 (2):43-63. doi: 10.1016/j.gendis.2017.04.001.

Lee, G. W., F. Melchior, M. J. Matunis, R. Mahajan, Q. Tian, and P. Anderson. 1998. "Modification of Ran GTPase-activating protein by the small ubiquitin-related modifier SUMO-1 requires Ubc9, an E2-type ubiquitin-conjugating enzyme homologue." *J Biol Chem* 273 (11):6503-7. doi: 10.1074/jbc.273.11.6503.

Lehming, N., A. Le Saux, J. Schuller, and M. Ptashne. 1998. "Chromatin components as part of a putative transcriptional repressing complex." *Proc Natl Acad Sci U S A* 95 (13):7322-6. doi: 10.1073/pnas.95.13.7322.

Leppard, K. N., and R. D. Everett. 1999. "The adenovirus type 5 E1b 55K and E4 Orf3 proteins associate in infected cells and affect ND10 components." *J Gen Virol* 80 (Pt 4):997-1008. doi: 10.1099/0022-1317-80-4-997.

Li, M., J. Luo, C. L. Brooks, and W. Gu. 2002. "Acetylation of p53 inhibits its ubiquitination by Mdm2." *J Biol Chem* 277 (52):50607-11. doi: 10.1074/jbc.C200578200.

Li, T., R. Santockyte, R. F. Shen, E. Tekle, G. Wang, D. C. Yang, and P. B. Chock. 2006. "Expression of SUMO-2/3 induced senescence through p53- and pRB-mediated pathways." *J Biol Chem* 281 (47):36221-7. doi: 10.1074/jbc.M608236200.

Liang, S. H., and M. F. Clarke. 2001. "Regulation of p53 localization." *Eur J Biochem* 268 (10):2779-83. doi: 10.1046/j.1432-1327.2001.02227.x.

Liang, Y. C., C. C. Lee, Y. L. Yao, C. C. Lai, M. L. Schmitz, and W. M. Yang. 2016. "SUMO5, a Novel Poly-SUMO Isoform, Regulates PML Nuclear Bodies." *Sci Rep* 6:26509. doi: 10.1038/srep26509.

Liebermann, H., R. Mentel, L. Dohner, S. Modrow, and W. Seidel. 1996. "Inhibition of cell adhesion to the virus by synthetic peptides of fiber knob of human adenovirus serotypes 2 and 3 and virus neutralisation by anti-peptide antibodies." *Virus Res* 45 (2):111-22. doi: 10.1016/s0168-1702(96)01369-x.

Lill, N. L., S. R. Grossman, D. Ginsberg, J. DeCaprio, and D. M. Livingston. 1997. "Binding and modulation of p53 by p300/CBP coactivators." *Nature* 387 (6635):823-7. doi: 10.1038/42981.

Lin, J. Y., T. Ohshima, and K. Shimotohno. 2004. "Association of Ubc9, an E2 ligase for SUMO conjugation, with p53 is regulated by phosphorylation of p53." *FEBS Lett* 573 (1-3):15-8. doi: 10.1016/j.febslet.2004.07.059.

Lin, K. H., Y. C. Lin, H. L. Chen, G. M. Ke, C. J. Chiang, K. P. Hwang, P. Y. Chu, J. H. Lin, D. P. Liu, and H. Y. Chen. 2004. "A two decade survey of respiratory adenovirus in Taiwan: the reemergence of adenovirus types 7 and 4." *J Med Virol* 73 (2):274-9. doi: 10.1002/jmv.20087.

Linne, T., H. Jornvall, and L. Philipson. 1977. "Purification and characterization of the phosphorylated DNA-binding protein from adenovirus-type-2-infected cells." *Eur J Biochem* 76 (2):481-90. doi: 10.1111/j.1432-1033.1977.tb11618.x.

Linne, T., and L. Philipson. 1980. "Further characterization of the phosphate moiety of the adenovirus type 2 DNA-binding protein." *Eur J Biochem* 103 (2):259-70. doi: 10.1111/j.1432-1033.1980.tb04310.x.

Linzer, D. I., and A. J. Levine. 1979. "Characterization of a 54K dalton cellular SV40 tumor antigen present in SV40-transformed cells and uninfected embryonal carcinoma cells." *Cell* 17 (1):43-52. doi: 10.1016/0092-8674(79)90293-9.

Lion, T. 2014. "Adenovirus infections in immunocompetent and immunocompromised patients." *Clin Microbiol Rev* 27 (3):441-62. doi: 10.1128/cmr.00116-13.

Lion, T., R. Baumgartinger, F. Watzinger, S. Matthes-Martin, M. Suda, S. Preuner, B. Futterknecht, A. Lawitschka, C. Peters, U. Potschger, and H. Gadner. 2003. "Molecular monitoring of adenovirus in peripheral blood after allogeneic bone marrow transplantation permits early diagnosis of disseminated disease." *Blood* 102 (3):1114-20. doi: 10.1182/blood-2002-07-2152.

Lion, T., K. Kosulin, C. Landlinger, M. Rauch, S. Preuner, D. Jugovic, U. Potschger, A. Lawitschka, C. Peters, G. Fritsch, and S. Matthes-Martin. 2010. "Monitoring of adenovirus load in stool by real-time PCR permits early detection of impending invasive infection in patients after allogeneic stem cell transplantation." *Leukemia* 24 (4):706-14. doi: 10.1038/leu.2010.4.

Liu, H., L. Jin, S. B. Koh, I. Atanasov, S. Schein, L. Wu, and Z. H. Zhou. 2010. "Atomic structure of human adenovirus by cryo-EM reveals interactions among protein networks." *Science* 329 (5995):1038-43. doi: 10.1126/science.1187433.

Liu, L., D. M. Scolnick, R. C. Trievel, H. B. Zhang, R. Marmorstein, T. D. Halazonetis, and S. L. Berger. 1999. "p53 sites acetylated in vitro by PCAF and p300 are acetylated in vivo in response to DNA damage." *Mol Cell Biol* 19 (2):1202-9. doi: 10.1128/mcb.19.2.1202.

Liu, X., and R. Marmorstein. 2006. "When viral oncoprotein meets tumor suppressor: a structural view." *Genes Dev* 20 (17):2332-7. doi: 10.1101/gad.1471706.

Liu, Y., A. L. Colosimo, X. J. Yang, and D. Liao. 2000. "Adenovirus E1B 55-kilodalton oncoprotein inhibits p53 acetylation by PCAF." *Mol Cell Biol* 20 (15):5540-53. doi: 10.1128/mcb.20.15.5540-5553.2000.

Liu, Y., A. Shevchenko, A. Shevchenko, and A. J. Berk. 2005. "Adenovirus exploits the cellular aggresome response to accelerate inactivation of the MRN complex." *J Virol* 79 (22):14004-16. doi: 10.1128/jvi.79.22.14004-14016.2005.

Lois, L. M., and C. D. Lima. 2005. "Structures of the SUMO E1 provide mechanistic insights into SUMO activation and E2 recruitment to E1." *Embo j* 24 (3):439-51. doi: 10.1038/sj.emboj.7600552.

Lois, L. M., C. D. Lima, and N. H. Chua. 2003. "Small ubiquitin-like modifier modulates abscisic acid signaling in Arabidopsis." *Plant Cell* 15 (6):1347-59. doi: 10.1105/tpc.009902.

Louie, J. K., A. E. Kajon, M. Holodniy, L. Guardia-LaBar, B. Lee, A. M. Petru, J. K. Hacker, and D. P. Schnurr. 2008. "Severe pneumonia due to adenovirus serotype 14: a new respiratory threat?" *Clin Infect Dis* 46 (3):421-5. doi: 10.1086/525261.

Lowe, S. W., and H. E. Ruley. 1993. "Stabilization of the p53 tumor suppressor is induced by adenovirus 5 E1A and accompanies apoptosis." *Genes Dev* 7 (4):535-45. doi: 10.1101/gad.7.4.535.

Luo, J., A. Y. Nikolaev, S. Imai, D. Chen, F. Su, A. Shiloh, L. Guarente, and W. Gu. 2001. "Negative control of p53 by Sir2alpha promotes cell survival under stress." *Cell* 107 (2):137-48. doi: 10.1016/s0092-8674(01)00524-4.

Luo, J., F. Su, D. Chen, A. Shiloh, and W. Gu. 2000. "Deacetylation of p53 modulates its effect on cell growth and apoptosis." *Nature* 408 (6810):377-81. doi: 10.1038/35042612.

Lutz, P., and C. Kedinger. 1996. "Properties of the adenovirus IVa2 gene product, an effector of late-phase-dependent activation of the major late promoter." *J Virol* 70 (3):1396-405.

Ma, X. F., Y. Tan, S. F. Li, W. Jin, and K. K. Wang. 2019. "[Post-translational Modifications of PML in Regulating the Functions of Nuclear Bodies --Review]." *Zhongguo Shi Yan Xue Ye Xue Za Zhi* 27 (5):1696-1700. doi: 10.19746/j.cnki.issn.1009-2137.2019.05.052.

MacLachlan, N. James, and Edward J. Dubovi. 2011. "Chapter 2 - Virus Replication." In *Fenner's Veterinary Virology (Fourth Edition)*, 21-42. San Diego: Academic Press.

Madu, Ikenna G., Shirley Li, Baozong Li, Haitang Li, Tammy Chang, Yi-Jia Li, Ramir Vega, John Rossi, Jiing-Kuan Yee, John Zaia, and Yuan Chen. 2015. "A Novel Class of HIV-1 Antiviral Agents Targeting HIV via a SUMOylation-Dependent Mechanism." *Scientific Reports* 5 (1):17808. doi: 10.1038/srep17808.

Mahajan, R., C. Delphin, T. Guan, L. Gerace, and F. Melchior. 1997. "A small ubiquitin-related polypeptide involved in targeting RanGAP1 to nuclear pore complex protein RanBP2." *Cell* 88 (1):97-107. doi: 10.1016/s0092-8674(00)81862-0.

Mahajan, R., L. Gerace, and F. Melchior. 1998. "Molecular characterization of the SUMO-1 modification of RanGAP1 and its role in nuclear envelope association." *J Cell Biol* 140 (2):259-70. doi: 10.1083/jcb.140.2.259.

Maki, C. G. 1999. "Oligomerization is required for p53 to be efficiently ubiquitinated by MDM2." *J Biol Chem* 274 (23):16531-5. doi: 10.1074/jbc.274.23.16531.

Marion, M. J., O. Hantz, and D. Durantel. 2010. "The HepaRG cell line: biological properties and relevance as a tool for cell biology, drug metabolism, and virology studies." *Methods Mol Biol* 640:261-72. doi: 10.1007/978-1-60761-688-7_13.

Maruzuru, Y., H. Fujii, M. Oyama, H. Kozuka-Hata, A. Kato, and Y. Kawaguchi. 2013. "Roles of p53 in herpes simplex virus 1 replication." *J Virol* 87 (16):9323-32. doi: 10.1128/jvi.01581-13.

Mathias, P., T. Wickham, M. Moore, and G. Nemerow. 1994. "Multiple adenovirus serotypes use alpha v integrins for infection." *J Virol* 68 (10):6811-4.

Matic, I., M. van Hagen, J. Schimmel, B. Macek, S. C. Ogg, M. H. Tatham, R. T. Hay, A. I. Lamond, M. Mann, and A. C. O. Vertegaal. 2008. "In vivo identification of human small ubiquitin-like modifier polymerization sites by high accuracy mass spectrometry and an in

vitro to in vivo strategy." *Mol Cell Proteomics* 7 (1):132-44. doi: 10.1074/mcp.M700173-MCP200.

Matunis, M. J., E. Coutavas, and G. Blobel. 1996. "A novel ubiquitin-like modification modulates the partitioning of the Ran-GTPase-activating protein RanGAP1 between the cytosol and the nuclear pore complex." *J Cell Biol* 135 (6 Pt 1):1457-70. doi: 10.1083/jcb.135.6.1457.

Matunis, M. J., J. Wu, and G. Blobel. 1998. "SUMO-1 modification and its role in targeting the Ran GTPase-activating protein, RanGAP1, to the nuclear pore complex." *J Cell Biol* 140 (3):499-509. doi: 10.1083/jcb.140.3.499.

Maul, G. G. 1998. "Nuclear domain 10, the site of DNA virus transcription and replication." *Bioessays* 20 (8):660-7. doi: 10.1002/(sici)1521-1878(199808)20:8<660::Aid-bies9>3.0.Co;2-m.

Maul, G. G., A. M. Ishov, and R. D. Everett. 1996. "Nuclear domain 10 as preexisting potential replication start sites of herpes simplex virus type-1." *Virology* 217 (1):67-75. doi: 10.1006/viro.1996.0094.

Maul, G. G., D. E. Jensen, A. M. Ishov, M. Herlyn, and F. J. Rauscher, 3rd. 1998. "Nuclear redistribution of BRCA1 during viral infection." *Cell Growth Differ* 9 (9):743-55.

McKinney, K., M. Mattia, V. Gottifredi, and C. Prives. 2004. "p53 linear diffusion along DNA requires its C terminus." *Mol Cell* 16 (3):413-24. doi: 10.1016/j.molcel.2004.09.032.

McLure, K. G., and P. W. Lee. 1998. "How p53 binds DNA as a tetramer." *Embo j* 17 (12):3342-50. doi: 10.1093/emboj/17.12.3342.

Mei, Ya-Fang, Balázs Harrach, and Göran Wadell. 2011. "Mastadenovirus." In *The Springer Index of Viruses*, edited by Christian Tidona and Gholamreza Darai, 33-48. New York, NY: Springer New York.

Mercado, N. B., R. Zahn, F. Wegmann, C. Loos, A. Chandrashekar, J. Yu, J. Liu, L. Peter, K. McMahan, L. H. Tostanoski, X. He, D. R. Martinez, L. Rutten, R. Bos, D. van Manen, J. Vellinga, J. Custers, J. P. Langedijk, T. Kwaks, M. J. G. Bakkers, D. Zuijdgeest, S. K. Rosendahl Huber, C. Atyeo, S. Fischinger, J. S. Burke, J. Feldman, B. M. Hauser, T. M. Caradonna, E. A. Bondzie, G. Dagotto, M. S. Gebre, E. Hoffman, C. Jacob-Dolan, M. Kirilova, Z. Li, Z. Lin, S. H. Mahrokhian, L. F. Maxfield, F. Nampanya, R. Nityanandam, J. P. Nkolola, S. Patel, J. D. Ventura, K. Verrington, H. Wan, L. Pessaint, A. Van Ry, K. Blade, A. Strasbaugh, M. Cabus, R. Brown, A. Cook, S. Zouantchangadou, E. Teow, H. Andersen, M. G. Lewis, Y. Cai, B. Chen, A. G. Schmidt, R. K. Reeves, R. S. Baric, D. A. Lauffenburger, G. Alter, P. Stoffels, M. Mammen, J. Van Hoof, H. Schuitemaker, and D. H. Barouch. 2020. "Single-shot Ad26 vaccine protects against SARS-CoV-2 in rhesus macaques." *Nature* 586 (7830):583-588. doi: 10.1038/s41586-020-2607-z.

Meroni, G., and G. Diez-Roux. 2005. "TRIM/RBCC, a novel class of 'single protein RING finger' E3 ubiquitin ligases." *Bioessays* 27 (11):1147-57. doi: 10.1002/bies.20304.

Miteva, M., K. Keusekotten, K. Hofmann, G. J. Praefcke, and R. J. Dohmen. 2010. "Sumoylation as a signal for polyubiquitylation and proteasomal degradation." *Subcell Biochem* 54:195-214. doi: 10.1007/978-1-4419-6676-6_16.

Mitra, S., D. L. Bodor, A. F. David, I. Abdul-Zani, J. F. Mata, B. Neumann, S. Reither, C. Tischer, and L. E. T. Jansen. 2020. "Genetic screening identifies a SUMO protease dynamically maintaining centromeric chromatin." *Nat Commun* 11 (1):501. doi: 10.1038/s41467-019-14276-x.

Mitsudomi, T., S. M. Steinberg, M. M. Nau, D. Carbone, D. D'Amico, S. Bodner, H. K. Oie, R. I. Linnoila, J. L. Mulshine, J. D. Minna, and et al. 1992. "p53 gene mutations in non-small-

cell lung cancer cell lines and their correlation with the presence of ras mutations and clinical features." *Oncogene* 7 (1):171-80.

Moll, U. M., M. LaQuaglia, J. Benard, and G. Riou. 1995. "Wild-type p53 protein undergoes cytoplasmic sequestration in undifferentiated neuroblastomas but not in differentiated tumors." *Proc Natl Acad Sci U S A* 92 (10):4407-11. doi: 10.1073/pnas.92.10.4407.

Moll, U. M., G. Riou, and A. J. Levine. 1992. "Two distinct mechanisms alter p53 in breast cancer: mutation and nuclear exclusion." *Proc Natl Acad Sci U S A* 89 (15):7262-6. doi: 10.1073/pnas.89.15.7262.

Momand, J., G. P. Zambetti, D. C. Olson, D. George, and A. J. Levine. 1992. "The mdm-2 oncogene product forms a complex with the p53 protein and inhibits p53-mediated transactivation." *Cell* 69 (7):1237-45. doi: 10.1016/0092-8674(92)90644-r.

Monaghan, A., A. Webster, and R. T. Hay. 1994. "Adenovirus DNA binding protein: helix destabilising properties." *Nucleic Acids Res* 22 (5):742-8. doi: 10.1093/nar/22.5.742.

Moran, E., T. Grodzicker, R. J. Roberts, M. B. Mathews, and B. Zerler. 1986. "Lytic and transforming functions of individual products of the adenovirus E1A gene." *J Virol* 57 (3):765-75.

Morin, N., and P. Boulanger. 1986. "Hexon trimerization occurring in an assembly-defective, 100K temperature-sensitive mutant of adenovirus 2." *Virology* 152 (1):11-31.

Morin, N., C. Delsert, and D. F. Klessig. 1989. "Nuclear localization of the adenovirus DNA-binding protein: requirement for two signals and complementation during viral infection." *Mol Cell Biol* 9 (10):4372-80. doi: 10.1128/mcb.9.10.4372.

Morris, S. J., and K. N. Leppard. 2009. "Adenovirus serotype 5 L4-22K and L4-33K proteins have distinct functions in regulating late gene expression." *J Virol* 83 (7):3049-58. doi: 10.1128/jvi.02455-08.

Morris, S. J., G. E. Scott, and K. N. Leppard. 2010. "Adenovirus late-phase infection is controlled by a novel L4 promoter." *J Virol* 84 (14):7096-104. doi: 10.1128/jvi.00107-10.

Mukhopadhyay, D., and M. Dasso. 2007. "Modification in reverse: the SUMO proteases." *Trends Biochem Sci* 32 (6):286-95. doi: 10.1016/j.tibs.2007.05.002.

Muller, S., and T. Dobner. 2008. "The adenovirus E1B-55K oncoprotein induces SUMO modification of p53." *Cell Cycle* 7 (6):754-8. doi: 10.4161/cc.7.6.5495.

Muncheberg, S., R. T. Hay, W. H. Ip, T. Meyer, C. Weiss, J. Brenke, S. Masser, K. Hadian, T. Dobner, and S. Schreiner. 2018. "E1B-55K-Mediated Regulation of RNF4 SUMO-Targeted Ubiquitin Ligase Promotes Human Adenovirus Gene Expression." *J Virol* 92 (13). doi: 10.1128/jvi.00164-18.

Murti, K. G., D. S. Davis, and G. R. Kitchingman. 1990. "Localization of adenovirus-encoded DNA replication proteins in the nucleus by immunogold electron microscopy." *J Gen Virol* 71 (Pt 12):2847-57. doi: 10.1099/0022-1317-71-12-2847.

Nakajima, T., K. Morita, H. Tsunoda, S. Imajoh-Ohmi, H. Tanaka, H. Yasuda, and K. Oda. 1998. "Stabilization of p53 by adenovirus E1A occurs through its amino-terminal region by modification of the ubiquitin-proteasome pathway." *J Biol Chem* 273 (32):20036-45. doi: 10.1074/jbc.273.32.20036.

Nakamura, S., J. A. Roth, and T. Mukhopadhyay. 2000. "Multiple lysine mutations in the C-terminal domain of p53 interfere with MDM2-dependent protein degradation and ubiquitination." *Mol Cell Biol* 20 (24):9391-8. doi: 10.1128/mcb.20.24.9391-9398.2000.

Natan, E., C. Baloglu, K. Pagel, S. M. Freund, N. Morgner, C. V. Robinson, A. R. Fersht, and A. C. Joerger. 2011. "Interaction of the p53 DNA-binding domain with its n-terminal

extension modulates the stability of the p53 tetramer." *J Mol Biol* 409 (3):358-68. doi: 10.1016/j.jmb.2011.03.047.

Neale, G. A., and G. R. Kitchingman. 1989. "Biochemical analysis of adenovirus type 5 DNA-binding protein mutants." *J Biol Chem* 264 (6):3153-9.

Negorev, D. G., O. V. Vladimirova, A. Ivanov, F. Rauscher, 3rd, and G. G. Maul. 2006. "Differential role of Sp100 isoforms in interferon-mediated repression of herpes simplex virus type 1 immediate-early protein expression." *J Virol* 80 (16):8019-29. doi: 10.1128/jvi.02164-05.

Nemerow, G. R., L. Pache, V. Reddy, and P. L. Stewart. 2009. "Insights into adenovirus host cell interactions from structural studies." *Virology* 384 (2):380-8. doi: 10.1016/j.virol.2008.10.016.

Nevins, J. R. 1981. "Mechanism of activation of early viral transcription by the adenovirus E1A gene product." *Cell* 26 (2 Pt 2):213-20. doi: 10.1016/0092-8674(81)90304-4.

Nevins, J. R., and J. E. Darnell. 1978. "Groups of adenovirus type 2 mRNA's derived from a large primary transcript: probable nuclear origin and possible common 3' ends." *J Virol* 25 (3):811-23.

Newhart, A., D. G. Negorev, I. U. Rafalska-Metcalf, T. Yang, G. G. Maul, and S. M. Janicki. 2013. "Sp100A promotes chromatin decondensation at a cytomegalovirus-promoter-regulated transcription site." *Mol Biol Cell* 24 (9):1454-68. doi: 10.1091/mbc.E12-09-0669.

Nicolas, J. C., P. Sarnow, M. Girard, and A. J. Levine. 1983. "Host range temperature-conditional mutants in the adenovirus DNA binding protein are defective in the assembly of infectious virus." *Virology* 126 (1):228-39. doi: 10.1016/0042-6822(83)90474-9.

Nie, L., M. Sasaki, and C. G. Maki. 2007. "Regulation of p53 nuclear export through sequential changes in conformation and ubiquitination." *J Biol Chem* 282 (19):14616-25. doi: 10.1074/jbc.M610515200.

Nisole, S., M. A. Maroui, X. H. Mascle, M. Aubry, and M. K. Chelbi-Alix. 2013. "Differential Roles of PML Isoforms." *Front Oncol* 3:125. doi: 10.3389/fonc.2013.00125.

Numazaki, Y., T. Kumasaka, N. Yano, M. Yamanaka, T. Miyazawa, S. Takai, and N. Ishida. 1973. "Further study on acute hemorrhagic cystitis due to adenovirus type 11." *N Engl J Med* 289 (7):344-7. doi: 10.1056/nejm197308162890704.

Okuma, T., R. Honda, G. Ichikawa, N. Tsumagari, and H. Yasuda. 1999. "In vitro SUMO-1 modification requires two enzymatic steps, E1 and E2." *Biochem Biophys Res Commun* 254 (3):693-8. doi: 10.1006/bbrc.1998.9995.

Orazio, N. I., C. M. Naeger, J. Karlseder, and M. D. Weitzman. 2011. "The adenovirus E1b55K/E4orf6 complex induces degradation of the Bloom helicase during infection." *J Virol* 85 (4):1887-92. doi: 10.1128/jvi.02134-10.

Ornelles, D. A., and T. Shenk. 1991. "Localization of the adenovirus early region 1B 55-kilodalton protein during lytic infection: association with nuclear viral inclusions requires the early region 4 34-kilodalton protein." *J Virol* 65 (1):424-9.

Ostapchuk, P., J. Yang, E. Auffarth, and P. Hearing. 2005. "Functional interaction of the adenovirus IVa2 protein with adenovirus type 5 packaging sequences." *J Virol* 79 (5):2831-8. doi: 10.1128/jvi.79.5.2831-2838.2005.

Owerbach, D., E. M. McKay, E. T. Yeh, K. H. Gabbay, and K. M. Bohren. 2005. "A proline-90 residue unique to SUMO-4 prevents maturation and sumoylation." *Biochem Biophys Res Commun* 337 (2):517-20. doi: 10.1016/j.bbrc.2005.09.090.

Pandolfi, P. P., M. Alcalay, M. Fagioli, D. Zangrilli, A. Mencarelli, D. Diverio, A. Biondi, F. Lo Coco, A. Rambaldi, F. Grignani, and et al. 1992. "Genomic variability and alternative splicing generate multiple PML/RAR alpha transcripts that encode aberrant PML proteins and PML/RAR alpha isoforms in acute promyelocytic leukaemia." *Embo j* 11 (4):1397-407.

Pearson, M., R. Carbone, C. Sebastiani, M. Cioce, M. Fagioli, S. Saito, Y. Higashimoto, E. Appella, S. Minucci, P. P. Pandolfi, and P. G. Pelicci. 2000. "PML regulates p53 acetylation and premature senescence induced by oncogenic Ras." *Nature* 406 (6792):207-10. doi: 10.1038/35018127.

Pennella, M. A., Y. Liu, J. L. Woo, C. A. Kim, and A. J. Berk. 2010. "Adenovirus E1B 55-kilodalton protein is a p53-SUMO1 E3 ligase that represses p53 and stimulates its nuclear export through interactions with promyelocytic leukemia nuclear bodies." *J Virol* 84 (23):12210-25. doi: 10.1128/jvi.01442-10.

Percherancier, Y., D. Germain-Desprez, F. Galisson, X. H. Mascle, L. Dianoux, P. Estephan, M. K. Chelbi-Alix, and M. Aubry. 2009. "Role of SUMO in RNF4-mediated promyelocytic leukemia protein (PML) degradation: sumoylation of PML and phospho-switch control of its SUMO binding domain dissected in living cells." *J Biol Chem* 284 (24):16595-608. doi: 10.1074/jbc.M109.006387.

Perez-Berna, A. J., R. Marabini, S. H. Scheres, R. Menendez-Conejero, I. P. Dmitriev, D. T. Curiel, W. F. Mangel, S. J. Flint, and C. San Martin. 2009. "Structure and uncoating of immature adenovirus." *J Mol Biol* 392 (2):547-57. doi: 10.1016/j.jmb.2009.06.057.

Petitjean, A., E. Mathe, S. Kato, C. Ishioka, S. V. Tavtigian, P. Hainaut, and M. Olivier. 2007. "Impact of mutant p53 functional properties on TP53 mutation patterns and tumor phenotype: lessons from recent developments in the IARC TP53 database." *Hum Mutat* 28 (6):622-9. doi: 10.1002/humu.20495.

Pichler, A., C. Fatouros, H. Lee, and N. Eisenhardt. 2017. "SUMO conjugation - a mechanistic view." *Biomol Concepts* 8 (1):13-36. doi: 10.1515/bmc-2016-0030.

Picksley, S. M., and D. P. Lane. 1993. "The p53-mdm2 autoregulatory feedback loop: a paradigm for the regulation of growth control by p53?" *Bioessays* 15 (10):689-90. doi: 10.1002/bies.950151008.

Pimentel, H., N. L. Bray, S. Puente, P. Melsted, and L. Pachter. 2017. "Differential analysis of RNA-seq incorporating quantification uncertainty." *Nat Methods* 14 (7):687-690. doi: 10.1038/nmeth.4324.

Plehn-Dujowich, D., P. Bell, A. M. Ishov, C. Baumann, and G. G. Maul. 2000. "Non-apoptotic chromosome condensation induced by stress: delineation of interchromosomal spaces." *Chromosoma* 109 (4):266-79. doi: 10.1007/s004120000073.

Pombo, A., J. Ferreira, E. Bridge, and M. Carmo-Fonseca. 1994. "Adenovirus replication and transcription sites are spatially separated in the nucleus of infected cells." *Embo j* 13 (21):5075-85.

Pronk, R., M. H. Stuiver, and P. C. van der Vliet. 1992. "Adenovirus DNA replication: the function of the covalently bound terminal protein." *Chromosoma* 102 (1 Suppl):S39-45. doi: 10.1007/bf02451784.

Prudden, J., S. Pebernard, G. Raffa, D. A. Slavin, J. J. Perry, J. A. Tainer, C. H. McGowan, and M. N. Boddy. 2007. "SUMO-targeted ubiquitin ligases in genome stability." *Embo j* 26 (18):4089-101. doi: 10.1038/sj.emboj.7601838.

Przybylski, M., T. Dzieciatkowski, J. Borysowski, R. Miedzybrodzki, and A. Gorski. 2019. "Inhibitory Effects of Bacteriophage Preparations on Adenoviral Replication." *Intervirology* 62 (1):37-44. doi: 10.1159/000500540.

Putzer, B. M., T. Stiewe, K. Parssanedjad, S. Rega, and H. Esche. 2000. "E1A is sufficient by itself to induce apoptosis independent of p53 and other adenoviral gene products." *Cell Death Differ* 7 (2):177-88. doi: 10.1038/sj.cdd.4400618.

Puvion-Dutilleul, F., J. P. Bachellerie, N. Visa, and E. Puvion. 1994. "Rearrangements of intranuclear structures involved in RNA processing in response to adenovirus infection." *J Cell Sci* 107 (Pt 6):1457-68.

Puvion-Dutilleul, F., J. Pedron, and C. Cajean-Feroldi. 1984. "Identification of intranuclear structures containing the 72K DNA-binding protein of human adenovirus type 5." *Eur J Cell Biol* 34 (2):313-22.

Puvion-Dutilleul, F., and E. Puvion. 1990. "Replicating single-stranded adenovirus type 5 DNA molecules accumulate within well-delimited intranuclear areas of lytically infected HeLa cells." *Eur J Cell Biol* 52 (2):379-88.

Querido, E., P. Blanchette, Q. Yan, T. Kamura, M. Morrison, D. Boivin, W. G. Kaelin, R. C. Conaway, J. W. Conaway, and P. E. Branton. 2001. "Degradation of p53 by adenovirus E4orf6 and E1B55K proteins occurs via a novel mechanism involving a Cullin-containing complex." *Genes Dev* 15 (23):3104-17. doi: 10.1101/gad.926401.

Rajagopalan, S., F. Huang, and A. R. Fersht. 2011. "Single-Molecule characterization of oligomerization kinetics and equilibria of the tumor suppressor p53." *Nucleic Acids Res* 39 (6):2294-303. doi: 10.1093/nar/gkq800.

Regad, T., and M. K. Chelbi-Alix. 2001. "Role and fate of PML nuclear bodies in response to interferon and viral infections." *Oncogene* 20 (49):7274-86. doi: 10.1038/sj.onc.1204854.

Reich, N. C., P. Sarnow, E. Duprey, and A. J. Levine. 1983. "Monoclonal antibodies which recognize native and denatured forms of the adenovirus DNA-binding protein." *Virology* 128 (2):480-4. doi: 10.1016/0042-6822(83)90274-x.

Ren, J., X. Gao, C. Jin, M. Zhu, X. Wang, A. Shaw, L. Wen, X. Yao, and Y. Xue. 2009. "Systematic study of protein sumoylation: Development of a site-specific predictor of SUMOsp 2.0." *Proteomics* 9 (12):3409-3412. doi: 10.1002/pmic.200800646.

Rice, S. A., D. F. Klessig, and J. Williams. 1987. "Multiple effects of the 72-kDa, adenovirus-specified DNA binding protein on the efficiency of cellular transformation." *Virology* 156 (2):366-76. doi: 10.1016/0042-6822(87)90416-8.

Riley, D., and S. J. Flint. 1993. "RNA-binding properties of a translational activator, the adenovirus L4 100-kilodalton protein." *J Virol* 67 (6):3586-95.

Riley, T., E. Sontag, P. Chen, and A. Levine. 2008. "Transcriptional control of human p53-regulated genes." *Nat Rev Mol Cell Biol* 9 (5):402-12. doi: 10.1038/nrm2395.

Rivas, C., S. A. Aaronson, and C. Munoz-Fontela. 2010. "Dual Role of p53 in Innate Antiviral Immunity." *Viruses* 2 (1):298-313. doi: 10.3390/v2010298.

Rodrigues, S. H., N. P. Silva, L. R. Delicio, C. Granato, and L. E. Andrade. 1996. "The behavior of the coiled body in cells infected with adenovirus in vitro." *Mol Biol Rep* 23 (3-4):183-9. doi: 10.1007/bf00351167.

Rodriguez, M. S., C. Dargemont, and R. T. Hay. 2001. "SUMO-1 conjugation in vivo requires both a consensus modification motif and nuclear targeting." *J Biol Chem* 276 (16):12654-9. doi: 10.1074/jbc.M009476200.

Rodriguez, M. S., J. M. Desterro, S. Lain, C. A. Midgley, D. P. Lane, and R. T. Hay. 1999. "SUMO-1 modification activates the transcriptional response of p53." *Embo j* 18 (22):6455-61. doi: 10.1093/emboj/18.22.6455.

Roelvink, P. W., A. Lizonova, J. G. Lee, Y. Li, J. M. Bergelson, R. W. Finberg, D. E. Brough, I. Kovesdi, and T. J. Wickham. 1998. "The coxsackievirus-adenovirus receptor protein can function as a cellular attachment protein for adenovirus serotypes from subgroups A, C, D, E, and F." *J Virol* 72 (10):7909-15.

Rosa-Calatrava, M., F. Puvion-Dutilleul, P. Lutz, D. Dreyer, H. de Thé, B. Chatton, and C. Kedinger. 2003. "Adenovirus protein IX sequesters host-cell promyelocytic leukaemia protein and contributes to efficient viral proliferation." *EMBO Rep* 4 (10):969-75. doi: 10.1038/sj.embor.embor943.

Rotter, V., H. Abutbul, and A. Ben-Ze'ev. 1983. "P53 transformation-related protein accumulates in the nucleus of transformed fibroblasts in association with the chromatin and is found in the cytoplasm of non-transformed fibroblasts." *Embo j* 2 (7):1041-7.

Rowe, W. P., R. J. Huebner, L. K. Gilmore, R. H. Parrott, and T. G. Ward. 1953. "Isolation of a cytopathogenic agent from human adenoids undergoing spontaneous degeneration in tissue culture." *Proc Soc Exp Biol Med* 84 (3):570-3. doi: 10.3181/00379727-84-20714.

Russell, W. C. 2009. "Adenoviruses: update on structure and function." *J Gen Virol* 90 (Pt 1):1-20. doi: 10.1099/vir.0.003087-0.

Russell, W. C., and B. Precious. 1982. "Nucleic acid-binding properties of adenovirus structural polypeptides." *J Gen Virol* 63 (Pt 1):69-79. doi: 10.1099/0022-1317-63-1-69.

Rux, J. J., and R. M. Burnett. 2004. "Adenovirus structure." *Hum Gene Ther* 15 (12):1167-76. doi: 10.1089/hum.2004.15.1167.

Sahin, U., O. Ferhi, M. Jeanne, S. Benhenda, C. Berthier, F. Jollivet, M. Niwa-Kawakita, O. Faklaris, N. Setterblad, H. de The, and V. Lallemand-Breitenbach. 2014. "Oxidative stress-induced assembly of PML nuclear bodies controls sumoylation of partner proteins." *J Cell Biol* 204 (6):931-45. doi: 10.1083/jcb.201305148.

Sahin, U., V. Lallemand-Breitenbach, and H. de The. 2014. "PML nuclear bodies: regulation, function and therapeutic perspectives." *J Pathol* 234 (3):289-91. doi: 10.1002/path.4426.

Saitoh, H., and J. Hinchey. 2000. "Functional heterogeneity of small ubiquitin-related protein modifiers SUMO-1 versus SUMO-2/3." *J Biol Chem* 275 (9):6252-8. doi: 10.1074/jbc.275.9.6252.

Salomoni, P., and P. P. Pandolfi. 2002. "The role of PML in tumor suppression." *Cell* 108 (2):165-70. doi: 10.1016/s0092-8674(02)00626-8.

Samuels-Lev, Y., D. J. O'Connor, D. Bergamaschi, G. Trigiante, J. K. Hsieh, S. Zhong, I. Campargue, L. Naumovski, T. Crook, and X. Lu. 2001. "ASPP proteins specifically stimulate the apoptotic function of p53." *Mol Cell* 8 (4):781-94. doi: 10.1016/s1097-2765(01)00367-7.

Sarnow, P., Y. S. Ho, J. Williams, and A. J. Levine. 1982. "Adenovirus E1b-58kd tumor antigen and SV40 large tumor antigen are physically associated with the same 54 kd cellular protein in transformed cells." *Cell* 28 (2):387-94. doi: 10.1016/0092-8674(82)90356-7.

Sarnow, P., C. A. Sullivan, and A. J. Levine. 1982. "A monoclonal antibody detecting the adenovirus type 5-E1b-58Kd tumor antigen: characterization of the E1b-58Kd tumor antigen in adenovirus-infected and -transformed cells." *Virology* 120 (2):510-7. doi: 10.1016/0042-6822(82)90054-x.

Scaglioni, P. P., T. M. Yung, L. F. Cai, H. Erdjument-Bromage, A. J. Kaufman, B. Singh, J. Teruya-Feldstein, P. Tempst, and P. P. Pandolfi. 2006. "A CK2-dependent mechanism for degradation of the PML tumor suppressor." *Cell* 126 (2):269-83. doi: 10.1016/j.cell.2006.05.041.

Schilling, R., B. Weingartner, and E. L. Winnacker. 1975. "Adenovirus type 2 DNA replication. II. Termini of DNA replication." *J Virol* 16 (4):767-74.

Schmid, M., T. Speiseder, T. Dobner, and R. A. Gonzalez. 2014. "DNA virus replication compartments." *J Virol* 88 (3):1404-20. doi: 10.1128/jvi.02046-13.

Schmidt, D., and S. Muller. 2002. "Members of the PIAS family act as SUMO ligases for c-Jun and p53 and repress p53 activity." *Proc Natl Acad Sci U S A* 99 (5):2872-7. doi: 10.1073/pnas.052559499.

Schmitz, M. L., and I. Grishina. 2012. "Regulation of the tumor suppressor PML by sequential post-translational modifications." *Front Oncol* 2:204. doi: 10.3389/fonc.2012.00204.

Schreiner, S., C. Burck, M. Glass, P. Groitl, P. Wimmer, S. Kinkley, A. Mund, R. D. Everett, and T. Dobner. 2013. "Control of human adenovirus type 5 gene expression by cellular Daxx/ATRX chromatin-associated complexes." *Nucleic Acids Res* 41 (6):3532-50. doi: 10.1093/nar/gkt064.

Schreiner, S., S. Kinkley, C. Burck, A. Mund, P. Wimmer, T. Schubert, P. Groitl, H. Will, and T. Dobner. 2013. "SPOC1-mediated antiviral host cell response is antagonized early in human adenovirus type 5 infection." *PLoS Pathog* 9 (11):e1003775. doi: 10.1371/journal.ppat.1003775.

Schreiner, S., R. Martinez, P. Groitl, F. Rayne, R. Vaillant, P. Wimmer, G. Bossis, T. Sternsdorf, L. Marcinowski, Z. Ruzsics, T. Dobner, and H. Wodrich. 2012. "Transcriptional activation of the adenoviral genome is mediated by capsid protein VI." *PLoS Pathog* 8 (2):e1002549. doi: 10.1371/journal.ppat.1002549.

Schreiner, S., P. Wimmer, and T. Dobner. 2012. "Adenovirus degradation of cellular proteins." *Future Microbiol* 7 (2):211-25. doi: 10.2217/fmb.11.153.

Schreiner, S., P. Wimmer, P. Groitl, S. Y. Chen, P. Blanchette, P. E. Branton, and T. Dobner. 2011. "Adenovirus type 5 early region 1B 55K oncoprotein-dependent degradation of cellular factor Daxx is required for efficient transformation of primary rodent cells." *J Virol* 85 (17):8752-65. doi: 10.1128/jvi.00440-11.

Schreiner, S., P. Wimmer, H. Sirma, R. D. Everett, P. Blanchette, P. Groitl, and T. Dobner. 2010. "Proteasome-dependent degradation of Daxx by the viral E1B-55K protein in human adenovirus-infected cells." *J Virol* 84 (14):7029-38. doi: 10.1128/jvi.00074-10.

Seeler, J. S., and A. Dejean. 2003. "Nuclear and unclear functions of SUMO." *Nat Rev Mol Cell Biol* 4 (9):690-9. doi: 10.1038/nrm1200.

Seeler, J. S., A. Marchio, R. Losson, J. M. Desterro, R. T. Hay, P. Chambon, and A. Dejean. 2001. "Common properties of nuclear body protein SP100 and TIF1alpha chromatin factor: role of SUMO modification." *Mol Cell Biol* 21 (10):3314-24. doi: 10.1128/mcb.21.10.3314-3324.2001.

Seeler, J. S., A. Marchio, D. Sitterlin, C. Transy, and A. Dejean. 1998. "Interaction of SP100 with HP1 proteins: a link between the promyelocytic leukemia-associated nuclear bodies and the chromatin compartment." *Proc Natl Acad Sci U S A* 95 (13):7316-21. doi: 10.1073/pnas.95.13.7316.

Sha, Z., T. Blyszcz, R. Gonzalez-Prieto, A. C. O. Vertegaal, and A. L. Goldberg. 2019. "Inhibiting ubiquitination causes an accumulation of SUMOylated newly synthesized nuclear proteins at PML bodies." *J Biol Chem* 294 (42):15218-15234. doi: 10.1074/jbc.RA119.009147.

Shauer, A., I. Gotsman, A. Keren, D. R. Zwas, Y. Hellman, R. Durst, and D. Admon. 2013. "Acute viral myocarditis: current concepts in diagnosis and treatment." *Isr Med Assoc J* 15 (3):180-5.

Shaulsky, G., A. Ben-Ze'ev, and V. Rotter. 1990. "Subcellular distribution of the p53 protein during the cell cycle of Balb/c 3T3 cells." *Oncogene* 5 (11):1707-11.

Shen, T. H., H. K. Lin, P. P. Scaglioni, T. M. Yung, and P. P. Pandolfi. 2006. "The Mechanisms of PML-Nuclear Body Formation." *Mol Cell* 24 (5):805. doi: 10.1016/j.molcel.2006.11.010.

Shen, Z., P. E. Pardington-Purtymun, J. C. Comeaux, R. K. Moyzis, and D. J. Chen. 1996. "UBL1, a human ubiquitin-like protein associating with human RAD51/RAD52 proteins." *Genomics* 36 (2):271-9. doi: 10.1006/geno.1996.0462.

Shenk, T.E. 2001. "Adenoviridae: the viruses and their replication." In *Fundamental virology.*, 1053-1088.

Shi, D., and W. Gu. 2012. "Dual Roles of MDM2 in the Regulation of p53: Ubiquitination Dependent and Ubiquitination Independent Mechanisms of MDM2 Repression of p53 Activity." *Genes Cancer* 3 (3-4):240-8. doi: 10.1177/1947601912455199.

Shi, X., I. Kachirskaia, H. Yamaguchi, L. E. West, H. Wen, E. W. Wang, S. Dutta, E. Appella, and O. Gozani. 2007. "Modulation of p53 function by SET8-mediated methylation at lysine 382." *Mol Cell* 27 (4):636-46. doi: 10.1016/j.molcel.2007.07.012.

Shieh, S. Y., J. Ahn, K. Tamai, Y. Taya, and C. Prives. 2000. "The human homologs of checkpoint kinases Chk1 and Cds1 (Chk2) phosphorylate p53 at multiple DNA damage-inducible sites." *Genes Dev* 14 (3):289-300.

Shishido-Hara, Y., K. Higuchi, S. Ohara, C. Duyckaerts, J. J. Hauw, and T. Uchihara. 2008. "Promyelocytic leukemia nuclear bodies provide a scaffold for human polyomavirus JC replication and are disrupted after development of viral inclusions in progressive multifocal leukoencephalopathy." *J Neuropathol Exp Neurol* 67 (4):299-308. doi: 10.1097/NEN.0b013e31816a1dd3.

Sloan, E., M. H. Tatham, M. Groslambert, M. Glass, A. Orr, R. T. Hay, and R. D. Everett. 2015. "Analysis of the SUMO2 Proteome during HSV-1 Infection." *PLoS Pathog* 11 (7):e1005059. doi: 10.1371/journal.ppat.1005059.

Smith, A. E., R. Smith, and E. Paucha. 1979. "Characterization of different tumor antigens present in cells transformed by simian virus 40." *Cell* 18 (2):335-46. doi: 10.1016/0092-8674(79)90053-9.

Sohn, S. Y., R. G. Bridges, and P. Hearing. 2015. "Proteomic analysis of ubiquitin-like posttranslational modifications induced by the adenovirus E4-ORF3 protein." *J Virol* 89 (3):1744-55. doi: 10.1128/jvi.02892-14.

Sohn, S. Y., and P. Hearing. 2011. "Adenovirus sequesters phosphorylated STAT1 at viral replication centers and inhibits STAT dephosphorylation." *J Virol* 85 (15):7555-62. doi: 10.1128/jvi.00513-11.

Sohn, S. Y., and P. Hearing. 2012. "Adenovirus regulates sumoylation of Mre11-Rad50-Nbs1 components through a paralog-specific mechanism." *J Virol* 86 (18):9656-65. doi: 10.1128/jvi.01273-12.

Sohn, S. Y., and P. Hearing. 2016a. "The adenovirus E4-ORF3 protein functions as a SUMO E3 ligase for TIF-1gamma sumoylation and poly-SUMO chain elongation." *Proc Natl Acad Sci U S A* 113 (24):6725-30. doi: 10.1073/pnas.1603872113.

Sohn, S. Y., and P. Hearing. 2016b. "Adenovirus Early Proteins and Host Sumoylation." *mBio* 7 (5). doi: 10.1128/mBio.01154-16.

Sohn, S. Y., and P. Hearing. 2019. "Mechanism of Adenovirus E4-ORF3-Mediated SUMO Modifications." *mBio* 10 (1). doi: 10.1128/mBio.00022-19.

Soria, C., F. E. Estermann, K. C. Espantman, and C. C. O'Shea. 2010. "Heterochromatin silencing of p53 target genes by a small viral protein." *Nature* 466 (7310):1076-81. doi: 10.1038/nature09307.

Sourvinos, G., and R. D. Everett. 2002. "Visualization of parental HSV-1 genomes and replication compartments in association with ND10 in live infected cells." *Embo j* 21 (18):4989-97. doi: 10.1093/emboj/cdf458.

Spector, D. L., and A. I. Lamond. 2011. "Nuclear speckles." *Cold Spring Harb Perspect Biol* 3 (2). doi: 10.1101/cshperspect.a000646.

Speir, E., R. Modali, E. S. Huang, M. B. Leon, F. Shawl, T. Finkel, and S. E. Epstein. 1994. "Potential role of human cytomegalovirus and p53 interaction in coronary restenosis." *Science* 265 (5170):391-4. doi: 10.1126/science.8023160.

Speiseder, T., H. Hofmann-Sieber, E. Rodríguez, A. Schellenberg, N. Akyüz, J. Dierlamm, T. Spruss, C. Lange, and T. Dobner. 2017. "Efficient Transformation of Primary Human Mesenchymal Stromal Cells by Adenovirus Early Region 1 Oncogenes." *J Virol* 91 (1). doi: 10.1128/jvi.01782-16.

St George, J. A. 2003. "Gene therapy progress and prospects: adenoviral vectors." *Gene Ther* 10 (14):1135-41. doi: 10.1038/sj.gt.3302071.

Stadler, M., M. K. Chelbi-Alix, M. H. Koken, L. Venturini, C. Lee, A. Saib, F. Quignon, L. Pelicano, M. C. Guillemin, C. Schindler, and et al. 1995. "Transcriptional induction of the PML growth suppressor gene by interferons is mediated through an ISRE and a GAS element." *Oncogene* 11 (12):2565-73.

Steegenga, W. T., A. Shvarts, N. Riteco, J. L. Bos, and A. G. Jochemsen. 1999. "Distinct regulation of p53 and p73 activity by adenovirus E1A, E1B, and E4orf6 proteins." *Mol Cell Biol* 19 (5):3885-94. doi: 10.1128/mcb.19.5.3885.

Stenger, J. E., P. Tegtmeyer, G. A. Mayr, M. Reed, Y. Wang, P. Wang, P. V. Hough, and I. A. Mastrangelo. 1994. "p53 oligomerization and DNA looping are linked with transcriptional activation." *Embo j* 13 (24):6011-20.

Sternsdorf, T., K. Jensen, B. Reich, and H. Will. 1999. "The nuclear dot protein sp100, characterization of domains necessary for dimerization, subcellular localization, and modification by small ubiquitin-like modifiers." *J Biol Chem* 274 (18):12555-66. doi: 10.1074/jbc.274.18.12555.

Sternsdorf, T., K. Jensen, and H. Will. 1997. "Evidence for covalent modification of the nuclear dot-associated proteins PML and Sp100 by PIC1/SUMO-1." *J Cell Biol* 139 (7):1621-34. doi: 10.1083/jcb.139.7.1621.

Stewart, P. L., C. Y. Chiu, S. Huang, T. Muir, Y. Zhao, B. Chait, P. Mathias, and G. R. Nemerow. 1997. "Cryo-EM visualization of an exposed RGD epitope on adenovirus that escapes antibody neutralization." *Embo j* 16 (6):1189-98. doi: 10.1093/emboj/16.6.1189.

Stewart, P. L., S. D. Fuller, and R. M. Burnett. 1993. "Difference imaging of adenovirus: bridging the resolution gap between X-ray crystallography and electron microscopy." *Embo j* 12 (7):2589-99.

Stindt, M. H., S. Carter, A. M. Vigneron, K. M. Ryan, and K. H. Vousden. 2011. "MDM2 promotes SUMO-2/3 modification of p53 to modulate transcriptional activity." *Cell Cycle* 10 (18):3176-88. doi: 10.4161/cc.10.18.17436.

Stommel, J. M., N. D. Marchenko, G. S. Jimenez, U. M. Moll, T. J. Hope, and G. M. Wahl. 1999. "A leucine-rich nuclear export signal in the p53 tetramerization domain: regulation of subcellular localization and p53 activity by NES masking." *Embo j* 18 (6):1660-72. doi: 10.1093/emboj/18.6.1660.

Stracker, T. H., C. T. Carson, and M. D. Weitzman. 2002. "Adenovirus oncoproteins inactivate the Mre11-Rad50-NBS1 DNA repair complex." *Nature* 418 (6895):348-52. doi: 10.1038/nature00863.

Stracker, T. H., D. V. Lee, C. T. Carson, F. D. Araujo, D. A. Ornelles, and M. D. Weitzman. 2005. "Serotype-specific reorganization of the Mre11 complex by adenoviral E4orf3 proteins." *J Virol* 79 (11):6664-73. doi: 10.1128/jvi.79.11.6664-6673.2005.

Stubbe, M., J. Mai, C. Paulus, H. C. Stubbe, J. Berscheminski, M. Karimi, S. Hofmann, E. Weber, K. Hadian, R. Hay, P. Groitl, M. Nevels, T. Dobner, and S. Schreiner. 2020. "Viral DNA Binding Protein SUMOylation Promotes PML Nuclear Body Localization Next to Viral Replication Centers." *mBio* 11 (2). doi: 10.1128/mBio.00049-20.

Stuiver, M. H., and P. C. van der Vliet. 1990. "Adenovirus DNA-binding protein forms a multimeric protein complex with double-stranded DNA and enhances binding of nuclear factor I." *J Virol* 64 (1):379-86.

Stuurman, N., A. de Graaf, A. Floore, A. Josso, B. Humbel, L. de Jong, and R. van Driel. 1992. "A monoclonal antibody recognizing nuclear matrix-associated nuclear bodies." *J Cell Sci* 101 (Pt 4):773-84.

Sugawara, K., Z. Gilead, W. S. Wold, and M. Green. 1977. "Immunofluorescence study of the adenovirus type 2 single-stranded DNA binding protein in infected and transformed cells." *J Virol* 22 (2):527-39.

Sullivan, K. D., M. D. Galbraith, Z. Andrysik, and J. M. Espinosa. 2018. "Mechanisms of transcriptional regulation by p53." *Cell Death Differ* 25 (1):133-143. doi: 10.1038/cdd.2017.174.

Sun, H., J. D. Leverson, and T. Hunter. 2007. "Conserved function of RNF4 family proteins in eukaryotes: targeting a ubiquitin ligase to SUMOylated proteins." *Embo j* 26 (18):4102-12. doi: 10.1038/sj.emboj.7601839.

Szostecki, C., H. H. Guldner, H. J. Netter, and H. Will. 1990. "Isolation and characterization of cDNA encoding a human nuclear antigen predominantly recognized by autoantibodies from patients with primary biliary cirrhosis." *J Immunol* 145 (12):4338-47.

Szostecki, C., H. Krippner, E. Penner, and F. A. Bautz. 1987. "Autoimmune sera recognize a 100 kD nuclear protein antigen (sp-100)." *Clin Exp Immunol* 68 (1):108-16.

Szostecki, C., H. Will, H. J. Netter, and H. H. Guldner. 1992. "Autoantibodies to the nuclear Sp100 protein in primary biliary cirrhosis and associated diseases: epitope specificity and immunoglobulin class distribution." *Scand J Immunol* 36 (4):555-64. doi: 10.1111/j.1365-3083.1992.tb03224.x.

Tamanoi, F., and B. W. Stillman. 1982. "Function of adenovirus terminal protein in the initiation of DNA replication." *Proc Natl Acad Sci U S A* 79 (7):2221-5. doi: 10.1073/pnas.79.7.2221.

Tang, Q., P. Bell, P. Tegtmeyer, and G. G. Maul. 2000. "Replication but not transcription of simian virus 40 DNA is dependent on nuclear domain 10." *J Virol* 74 (20):9694-700. doi: 10.1128/jvi.74.20.9694-9700.2000.

Tang, Y., J. Luo, W. Zhang, and W. Gu. 2006. "Tip60-dependent acetylation of p53 modulates the decision between cell-cycle arrest and apoptosis." *Mol Cell* 24 (6):827-39. doi: 10.1016/j.molcel.2006.11.021.

Tang, Z., W. Y. Chen, M. Shimada, U. T. Nguyen, J. Kim, X. J. Sun, T. Sengoku, R. K. McGinty, J. P. Fernandez, T. W. Muir, and R. G. Roeder. 2013. "SET1 and p300 act synergistically, through coupled histone modifications, in transcriptional activation by p53." *Cell* 154 (2):297-310. doi: 10.1016/j.cell.2013.06.027.

Tatham, M. H., M. C. Geoffroy, L. Shen, A. Plechanovova, N. Hattersley, E. G. Jaffray, J. J. Palvimo, and R. T. Hay. 2008. "RNF4 is a poly-SUMO-specific E3 ubiquitin ligase required for arsenic-induced PML degradation." *Nat Cell Biol* 10 (5):538-46. doi: 10.1038/ncb1716.

Tatham, M. H., E. Jaffray, O. A. Vaughan, J. M. Desterro, C. H. Botting, J. H. Naismith, and R. T. Hay. 2001. "Polymeric chains of SUMO-2 and SUMO-3 are conjugated to protein substrates by SAE1/SAE2 and Ubc9." *J Biol Chem* 276 (38):35368-74. doi: 10.1074/jbc.M104214200.

Tatsis, N., and H. C. Ertl. 2004. "Adenoviruses as vaccine vectors." *Mol Ther* 10 (4):616-29. doi: 10.1016/j.ymthe.2004.07.013.

Tauber, B., and T. Dobner. 2001. "Molecular regulation and biological function of adenovirus early genes: the E4 ORFs." *Gene* 278 (1-2):1-23. doi: 10.1016/s0378-1119(01)00722-3.

Tavalai, N., and T. Stamminger. 2008. "New insights into the role of the subnuclear structure ND10 for viral infection." *Biochim Biophys Acta* 1783 (11):2207-21. doi: 10.1016/j.bbamcr.2008.08.004.

Temperley, S. M., and R. T. Hay. 1991. "Replication of adenovirus type 4 DNA by a purified fraction from infected cells." *Nucleic Acids Res* 19 (12):3243-9. doi: 10.1093/nar/19.12.3243.

Teodoro, J. G., and P. E. Branton. 1997. "Regulation of p53-dependent apoptosis, transcriptional repression, and cell transformation by phosphorylation of the 55-kilodalton E1B protein of human adenovirus type 5." *J Virol* 71 (5):3620-7.

Teufel, D. P., M. Bycroft, and A. R. Fersht. 2009. "Regulation by phosphorylation of the relative affinities of the N-terminal transactivation domains of p53 for p300 domains and Mdm2." *Oncogene* 28 (20):2112-8. doi: 10.1038/onc.2009.71.

Thut, C. J., J. L. Chen, R. Klemm, and R. Tjian. 1995. "p53 transcriptional activation mediated by coactivators TAFII40 and TAFII60." *Science* 267 (5194):100-4. doi: 10.1126/science.7809597.

Tollefson, A. E., A. Scaria, T. W. Hermiston, J. S. Ryerse, L. J. Wold, and W. S. Wold. 1996. "The adenovirus death protein (E3-11.6K) is required at very late stages of infection for efficient cell lysis and release of adenovirus from infected cells." *J Virol* 70 (4):2296-306.

Tormanen, H., E. Backstrom, A. Carlsson, and G. Akusjarvi. 2006. "L4-33K, an adenovirus-encoded alternative RNA splicing factor." *J Biol Chem* 281 (48):36510-7. doi: 10.1074/jbc.M607601200.

Treacy, A., M. J. Carr, L. Dunford, G. Palacios, G. A. Cannon, A. O'Grady, J. Moran, J. Hassan, A. Loy, J. Connell, D. Devaney, P. Kelehan, and W. W. Hall. 2010. "First report of sudden death due to myocarditis caused by adenovirus serotype 3." *J Clin Microbiol* 48 (2):642-5. doi: 10.1128/jcm.00815-09.

Trentin, J. J., Y. Yabe, and G. Taylor. 1962. "The quest for human cancer viruses." *Science* 137 (3533):835-41. doi: 10.1126/science.137.3533.835.

Tsernoglou, D., A. Tsugita, A. D. Tucker, and P. C. van der Vliet. 1985. "Characterization of the chymotryptic core of the adenovirus DNA-binding protein." *FEBS Lett* 188 (2):248-52. doi: 10.1016/0014-5793(85)80381-1.

Tucker, P. A., D. Tsernoglou, A. D. Tucker, F. E. Coenjaerts, H. Leenders, and P. C. van der Vliet. 1994. "Crystal structure of the adenovirus DNA binding protein reveals a hook-on model for cooperative DNA binding." *Embo j* 13 (13):2994-3002.

Turnell, A. S., and R. J. Grand. 2012. "DNA viruses and the cellular DNA-damage response." *J Gen Virol* 93 (Pt 10):2076-2097. doi: 10.1099/vir.0.044412-0.

van Amerongen, H., R. van Grondelle, and P. C. van der Vliet. 1987. "Interaction between adenovirus DNA-binding protein and single-stranded polynucleotides studied by circular dichroism and ultraviolet absorption." *Biochemistry* 26 (15):4646-52. doi: 10.1021/bi00389a009.

van Breukelen, B., A. B. Brenkman, P. E. Holthuizen, and P. C. van der Vliet. 2003. "Adenovirus type 5 DNA binding protein stimulates binding of DNA polymerase to the replication origin." *J Virol* 77 (2):915-22. doi: 10.1128/jvi.77.2.915-922.2003.

van Breukelen, B., P. N. Kanellopoulos, P. A. Tucker, and P. C. van der Vliet. 2000. "The formation of a flexible DNA-binding protein chain is required for efficient DNA unwinding and adenovirus DNA chain elongation." *J Biol Chem* 275 (52):40897-903. doi: 10.1074/jbc.M005745200.

Van Damme, E., K. Laukens, T. H. Dang, and X. Van Ostade. 2010. "A manually curated network of the PML nuclear body interactome reveals an important role for PML-NBs in SUMOylation dynamics." *Int J Biol Sci* 6 (1):51-67. doi: 10.7150/ijbs.6.51.

van der Vliet, P. C., and A. J. Levine. 1973. "DNA-binding proteins specific for cells infected by adenovirus." *Nat New Biol* 246 (154):170-4. doi: 10.1038/newbio246170a0.

Varga, M. J., C. Weibull, and E. Everitt. 1991. "Infectious entry pathway of adenovirus type 2." *J Virol* 65 (11):6061-70.

Velicer, L. F., and H. S. Ginsberg. 1970. "Synthesis, transport, and morphogenesis of type adenovirus capsid proteins." *J Virol* 5 (3):338-52.

Vellinga, J., S. Van der Heijdt, and R. C. Hoeben. 2005. "The adenovirus capsid: major progress in minor proteins." *J Gen Virol* 86 (Pt 6):1581-8. doi: 10.1099/vir.0.80877-0.

Vertegaal, A. C., S. C. Ogg, E. Jaffray, M. S. Rodriguez, R. T. Hay, J. S. Andersen, M. Mann, and A. I. Lamond. 2004. "A proteomic study of SUMO-2 target proteins." *J Biol Chem* 279 (32):33791-8. doi: 10.1074/jbc.M404201200.

Vink, E. I., M. A. Yondola, K. Wu, and P. Hearing. 2012. "Adenovirus E4-ORF3-dependent relocalization of TIF1α and TIF1γ relies on access to the Coiled-Coil motif." *Virology* 422 (2):317-25. doi: 10.1016/j.virol.2011.10.033.

Vink, E. I., Y. Zheng, R. Yeasmin, T. Stamminger, L. T. Krug, and P. Hearing. 2015. "Impact of Adenovirus E4-ORF3 Oligomerization and Protein Localization on Cellular Gene Expression." *Viruses* 7 (5):2428-49. doi: 10.3390/v7052428.

Voelkerding, K., and D. F. Klessig. 1986. "Identification of two nuclear subclasses of the adenovirus type 5-encoded DNA-binding protein." *J Virol* 60 (2):353-62.

Vousden, K. H., and C. Prives. 2009. "Blinded by the Light: The Growing Complexity of p53." *Cell* 137 (3):413-31. doi: 10.1016/j.cell.2009.04.037.

Wang, B., T. H. Lam, M. K. Soh, Z. Ye, J. Chen, and E. C. Ren. 2018. "Influenza A Virus Facilitates Its Infectivity by Activating p53 to Inhibit the Expression of Interferon-Induced Transmembrane Proteins." *Front Immunol* 9:1193. doi: 10.3389/fimmu.2018.01193.

Wang, L., X. M. Ren, J. J. Xing, and A. C. Zheng. 2010. "The nucleolus and viral infection." *Virol Sin* 25 (3):151-7. doi: 10.1007/s12250-010-3093-5.

Wang, Y., and M. Dasso. 2009. "SUMOylation and deSUMOylation at a glance." *J Cell Sci* 122 (Pt 23):4249-52. doi: 10.1242/jcs.050542.

Webster, A., I. R. Leith, J. Nicholson, J. Hounsell, and R. T. Hay. 1997. "Role of preterminal protein processing in adenovirus replication." *J Virol* 71 (9):6381-9. doi: 10.1128/jvi.71.9.6381-6389.1997.

Webster, A., S. Russell, P. Talbot, W. C. Russell, and G. D. Kemp. 1989. "Characterization of the adenovirus proteinase: substrate specificity." *J Gen Virol* 70 (Pt 12):3225-34. doi: 10.1099/0022-1317-70-12-3225.

Weger, S., E. Hammer, and R. Heilbronn. 2005. "Topors acts as a SUMO-1 E3 ligase for p53 in vitro and in vivo." *FEBS Lett* 579 (22):5007-12. doi: 10.1016/j.febslet.2005.07.088.

Weinberg, R. L., D. B. Veprintsev, and A. R. Fersht. 2004. "Cooperative binding of tetrameric p53 to DNA." *J Mol Biol* 341 (5):1145-59. doi: 10.1016/j.jmb.2004.06.071.

Weinmann, R., H. J. Raskas, and R. G. Roeder. 1974. "Role of DNA-dependent RNA polymerases II and III in transcription of the adenovirus genome late in productive infection." *Proc Natl Acad Sci U S A* 71 (9):3426-39. doi: 10.1073/pnas.71.9.3426.

Weis, K., S. Rambaud, C. Lavau, J. Jansen, T. Carvalho, M. Carmo-Fonseca, A. Lamond, and A. Dejean. 1994. "Retinoic acid regulates aberrant nuclear localization of PML-RAR alpha in acute promyelocytic leukemia cells." *Cell* 76 (2):345-56. doi: 10.1016/0092-8674(94)90341-7.

Weisshaar, S. R., K. Keusekotten, A. Krause, C. Horst, H. M. Springer, K. Gottsche, R. J. Dohmen, and G. J. Praefcke. 2008. "Arsenic trioxide stimulates SUMO-2/3 modification leading to RNF4-dependent proteolytic targeting of PML." *FEBS Lett* 582 (21-22):3174-8. doi: 10.1016/j.febslet.2008.08.008.

Wells, M., H. Tidow, T. J. Rutherford, P. Markwick, M. R. Jensen, E. Mylonas, D. I. Svergun, M. Blackledge, and A. R. Fersht. 2008. "Structure of tumor suppressor p53 and its intrinsically disordered N-terminal transactivation domain." *Proc Natl Acad Sci U S A* 105 (15):5762-7. doi: 10.1073/pnas.0801353105.

Wesierska-Gadek, J. 2018. "Targeting p53 as a promising therapeutic option for cancer by re-activating the wt or mutant p53's tumor suppression." *Future Med Chem* 10 (7):755-777. doi: 10.4155/fmc-2017-0175.

Whyte, P., K. J. Buchkovich, J. M. Horowitz, S. H. Friend, M. Raybuck, R. A. Weinberg, and E. Harlow. 1988. "Association between an oncogene and an anti-oncogene: the adenovirus E1A proteins bind to the retinoblastoma gene product." *Nature* 334 (6178):124-9. doi: 10.1038/334124a0.

Wickham, T. J., E. J. Filardo, D. A. Cheresh, and G. R. Nemerow. 1994. "Integrin alpha v beta 5 selectively promotes adenovirus mediated cell membrane permeabilization." *J Cell Biol* 127 (1):257-64. doi: 10.1083/jcb.127.1.257.

Wiethoff, C. M., H. Wodrich, L. Gerace, and G. R. Nemerow. 2005. "Adenovirus protein VI mediates membrane disruption following capsid disassembly." *J Virol* 79 (4):1992-2000. doi: 10.1128/jvi.79.4.1992-2000.2005.

Wilkinson, K. A., and J. M. Henley. 2010. "Mechanisms, regulation and consequences of protein SUMOylation." *Biochem J* 428 (2):133-45. doi: 10.1042/bj20100158.

Wimmer, P., J. Berscheminski, P. Blanchette, P. Groitl, P. E. Branton, R. T. Hay, T. Dobner, and S. Schreiner. 2016. "PML isoforms IV and V contribute to adenovirus-mediated oncogenic transformation by functionally inhibiting the tumor-suppressor p53." *Oncogene* 35 (1):69-82. doi: 10.1038/onc.2015.63.

Wimmer, P., P. Blanchette, S. Schreiner, W. Ching, P. Groitl, J. Berscheminski, P. E. Branton, H. Will, and T. Dobner. 2013. "Cross-talk between phosphorylation and SUMOylation regulates transforming activities of an adenoviral oncoprotein." *Oncogene* 32 (13):1626-37. doi: 10.1038/onc.2012.187.

Wimmer, P., and S. Schreiner. 2015. "Viral Mimicry to Usurp Ubiquitin and SUMO Host Pathways." *Viruses* 7 (9):4854-72. doi: 10.3390/v7092849.

Wimmer, P., S. Schreiner, R. D. Everett, H. Sirma, P. Groitl, and T. Dobner. 2010. "SUMO modification of E1B-55K oncoprotein regulates isoform-specific binding to the tumour suppressor protein PML." *Oncogene* 29 (40):5511-22. doi: 10.1038/onc.2010.284.

Windheim, M., A. Hilgendorf, and H. G. Burgert. 2004. "Immune evasion by adenovirus E3 proteins: exploitation of intracellular trafficking pathways." *Curr Top Microbiol Immunol* 273:29-85. doi: 10.1007/978-3-662-05599-1_2.

Wold, W., M. Horwitz. 2007. "Adenoviruses." In *Fields Virology*.

Wu, E., L. Pache, D. J. Von Seggern, T. M. Mullen, Y. Mikyas, P. L. Stewart, and G. R. Nemerow. 2003. "Flexibility of the adenovirus fiber is required for efficient receptor interaction." *J Virol* 77 (13):7225-35. doi: 10.1128/jvi.77.13.7225-7235.2003.

Wu, K., D. Guimet, and P. Hearing. 2013. "The adenovirus L4-33K protein regulates both late gene expression patterns and viral DNA packaging." *J Virol* 87 (12):6739-47. doi: 10.1128/jvi.00652-13.

Wu, L., and A. J. Levine. 1997. "Differential regulation of the p21/WAF-1 and mdm2 genes after high-dose UV irradiation: p53-dependent and p53-independent regulation of the mdm2 gene." *Mol Med* 3 (7):441-51.

Xie, Y., O. Kerscher, M. B. Kroetz, H. F. McConchie, P. Sung, and M. Hochstrasser. 2007. "The yeast Hex3.Slx8 heterodimer is a ubiquitin ligase stimulated by substrate sumoylation." *J Biol Chem* 282 (47):34176-84. doi: 10.1074/jbc.M706025200.

Yanagawa-Matsuda, Aya, Yohei Mikawa, Umma Habiba, Tetsuya Kitamura, Motoaki Yasuda, Mohammad Towfik-Alam, Yoshimasa Kitagawa, Kazuyuki Minowa, Masanobu Shindoh, and Fumihiro Higashino. 2019. "Oncolytic potential of an E4-deficient adenovirus that can recognize the stabilization of AU-rich element containing mRNA in cancer cells." *Oncol Rep* 41 (2):954-960. doi: 10.3892/or.2018.6865.

Yates, A. D., P. Achuthan, W. Akanni, J. Allen, J. Allen, J. Alvarez-Jarreta, M. R. Amode, I. M. Armean, A. G. Azov, R. Bennett, J. Bhai, K. Billis, S. Boddu, J. C. Marugán, C. Cummins, C. Davidson, K. Dodiya, R. Fatima, A. Gall, C. G. Giron, L. Gil, T. Grego, L. Haggerty, E. Haskell, T. Hourlier, O. G. Izuogu, S. H. Janacek, T. Juettemann, M. Kay, I. Lavidas, T. Le, D. Lemos, J. G. Martinez, T. Maurel, M. McDowall, A. McMahon, S. Mohanan, B. Moore, M. Nuhn, D. N. Oheh, A. Parker, A. Parton, M. Patricio, M. P. Sakthivel, A. I. Abdul Salam, B. M. Schmitt, H. Schuilenburg, D. Sheppard, M. Sycheva, M. Szuba, K.

Taylor, A. Thormann, G. Threadgold, A. Vullo, B. Walts, A. Winterbottom, A. Zadissa, M. Chakiachvili, B. Flint, A. Frankish, S. E. Hunt, I. Isley G, M. Kostadima, N. Langridge, J. E. Loveland, F. J. Martin, J. Morales, J. M. Mudge, M. Muffato, E. Perry, M. Ruffier, S. J. Trevanion, F. Cunningham, K. L. Howe, D. R. Zerbino, and P. Flicek. 2020. "Ensembl 2020." *Nucleic Acids Res* 48 (D1):D682-d688. doi: 10.1093/nar/gkz966.

Yew, P. R., and A. J. Berk. 1992. "Inhibition of p53 transactivation required for transformation by adenovirus early 1B protein." *Nature* 357 (6373):82-5. doi: 10.1038/357082a0.

Yondola, M. A., and P. Hearing. 2007. "The adenovirus E4 ORF3 protein binds and reorganizes the TRIM family member transcriptional intermediary factor 1 alpha." *J Virol* 81 (8):4264-71. doi: 10.1128/jvi.02629-06.

Yoshitomi, H., N. Sera, G. Gonzalez, N. Hanaoka, and T. Fujimoto. 2017. "First isolation of a new type of human adenovirus (genotype 79), species Human mastadenovirus B (B2) from sewage water in Japan." *J Med Virol* 89 (7):1192-1200. doi: 10.1002/jmv.24749.

Young, M. D., M. J. Wakefield, G. K. Smyth, and A. Oshlack. 2010. "Gene ontology analysis for RNA-seq: accounting for selection bias." *Genome Biol* 11 (2):R14. doi: 10.1186/gb-2010-11-2-r14.

Yousef, A. F., G. J. Fonseca, P. Pelka, J. N. Ablack, C. Walsh, F. A. Dick, D. P. Bazett-Jones, G. S. Shaw, and J. S. Mymryk. 2010. "Identification of a molecular recognition feature in the E1A oncoprotein that binds the SUMO conjugase UBC9 and likely interferes with polySUMOylation." *Oncogene* 29 (33):4693-704. doi: 10.1038/onc.2010.226.

Yu, X., S. L. Harris, and A. J. Levine. 2006. "The regulation of exosome secretion: a novel function of the p53 protein." *Cancer Res* 66 (9):4795-801. doi: 10.1158/0008-5472.Can-05-4579.

Zhang, W., J. A. Low, J. B. Christensen, and M. J. Imperiale. 2001. "Role for the adenovirus IVa2 protein in packaging of viral DNA." *J Virol* 75 (21):10446-54. doi: 10.1128/jvi.75.21.10446-10454.2001.

Zhang, X., A. S. Turnell, C. Gorbea, J. S. Mymryk, P. H. Gallimore, and R. J. Grand. 2004. "The targeting of the proteasomal regulatory subunit S2 by adenovirus E1A causes inhibition of proteasomal activity and increased p53 expression." *J Biol Chem* 279 (24):25122-33. doi: 10.1074/jbc.M403287200.

Zhao, Q., Y. Xie, Y. Zheng, S. Jiang, W. Liu, W. Mu, Z. Liu, Y. Zhao, Y. Xue, and J. Ren. 2014. "GPS-SUMO: a tool for the prediction of sumoylation sites and SUMO-interaction motifs." *Nucleic Acids Res* 42 (Web Server issue):W325-30. doi: 10.1093/nar/gku383.

Zhao, Y., S. W. Kwon, A. Anselmo, K. Kaur, and M. A. White. 2004. "Broad spectrum identification of cellular small ubiquitin-related modifier (SUMO) substrate proteins." *J Biol Chem* 279 (20):20999-1002. doi: 10.1074/jbc.M401541200.

Zhong, S., S. Muller, S. Ronchetti, P. S. Freemont, A. Dejean, and P. P. Pandolfi. 2000. "Role of SUMO-1-modified PML in nuclear body formation." *Blood* 95 (9):2748-52.

Zhu, J. Y., M. Abate, P. W. Rice, and C. N. Cole. 1991. "The ability of simian virus 40 large T antigen to immortalize primary mouse embryo fibroblasts cosegregates with its ability to bind to p53." *J Virol* 65 (12):6872-80. doi: 10.1128/jvi.65.12.6872-6880.1991.

Zijderveld, D. C., M. H. Stuiver, and P. C. van der Vliet. 1993. "The adenovirus DNA binding protein enhances intermolecular DNA renaturation but inhibits intramolecular DNA renaturation." *Nucleic Acids Res* 21 (11):2591-8. doi: 10.1093/nar/21.11.2591.

7 Addendum

7.1 Abbreviations

µg	Microgram
µl	Microliter
aa	Amino acid
Ads	Adenoviruses
AIDS	Acquired immune deficiency syndrome
APS	Ammonium persulfate
ATP	Adenosine triphosphate
ATM	Ataxia telangiectasia mutated protein
ASPP	Apoptosis-stimulating of p53 protein
Bax	Bcl-2-like protein x
Bak	Bcl-2 homologous antagonist/killer
Bcl-2	B-cell lymphoma 2
BLM	Bloom Helicase
bp	Base pair
BSA	Bovine serum albumin
CAR	Coxsackievirus-adenovirus receptor
CB	Cajal bodies
CBP	CREB-binding protein
CDK	Cyclin-dependent kinase
Chk	Checkpoint kinase
CK2	Casein Kinase 2
CMV	Cytomegalovirus
DAPI	4′,6-diamidino-2-phenylindole
Daxx	Death domain associated protein 6
DBD	DNA binding domain
DBP	DNA-binding protein
DDR	DNA damage response
DMEM	Dulbecco's Modified Eagle Medium

DMSO	Dimethyl sulfoxide
DNA	Desoxyribonucleic acid
dNTP	Desoxyribonucleoside-5'-Triphosphate
ds	Double-stranded
DTT	Dithiotreithol
E.coli	*Escherichia coli*
ECL	Enhanced Chemiluminescence
EDTA	Ethylenediaminetetraacetic acid
EtOH	Ethanol
FBS	Fetal bovine serum
FFU	Fluorescent forming units
fwd	Forward
h	Hours
H1299	Human non-small cell lung carcinoma cell line
HAdV	Human Adenovirus
HAT	Histone acetyltransferase
HCMV	Human cytomegalovirus
HDAC	Histone deacetylase complex
HEK	Human embryonic kidney
HeLa	Human cervical carcinoma cell line
HepaRG	Human hepatic progenitor cell line
HMG	High Mobility Group
h p.i.	Hours post infection
HRP	Horse-radish peroxidase
HSR	Homogenously stained region
HSV-1	Herpes simplex virus 1
HP1	Heterochromatin protein 1
HPV	Human papillomavirus
HRP	Horseradish peroxidase
ICP0	Infected Cell Polypeptide 0 protein
IG	Interchromatin granules

IP	Immunoprecipitation
ITR	Inverted terminal repeats
K	Lysine
KAP1	KRAB-associated protein 1
kb	Kilobase
kbp	Kilobase pairs
kDa	Kilodalton
LB	Luria-bertani
mA	Milliampere
Mdm2	Mouse double minute 2 homolog
mg	Milligram
ml	Milliliter
MLTU	Major late transcription unit
MLP	major late promoter
MOI	Multiplicity of infection
MTOC	Microtubule organizing center
Mre11	Meiotic recombination 11 homolog 1
MRN	Mre11-Rad50-Nbs1
mRNA	Messenger RNA
NEM	N-ethylmaleimide
NES	Nuclear export signal
NLS	Nuclear localization signal
NFI	Nuclear factor I
Ni-NTA	Nickel-nitrilotriacetic acid
nm	Nanometer
nt	Nucleotide
OD	Optical density
ORF	Open reading frame
PAGE	Polyacrylamide gel electrophoresis
PBS	Phosphate buffered saline
PCAF	P300/CBP-associated factor

PCR	Polymerase chain reaction
PEI	Polyethylenimine
PFA	Paraformaldehyde
PHD	Plant homeo-domain
PIAS	Protein inhibitors of activated STAT
PML	Promyelocytic leukemia protein
PML-NB	PML nuclear body
PMSF	Phenylmethylsulfonyl fluoride
Pol	Viral DNA polymerase
P-rich	Proline-rich domain
PRZ	Peripheral replicative zone
PTM	Posttranslational modification
pTP	Precursor of the terminal protein
R	Arginine
Rad	DNA repair protein
Rb	Retinoblastoma protein
RBCC motif	RING, B-Box, coiled-coil domain
RC	Viral replication center
REG	Regulatory C-terminal domain
rev	Reverse
RGD	Arg-Gly-Asp
RING	Really interesting new gene
RIPA	Radioimmunoprecipitation assay
RNA	Ribonucleic acid
ROS	Reactive oxygen species
rpm	Rotations per minute
RT	Room temperature
SAE	SUMO activating enzyme
SAND	Sp100, AIRE-1, NucP41/45, DEAF1-domain
SCM	SUMO conjugation motif
SDS	Sodium dodecyl sulphate

SDS-PAGE	SDS-polyacrylamid gel electrophoresis
SENP	Sentrin specific protease
shRNA	Small hairpin RNA
SIM	SUMO interacting motif
ss	Single-stranded
SPOC1	Survival time associated PHD finger protein in Ovarian Cancer 1
Sp100	Speckled protein 100
STUbL	SUMO-targeted ubiquitin ligases
SUMO	Small ubiquitin-related modifier
SV40	Simian Vacuolating Virus 40
TAD	Transactivation domain
TAFII3	TBP-associated factor 3
TBE	Tris/Borate/EDTA buffer
TBS-BG	Tris-buffered saline with BSA and glycine
TD	Tetramerization domain
TEMED	N, N, N‘, N‘-Tetra-methylethylendiamine
TGS	Tris, glycine, SDS
TP	Terminal protein
TRIM	Tripartite motif
Tris	Tris-(hydroxymethyl)-aminomethane
Ub	Ubiquitin
Usp	Ubiquitin specific protease
UV	Ultraviolet
V	Volt
v/v	Volume per volume
VA-RNAs	Virus associated RNAs
w/v	Weight per volume
wt	Wild type

7.2 List of figures

7.3 Publications and Conferences

7.3.1 Articles in peer-reviewed journals

- Berscheminski J, Brun J, Speiseder T, Wimmer P, Wing Hang Ip, **Terzic M**, Dobner T, Schreiner S. 2015. *Sp100A is a tumor suppressor that activates p53-dependent transcription and counteracts E1A/E1B-55K-mediated transformation.* Oncogene doi:10.1038/onc.2015.378

- **Stubbe M**, Mai J, Paulus C, Stubbe HC, Berscheminski J, Karimi M, Hofmann S, Weber E, Hadian K, Hay R, Groitl P, Nevels M, Dobner T, Schreiner S. *Viral DNA Binding Protein SUMOylation Promotes PML Nuclear Body Localization Next to Viral Replication Centers.* mBio. 2020 Mar 17;11(2): e00049-20. doi:10.1128/mBio.00049-20.

- Hofmann S, **Stubbe M**, Mai J, Schreiner S. *Double-edged Role of PML Nuclear Bodies during Human Adenovirus Infection*. Virus Res. 2020 Dec 25: 198280. doi: 10.1016/j.virusres.2020.198280.

- Mai J[#], **Stubbe M**[#], Hofmann S, Masser S, Everett R, Dobner T, Boutell C, Groitl P, Schreiner S. *PML alternative splice products differentially regulate HAdV productive infection in stably transformed lung/liver cell lines*. Microbiology spectrum, 4/2022. Manuscript accepted
  [#] These authors contributed equally to this work.

- Weiß C, Göttig L, **Stubbe M**, Hofmann S, Stadler D, Protzer U, Schreiner S. *Apobec3A deamination capacity antagonizes efficient human adenovirus replication and gene expression*. PLOS Pathogens, under review

- **Stubbe M**, Mai J, Plank V, Hofmann S, Stubbe HC, Göttig L, Groitl P, Hay R, Dobner T, Schreiner S. *E2A SUMOylation promotes HAdV-mediated inhibition of the tumor suppressor p53.* Manuscript in preparation

- **Stubbe M**, Mai J, Plank V, Hofmann S, Stubbe HC, Göttig L, Groitl P, Hay R, Schreiner S. *HAdV E2A regulates localization and SUMOylation of the tumor supressor p53.* Manuscript in preparation

7.3.2 Presentations at scientific conferences

2016 - Retreat of the Institute of Virology 2016, Schliersee, Germany
Oral presentation: *Covalent SUMO attachment to HAdV E2A by host-cell cascades is beneficial for productive virus replication*

2017 - Retreat of the Institute of Virology 2017, Tutzing, Germany
Oral presentation: *HAdV-C5 E2A protein counteracts host antiviral response in a SUMO-dependent manner*

2017 - 27th annual Meeting of the Society of Virology, Marburg, Germany
Oral presentation: *Covalent SUMO attachment to HAdV-C5 E2A/DBP by host-cell cascades is beneficial for HAdV-C5 productive replication*

2017 - DNA Tumour Virus Conference 2017, University of Birmingham, England, UK
Oral presentation: *HAdV-C5 E2A protein counteracts host antiviral response in a SUMO-dependent manner*

2018 - 28th annual Meeting of the Society of Virology, Würzburg, Germany
Oral presentation: *Covalent SUMO attachment to HAdV-C5 E2A/DBP by host-cell cascades is beneficial for HAdV-C5 productive replication*

2018 - Retreat of the Institute of Virology 2018, Herrsching, Germany
Oral presentation: *HAdV E2A/DBP recruits p53 to antagonize E1B-55K-mediated SUMOylation of the tumor suppressor protein*

2019 - 29th annual Meeting of the Society of Virology, Düsseldorf, Germany
Poster presentation: *HAdV E2A modulates anti-apoptotic E1B-55K regulation by recruiting the p53 tumor suppressor protein*

2019 - Retreat of the Institute of Virology 2019, Herrsching, Germany
Oral presentation: *HAdV E2A modulates anti-apoptotic E1B-55K regulation by recruiting p53 tumor suppressor*

2019 - Chromatin Dynamics 2019-5th International Munich Symposium, Munich, Germany
Poster presentation: *HAdV E2A SUMOylation manipulates host cellular immune response to promote efficient infection*

2021 - 30th annual Meeting of the Society of Virology, Online
Oral presentation: *E2A SUMOylation promotes HAdV mediated inhibition of the tumor suppressor p53*

2022 - 31th annual Meeting of the Society of Virology, Munich, Germany
Poster Presentation: *HAdV E2A regulates localization and SUMOylation of the tumor suppressor p53*

8 Acknowledgments

First and foremost, I want to express my sincere gratitude to my first supervisor Prof. Dr. Sabrina Schreiner for giving me the opportunity to embark the science adventure with her and work on this interesting project. She pushed me forward with her continuous support, encouraged me to follow my own ideas and thought me how to be a scientist. We shared so many wonderful professional and personal moments, that I will never forget.

I also want to thank my second supervisor Prof. Dr. Thomas Floss and my mentor PD. Dr. Martina Anton for their great support with helpful suggestions and friendly scientific discussions.

I extend my gratitude to all people involved in this work and our collaborators for great scientific discussions, as well as for sharing their expertise and reagents. Thank you to Prof. Dr. Ruth Brack-Werner (Helmholtz Center Munich, Germany), Dr. Michelle Vincendeau (Helmholtz Center Munich, Germany), Prof. Dr. Thomas Dobner (HPI, Hamburg, Germany) Prof. Dr. Ron Hay (University of Dundee, UK), Prof. Dr. Michael Nevels (University of St. Andrews, UK), Dr. Christina Paulus (University of St. Andrews, UK), Dr. Kamyar Hadian (Helmholtz Center Munich, Germany) and Dr. Elisabeth Weber (Helmholtz Center Munich, Germany).

Particularly, I want to thank my lab colleagues Peter Groitl, Dr. Christina Weiss, Dr. Sawinee Masser, Dr. Julia Mai, Dr. Verena Plank, Dr. Samuel Hofmann, Lilian Göttig, Johanna Markert, Maryam Karimi, Ilka Simons, Anna Hoffrek and Ute Finkel, for all the support and great scientific discussions. I am especially grateful for their friendship that made my PhD time full of fun and wonderful memories.

I owe special thanks to Prof. Dr. Hans Will for his trust and help to step into the world of science.

I also want to say thank you to Svetlana Dragicevic for her friendship, warm and open heart, and all the help I got from her, which I will always remember.

My deepest gratitude goes to my parents Mirjana and Aca Terzic, to my siblings Isidora and Nikola, to my grandma Dragica Lucic and my aunt Gordana Terzic for having faith in me and always giving me unconditional love and support without which I would not be who I am today.

Finally, I want to thank my husband Hans Christian Stubbe for his love, support, and faith in me. Thank you for making me happy every day, for always being there for me and for even letting me brainwash you with adenovirus stories. Very special thank you goes to our daughter Lara Katharina Stubbe for supervising the final writing steps of this thesis.